EXPERIMENTAL AND ANALYTICAL INVESTIGATION

OF

DOUBLE CHORD HSS TRUSSES

By

ERNEST TIN-CHUNG CHIU, B.Sc.

A Thesis

Submitted to the School of Graduate Studies

in Partial Fulfillment of the Requirements

for the Degree

Master of Engineering

McMASTER UNIVERSITY

February 1982

DOUBLE CHORD HSS TRUSSES

MASTER OF ENGINEERING (1982) McMASTER UNIVERSITY
(Civil Engineering) Hamilton, Ontario

TITLE: Experimental and Analytical Investigation of Double Chord HSS Trusses

AUTHOR: Ernest Tin-Chung Chiu, B.Sc. (University of Wisconsin), U.S.A.

SUPERVISORS: Dr. R. M. Korol
Dr. F. A. Mirza

NUMBER OF PAGES: xix, 205

ABSTRACT

A research program into the investigation of the behaviour of double chord HSS Warren trusses is presented. The experimental results of eleven tests on five different types are reported; these include two Back-to-Back trusses, two Standard trusses and a Bolted type. One of the Back-to-Back trusses employed stiffening plates to reinforce gapped connections while the other had web members fully overlapped. The two Standard trusses had different eccentricities depending on whether the ends of the web members were square cut or angle cut. Gusset plates and tie plates were used to stiffen the connections for the Bolted truss. Retests after reparations were undertaken in the event of a localized joint or member failure so that maximum information could be obtained from the program.

An analytical model has been developed and incorported into an existing plane frame program for analysis of the double chord HSS trusses. Three types of yield mechanisms that are accounted for are plastic hinge formation at the end of a member, member failure due to plastic limit load and yielding of the spring for modelling a connection.

The experimental and analytical results are then compared thus confirming the validity of the analytical model. Finally, conclusions and recommendations are outlined for the analysis, design and feasibility of double chord Warren trusses with hollow structural sections.

ACKNOWLEDGEMENTS

I wish to express my sincere appreciation to my research supervisors, Dr. R. M. Korol and Dr. F. A. Mirza for their patience, guidance and encouragement during the course of this study.

Financial support from McMaster University and the Natural Sciences and Engineering Research Council, Canada (Grant number A 1003) are gratefully acknowledged. Much appreciation is extended to C.I.D.E.C.T. (Comite International pour le developpement et l'Etude de la Construction Tubulaire) and C.S.C.C. (Canadian Steel Construction Council) for sponsoring this research program.

The provision of the hollow structural sections for the test program by the Steel Company of Canada and the fabrication of the trusses by Marshall Steel, Niagara Structural Steel and T.I.W. Central Bridge is also appreciated.

I am grateful to the staff of the Applied Dynamics Laboratory for their assistance during the testing program and my thanks also to Ms. Marlene Fletcher for the expert typing of the thesis.

I would also like to thank my lovely fiancée, Caroline, in recognition of the sacrifices which she has made during the period of this investigation.

To my dear parents

TABLE OF CONTENTS

TABLE OF CONTENTS (Continued)

TABLE OF CONTENTS (Continued)

LIST OF FIGURES

LIST OF FIGURES (Continued)

LIST OF FIGURES (Continued)

LIST OF FIGURES (Continued)

LIST OF TABLES

LIST OF TABLES (Continued)

NOMENCLATURE

A	Cross-sectional area of member
A_s	Area of stiffening plate in resisting shear
A_w	Area of rectangular hollow section in resisting shear
a	Constant for m-ϕ relationship when $\phi \leq \phi_1$
b	Constant for m-ϕ relationship when $\phi_1 < \phi < \phi_2$
b_s	Width of stiffening plate
c	Value of P/P_y when $M = M_p$
d	S/Z
e	Eccentricity
f	Constant for $m - \phi$ relationship when $\phi_2 < \phi$
G	Shear modulus of elasticity
g	Constant for $m - \phi$ relationship when $\phi_1 < \phi < \phi_2$
h_0	Height of section
I	Momet of inertia of member
k_{sp}	Stiffness of shear spring
ℓ_i	Distance to the yield surface
ℓ_c	Length of short member next to shear spring
M	Bending moment across section
M_p	Plastic yield moment
M_y	Yield moment when the outer front fibre stress is σ_y
m	Ratio of applied moment to plastic yield moment, M/M_p
$\tilde{m}$	Ratio of applied moment to yield moment, M/M_y
$\tilde{m}_1$	Initial yield moment
$\tilde{m}_2$	Secondary yield moment

NOMENCLATURE (Continued)

$\tilde{m}_{pc}$	Ultimate flow moment
P	Axial force in member
P_w	Force in web member
P_y	Yield axial force
p	Ratio of axial force to yield axial force, P/P_y
Q	Panel point load on truss
S	Section modulus
t	Effectiveness of section in resisting shear
t_0	Web thickness
t_s	Thickness of stiffening plate
V	Shear force at a section
V_i^k	Shear force in the i^{th} spring at the k^{th} load increment
V_p	Fully plastic shear force
W	Total load on truss
W_{max}	Truss failure load
Z	Plastic sectional modulus
α_i^k	Distance to yield surface for member 'i' at the k^{th} load increment
β_k	Load increment factor at the k^{th} load increment
β_{kh}	Critical load increment factor to cause hinge formation at the k^{th} load increment
β_{km}	Critical load increment factor to cause member removal at the k^{th} load increment
β_{ks}	Critical load increment factor to cause shear failure at the

NOMENCLATURE (Continued)

	k^{th} load increment
Δ	Total mid-span displacement of truss
ΔV_i^k	Shear force increment for the i^{th} spring to cause failure at the k^{th} load increment
ΔV_{il}^k	Change in shear force in the i^{th} spring at the k^{th} load increment when $\beta_{ks} = 1.0$
Δ_c	Allowable displacement of shear spring
ΔM_{pj}^k	Incremental limit moment of the j^{th} hinge during the k^{th} load increment
Δ_0	Displacement of web member
Δ_{sp}	Displacement of shear spring
δ_{ij}	Kronecker delta
ε	Maximum principal strain
γ_y	Maximum shear strain
κ	Constant in computing web area in resisting shear
ϕ	Ratio of curvature to yield curvature corresponding to M_y, ϕ_c/ϕ_y
ϕ_c	Curvature of a section under the applied moment
ϕ_y	Yield curvature
ϕ_1	Initial yield curvature
ϕ_2	Secondary yield curvature
ρ_{ij}^{LK}	Bending moment at end 'L' of the i^{th} member due to unit moment at hinge 'j' for the k^{th} load increment
ρ_{ij}^{GK}	Bending moment at end 'G' of the i^{th} member due to unit moment at hinge 'j' for the k^{th} load increment

NOMENCLATURE (Continued)

σ_u	Ultimate stress
σ_y	Yield stress
τ_y	Yield stress in shear
$\{f\}_j^k$	Axial force due to unit moment at hinge 'j' at the k^{th} load increment
$[K]$	Global stiffness matrix
$[k]_{sp}$	Stiffness matrix for shear spring
$\{\Delta M^L\}^k$	Bending moment increment at end 'L' of member at the k^{th} load increment
$\{\Delta M^G\}^k$	Bending moment increment at end 'G' of member at the k^{th} load increment
$\{\Delta M_y^{L1}\}$	Bending moment increment at end 'L' of member due to load increment and zero moment at hinge
$\{\Delta M_y^{G1}\}$	Bending moment increment at end 'G' of member due to load increment and zero moment at hinge
$\{P\}$	Load vector
$\{P_y\}$	Load vector to cause yielding
$\{\Delta P\}^k$	Axial force increment at the k^{th} load increment
$\{\Delta P_y^1\}^k$	Axial force increment due to $\beta_k = 1.0$ and zero moment at hinge
$\{\Delta P_y^2\}^k$	Axial force increment due to incremental limit moment applied at the hinges
$\{x\}$	Displacement vector

CHAPTER 1

INTRODUCTION

1.1 Background to the Study

A major consideration in employing hollow structural sections in long span truss applications has been one of size availability for the chord members. This problem has been overcome in offshore structural applications with the use of large diameter round tubular members as the main members. However, in the quest for oil and gas resources, the economic stakes are so high that high fabrication costs for building oil rigs and associated structures can be tolerated. In the case of building construction or in industrial site applications, prudent reductions in fabrication costs will make conceived structural systems more competitive. Thus, trusses consisting of rectangular hollow structural sections have a distinct edge over round tubular sections because of the simplified end preparations needed for welding.

If, however, the largest size square hollow members of 304.8 × 304.8 × 12.7 mm that is currently manufactured in Canada was used for chord members in a Warren truss structure, the clear span would need to be restricted to the 30 to 40 m range. Many applications such as sports and recreational centres, convention halls and manufacturing plants necessitate clear spans exceeding 50 m. It was for this reason that the double chord concept suggested itself for long span possiblities with economically viable designs.

Double chord systems are more advantageous over the traditional single chord systems in many aspects. The most profound effect is that forces from the diagonal members are transferred to the webs of the double chord as compared to the weaker flange of the chord plate for single chord systems, thus resulting in stiffer connections and higher load carrying capacity of the truss. Since a double chord truss will have a longer unsupported span than that utilizing single chord members, greater interior design flexibility within buildings will be achieved. Moreover, double chord systems will result in higher lateral rigidity and consequently, less lateral bracing will be required to prevent instability of the top chord subjected to compressive stress. At present, the major example of a double chord system is the Hamilton Convention Centre. Its design was based on work done at McMaster University [1] on double chord joints. Hence it is appropriate at this juncture to discuss the findings of Korol and Chidiac involving double chord joints and to present reasons for the need to have undertaken the truss program described herein.

The initial research project involving double chord connections was sponsored by Comite International pour le Developpement et l'Etude de la Construction Tubulaire (C.I.D.E.C.T.) (5V) and the Canadian Steel Construction Council (C.S.C.C.) and conducted study on four different types of joints [2]. These included Back-to-Back, Channel, Standard and Bolted types. It was stated in the conclusions of that study that Back-to-Back, Standard and Bolted connections showed the most promise whereas the Channel type connections were found to be unsatisfactory.

From experience gained with single chord trusses and joints, it was felt that additional research on double chord joint behaviour was essential. For example, as part of C.I.D.E.C.T Program 5F, eight Pratt trusses with single chord rectangular hollow sections (RHS) having spans of between 14 and 16 meters were tested at Pisa University, Italy [3]. Isolated joints were also fabricated and tested in an attempt to draw possible correlations with those forming the trusses [4]. It was found that many of the isolated joints failed by local buckling of the chord which did not occur in the truss experiments. The truss tests also showed no appreciable difference between the strengths of joints on the compression chord and those on the tension chord [5].

This difference in results is further noticed in the testing of eleven welded steel trusses of 6 m span and 0.84 m deep by Dasgupta [6] conducted at Nottingham University. The connections were designed in accordance with previous test results on individual joints undertaken at the University of Sheffield [7] while rectangular hollow sections were used to form the gapped N-joints. Failure loads of the truss joints were found to be up to 30% lower than the equivalent joint failure loads. Therefore it appears that the joint behaviour in a full scale truss may be quite different from the results obtained for isolated joints.

1.2 Objectives and Scope

A decision to extend the double chord joint work to include

large scale trusses was therefore taken. This project, known as C.I.D.E.C.T. (5VI), was intended to study the behaviour of trusses comprised of the joints deemed to be most likely to lead to structurally efficient and economic designs. One of the primary objectives of the investigation was to ascertain whether the joint test findings [2] would be substantiated in actual truss tests. Such a verification was not necessarily to be expected in light of the experience with the single chord connections.

Another objective was to determine whether the type of joint or its detailing would cause localized weakness or unanticipated overall buckling of the associated truss. For example, lateral bracing of the top chord is required if the ratio of unsupported length to its radius of gyration is excessive. There are some questions about the effective moment of inertia of the double chord about an axis in the plane of the truss; particularly when the chords are separated intermittently by the diagonal members at the connnections. Also of concern was the possible local buckling at the ends of diagonal members due to moment and axial force transfer mechanisms.

Large deformations prior to failure usually alter a structure's original geometry to the extent that secondary forces may become significant. This consideration, in additon to the truss' overall ductility prior to failure is important in the limit state design philosophy. Laboratory experiments on trusses are therefore essential to shed light on the above mentioned aspects of the overall behaviour.

It was decided to test a total of five trusses, two with double chords placed back-to-back, two with standard type connections and one with bolted connections. The trusses were conceived to be one-half to one-third scale of the possible long span prototype structures. These large scale sizes avoid scale effects for residual stresses due to welding or manufacturing and from general fabrication procedures.

Finally an analytical method, to predict the stiffness and strength characteristics of a double chord truss was deemed essential to permit an assessment of the effect of varying parameters, e.g. eccentricity, diagonal to chord angle and joint characteristics, etc.

1.3 Truss Types

Three different types of connections were used for the five trusses tested. These included the Back-to-Back, Standard and Bolted connections and are shown in Fig. 1.1.

In the case of the Back-to-Back or "BB" connection, the two chord members are placed together in a back-to-back manner and the chord members are welded onto their composite flanges as indicated in Fig. 1.1(a). This type of connection can be reinforced by overlapping the web members (OV designation) or by employing stiffening plates (ST designation). Thus the truss BBST employed the Back-to-Back with stiffening plate type connections. In both cases, with or without stiffening plate, diagonal end preparation is required to ensure an effective weldment.

The Standard or "S" connection has the web members sandwiched between the chord members and are attached to the latter by simple fillet welds as illustrated in Fig. 1.1(b). The two trusses tested of this type were identified as S1 and S2 because of different joint eccentricities.

The Bolted or "BO" connection is similar to the Standard connection except that the web members are bolted to gusset plates that in turn are welded to the chord members. This type is shown in Fig. 1.1(c)..

1.3.1 Eccentricity

Large eccentricities are normally to be avoided when designing joints since these induce moments on the ends of members framing into a joint. However, recent studies at the University of New Brunswick [8] noted that very high stresses were caused by bridging action at the ends of the diagonal members thus tending to cause localized rupturing of the chords webs. This effect is particularly pronounced in Standard trusses. In defining geometries of the two Standard trusses, it was originally thought that a smaller eccentricity would yield a larger load carrying capacity. Nonetheless, it is possible to minimize eccentricity by angle-cutting the ends of the diagonal members. The two types of detailing for Truss S2 and Truss S1 joints are shown in Fig. 1.2(a) and Fig. 1.2(b), respectively. Eccentricities are positive in both instances.

Positive, zero or negative eccentricity can be obtained for the Bolted and Back-to-Back connections. For the Back-to-Back connection, a gap joint (as for Truss BBST) produces partial eccentricity, partial overlapping produces zero eccentricity while full overlapping (as for Truss BBOV) results in negative eccentricity. These cases are illustrated in Fig. 1.3.

The gusset plates for the Bolted truss permits complete freedom of choice regarding eccentricity. The eccentricity of Truss BO is taken as zero.

1.3.2 Diagonal to Chord Angle

The angle between the diagonal and the chord members affects the performance of the connections as well as that of the entire truss. A small angle produces a small eccentricity at the connection but results in longer diagonals and the ones in compression will be more susceptible to buckling. Panel point spacings would also be increased giving greater unsupported length for the top chord. The effect of varying the diagonal to chord angle was not investigated in this research work. The diagonals were positioned so as to have an approximately 2:1 slope (63.4°) with the chords.

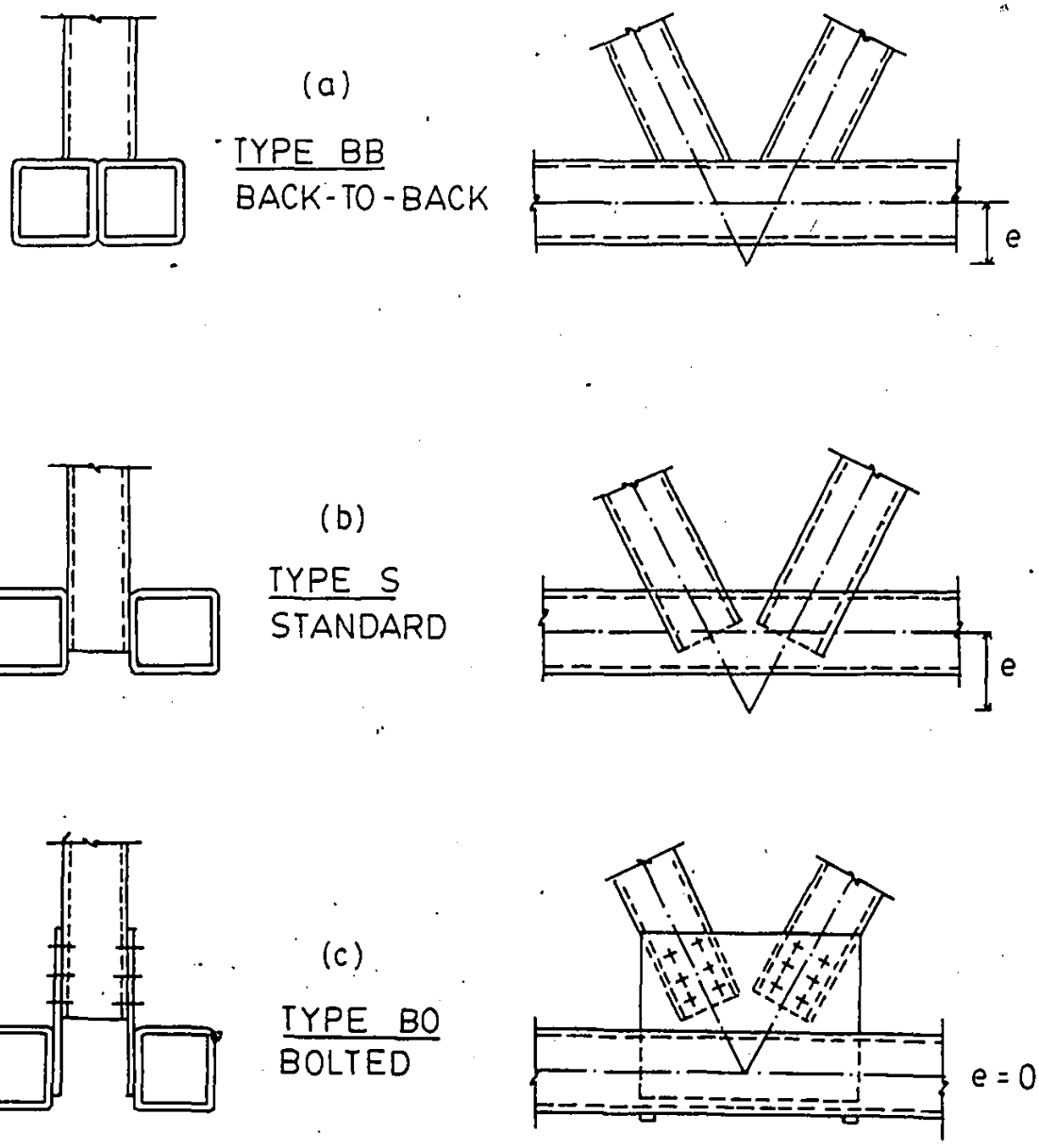

FIGURE 1.1 TYPE OF CONNECTIONS

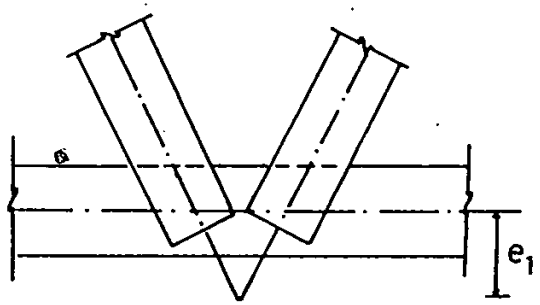

(a) SQUARE CUTS (S2)

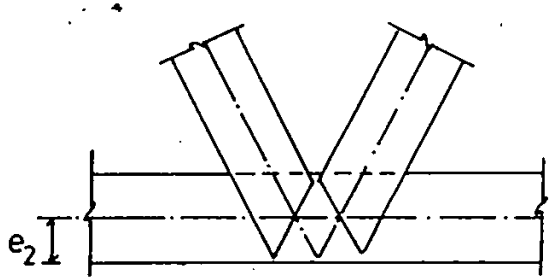

(b) ANGLE CUTS (S1)

FIGURE 1.2 ECCENTRICITY IN STANDARD CONNECTION

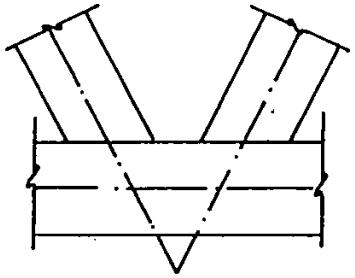

GAP JOINT

+ve e

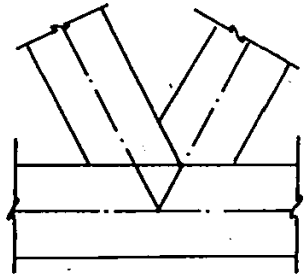

PARTIAL OVERLAPPING

e = 0

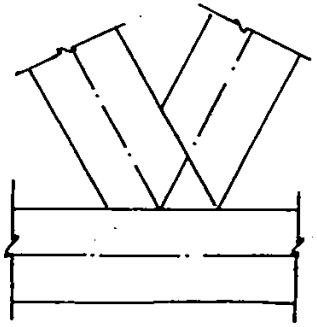

FULL OVERLAPPING

-ve e

FIGURE 1.3 ECCENTRICITY IN BACK-TO-BACK CONNECTION

CHAPTER 2

DESCRIPTION OF THE EXPERIMENTAL PROGRAM

2.1 General Truss Details

From previous joint test results [2], the Back-to-Back or BB, Standard or S and Bolted or BO type connections showed promising results while the Channel type did not. As such, the former three were deemed worthy of further study regarding their performance as parts of the overall trusses. A total of five trusses were tested, of which there were two Back-to-Back, two Standard and one Bolted type. In order to assess their performances, the overall dimensions were designed to have a common height of 1.83 m and length of 15.09 m as shown in Fig. 2.1. The slope of web members was maintained at 2:1 with minor differences due to end detailing of the diagonals. A general view of the Truss S1 with spreader beams and loading assembly is shown in Fig. 2.2. A similar setup was also used for the other trusses.

The steel used in all trusses was CSA Grade 40.21M 350 Class H. Sections were cold formed from flat-rolled steel with the following mechanical properties:

(a) a minimum yield strength of 350 MPa (50.8 ksi);

(b) tensile strength of 450-620 MPa (65.3 - 89.9 ksi);

(c) miniminum elongation of 22% in 50.8 mm.

Upon completion of each test, coupons were cut from the chord and web members of each truss. These coupons were then used in the standard tensile tests on a Tinius Olson machine in accordance with the ASTM specifications [9]. The results obtained are representative of the strength properties of different members comprising each truss and are listed in Table 2.1.

All chord members consisted of two square hollow structural sections (HSS) of dimensions 152.4 mm × 152.4 mm × 6.35 mm while the web members were single square HSS of size 127.0 mm × 127.0 mm. Different thicknesses were used for the web members to account for the anticipated differences in levels of axial forces developed depending on their positions in the truss. Exterior web members with the highest axial forces were proportioned with a thickness of 9.53 mm while interior web members had thicknesses of 6.35 mm and 4.78 mm. It was expected that by utilizing the above mentioned web member dimensions, approximately equal stresses would be developed during testing.

Because of the high cost of fabricating such large structures, it was deemed prudent to reinforce members or joints and their symmetric counterparts that suffered from localized failures and to undertake retests. In the event that a major failure of the structure would occur, as for example, top chord overall buckling or rupturing of a joint, testing would be discontinued. It was felt that the necessary repair work and altered geometry would have a major influence on the truss' behaviour when compared to that of the original structure.

2.2 Testing Arrangement

Trusses to be tested were simply supported at the ends of the bottom chord members which rested on two massive concrete blocks. The ends of the top chord members were restrained against lateral movement by placing wooden blocks between the webs and the vertical W14 x 119 steel columns that were securely bolted to the test floor.

Two single-acting hydraulic jacks were used to simulate in-plane gravity loading at the top panel points of the trusses. Two load cells, each having a capacity of 1780 kN in compression were used along with the hydraulic jacks. These were connected to two strain gauge indicators and the readings were recorded for prescribed loadings in accordance with the precalibration.

By employing systems of spreader beams under each of the hydraulic jacks, equal loadings could then be transferred to each of the eight top panel points. Since the loadings and truss geometry were symmetrical about the centre line, testing arrangement for half of a typical truss is illustrated in Fig. 2.3.

2.3 Measuring Devices

A large number of strain gauges were placed at the approximately computed critical sections of each truss. Sets of 90° rosettes were also located along a line through the connection center and perpendicular to the double chord members in order to measure the principal

strains, and in particular the maximum shearing strains at the connections [10]. The two types of linear gauges used had gauge lengths of 12.7 mm and 5.0 mm with gauge factors of 2.10 and 2.09, respectively. The rosettes used were general purpose 3 element 45° of rectangular shape (model 90-EA06125RS-120) having an individual gauge length of 3.2 mm and a gauge factor of 2.03. To ensure a proper bond between the strain gauges and the metal surfaces, rust proof paint applied by the fabricators was first removed. Bonding was then performed according to the manufacturer's specifications with the necessary drying periods allowed. These gauges were connected to a nominal 100 channel Autodata recording device (80 channels only for single gauges) which gives an output on a paper tape. Since more than 80 channels were normally needed, strain indicator boxes were used for the additional gauges required.

Eight dial gauges, mounted on one side of the top chord members, were used to indicate the amount of lateral displacement of a truss. Three more dial gauges were attached to the upper sides of the top chord members to determine vertical displacement of the mid span of the truss at various loading stages.

In order to compare performances of various trusses the strain gauges, rosettes, and dial gauges were arranged in a consistent manner and will be discussed in more detail in the subsequent chapters.

2.4 Test Procedures

Just prior to testing, the two load cells were calibrated while

the resistances of all strain gauges and rosettes were checked to indicate the amount of drift, if any. After identical readings had been taken, identical loads were applied incrementally to the top chord in increments of about 5% of the estimated capacity of the truss. The strain and displacement readings and general observations were recorded at each load step. This procedure was repeated until significant deformations of joints or members had occured which was indicated by a drop in strain readings for the load cells. The truss would then be examined for a possible failure condition. In some cases a small drop in load was associated with a displaced shim or bolt slippage. Loading was continued until a true maximum was reached and a mode of failure observed.

In order to check for possible unsymmetrical loadings, strains in members were checked against their mirror image members. If there were any significant discrepancies between the two strains readings, the loading arrangements and/or load cells would be checked for possible eccentricity and/or non-uniform applied pressure, respectively. Further loadings would commence only after the necessary adjustments had been made satisfactorily.

2.5 Specific Truss Features

The detailed descriptions of the trusses, their construction and strain gauging are presented in the subsections to follow. The subsequent reinforcing measures conducted on the trusses that were retested are outlined in Chapter 4 along with their performances.

2.5.1 Back-to-Back Trusses

Two Back-to-Back trusses, BBST and BBOV with eccentricities of 117 mm and -76 mm respectively, were tested for comparisons. Truss BBST employed stiffening plates of thickness 19.05 mm at the connections where the web members were connected to the chord members. Truss BBOV had fully overlapped connnections where the compression web members were welded to the tension web members. Details and dimensions of interior joints are shown in Fig. 2.4 and Table 2.2 for both types.

Truss BBST was expected to develop relatively high shear forces at the connections. The provision of the 19.05 mm stiffening plates, however, tended to transfer much of these shear forces from one web member to the other thereby minimizing the possibility of a shear failure. Previous test results on individual connections [2] showed that the maximum shear stresses developed in the chord members with equivalent stiffening plates were not sufficient to cause a failure. One of the principal objectives was to establish whether this conclusion would be reaffirmed in the truss test. As such, strain rosettes were located along the joint centerlines (critical sections) on the outer webs of exterior joint to measure maximum shear strains occuring at different loads. In addition, strain gauges were mounted at the ends and at mid-length of some members to determine axial forces and moments at the approximately precomputed high stressed locations. The layout of the strain gauges and rosettes is shown in Fig. 2.5.

Truss BBOV with eccentricity of -76 mm had the advantage of a more efficient transfer of web forces due to its fully overlapped connections. This is also confirmed by the previous test results [2] where the shear strains developed on the chord members at the connections were significantly lower than the stiffened gap joint case. Figure 2.6 illustrates layout of the strain gauges and rosettes employed for studying the above mentioned effects.

2.5.2 Standard Trusses

Two Standard trusses, S1 and S2 with eccentricities of 108 mm and 178 mm, respectively, were tested. They were fabricated by continuous fillet welding the web members to the chord members. Ends of the web members for Truss S2 were square-cut whereas those for Truss S1 were angle cut (Fig. 1.2) to permit a smaller eccentricity. Details of the square cut connection and dimensions of both types are presented in Fig. 2.7 and Table 2.3.

From previous joint tests [2], it was anticipated that a failure would perhaps be precipitated by shear at the connections rather than buckling of the compression diagonals. As a consequence, strain rosettes were located at inner and outer webs at exterior joints and crtical sections as shown in Fig. 2.8. However, due to the interference of the web members there was at best room to accomodate only two rosettes, e.g. joints of Truss S1. For Truss S2, it was only possible to include a single inner chord rosette per web surface and, as such, No. 29 at joint 1 and No. 34 at joint 2 were omitted. These arrange-

ments are indicated in Fig. 2.9.

2.5.3 Bolted Truss

Only one bolted truss, BO with zero eccentricity, was tested. Gusset plates bolted to the web members and welded to the chord members were employed at the connections. Tie plates composed of two flat bars spanning the double chord members were also utilized to stiffen the connections. Dimensions and details of a typical bolted connection are shown in Fig. 2.10 and Table 2.4.

Once again the previous joint tests [2] showed that a negligible amount of shear stresses were developed in the chord members at the connections. This suggests that the introduction of gusset plates and tie plates can significantly increase the rigidity of the connections. Only strain gauges were mounted at the ends and at the middle of some members to determine axial forces and moments at the critical sections. The layout of strain gauges is shown in Fig. 2.11.

2.6 Moment-Curvature-Thrust Relationships

Each member of a truss experiences an increase in both the axial force and the bending moments as the loading on the truss increases. This combination of forces has a significant effect on the curvature of a member. Chen and Atsuta [11] have proposed a set of parametric functions for the approximate moment-curvature-thrust (m-ϕ-p) expressions for tubular sections without taking residual stresses into account, and

enables one to relate the curvature of a section subjected to combined axial force and bending moment. These functions and typical $m-\phi-p$ interaqtion diagrams are shown in Appendices III and IV, respectively.

In order to fully utilize the experimental results, strain readings are converted into the corresponding curvatures at the ends of the members which are then incorporated into the $m-\phi-p$ interaction diagrams to obtain the end moments at various stages of loading. These experimental load-moments (W-M) curves are then compared with the analytical curves for verification purposes.

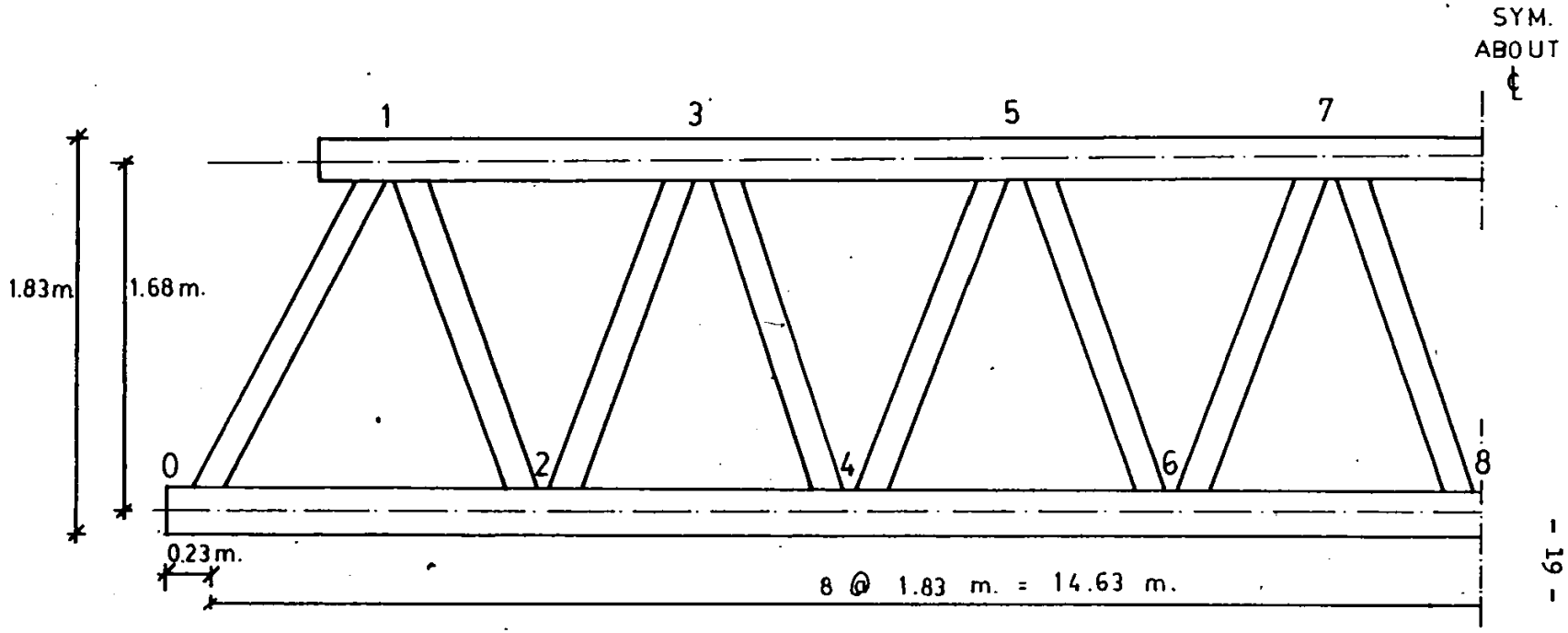

NOTE: 1) Chords were 2 152.4 × 152.4 mm.; webs were 127.0 × 127.0 mm.

2) Thickness of chord members, top & bottom were 6.35 mm.

Thickness of web members 0-1 were 9.53 mm.

1-2 to 4-5 were 6.35 mm.

5-6 to 7-8 were 4.78 mm.

FIGURE 2.1 GENERAL DIMENSIONS OF TRUSS

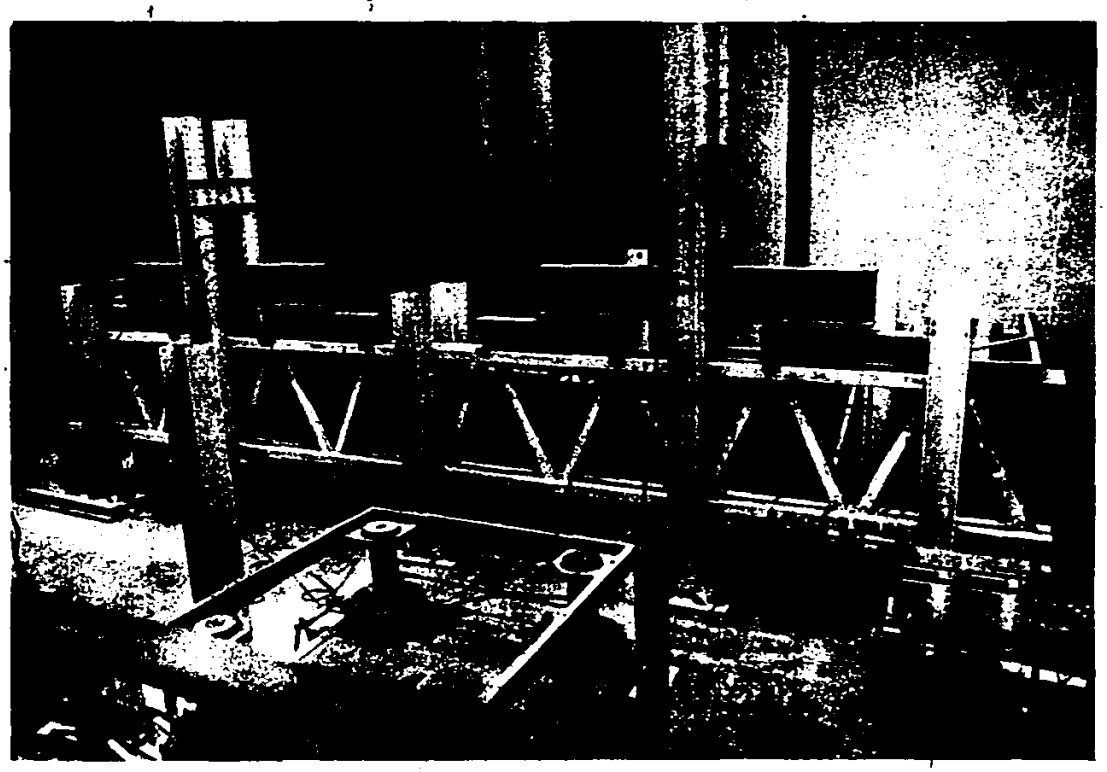

FIGURE 2.2 GENERAL VIEW OF TRUSS AND LOADING SYSTEM

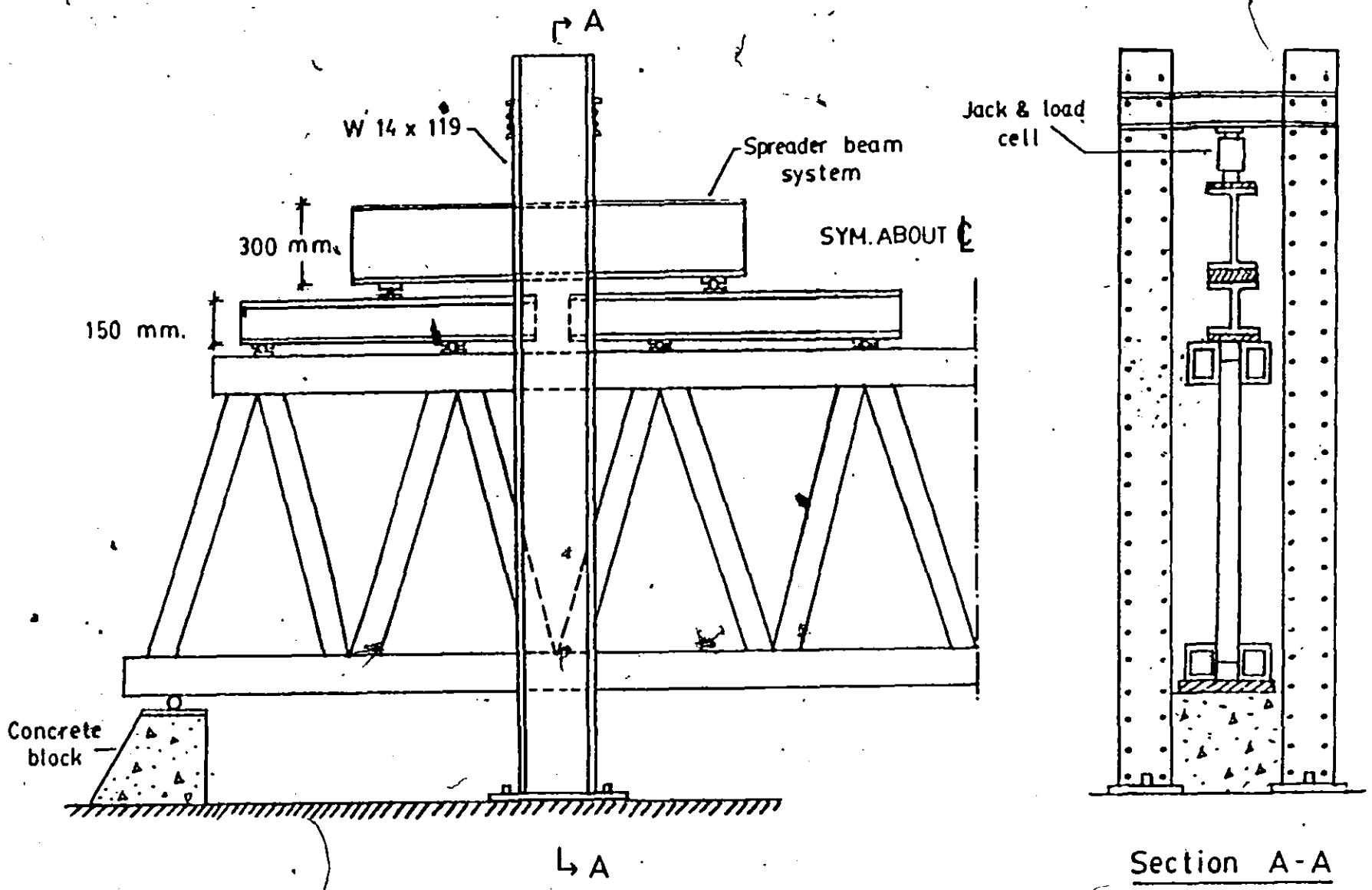

FIGURE 2.3 GENERAL TESTING ARRANGEMENT

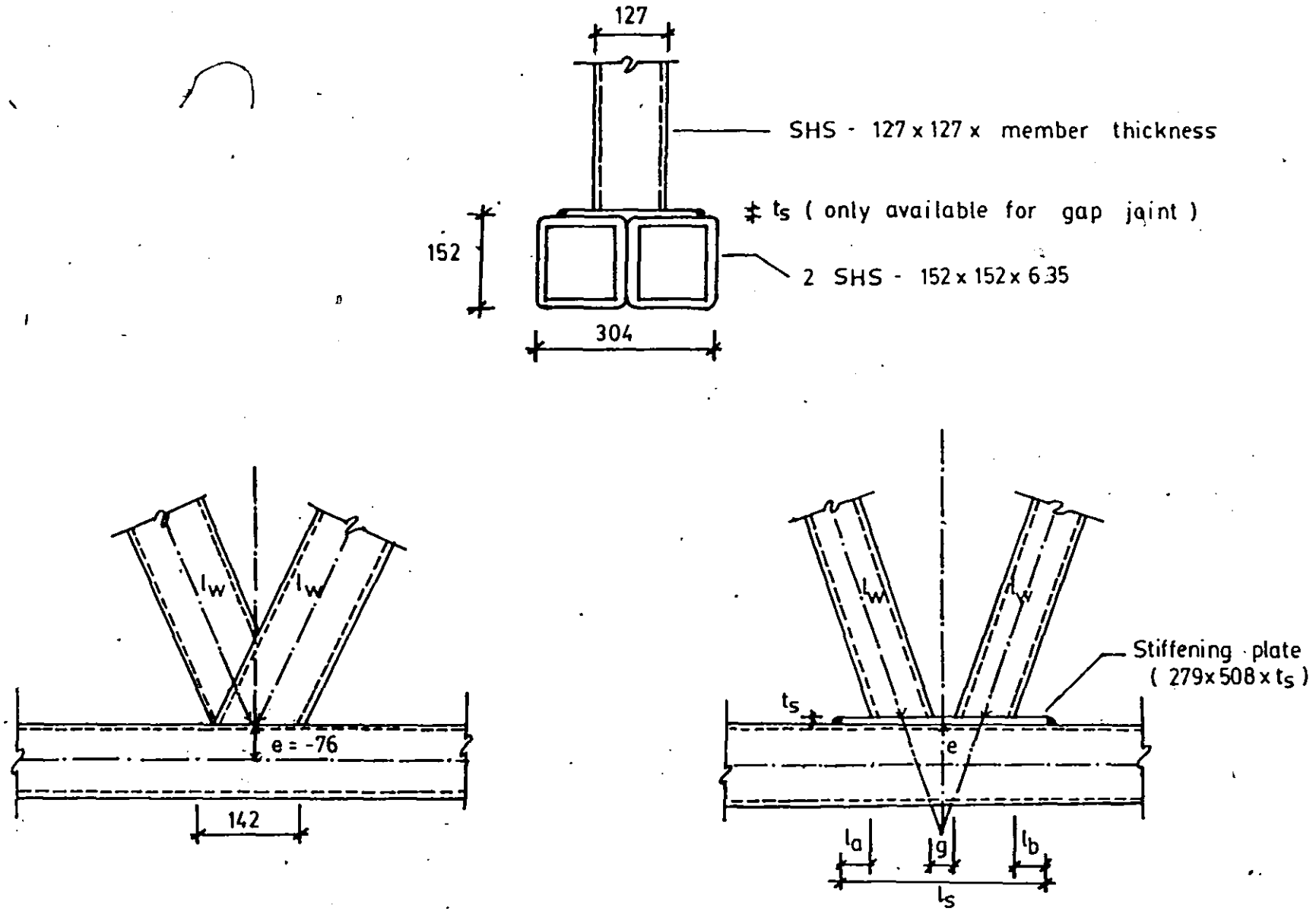

FIGURE 2.4 DETAILS OF BACK-TO-BACK CONNECTION (Dimensions in mm.)

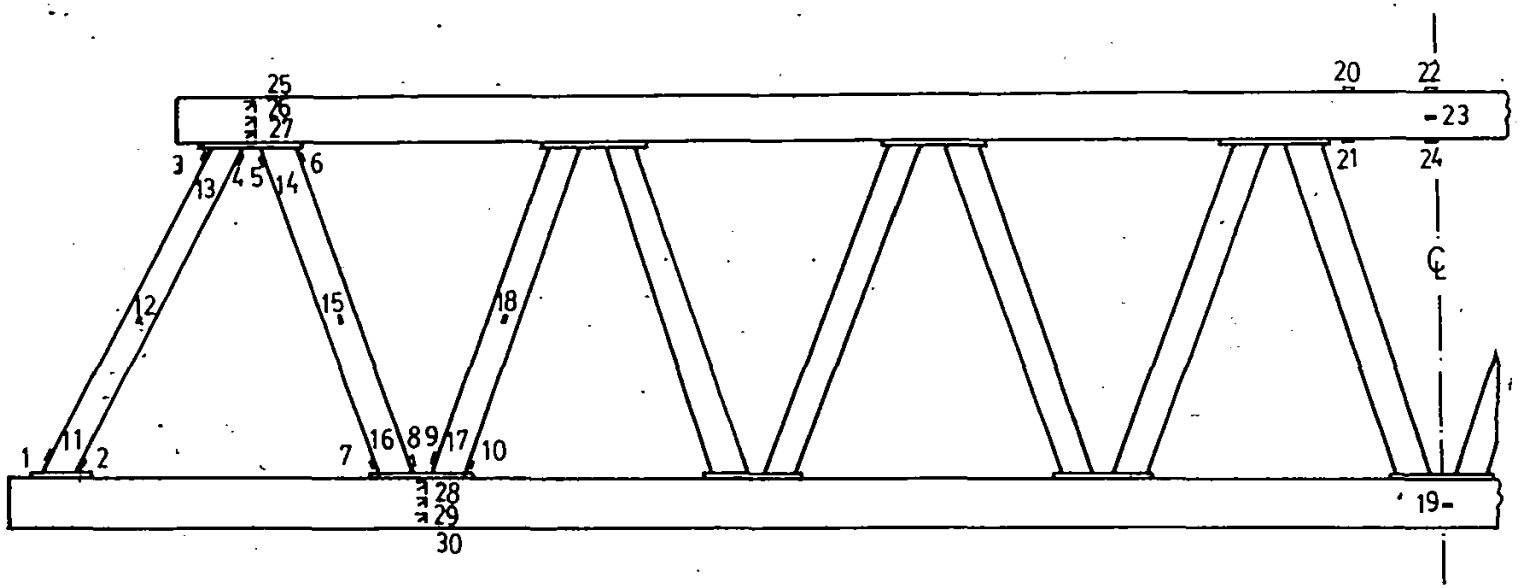

FIGURE 2.5 LAYOUT OF STRAIN GAUGES & ROSETTES FOR TRUSS BBST

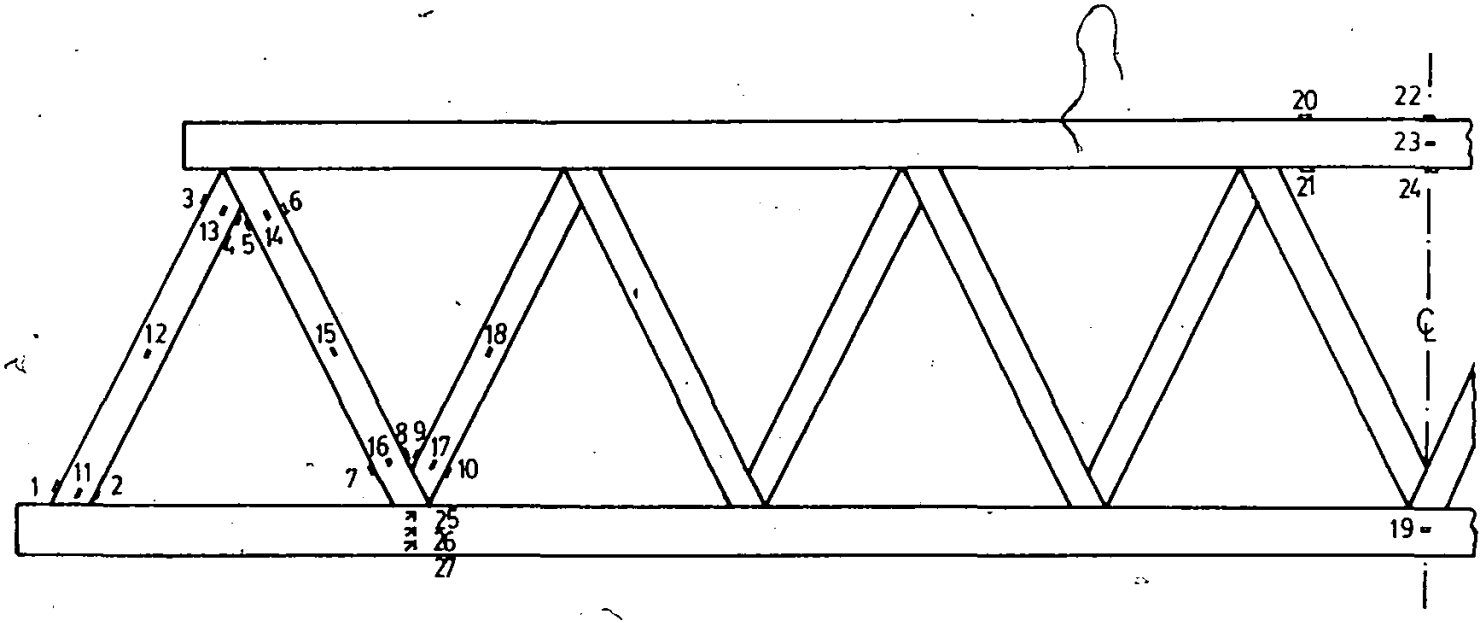

FIGURE 2.6 LAYOUT OF STRAIN GAUGES & ROSETTES FOR TRUSS BBOV

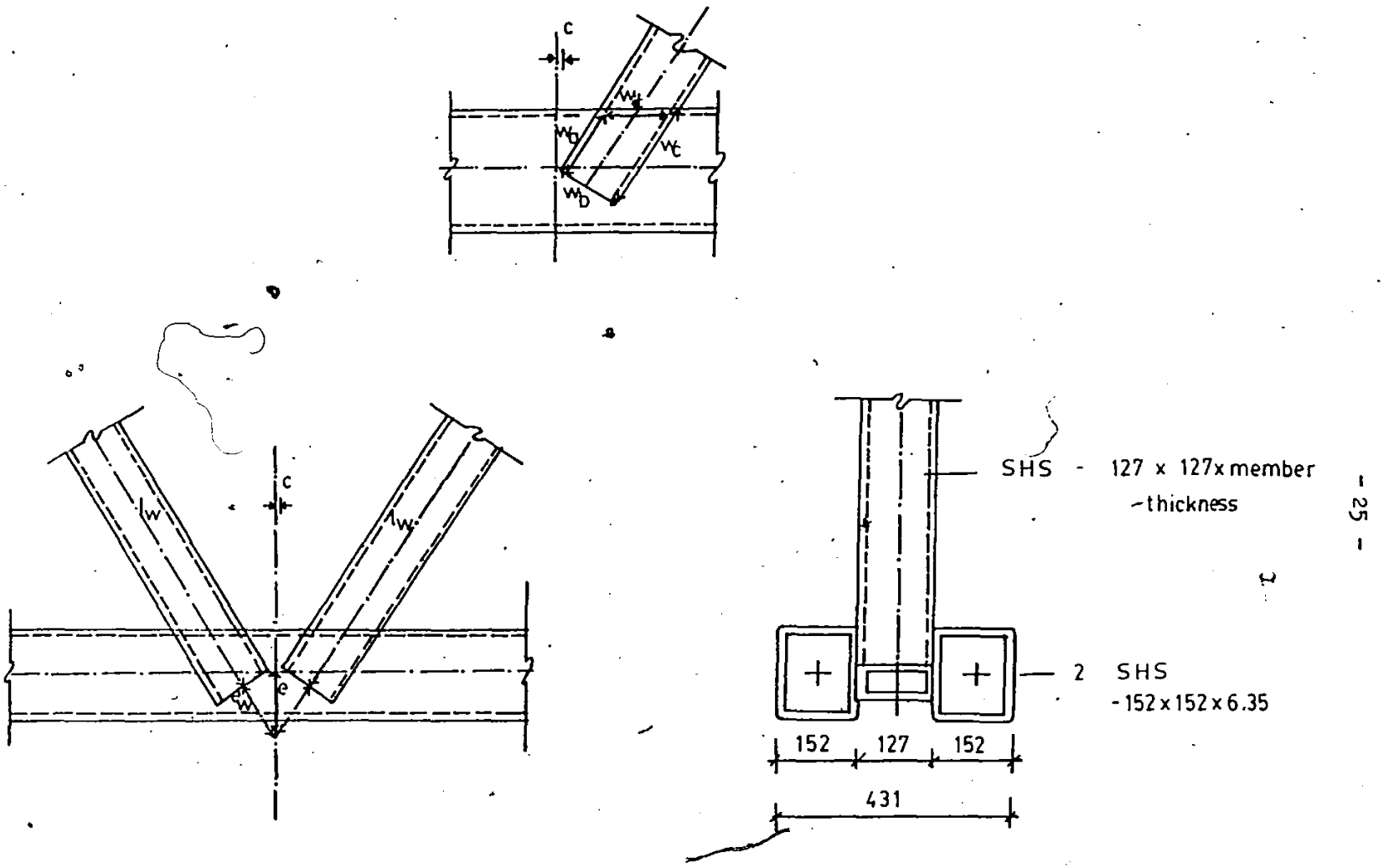

FIGURE 2.7 DETAILS OF STANDARD CONNECTION (Dimensions in mm.)

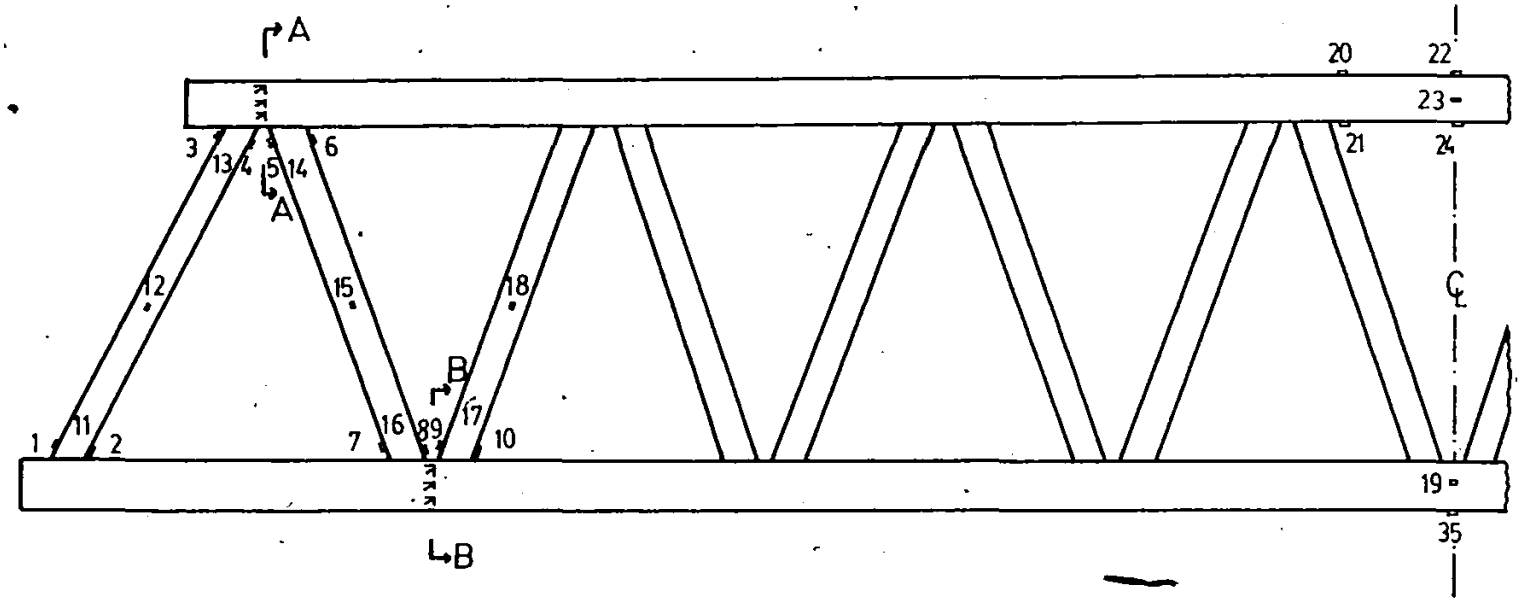

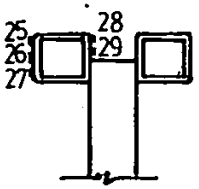

JOINT 1 (Sec.A-A)

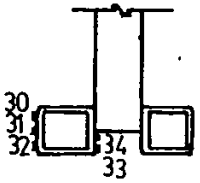

JOINT 2 (Sec.B-B)

FIGURE 2.8 LAYOUT OF STRAIN GAUGES & ROSETTES FOR STANDARD TRUSS

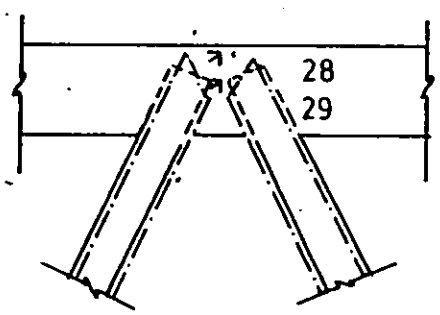

— S 2 (29 N/A)
—·— S 1

INNER CHORD DETAILS

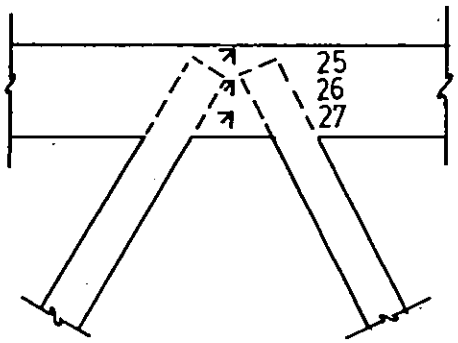

OUTER CHORD DETAILS

NOTE: 1) Similar arrangements for joint 2 with different nomenclature for rosettes

2) Joint 2 is a mirror image of joint 1 about a horizontal axis

FIGURE 2.9 ROSETTES ARRANGEMENTS FOR STANDARD TRUSS AT JOINT 1

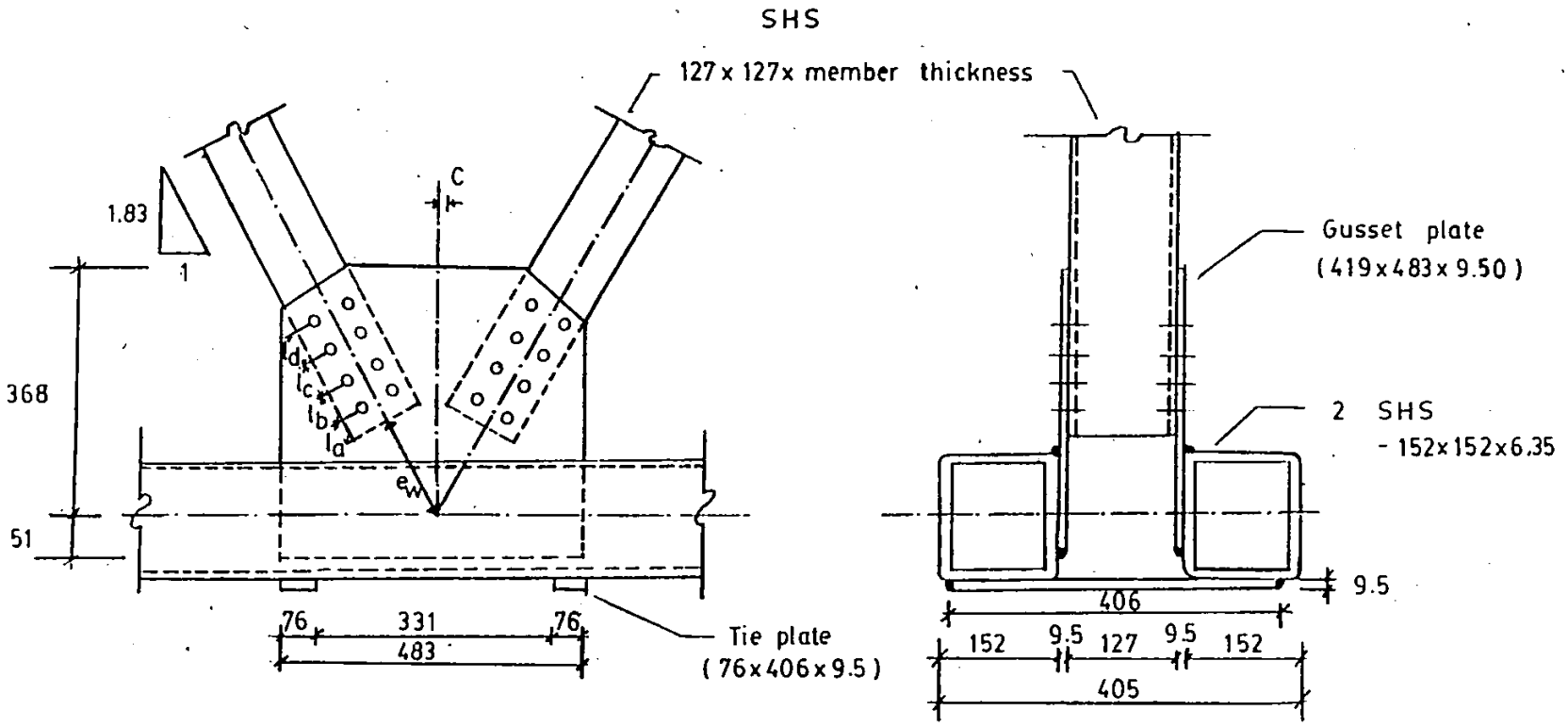

FIGURE 2.10 DETAILS OF BOLTED CONNECTION (Dimensions in mm.)

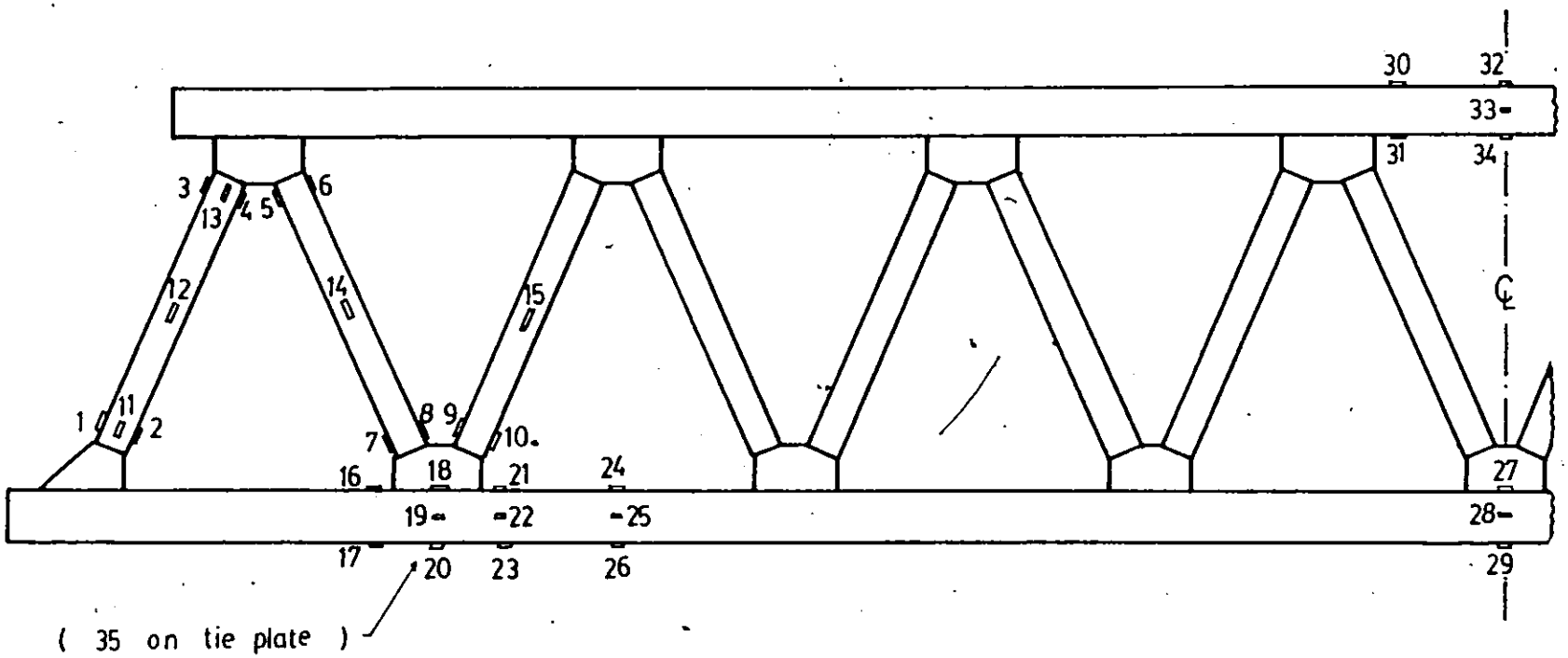

FIGURE 2.11 LAYOUT OF STRAIN GAUGES FOR TRUSS B0

Truss	Members		σ_y (MPa)	σ_u (MPa)
BBST	Chord	7-7	394.9	488.2
	Diagonal	0-1	397.7	496.1
		1-2	396.0	489.4
		2-3	389.1	495.7
BBOV	Chord	7-7	401.2	490.2
	Diagonal	0-1	409.1	499.6
		1-2	412.0	513.8
		2-3	390.7	485.8
S1	Chord	7-7	370.3	470.9
	Diagonal	0-1	393.0	502.0
		1-2	374.4	481.3
		2-3	386.1	485.4
S2	Chord	7-7	390.1	487.8
	Diagonal	0-1	382.2	488.8
		1-2	368.7	459.2
		2-3	360.7	461.7
BO	Chord	7-7	374.4	472.0
	Diagonal	0-1	402.0	506.1
		1-2	407.5	510.2
		2-3	408.2	512.3

Table 2.1 Tensile Properties for Diagonal and Chord Members for Various Trusses

Truss	Web Member Details		Joint Details							
				Dimensions at connections (mm)						
	Member	ℓ_w (mm)	Joint	ℓ_a	ℓ_b	g	ℓ_s	t_s	e	General Remarks
BBST	0-1	1711	0	76	74	0	295	19.05	117	Gap joint with stiffening plates.
	1-2 to 7-8	1690	1 to 8	76	76	74	508	19.05	117	
BBOV	0-1 to 7-8	1629	0 to 8	N/A				N/A	-76	Compression diagonals welded to tension diagonals. 100% overlap.

Table 2.2 Dimensions for Back-to-Back Trusses

Truss	Web Member Details				Joint Details							
	Member	ℓ_w (mm)	Weld Size (mm)		Joint	Web dimensions at connections (mm)					Ecc. (mm)	
			W_a, W_c, W_d	W_b		W_a	W_b	W_c	W_d	c	e	e_w
S1	0-1	1712	19.1	7.9	0	159	142	159	142	0	108	109
	1-2 to 4-5	1693	14.3	4.8	1	32	142	159	142	6.35	108	109
	5-6 to 7-8	1693	11.1	3.2	2 to 8	32	142	159	142	6.35	108	109
S2	0-1	1699	15.9	7.9	0	159	142	159	142	0	178	159
	1-2 to 4-5	1671	14.3	4.8	1	94	127	157	142	12.70	178	159
	5-6 to 7-8	1671	9.5	3.2	2 to 8	89	127	146	142	6.35	178	159

Table 2.3 Dimensions for Standard Trusses

Truss	Web Member Details		Joint Details										
	Member	ℓ_w (mm)	Joint	Dimensions at connections (mm)					Tie plates (mm)	19.05 mm ϕ bolts		Eccentricity (mm)	
				ℓ_a	ℓ_b	ℓ_c	ℓ_d	c		Type	Number	e	e_w
B0	0-1 to 7-8	1736	0	32	57	57	57	0	2 - 76×406×9.5	A 490	16	0	127
			1	32	57	57	57	12.70	2 - 76×406×9.5	A 490	32	0	133
			2 to 5	32	57	57	57	12.70	2 - 76×406×9.5	A 325	32	0	133
			6 to 7	32	76	76	0	12.70	2 - 76×406×9.5	A 325	24	0	133

Table 2.4 Dimensions for Bolted Truss

CHAPTER 3

ANALYTICAL AND COMPUTER MODELLING OF ELASTIC-PLASTIC BEHAVIOUR OF HOLLOW STRUCTURAL SECTION (HSS) TRUSSES

3.1 Introduction

The progressive transition from allowable or working stress approach to a limit states design has been due to a combination of factors which strike at the heart of engineering design - to produce a structure for the least cost with satisfactory performance and a very low probability of failure. Greater understanding by the practicing engineering fraternity of plastic design principles [12, 13], validated by tests [14, 15], has provided a basis for this new design direction.

Some important pioneering work was undertaken in the United Kingdom in the late 1950's and early 1960's. Jennings and Majid [16] developed a computer program to analyse plane frameworks under static loading in the elastic-plastic range by the displacement method. Their analysis focussed on the prediction of load at which moment across a section of a member reaches the plastic moment, thus forming a plastic hinge. The analysis is further limited by neglecting the reduction in the fully plastic moment capacity of a member due to the axial load.

In Canada, Casgoly and Bakht [17] recently proposed a technique to determine the collapse load of steel trusses taking into account the non-linear behaviour of end fixities of members under applied loads.

Although the failure mode due to very large rotation of a joint was considered, no treatment was suggested for the shearing action at a connection and the axial force-bending moment interaction.

The analytical model developed in this study is an extension of the linear elastic plane frame stiffness analysis [18, 19]. An incremental load process is used to compute member forces and joint displacements at various stages of loading hence resulting in a piece-wise linear load-deflection response. This technique uses the elastic-perfectly plastic moment-rotation characteristics. The subsequently developed computer program is limited to stocky members as are manufactured by the Steel Company of Canada (STELCO) (i.e., the width to thickness ratio of the flat plate elements is less than that for which local plate buckling is likely to occur). Furthermore, the overall buckling of members, in the expected range of compressive stress, is unlikely since the slenderness ratio will generally be small and at the same time the occurence of end moments of opposite signs in the truss diagonals will tend to retard the onset of buckling. Therefore, these possible mechanisms of failures have been ignored in the inelastic analysis.

The reduction in plastic moment capacity of the members due to axial forces is taken into account through a bilinear interaction relationship. It is assumed that there is no distinction between the interaction relationships whether the axial forces are in tension or compression. Three types of yield mechanisms are included in the model; two involve the members while the third affects the joints. These are: plastic hinge formation, plastic limit load failure of a member (com-

pression or tension) and the maximum shear force resisted by a chord member at a joint. The member end stress resultants are checked at each load level to establish whether the maximum permitted forces have been exceeded anywhere in the truss and hence an onset of one of the three yield mechanisms above.

The major steps in the analysis are as follows:

1. The global stiffness matrix [K] of the truss is computed by inputing all joint and member details. The loads applied to the truss are incorporated through the load vector {P}. The equilibrium matrix equation $[K]\{x\} = \{P\}$, is solved for the displacements $\{x\}$ and member forces are computed.
2. The elastic range is terminated when either one of the yield conditions occurs; i.e. plastic hinging, axial load limit of members and plastic shearing of joints. The details of yield mechanisms are discussed in later sections.
3. After the most highly stressed section of a member reaches the load-moment limit defined by the interaction relationship, a hinge is then introduced at this section along with the yield moment and the axial force. This, of course, reduces stiffness of the truss while it maintains the load capacities. The next load increment is applied and scaled so as to allow formation of the next hinge at the most highly stressed section. This process is repeated.
4. A check is made to determine whether the truss has undergone excessive deflections or whether a collapse mechanism has formed

due to introduction of the hinges causing deterioration of stiffness. If either one of the above conditions occurs, the truss is deemed to have failed.

The details of the above mentioned steps are described in the following sections. However, a flow chart for the subsequent computer program developed is presented in Figure 3.1.

3.2 Analytical Modelling of Yield Mechanisms

The three types of yield mechanisms proposed are presented below. The overall behaviour beyond the elastic limit of a truss is explained in terms of the interactive formation of the above mentioned yield mechanisms.

3.2.1 Progressive Formation of Plastic Hinges

This yield mechanism is based on a simplified moment-axial force interaction diagram. Below a certain p ratio (P/P_y) of c, the value of m (M/M_p) is 1.0 and reduces to zero linearly for $c < p < 1$. A typical interaction diagram is shown in Fig. 3.2(a) using the member properties, $P_y = \sigma_y A$ and $M_p = \sigma_y Z$, where P_y is the yield load; σ_y, the yield stress; A, the area of member cross section; M_p, the plastic moment capacity and Z is the plastic section modulus.

When the truss is subjected to a loading {P} in the elastic range, each member experiences a different combination of axial force

and bending moment, e.g., point A in Figure 3.2(a). A check is made at both ends of each member to determine which stress point (e.g. point A) would reach the interaction line first. The scaling factor β_{0h}, which designates the ratio of OA to OB for the most highly stressed of the member ends, is given by

$$\beta_{0h} = \frac{1}{\ell_i} \tag{3.1}$$

where ℓ_i = distance OA on the interaction diagram. For the assumed linear elastic behaviour within the first load increment, the loading $\{P_y\}$ that causes the first joint to reach the yield surface is scaled by

$$\{P_y\} = \beta_{0h}\{P\} \tag{3.2}$$

where β_{0h} = minimum value of all β_{0h}'s associated with members in a truss.

The truss is now in the post-elastic range. A hinge, along with the axial force and the bending moment capacities, is introduced which alters the stiffness of the truss. The load $\{P_y\}$ is then incremented by an amount $\beta_{0h}\{P_y\}$ so as to cause occurrence of the second hinge. What load increment and where the second hinge forms are yet to be determined. The analysis is a combination of two load cases; namely case 'a' with $\beta_{1h} = 1.0$ and case 'b' in which a unit moment is applied at the hinge and the internal forces determined are used to set up the constraint equations allowing the axial forces and end moments at the plas-

tic hinges to change and follow the interaction curves. Note the stiffness matrix for both cases 'a' and 'b' is the same thus requiring only one Choleski decomposition during the load increment.

Let us consider a member which has a plastic hinge formed at one of its ends. Since the load is assumed to increase monotonically, the hinge is not expected to return to within its elastic range (i.e. no unloading) and the state of stress (P and M) on it has to move along the yield envelope constrained by the following equation:

$$\frac{P}{P_y} + (1 - c)\frac{M}{M_p} = 1.0 \qquad (3.3)$$

For the analysis undertaken in this investigation, a value of c = 0.15 has been used throughout. This value is consistent with the analytical interaction curves developed for square and rectangular hollow sections [20].

When case 'a' has been carried out for the truss in the post-elastic range, moment at the hinge is zero while the associated axial forces in the members change. In order for a member end, which has a plastic hinge formed, to satisfy the constraint Equation (3.3), case 'b' with a unit moment applied at the hinge is employed to determine the actual incremental limit moment which when combined with case 'a' yields the correct proportions of axial force and bending moment increments. This superposition holds only within a load increment because a linear elastic behaviour has been assumed until the next hinge formation.

Therefore,

$$\{\Delta P\}^k = \beta_{kh}\{\Delta P_y{}^1\}^k + \{\Delta P_y{}^2\}^k \qquad (3.4)$$

and

$$\{\Delta P_y{}^2\}^k = \Delta M_{pj}{}^k \{f\}_j^k \qquad (3.5)$$

where $\{\Delta P\}^k$ = axial force increment due the k^{th} load increment = $\beta_{kh}\{P\}^k$

$\{\Delta P_y{}^1\}^k$ = axial force increments due to $\beta_{kh} = 1.0$ and zero moments at the hinges (case 'a')

$\{\Delta P_y{}^2\}^k$ = axial force increments due to the incremental limit moments applied at the hinges

$\Delta M_{pj}{}^k$ = incremental limit moment at the j^{th} hinge during the k^{th} load increment

$\{f\}_j^k$ = axial forces in the members due to a unit moment at the j^{th} hinge

β_{kh} = load increment factor due to formation of the next hinge.

From Equation (3.3), the change in P/P_y with respect to M/M_p is given by:

$$\frac{\Delta P}{P_y} = (c - 1) \frac{\Delta M_p}{M_p} . \qquad (3.6)$$

Equation (3.6) is substituted into Equation (3.4) so that the yield surface constraint can be satisfied. For example, when the first hinge forms at one of the ends of member 'n',

$$\beta_{1h} \Delta P_{yn}^{1} + \Delta M_{p1}^{1} f_{n1}^{1} = (c - 1) \left(\frac{P_y}{M_p}\right)_n \Delta M_{p1}^{1} \qquad (3.7)$$

Therefore

$$\Delta M_{p1}^{1} = \frac{-\beta_{1h} \Delta P_{yn}^{1}}{\left(f_{n1}^{1} + (1 - c) \left(\frac{P_y}{M_p}\right)_n\right)} \qquad (3.8)$$

Although $\beta_{1h} = 1.0$ is used in case 'a', the actual proportion that causes the next hinge to form is not yet known. Once the incremental moment has been obtained, the incremental forces for all members can be readily calculated.

$$\{\Delta P\}^k = \beta_{kh} \{\Delta P_y^{1}\}^k + \Delta M_{pj}^{k} \{f\}_j^k$$

$$\{\Delta M^L\}^k = \{\Delta M_y^{L1}\}^k + \Delta M_{pj}^{k} \{\rho^L\}_j^k \qquad (3.9)$$

$$\{\Delta M^G\}^k = \{\Delta M_y^{G1}\}^k + \Delta M_{pj}^{k} \{\rho^G\}_j^k$$

where $\{\Delta M_y^{L1}\}$ = bending moment increments at ends 'L' of members due to load increment and zero moment at hinges

$\{\Delta M_y^{G1}\}$ = bending moment increments at ends 'G' of members due to load increment and zero moment at hinges

ρ_{ij}^{Lk} = bending moment at end 'L' of i^{th} member due to unit moment at hinge 'j' for the k^{th} load increment

ρ_{ij}^{Gk} = bending moment at end 'G' of i^{th} member due to unit moment at hinge 'j', for the k^{th} load increment.

For the above cited example where the first hinge is formed at the end of member 'n', the following force increments for member 'n' are obtained from Equations (3.9) where

$$\Delta P_n^1 = \beta_{1h}\Delta P_{yn}^1 + \Delta M_{p1}^1 f_{n1}^1$$

$$\Delta M_n^{L1} = \Delta M_{yn}^{L1} + \Delta M_{p1}^1 \rho_{n1}^{L1} \qquad (3.10)$$

$$\Delta M_n^{G1} = \Delta M_{yn}^{G1} + \Delta M_{p1}^1 \rho_{n1}^{G1}$$

The force increments for all members from Equations (3.9) are then added to the forces from the last increment (points A) to arrive at the new positions (points C) on the m-p interaction diagram, as illustrated in Fig. 3.2(b). The loading paths for all members are different in general because of different internal forces. Due to the k^{th} load increment and for $\beta_{kh} = 1.0$ initially, some member ends may very well be

within the elastic range and others superficially past the elastic range, point C for each loading path in Figure 3.2(b). However, the load increment factor β_{kh} is determined by searching for a member end where the next hinge forms with previously formed hinges, points B, moving along the yield constraint line to points B'. Thus all those sections without the hinges, are brought back to within the elastic range, points C'. Therefore, the appropriate β_{kh} is the smallest of the β_{kh}'s determined for the member ends. The factor β_{kh} for the i^{th} member is computed by:

$$\beta_{kh}^{i} = \left| \frac{\alpha_i^k - 1}{\alpha_i^k - \alpha_i^{k-1}} \right| \qquad (3.11)$$

where

$$\alpha_i^k = \left(\frac{P}{P_y}\right)^k + (1 - c) \left(\frac{M}{M_p}_i\right)^k$$

Note that for the i^{th} member, β_{kh}^{i} is the lower of the values determined for the two ends, of course, deleting the end which already has a hinge formed. It is of interest to note that point C for a member, which is the farthest away, i.e. $\alpha_{i\ max}^{k}$, does not necessarily govern the load increment factor β_{kh}.

We can now generalize the approach mentioned above in the following manner.

Suppose, prior to the k^{th} load increment and before the next hinge is formed, there are 't' hinges formed in the structure. Equation (3.7) can be generalized to the following set of 't' linear equations with ΔM^k_{pj}, the incremental limit moments as the unknowns.

$$\left(f^k_{ij} + (1 - c)\left(\frac{P_y}{M_p}\right)_i \delta_{ij}\right) \Delta M^k_{pj} = -\beta_{kh} \Delta P^k_{yi} \qquad (3.12)$$

where i = member with hinges, j = hinge member and δ_{ij} is the Kronecker delta.

Again, β_{kh} can be treated as unity and scaled later. The analysis is as before divided into two load cases; case 'a' involves determining the axial force increments $\{\Delta P^1_y\}^k$ due to $\beta_{kh} = 1.0$ with 't' plastic hinges introduced in the structure, and case 'b' involves applying a unit moment at each of 't' hinges, one at a time to determine $\{f\}^k_j$, $\{\rho^L\}^k_j$ and $\{\rho^G\}^k_j$.

Equation (3.12) is solved for ΔM^k_{pj} with $\beta_{kh} = 1.0$, then scaled using Equation (3.11) and substituted into Equations (3.9) to obtain the internal force increments $\{\Delta P\}^k$, $\{\Delta M^L\}^k$ and $\{\Delta M^G\}^k$.

$$\{\Delta P\}^k = \beta_{kh}\{\Delta P^1_y\} + \beta_{kh}\Delta M_{pj}{}^k \{f\}^k_j$$

$$\{\Delta M^{L}\}^{k} = \beta_{kh}\{\Delta M_{y}^{L1}\}^{k} + \beta_{kh}\,\Delta M_{pj}{}^{k}\,\{\rho^{L}\}_{j}^{k} \qquad (3.13)$$

$$\{\Delta M^{G}\}^{k} = \beta_{kh}\{\Delta M^{G1}{}_{y}\}^{k} + \beta_{kh}\,\Delta M_{pj}{}^{k}\{\rho^{G}\}_{j}^{k}$$

These values are then added to the corresponding internal forces obtained after the $(k-1)^{th}$ increment, i.e.

$$\{P\}^{k} = \{P\}^{k-1} + \{\Delta P\}^{k}.$$

$$\{M^{L}\}^{k} = \{M^{L}\}^{k-1} + \{\Delta M^{L}\}^{k} \qquad (3.14)$$

$$\{M^{G}\}^{k} = \{M^{G}\}^{k-1} + \{\Delta M^{G}\}^{k}.$$

It should be pointed out that when a member has axial force less than the value of cP_y its moment capacity is assumed to be M_p and a hinge along with M_p is introduced at its end. The constraint Equation (3.12) is not applicable in this range since P/P_y and M/M_p are independent of each other. When there is a hinge at one end of a member and a new hinge is about to form at the other end of the same member, the member will have the same ratio for $(M/M_p)_i$ at both ends and the two points will coincide on the yield limit line.

3.2.2 Plastic Limit Load Failure of a Member

This type of localized failure is also based on the simplified m-p interaction diagram illustrated in Fig. 3.2(a). As the loading on

the truss increases, axial force in all members will increase accordingly except when a joint failure by shear occurs. If a second hinge has already formed at the other end of a member, the points describing P/P_y and M/M_p at the two ends will coincide on the yield surface (Figure 3.2(b)). Hence, during the load increment, the two will move together. In the case where P/P_y reaches unity, this member must be removed and replaced by the axial load capacity P_y at the end joints. The overall stiffness of the truss, therefore, decreases due to the equivalent loss of this member. The incremental load factor β_{km} for member removal has to be determined before either the formation of the next hinge elsewhere in the truss or yielding of a shear spring described in the next subsection. This factor is calculated for increasing axial load in the i^{th} member in the following manner.

$$\beta_{km}^{i} = \left(\frac{P}{P_y}\right)_i \tag{3.15}$$

Again smallest of β_{km}^{i} governs and gives the load increment $\beta_{km}\{P_y\}$ at which the corresponding member must be removed.

3.2.3 Modelling of Shear Behaviour at Connections

The shear behaviour of a connection is modelled by incorporating an elastic-plastic shear spring which connects two neighbouring joints (Figure 3.3(a)) at the centerline of a connection. These two joints have the same coordinates, the same displacement along the chord and the same rotation. The spring has the stiffness and strength characteris-

tics which simulate shearing action of the chord portion of the connection between intersections of centerlines of the diagonals with the chord centerline. A sketch of the shear spring model and the neighbouring arrangement are given in Fig. 3.3(a). The properties of the shear spring depend on the properties of the connection which include the maximum allowable shear force and the allowable displacement.

In the case of the standard K-connections, the distribution of shear forces across the critical section by the inner and outer webs of the chord members is different. This is due to the inefficient transfer of forces across the flanges of the chord members. The inner webs resist larger proportions of the shear forces than the outer webs at the same load level. For analytical modelling, the inner webs are assumed to be 100% effective while the outer webs' effectiveness is a prescribed fraction of the former. This ratio is estimated by comparing the maximum shear strains at the outer and inner webs at loads initiating yielding and causing a possible failure. The combined effect of the outer and inner webs as illustrated by the force-displacement relationship for the shear spring, is shown in Fig. 3.3(b).

In the case of a double chord rectangular hollow section, the area provided to resist shear is

$$A_w = \kappa h_0 t_0 \qquad (3.16)$$

where h_0 = height of the section

t_0 = the web thickness

and κ = a constant that depends on the type of double chord gap joint (see Table 3.1).

In the case of the back-to-back connection, all four webs are effective in resisting shear and therefore κ is taken as 4.0. On the other hand the outer webs of the standard connection are much less effective and their contribution depends on joint eccentricity, i.e. the gap spacing bewtween the diagonal members. This configuration lowers the value of κ to reflect the actual contribution of all four webs.

Where a stiffening plate is used, as for a back-to-back connection, a parabolic shear stress distribution through the thickness may be assumed. As such, the equivalent area of plate that resists shear is

$$A_s = \frac{2}{3} b_s t_s \tag{3.17}$$

where b_s = the width of stiffener t_s = the thickness of stiffener. Therefore, the fully plastic shear force V_p as given by the Von Mises yield criterion in a rectangular hollow section [21] with a stiffening plate is

$$V_p = \frac{\sigma_y}{\sqrt{3}} (A_w + A_s) = \frac{\sigma_y}{\sqrt{3}} \left[\kappa h_0 t_0 + \frac{2}{3} b_s t_s\right] \tag{3.18}$$

The assumption of an elastic response for shear stress versus shear strain up to V_p provides a basis for calculating the relative displacement [illegible] connection prior to yielding. It is, therefore,

given by

$$\Delta_c = \gamma_y \ell_c = \frac{\tau_y \ell_c}{G} \tag{3.19}$$

where ℓ_c = length of a short member on either side of the shear spring

γ_y = shear strain when yield just begins

τ_y = yield stress in shear

G = shear modulus of elasticity.

The shear spring stiffness k_{sp} is then given by

$$k_{sp} = \frac{V_p}{\Delta_c} = \left(\kappa h_0 t_0 + \frac{2}{3} b_s t_s\right) \frac{G}{\ell_c} \tag{3.20}$$

Since the shear spring member has degrees of freedom only in the y-direction, the member stiffness matrix to be incorporated into the computer program is given by

$$[k]_{sp} = \begin{bmatrix} 0 & 0 & 0 & 0 & 0 & 0 \\ 0 & k_{sp} & 0 & 0 & -k_{sp} & 0 \\ 0 & 0 & 0 & 0 & 0 & 0 \\ 0 & 0 & 0 & 0 & 0 & 0 \\ 0 & -k_{sp} & 0 & 0 & k_{sp} & 0 \\ 0 & 0 & 0 & 0 & 0 & 0 \end{bmatrix}$$

Note that there are three degrees of freedom (two translations and one rotation) at each joint (Figure 3.3(a)) while only the degrees of freedom that correspond to the y-direction have non-zero entries in $[k]_{sp}$. It is assumed that the combined action of a diagonal member in tension and the other in compression at a connection produces shear force in the spring. Axial forces and bending moments were not observed to be as important for the 63.4° angle for the diagonals tested. Therefore, for simplicity, these effects are neglected and the vertical displacements of the shear spring, gives the relative displacement at the ends of the web members. The shear force V at a given joint is given by the linear force-relative displacement relationship as

$$V = k_{sp} \Delta_c \tag{3.21}$$

where k_{sp} = stiffness of shear spring, and Δ_c = relative displacement of shear spring. A check is necessary in order to determine where a shear spring has reached the elastic limit, i.e. $V = V_p$. This is accomplished in the following manner.

When the i^{th} shear spring experiences the k^{th} load increment, the increase in shear force required to cause yielding is given by

$$\Delta V_i^k = V_{pi} - V_i^{k-1} \tag{3.22}$$

where V_i^{k-1} = shear force in the i^{th} spring at the $(k-1)^{th}$ load increment and V_{pi} = fully plastic shear force for the i^{th} shear spring. The

load factor β_{ks}^{i} that would cause yielding of the i^{th} shear spring is therefore given by

$$\beta_{ks}^{i} = \frac{\Delta V_i^k}{\Delta V_{il}^k} \tag{3.23}$$

where ΔV_{il}^k = the change in shear force in the i^{th} spring at the k^{th} load increment when $\beta_{ks} = 1.0$. The shear spring with the smallest β_{ks} governs the next load increment which will cause yielding of this spring. Of course, it must be compared with the smallest β_{kh} value for the possible next hinge formation and the smallest β_{km} value for member removal.

3.2.4 Summary

The three types of mechanisms have been discussed and either one of them can control the next load increment $\beta_k\{P_y\}$. There may be a number of hinges about to be formed, members reaching P_y to be removed and also certain number of shear springs about to be yielding. This may occur at different levels of load increments. Hence, to determine the correct β_k, the smallest of the individually determined smallest β_{kh}, β_{km} and β_{ks} for hinge formation, member removal and shear spring yielding respectively, governs.

The flow chart for the computer program developed is shown in Fig. 3.1. The three types of yield mechanisms are incorporated which

can cause localized failures while the truss can fail either due to excessive deflection or formation of an overall mechanism.

3.3 Modelling of Various Trusses

Different arrangements of joints and members of the trusses can greatly enhance their behaviour under various loadings. With reference to their properties, the simulation model for each truss to be analyzed by the compter program is presented in the following sections.

All chord and diagaonal members were taken as rigidly connected and hence referred to as the "Fix-Fix" type. For best simulation of the rigid connections as in the case of gusset plates and overlapped joints, small rigid members of cross-sectional area and moment of inertia of 7000 mm^2 and 4.2×10^8 mm^4 were used, respectively. The value of area chosen was the average of chord and web members while the moment of inertia was about fifteen times that of the chord member.

3.3.1 Back-to-Back Truss BBST

A shear spring was incorporated at the joints of this truss to reflect the influence of a 19.05 mm stiffening plate. Therefore, higher V_p and k_{sp} values were obtained than was the case when the stiffening plates were omitted. The values can be determined from Equation (3.18) and Equation (3.20), respectively. In addition, short rigid members were used to account for the positive eccentricity that occurs at the connections which join the main diagonal and chord members to the shear

spring joints.

Loads were applied to the top eight panel points with half of each joint load on each of the shear spring joints as indicated in Fig. 3.4. The intra-joint member dimensions are also shown.

3.3.2 Back-to-Back Truss BBOV

A system of small rigid members were incorporated at the joints to simulate rigid connections that result from overlapping the ends of the diagonal members. No shear springs were used in these connections.

Loading was to act on the middle joints of the rigid connections on the top panel points. These arrangements are shown in Fig. 3.5.

3.3.3 Standard Trusses S1 and S2

Shear springs were incorporated at the connections of these types of trusses to simulate joint behaviour as in the case of Truss BBST. The V_p and k_{sp} values computed for each truss are shown in Table 3.1. Short rigid members were also used to connect the diagonal and chord members to the shear spring joints.

Loading was applied as before to the top panel points (half on each side of the shear spring). The details are illustrated in Fig. 3.6.

3.3.4 Bolted Truss BO

A system of small rigid members was incorporated at the joints to reflect the influence of the gusset plates in providing additional rigidity. No shear springs were used in these connections. Figure 3.7 shows the loading and small member dimensions assumed for this case.

A table that summarizes all of the computer program input characteristics for the original trusses appears in Table 3.1.

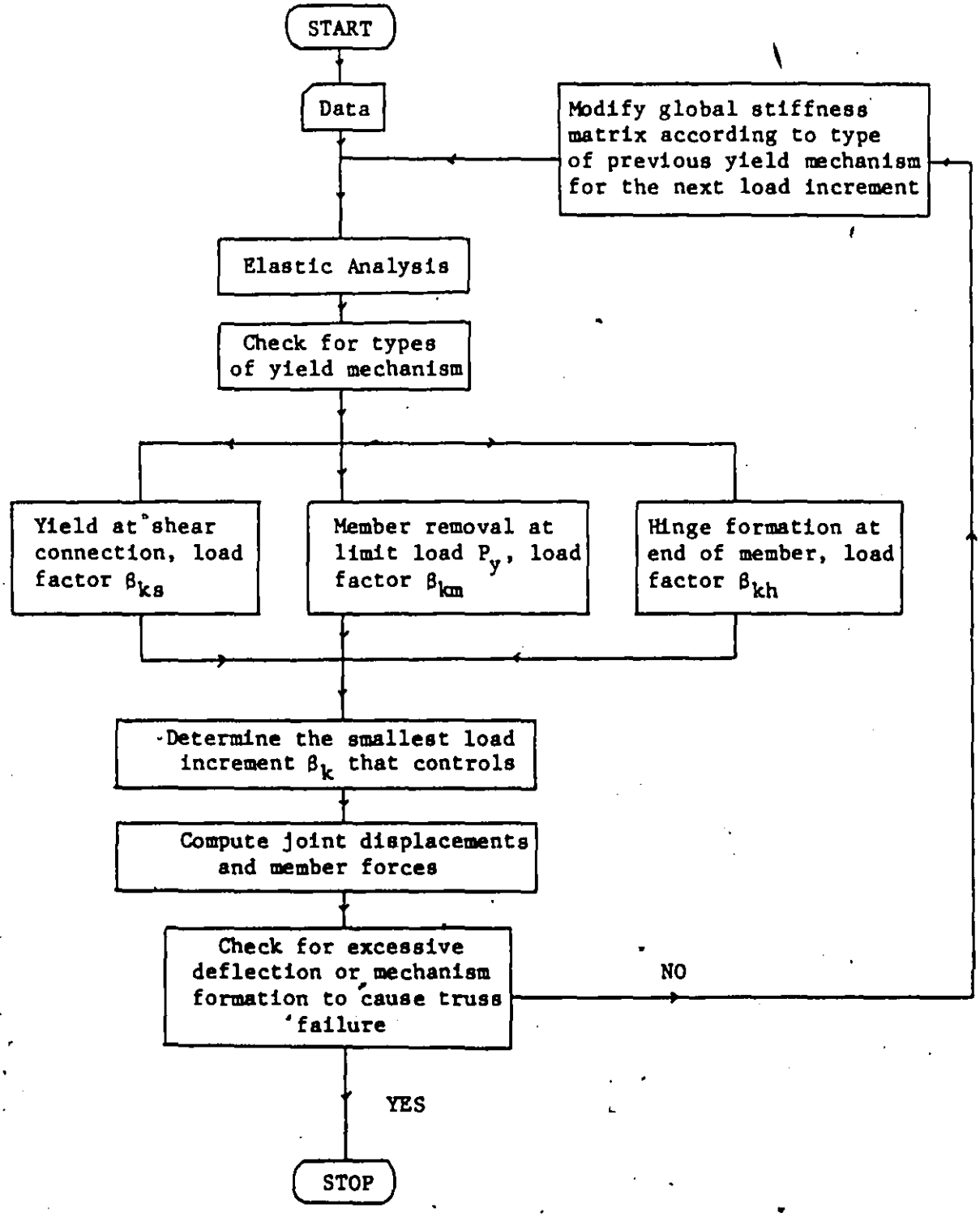

Figure 3.1 Flow Diagram for the Computer Program to Perform the Elastic-Plastic Analysis

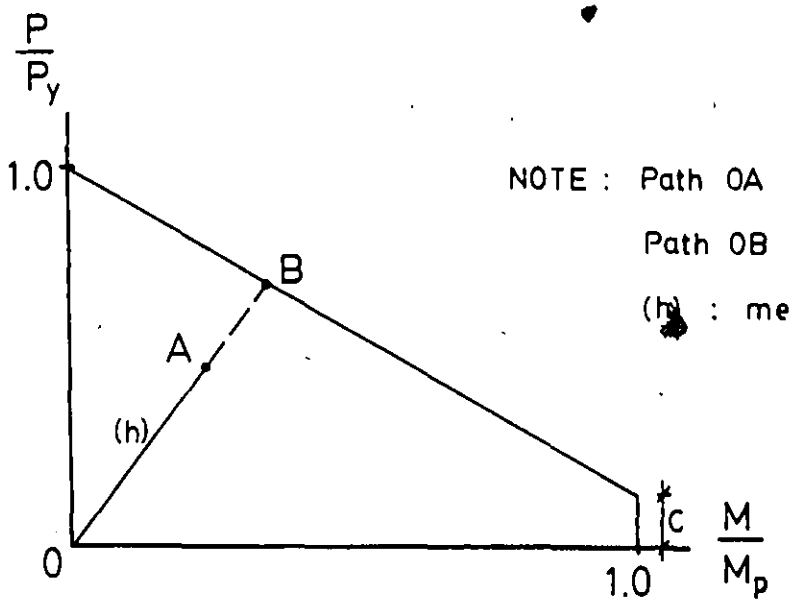

FIGURE 3.2(a) TYPICAL m-p INTERACTION DIAGRAM

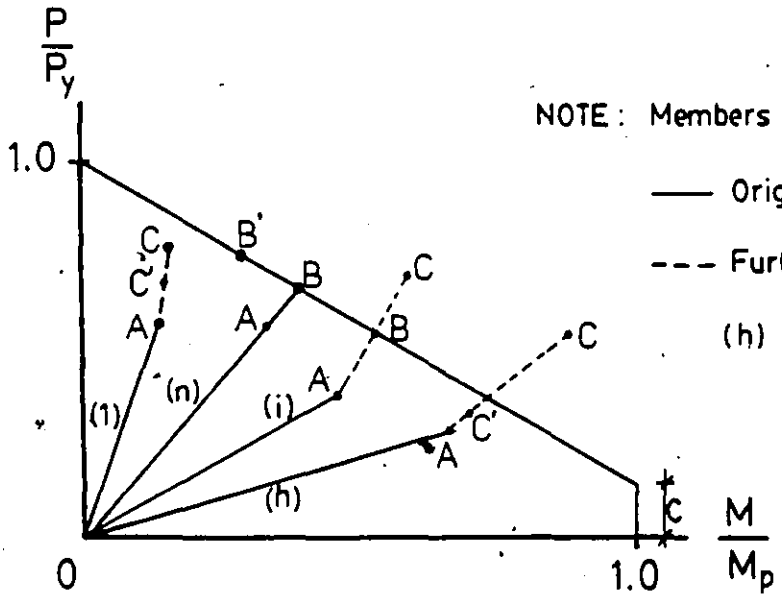

FIGURE 3.2(b) BEHAVIOUR OF ALL MEMBERS FOR FURTHER LOADING

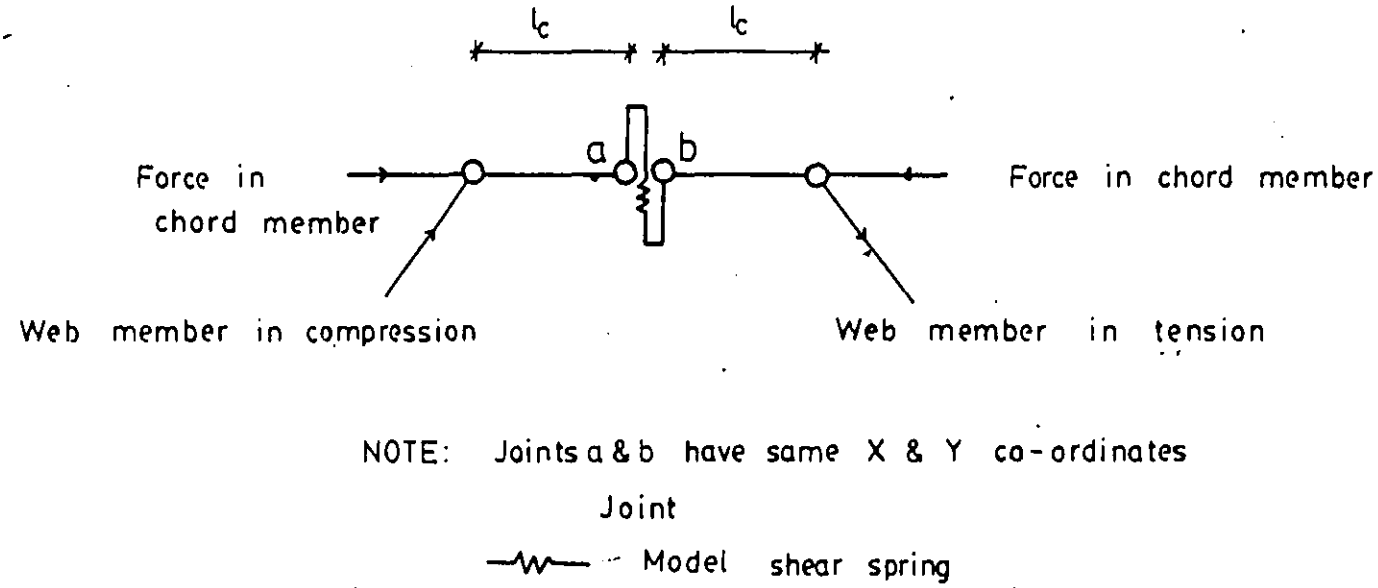

FIGURE 3.3 (a) ARRANGEMENTS OF SHEAR SPRING AND JOINTS AT CONNECTION

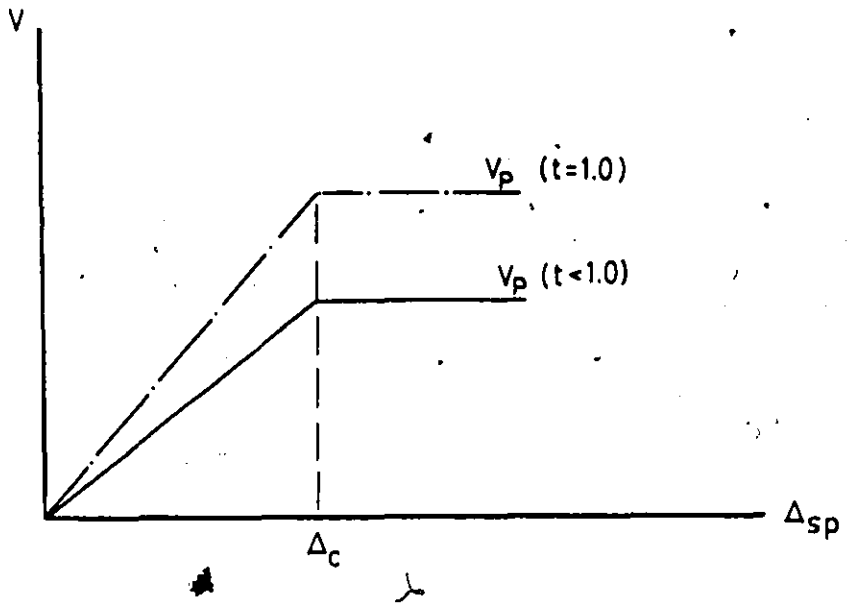

FIGURE 3.3 (b) FORCE - DISPLACEMENT RELATIONSHIP IN SHEAR SPRING

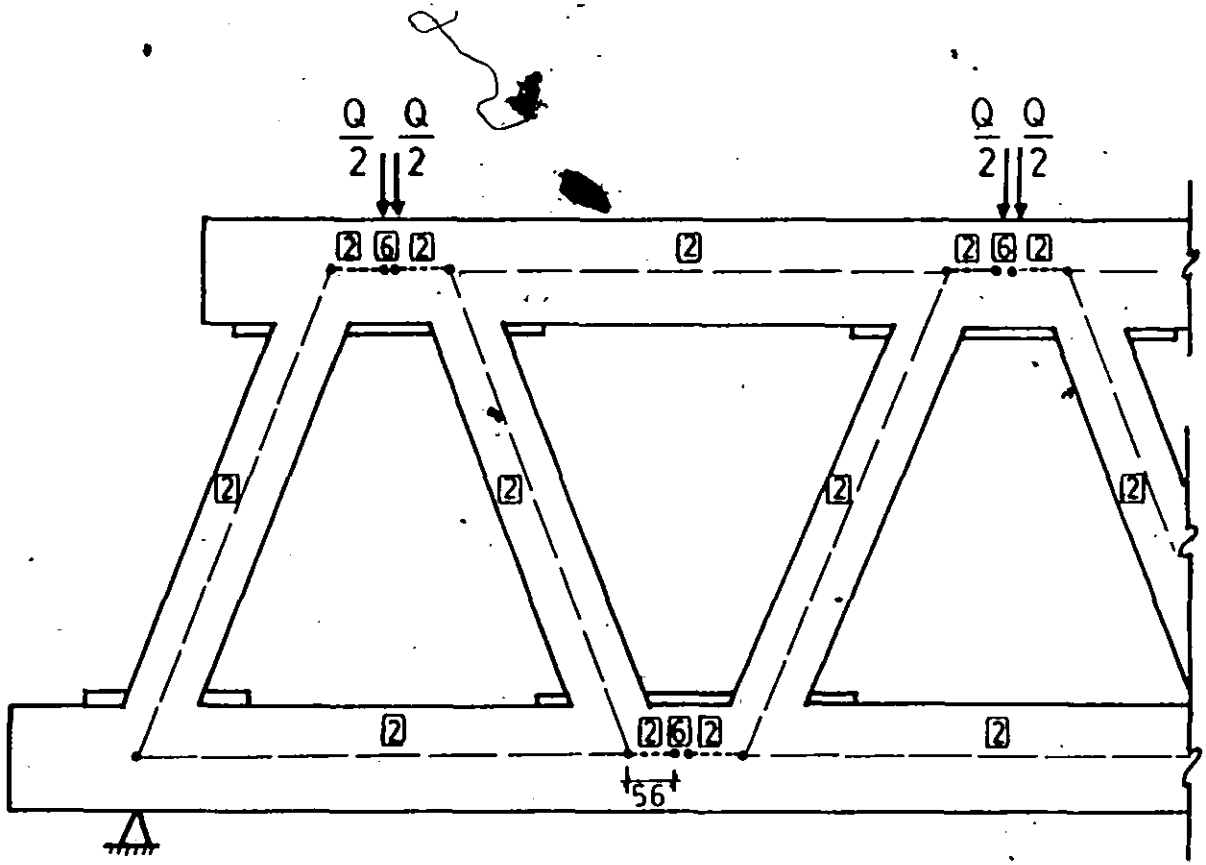

LEGEND: Q - Joint load

[2] - Member type 2 ; FIX - FIX

[6] - Member type 6 ; SHEAR SPRING

• - Joint

Dimensions in mm.

FIGURE 3.4 ARRANGEMENTS OF JOINTS & MEMBERS IN TRUSS BBST

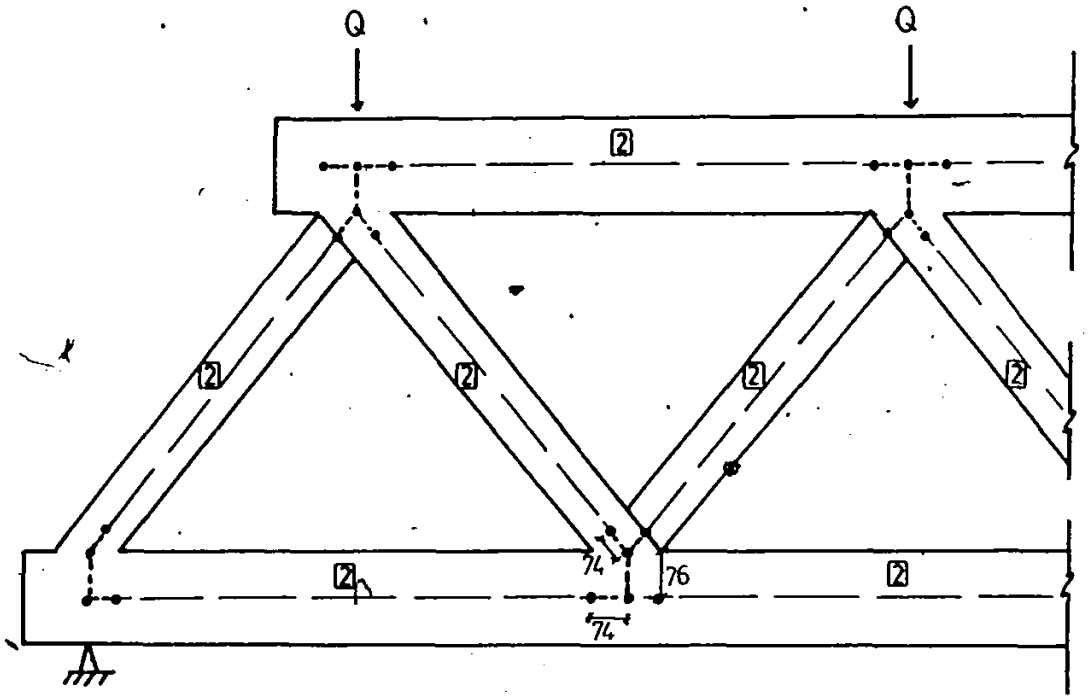

LEGEND : Q - Joint load

2 - Member type 2 ; FIX - FIX

-- - Small rigid member

• - Joint

Dimensions in mm.

FIGURE 3.5 ARRANGEMENTS OF JOINTS & MEMBERS IN TRUSS BBOV

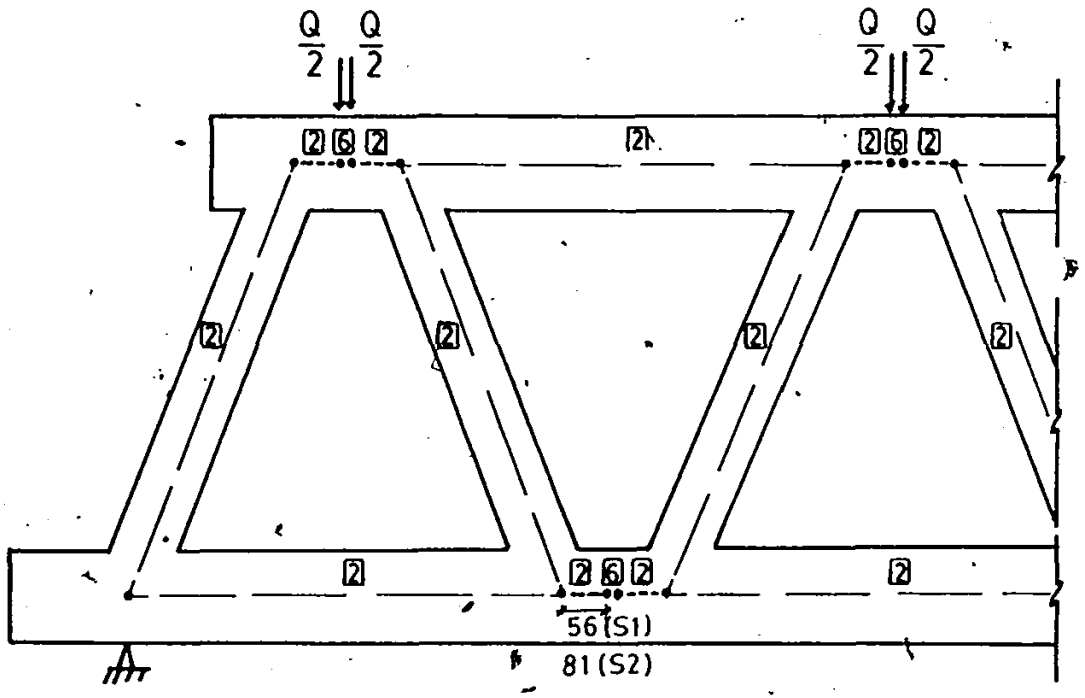

LEGEND : Q - Joint load

2 - Member type 2 ; FIX - FIX

6 - Member type 6 ; SHEAR SPRING

• - Joint

Dimensions in mm.

FIGURE 3.6 ARRANGEMENTS OF JOINTS & MEMBERS IN STANDARD TRUSS

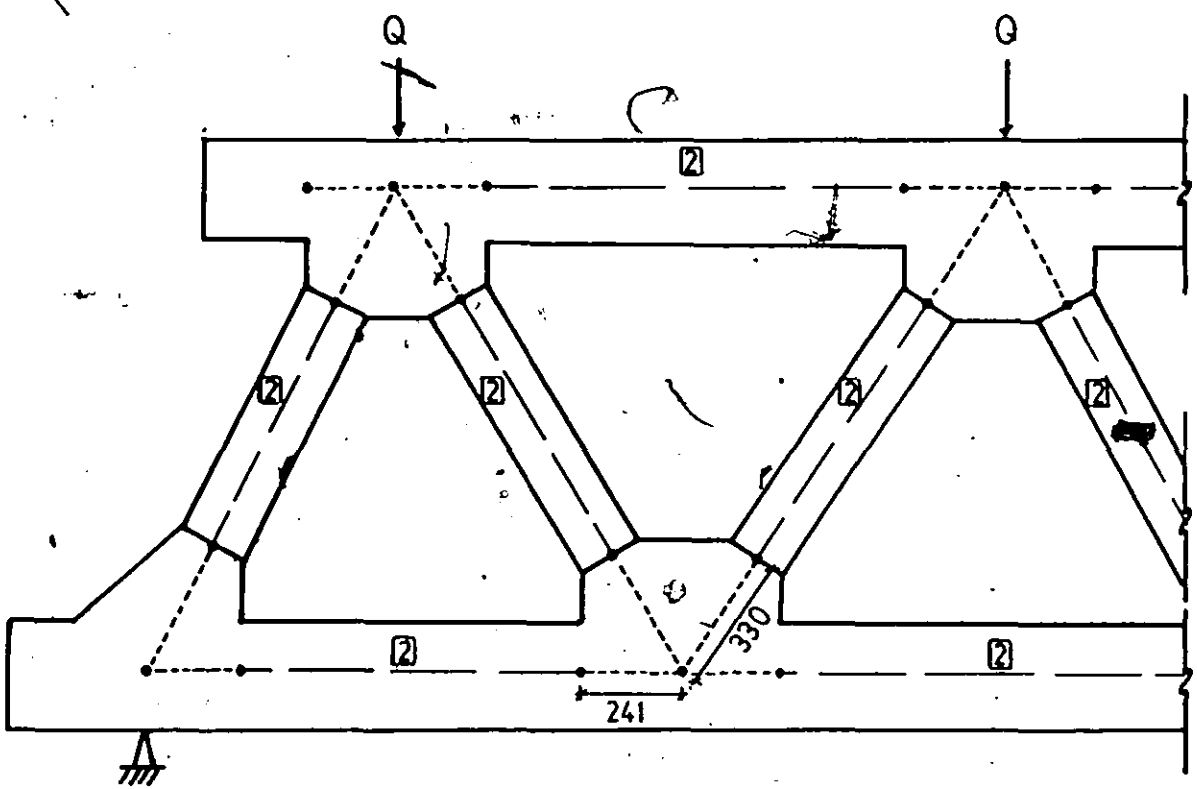

LEGEND : Q - Joint load

2 - Member type 2 ; FIX - FIX

--- - Small rigid member

• - Joint

Dimensions in mm

FIGURE 3.7 ARRANGEMENTS OF JOINTS & MEMBERS IN TRUSS B0

Truss	σ_y + (MPa).	κ †	V_p(kN)	k_{sp}(kN/mm)
BBST*	394.9	4.00	1691.6	10104.0
BBOV	401.2	4.00	896.6	N/A
S1	370.3	2.60	537.9	3426.3
S2	390.1	2.88	627.7	2494.1
BO	374.2	4.00	836.8	N/A

* Equivalent area of plate that resists shear, A_s = 3543.3 mm^2.

\+ Yield stress for chord member obtained from tensile tests.

† κ values were obtained from truss test strain rosette measurements (Chapter 2).

Table 3.1 Computer Program Input Characteristics for Various Trusses

CHAPTER 4

RESULTS OF EXPERIMENT AND ANALYSIS

In reporting the experimental and the analytical results, the forces, reinforcing, hinge formation and strains reported for various members should also be interpreted for their symmetric parts.

4.1 Back-to-Back Trusses

In testing, increments of 90 kN were applied on each of the two jacks up to the elastic limit while readings of strain gauges and rosettes were taken. These increments were reduced substantially after pronounced yielding or joint shearing was observed.

4.1.1 Truss BBST

For this truss possessing gap joints and stiffening plates, failure occurred by combined local and overall buckling of the top chord member at center span (member 7-7 in Fig. 2.1) at a total load of 2535 kN. The failure mode is shown by the photograph in Fig. 4.1(a).

Table 4.1 shows the ratio of the applied load to truss failure load when yielding was observed to occur at the extreme fibres of various critical members. It is evident that yielding of the extreme fibres at joint 2 of member 2-3 had begun when the applied load was 52% of the failure load. This compares to a predicted value of 64% from the analy-

tical solution. Somewhat later, joint 1 of members 1-2 and then 0-1 yielded when the applied loading was 64% and 85% of the failure load respectively. These values compare with computed values of 60% and 73%.

Despite early yielding, the presence of stiffening plates significantly stiffened and strengthed the connections. As a consequence, the truss was able to resist additional loading before excessive plastification caused ultimate failure. To provide an indication of the joint deformations occuring during load application, strain rosettes mounted along the centerline of the connection on the chord web faces were used to determine maximum shear stresses. Because of the large amount of data so obtained, this information is contained in Appendix II. As observed from load-shear strain curves for connections 1 and 2, the maximum shear strain developed was 1.2 times the yield strain, i.e. 3400×10^{-6} mm/mm. This value is small when compared with the results from other joint types. Evidently, the stiffening plates played an important role in transferring large portions of shear forces from one web member to the other.

The experimental and analytical vertical displacement curves for the mid-span top chord deflection are shown in Fig. 4.2. The experimental curve begins to deviate from the analytical curve when the total load on the truss reaches about 1650 kN. This is due to yielding that occurred in the actual truss. It is evident as well that at a load of 1646 kN, formation of plastic hinge at the higher stressed end (Joint 1) of member 1-2 takes place but does not result in a major loss in stiff

ness. The same phenomenon occurs for members 2-3 and 0-1 at total loads of 1779 kN and 2019 kN, respectively. Failure is predicted to occur at 2575 kN, which is 1.6% higher than the experimental value. Twenty-eight plastic hinges were predicted to have formed thus leading to formation of a mechanism. The sequence of hinge formation is illustrated in the load-deflection curves in Fig. 4.3. Failure of member 2-3, however, is observed when the loading reaches 2553 kN and results in pronounced loss of stiffness. The analytical curve then is seen to more closely approximate the experimental curve.

In order to determine how well the analytical model predicts member forces during loading, strain gauge measurements taken near the ends of members framing into their respective joints have been used. Appendix III gives theoretically derived relationships for moment-curvature-axial force applied to "prismatic" members. Therefore, at a prescribed point at which strain gauge readings were taken, the strain gradient through the thickness and the average strain can be computed and used to determine the axial force and moment at that section. The bending moment so obtained is considered to be an experimental quantity.

The load-moment curves from both the experimental results and the analytical solution as found for the most highly stressed locations are shown in Fig. 4.4 to Fig. 4.7 inclusive. It is noted that as the loading on the truss increases, the analytical solution gives a general moment reduction pattern for those members which have plastic hinges formed at the ends. Similar behaviour is observed from the experimental

curves thus confirming the trends exhibited by the analytical solution. It is noted that the actual bending moments are lower than those predicted by the analytical solution for ends of members 0-1 and 1-2. This is likely due to a combination of factors -- partial moment release at the junctions with the stiffening plates and a localized stress distribution that may not be linear in the neighbourhood of the joint in the actual structure. However, there is good agreement between analytical and experimental moments for the other joints. More refined modelling of the behaviour of connections would perhaps provide better correlation between the experimental and analytical results.

4.1.2 Truss BBOV

An inadequate design detail was detected at the end supports of this truss during testing. It was observed that crippling of the two middle webs of the bottom chord members was occurring at the ends. The reason is simply insufficient web areas needed to resist force from the end diagonals (0-1) and reaction from the support. The truss was, therefore, unloaded after reaching a load of 2224 kN when crippling of the chord webs began. Since the objective was to determine the overall capacity rather than a local failure, wooden blocks were installed in the ends of the bottom chord member. This permitted improved transfer of forces from the diagonal member to the support, thus avoiding a local failure. In future design detailing, a stiffening plate similar to that for Truss BBST at joint 0 would help to distribute the end diagonal forces to four webs and alleviate the problem. After making the necessary adjustments the truss was re-loaded. The strain gauges indicated

that loading proceeded very closely to the unloading line. As such, the load deformation relationships were based on the original loading curves assumed to continue in the re-test after reaching the previous maximum load. In this case, failure took place at a total load of 2553 kN. The mode of failure was combined local and overall buckling of the center top chord member (member 7-7) as shown in the photograph of Fig. 4.1(b). The experimental and analytical vertical displacement curves for the mid-span are shown in Figs. 4.8 and 4.9.

It is evident that the analytical model gives a good prediction of load-deflection relationships up to the elastic limit of 2376 kN. There is subsequently a progressive formation of plastic hinges at various locations until members 7-7 and 6-8 reach their load carrying capacities. This occurs at a total load of about 2670 kN. The loss of these members greatly reduces the overall stiffness and leads to the formation of four other plastic hinges thus leading to the failure of the truss at 2687 kN due to excessive deflection. The criterion used for deflection was five times the elastic limit value. A larger mid-span deflection is not only excessive from the viewpoint of serviceability but also violates assumption of the original geometry being employed for the analysis. The analytical solution predicts a total of sixteen plastic hinges with a failure of three members. The failure load of 2687 kN is 5.2% higher than the experimental value which is considered to be in excellent agreement.

From Table 4.2 which shows the ratio of applied load to truss failure load for yielding at extreme fibres of various members, it is

noted that the center of member 7-7 starts to yield when the loading on the truss reaches 87% of the experimental failure load. This compares to 93% for the analytical solution. All other members remain elastic up to truss failure load except member 0-1 which has just started to yield. The partial overlapping of web members at the connection here tended to reduce the bending moment at the ends of the members which consequently led to higher yielding loads as compared to the previous Truss BBST.

Using the m-ϕ-p interaction curves for the critical members, presented in Appendix IV, the load-moment curves from the experimental results and the analytical solutions for the most highly stressed location are shown in Fig. 4.10 to Fig. 4.13. There is reasonable correlation between the experimental and analytical results for all connections, except for member 1-2 at joint 1. Analytically, a complete loss of moment resistance is predicted for both ends of the mid-span top chord member (due to hinges forming) at failure whereas experimentally this did not happen. Furthermore, yielding of member 7-7 occurs under a total load of 2652 kN versus the experimental value of 2553 kN.

The m-p interaction diagram was introduced in Chapter 3, it would be appropriate to further investigate the behaviour of various members under end loadings. From the strain gauges mounted along the members, it is possible to determine the relationship between axial force and bending moments at the member ends. These values for members 0-1 and 1-2 are plotted along with the analytically determined values as shown in Fig. 4.14 and Fig. 4.15 for Truss BBST and Fig. 4.16 and

Fig. 4.17 for Truss BBOV. A better correlation is observed for the experimental and analytical curves for Truss BBOV while the deviation for Truss BBST follows the same reasoning as has been explained in the previous section.

A summary of both the experimental and the analytical results for the two Back-to-Back trusses is presented in Table 4.3. Close correspondence between experimental and analytical failure loads is evident except for the failure mode differences. It is expected because the analytical model excludes a check on buckling of members. Repair and retesting were not undertaken for these trusses because major failure of the top chord occurred for both cases. This precluded the possibility of retesting trusses exhibiting properties consistent with the original trusses.

4.2 Standard Trusses

The load increments used for these trusses were similar to those used for the Back-to-Back cases, i.e., load was applied in 90 kN increments and then reduced as yielding progressed. Results for the two standard type trusses are discussed separately in the following subsections.

4.2.1 Truss S1

There are two features of this truss different from those of Truss S2. Firstly, the diagonal ends were angle cut in Truss S1 which

permitted a smaller eccentricity than that of Truss S2. Secondly, the chord ends for Truss S1 were open, while for Truss S2, the top chord ends were capped. The reason for end capping for Truss S2 was due to observed premature failure of Truss S1.

During testing, when Truss S1 was being loaded beyond 1710 kN (where readings were taken), a sudden failure occurred at a load of 1727 kN with a middle span deflection of about 70 mm. On examination it was found that one of the chord end connections (joint 1) had failed by shearing and large end twisting. In fact, due to shearing action a rupture occurred in the chord's inner webs. This failure mode is shown in Fig. 4.18. Significant distortion of corresponding joint 1' had also developed on the right hand side of line of symmetry.

This premature joint failure is evident from Table 4.4 where only the extreme fibres of member 0-1 at joint 0 start to yield at 97% of the experimental failure load. The other members are still within the elastic range when truss failure occurs. These results predict higher yielding values as compared to the analytical solution.

After testing, the rosette readings for shear strains across the critical section at joint 1 were analyzed. It was found that the shear strains developed in the inner webs of the chord members were much larger than those in the outer webs. The difference in shear strains increased from about three in the elastic range to more than ten times when the last readings were recorded. This suggests that the outer webs were much less effective than the inner webs in resisting shear. The

plots for load versus strains are given in Fig. 4.19 and Fig. 4.20 for joints 1 and 2, respectively. The numbers on the curves in Fig. 4.19 and Fig. 4.20 refer to the identified rosettes located across the sections of the chord webs (see Fig. 2.8). Note that the curves cluster to the left side of the plots pertaining to outer web shear strains whereas the two to the right are for the inner webs.

The efficiency of the outer webs can be estimated by comparing their maximum average shear strain just prior to failure with a computed plastic shear strain γ_y value. The value so obtained by the test for the two joints is about 30% of the value $\gamma_y = 2850 \times 10^{-6}$ based on a 350 MPa yield in tension. Therefore, only about 30% of each of the outer webs was effective in resisting the shear force near the failure load. For analytical purposes, however, the inner webs were assumed to be 100% effective in resisting shear. Another way of interpreting these results is that 65% of the total four webs was effective in resisting shear forces across the section.

Strain gauge readings on various members showed that strains developed along the length of the members were below the yield value when failure of the truss occurred. This further indicates the weakness of the connections in resisting shear forces which led to a premature failure.

Because the actual contribution of the outer webs to the overall truss behaviour is to some degree uncertain, analytical load-deflection

curves employing 75% and 100% effectiveness of the four webs are also used for comparison. These are plotted along with the curve that used 65% effectiveness as obtained from the test and compared with the experimental load-deflection curve in Fig. 4.21.

A general pattern of major reduction in stiffness is observed with the occurance of shear failures at critical connections. The plastic hinge numbering and the joint failure sequences are presented in Table 4.5 and Fig. 4.22. Note that the failure load increases significantly as the effectiveness of the outer webs increases. The stiffness of the truss decreases considerably once a joint suffers shear yield. A reduction in joint shear capacity leads to an early joint failure which, in turn, results in a lower overall load capacity. Therefore, as the overall web effectiveness decreases from 100% to 75% and then to 65%, the failure load drops from 2217 kN to 1754 and then to 1581 kN, respectively.

Apparently, the 65% effectiveness curve obtained from the analytic model gives a lower bound whereas the 100% effectiveness curve gives an upper bound solution. The best correlation with the experimental result is obtained with the 75% effectiveness case. However, there is some uncertainty as to what percentage is appropriate and hence a more detailed study of the shear resisting capacity of the outer webs is necessary to predict the capacity of the connections and hence to more accurately ascertain the response of the truss. Since the 65% effectiveness of the total four webs is the value assumed to be applicable based on the load-strain curves, an analytical solution for this case is

used for plotting the load-moment curves for presumed critical locations with their experimentally obtained counterparts. These are shown in Fig. 4.23 through to Fig. 4.26.

The analysis predicts a shear failure at joint 1 at 1317 kN. As can be observed from the load-moment curves for the diagonal members at joints 0, 1 and 2, a significant increase in bending moments takes place at these critical sections due to redistribution of forces throughout the truss. Joints 2 and 3 also experience shear failure at loadings of 1521 kN and 1539, respectively. Thus a mechanism was imminent which finally led to overall failure at 1581 kN. Twelve plastic hinges had also formed along with failures of joints 2 and 3 in shear during the analysis. In general, a resonably good agreement with the experimental load displacement curves is evident for the 65% and 75% effectivness cases. However, a 70% effectiveness curve could have provided a better correlation.

From the test results of Truss S1, it is noted that failure of joint 1 due to shear was the cause of failure for the whole truss. The primary objective was to continue testing until all joints or connections had failed. This, therefore, led to the retesting of Truss S1 with joint 1 reinforced by welding two 610 mm × 305 mm × 11.1 mm gusset plates onto both webs of the diagonal members at that connection. With this arrangement undertaken, the truss is identified as Truss S1A.

The same loading and measuring procedures were re-applied until failure. Joint 2 of Truss S1A failed under a total loading of 2108 kN.

The failure mode was different from that of Truss S1 in that torsional distorsion was prevented due to the continuity provided by the chord extending to joint 0. Excessive shear forces from the diagonal members caused failure at the connection. In-plane shear distortion, as shown pictorally in Fig. 4.27(a), led to the failure of the truss. By incorporating the gusset plates at joint 1, the failure load was increased by 22.1% compared to that of Truss S1 without any reinforcement.

For analytical purposes, the gusset plates at joint 1 were presumed to provide sufficient stiffness that small members having an area $A = 7000\ mm^2$ and moment of inertia $I = 4.2 \times 10^8\ mm^4$ were incorporated. The resulting theoretical load-deflection curves using 65%, 75% and 100% effectiveness factors for the four webs were computed and plotted with the experimental curve in Fig. 4.28. The 65% and 100% effectiveness curves again gives respectively a lower and upper bound solution. Sensitivity is also high as the failure load increased from 1762 kN to 1913 kN and to 2452 kN as the chord webs' efficiency increasingly improved from 65% to 75% and then to 100%, respectively.

The analytical solution using 65% efficiency predicts joint 2 to yield plastically in shear at a load of 1459 kN. Eventually, twelve plastic hinges had formed to create a mechanism at a total load of 1762 kN. In this case it is noted that an analytical curve having a web efficiency of about 85% would give a very good load-deflection relationship with the experimental curve. Again, it is clear the truss failure load is very sensitive to the shear resistance offerred by the entire chord cross section.

Truss S1A was again reinforced with 11.1 mm thick gusset plates on both sides of joint 2. This truss is referred to as Truss S1B. It was then re-tested to ultimate load. The mode of failure was plastic shearing of joint 3 as shown in Fig. 4.27(b), at a total loading of 2393 kN. The failure load increased by 13.5% over that of Truss S1A. Joints 1 and 2 of the analytical model were now stiffened as during the actual testing of the truss. The analytical solution using the 65% efficiency of the four webs in resisting shear predicts a shear failure at joint 3 under a load of 1761 kN. The slope of the load-deflection curve then decreases as the overall stiffness of the truss is reduced. A mechanism finally developed in the structure when a total of twelve plastic hinges had formed.

The analytical load-deflection curves employing 65%, 75% and 100% effectiveness of the four webs are shown in Fig. 4.29. Artificial members replacing the gusset plates were again employed. Here, 75% and 100% effectiveness curves give lower and upper bounds to the experimental curve, respectively. The predicted failure load increases from 1995 kN to 2169 kN and to 2668 kN as the efficiency increases from 65% to 75% and then to 100%, respectively. Again, an efficiency of about 85% would provide a good correlation with the experimental curve.

The systematic reinforcement of connections was then continued as Truss S1C was formed by welding additional gusset plates on the web faces of joint 3. It is noted at this conjuncture that joints 1, 2, and 3 of Truss S1C were all reinforced with additional gusset plates. The

truss was then loaded by employing the same procedure. When the loading on the truss reached 2420 kN, local buckling occurred at one end of member 7-7 as shown in Fig. 4.27(c). This failure load represented an increase of 1.1% over that of Truss S1B. With all the critical connections reinforced to prevent a joint shear failure, the failure mode was thus transferred to member 7-7. This suggests that joints 1, 2 and 3 ought to be reinforced to ensure a member failure (in this case the top chord). The analytical solution using 65% efficiency of the webs in resisting shear predicts a shear failure at joint 4 under a loading of 2206 kN. Eventually, a sufficient number of plastic hinges have formed to cause a mechanism which leads to a failure at 2539 kN.

The analytical load-deflection curves using 65%, 75% and 100% efficiencies of the four webs are plotted against the experimental curve as shown in Fig. 4.30. Sensitivity with web efficiency of the curves is not as high as those of the previous trusses. The failure load increases from 2539 kN to 2564 kN and then to 2666 kN as the effectiveness of the webs in resisting shear increases from 65% to 75% and to 100%, respectively. All three of these analytical cuves give an upper bound solution in contrast to the previous cases. Once again, the analytical model does not check buckling of a member and the higher failure loads above are, perhaps, due to shear failure of joint 4 instead of buckling of member 7-7.

No further repair work was attempted since damage to the top chord during local and overall buckling was substantial.

4.2.2 Truss S2

As discussed in the previous section, the inefficient transfer of shear forces to the outer webs of the chord members is worsened if continuity across a joint is terminated. One method of improving this condition is to weld end plates onto the ends of the top chord members as shown in Fig. 4.31. Therefore, for efficient transfer of shear forces, joint 1 was reinforced with end caps and prevented from chord distortion as observed during the previous truss test.

With the above adjustments made, load increments of 90 kN on each of the two jacks were applied while readings on strain gauges and rosettes were recorded. When the total load on the truss reached 2045 kN, again a shear failure occurred at joint 1. The geometry of the chord members at the connection was distorted but to a lesser extent than that for the previous test which is also evident from the photograph in Fig. 4.32(a).

Table 4.6 indicates the ratio of applied load to truss failure load when yielding occurred at extreme fibres of various members. It is evident that the extreme fibres of members 1-2 and 0-1 at joint I started to yield when the applied load reaches 66% and 78% of the experimental failure load, respectively. This corresponds to the predicted values of 79% and 87% from the analytical solution. The early yielding attributed to the shear failure at joint 1.

The effectiveness of the outer webs in resisting shear forces

across the critical section is estimated by the same procedure as outlined in the previous section. The efficiency of the four webs is very different for the two joints where strain rosettes were located. From Fig. 4.33 and Fig. 4.34, it is found that the outer webs are only 14% effective for joint 1 as compared to 44% for joint 2. A possible explanation for this large variation of effectivness of the outer webs to resist shear forces at joints 1 and 2 is now suggested. The large eccentricity at the connections resulted in a large gap between the diagonal members. Joint 1 was loaded by the spreader beam system directly onto a pad plate of width 152 mm. The combined action of compressive forces from member 0-1 and tension force from member 1-2 had the effect of shifting the joint towards the centre of the truss. This tended to cause a change in the stress pattern at the gap due to the apparent change in loading position. The localized stresses embracing compression from the pad plate and those stresses from the joint itself complicated the distribution of stresses at joint 1.

For joint 2, where the forces were more regularly distributed, one would expect a more uniform distribution of stresses across the section. As such, the results from joint 2 are considered to be more reliable than those of joint 1 in postulating connection behaviour of this truss. Furthermore, since end-capping of the top chord members tended to produce the same effect on both joints 1 and 2, the study of the efficiency of outer webs of chord members in resisting shear forces based on joint 2 would then form a more realistic basis for analysis.

For purposes of predicting strength and deformation of the

truss, the efficiency of the outer webs of the chord members in resisting shear is therefore taken as 44%. Since the inner webs are assumed to be 100% effective in resisting shear, the overall efficiency of the webs in resisting shear is then 72% of the theoretical plastic shear capacity for four webs. Two other values, namely, 85% and 100% were used to investigate the sensitivity of effectiveness of the total web thickness in resisting shear on the overall behaviour of the truss. The experimental and analytical load-deflection curves for these cases are shown in Fig. 4.35. As the effectiveness of the four webs in resisting shear increases from 72% to 85% and to 100%, the failure load increases from 1613 kN to 1842 kN and to 2097 kN, respectively. All of these cases predict shear failure at joint 1.

The analytical model (plane-frame analysis program), using 72% effectiveness of the four webs, predicted joint 1 to fail under shear at a load of 1415 kN. As more plastic hinges formed in the truss, joints 2 and 3 also failed by shear at loadings of 1548 kN and 1601 kN. A mechanism then formed with a total of sixteen plastic hinges which caused failure of the truss at a load of 1613 kN. The failure sequences for Truss S2, including all three cases of web effectiveness, are shown in Fig. 4.36, and the plastic hinge progression appears in Table 4.5. It is noted that with an improvement in the effectiveness of the outer webs in resisting shear, the load level for joint shear failure increases. The 72% and 100% effectiveness curves give lower and upper bound solutions, respectively, while a closer correlation with the experimental curve would be obtained if 95% effectiveness were used for the four webs.

The analytical load-moment curves using 72% effectiveness of the four webs and the experimental load-moment curves for the members with most highly stressed ends are shown in Fig. 4.37 to Fig. 4.40 inclusively. It is observed that the bending moment at joint 0 of member 0-1 increases rapidly as the loading reaches 1415 kN. This load coincides with the load level at which joint 1 fails in shear, resulting in redistribution of the forces throughout the truss. Other members also react to this sudden loss of stiffness but to a lesser extent.

For similar reasons as were presented for Truss S1, Truss S2 was reinforced with 610 mm × 305 mm × 11.1 mm gusset plates at the failed joints to provide the needed joint strength and stiffness for retesting. This truss is identified as Truss S2A. The truss was retested following the same procedure as for the original truss. In this instance, joint 2 of Truss S2A failed at a loading of 2162 kN. The failure mode was by shear at the connection as shown in Fig. 4.32(b). It was not possible to release the load quickly enough to avoid the substantial distortion of the double chord section at the joint. Major rupturing of the inner webs resulted and consequently it was decided that repair work would seriously alter the truss' configuration and hence, was not undertaken. The failure load of Truss S2A was 5.7% higher than the ultimate load attained by Truss S2. It is also to be noted that by reinforcing joint 1 of the truss, the failure mode was transferred to joint 2 as was the case for Truss S1.

The analytical load-deflection curves using 72%, 85% and 100%

efficiencies of shear transfer of the total four webs in resisting shear are plotted along with the experimental curve in Fig. 4.41. The experimental curve is bounded by the 85% effectiveness and 100% effectiveness solutions. The failure load for the 100% effectiveness solution is 2212 kN while the 72% and 85% effectiveness curves are at lower levels of 1717 kN and 1947 kN, respectively. High sensitivity to this variation in shear resistance at the joints is once again demonstrated.

Using the 72% effectiveness factor for the four webs, the analysis predicts joint 2 to fail at a loading of 1512 kN. Sixteen plastic hinges were identified throughout the structure culminating in a failure mechanism formation of the truss. As observed from the load-deflection curves, a joint efficiency of nearly 100% would appear to provide the best match to the experimental curve.

The analytical and experimental m-p interaction diagram for members 0-1 and 1-2 are plotted in Fig. 4.42 and Fig. 4.43 for Truss S1 and Fig. 4.44 and Fig. 4.45 for Truss S2. As Truss S1 experienced premature joint failure at an early stage, the experimental curves tend to give lower values than the analytical cuves. The complex distribution of stresses at the connections during the testing of Truss S2 tends to cause a disparity between the experimental and analytical curves for both members. A summary of the principle results for both standard trusses is presented in Table 4.7.

The analytical results cited are for shear efficiency factors of 65% and 72% for Truss S1 and Truss S2 respectively. These values were

obtained from strain rosette readings and represent lower bound solutions to the experimental results. Better agreement would result with higher values, since the ultimate strength of the truss is sensitive to individual joint resistance in shear.

4.3 Bolted Truss BO

As was done with the previous trusses, load increments of 90 kN at each jack was applied to the truss while strain gauge readings were taken. The truss failed at a total load of 2528 kN by local buckling of the central top chord member (member 7-7). Fig. 4.46 shows the small buckle that formed when the truss reached its ultimate load carrying capacity.

From the experimental load-strain curves given in Appendix II, the ratio of applied load to truss failure load when yielding occurred at extreme fibres of members is shown in Table 4.8. It is noted that yielding of the extreme fibres of the end and center of member 7-7 has begun at an average of 82% and 92% of the truss failure load, respectively. This compares very well with the analytical values of 84% and 93%. Member 0-1 was in the elastic range when member 7-7 failed during the experiment.

From observations made throughout the testing program, there was no duress of the connections or the members framing into them. The tie plates connecting the chord members effectively transfered the diagonal member forces, thereby preventing the chord members from displacing

relative to each other. From the strain readings on the tie plates, it can be concluded that the tie plates transferred about 33 kN in tension and compression near the ultimate load, from one chord member to the other. The provision of the tie plates and the gusset plates had the effect of increasing the rigidity of the connections and the overall stiffness of the entire truss.

The experimental and computed vertical displacement curves for mid span are shown in Fig. 4.47. Very good agreement is evident between the two curves. The analytical curve is linear up to a total loading of 2162 kN with the formation of the initial plastic hinge in member 2-3. A signficiant decrease in slope does not take place however until failure of member 7-7 occurs. This is shown by the detailed load-displacement curve in Fig. 4.48. After a substantial loss in overall stiffness, a maximum loading of 2624 kN or 3.8% higher than the experimental failure load is obtained when a specified maximum deflection of 278.0 mm (five times the elastic deflection) is reached. The analytical model predicts member 7-7 to reach its load carrying capacity at 2589 kN. As loading increases to 2612 kN, members 6-8 also reach their load capacity. Excessive deflection occurred as the load reached 2624 kN. A total of twenty-eight hinges had formed at this stage. The failure sequence is shown in Fig. 4.48. It can be observed that there is good correlation with the experimental values throughout the loading process.

From the m-ϕ-p interaction curves of Appendix IV the experimental load-moment curves for the most highly stressed members are plotted

along with the analytical curves as shown in Fig. 4.49 to Fig. 4.52 inclusively. Good correlation is obtained for all the cited members except member 0-1 at joint 0 which shows disparity. This is probably due to the lack of continuity at the connection.

An additional test was undertaken on the bolted truss to establish the effective moment of inertia of the top chord for resisting top chord buckling. The truss was laid horizontally onto four blocks that rested on the floor. Each was located to support each end of the top and bottom chord. Two loads were applied to the inner most joints of the top chord to cause out-of-plane bending while top and bottom chord deflections were measured. When comparing measured top chord deflections with those obtained by assuming top chords as a single integrated unit, it was found that the latter gave predicted deflections of 96% of the measured values. It would, therefore, seem reasonable to state that the effective moment of inertia of the top chord as a single unit may be assumed to be that obtained by elementary beam theory; that is, plane sections remain plane for the components of the chord section when bending out-of-plane.

Having completed the original test, a decision had to be made about repairing the top chord sufficiently and yet without altering the behavioural characteristics unduly. Because of the cross ties obstructing any possibilty of attaching reinforcements to the chord's flanges, the truss was reinforced by welding 127 mm × 15.8 mm external side plates along the top chords of the three middle panels and also across the two middle panels of the bottom chords. It was felt that such a

truss would provide a better basis for establishing the joint strength than was the case with Truss BO. This reinforced truss is referred to as Truss BOA.

On testing, buckling occurred in member 2-3 when the total loading reached was 3176 kN. The failure mode is shown in Fig. 4.53(a). About 5 mm of slippage of the bolts was observed at the bottom end of member 2-3 at failure. This was, however, the first sign of any bolt duress. It is noted that by reinforcing the top and bottom chords, the truss failure load is increased by 25.6% while the failure mode is transferred to the next critical member. For analytical purposes, the I and A values of 5.41×10^6 mm^4 and 4032 mm^2, respectively, for the side plates are added onto the original values of the various members to simulate the addition of side plates.

The experimental and analytical load-deflection curves for Truss BOA are shown in Fig. 4.54.. Member 1-2 reaches its axial load carrying capacity at a loading of 2847 kN. As loading progresses, member 2-3 also reaches its loading capacity at a load of 2927 kN (7.8% lower than the experimental value). Member 4-6 also reaches its capacity at a loading of 2980 kN when the truss failed under excessive deflection. A total of twenty-six hinges had formed in the analysis. Close agreement with the experimental result is again obtained using the analytical model for the truss.

Following testing of Truss BOA, it was decided to reinforce member 2-3 with 114.3 mm × 18.8 mm plates on both sides (webs) along

their full lengths. This reinforced truss is referred to as Truss BOB. It was tested as before and sustained a total loading of 3327 kN at which time local buckling of member 5-7 occurred in the side wall of the chord at joint 5 where the chord side plate was terminated. The failure mode is shown in Fig. 4.53(b). It is evident that if the end plates had been extended beyond the panel points a short distance, this local buckling failure would have been prevented. As was the case for Truss BOA, the properties of the side plates are incorporated in member 2-3 to simulate the reinforcement in the modelling of the truss. The experimental and analytical load-deflection curves for Truss BOB are shown in Fig. 4.55. The analytical solution predicts members 1-2 and 4-6 to reach their axial load carrying capacities at loadings of 2838 kN and 2998 kN, respectively. Of course, plastic hinges had formed earlier in these members. The effect of limiting member strength is to reduce the overall stiffness of the truss significantly. This suggests sensitivity of truss stiffness to the plastic limit load for the members cited. When the total load on the truss reached 3060 kN and twenty-six plastic hinges had formed, the mid-span deflection reached the limiting value of five times the elastic limit value and led to ultimate failure by excessive deflection. Another attempt was made to restore the truss' integrity by reinforcing the truss with 30 cm long plates welded along the chord webs to extend those installed for Truss BOA. This truss, identified as Truss BOC, was altered in another way. From the previous tests, there had been little indication of an ensuing joint failure. It was felt that the joints had been over-designed and therefore one row of inner bolts fastening the gusset plates was removed on both sides of each end of all members. The truss was then reloaded in the usual

manner. This time, numerous cracking sounds were heard with bolt slippages occuring until the total load on the truss reached 3123 kN when local buckling of member 2-3 at joint 3 was observed. About 3 mm of slippage had occured at the bottom chord end of member 1-2. The failure mode is shown in Fig. 4.53(c).

It was expected that with the addition of side plates to the top chord members, somewhat higher strength could be achieved. In fact, the experimental failure load for Truss BOC is 6.9% lower than the experimental failure load of Truss BOB. Although the inner row of bolts was removed from all gusset plates, the failure load is still 18.3% higher than that Truss BO where all bolts were present. Since failure occurred in the vicinity of the removed bolts, this suggests that the bolts can significantly affect the localized stress distribution at the connections. If the bolts had been present during the testing of Truss BOC, local buckling would not occur while a higher failure load would be obtained. In order to simulate the extension of side plates to the chord members, the properties of these side plates are added to member 3-5 for modelling of the truss.

The experimental and analytical load-deflection curves for Truss BOC are shown in Fig. 4.56. The analytical solution predicted member 1-2 to fail by yielding at a load of 2866 kN. Loss of stiffness is indicated by a major change in slope of the load-deflection curve. As members 0-1 and 4-6 also reach their load carrying capacities at 2989 kN and 3069 kN, respectively, and together with various plastic hinges the truss finally failed at a loading of 3123 kN due to excessive deflec-

tion. A total of twenty-six plastic hinges were associated with failure. Better agreement with the experimental curve resulted for this truss than for Truss BOB.

The m-p interaction diagrams for members 0-1 and 1-2 for Truss BO are presented in Fig. 4.57 and Fig. 4.58, respectively. The analytical solution suggests higher bending moment values over the experimental results and consequently predicts both members to reach the failure envelope. As explained in the previous section, these higher values are a result of the upper bound values given by the analytical solution. However, close agreement between the experimental and analytical results is obtained.

A summary of the principle results for the bolted truss is presented in Table 4.9. The experimental failure load of the truss generally increases as more reinforcements are incorporated. The onset of premature failure at the joint which led to a 6.9% reduction in total load capacity for Truss BOC as compared with Truss BOB is probably due to removal of a row of bolts which, consequently, reduce the stiffness of the connection.

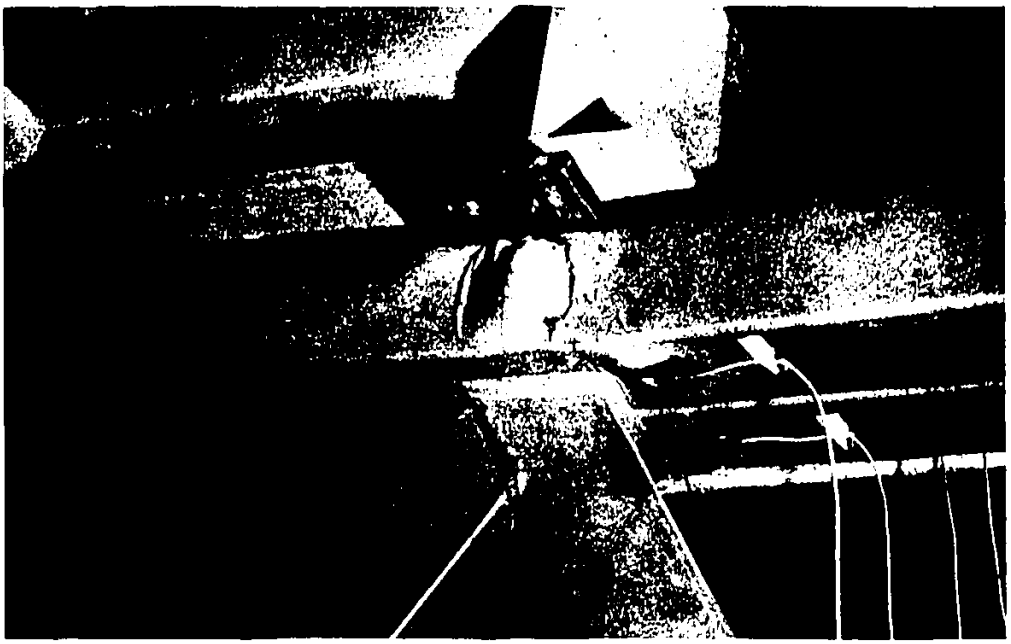

(a) Truss BBST

(b) Truss BBOV

FIGURE 4.1 FAILURE MODE OF BACK-TO-BACK TRUSSES.

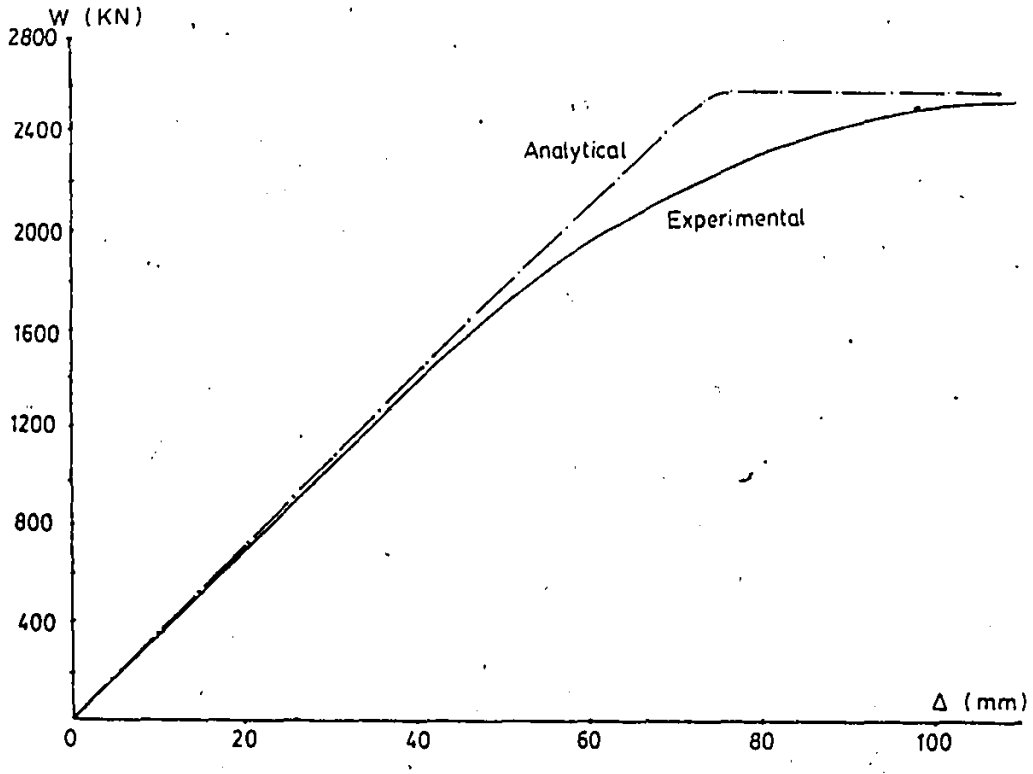

FIGURE 4.2 LOAD-DEFLECTION CURVES OF MID-SPAN FOR TRUSS BBST

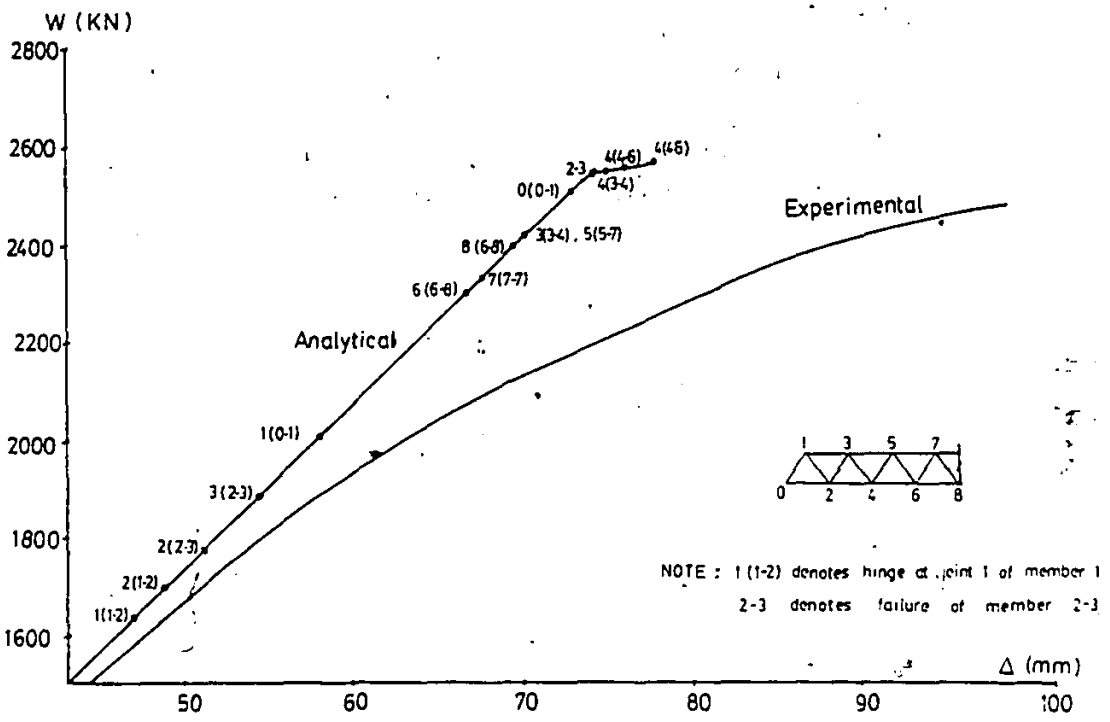

FIGURE 4.3 FAILURE SEQUENCE FOR TRUSS BBST

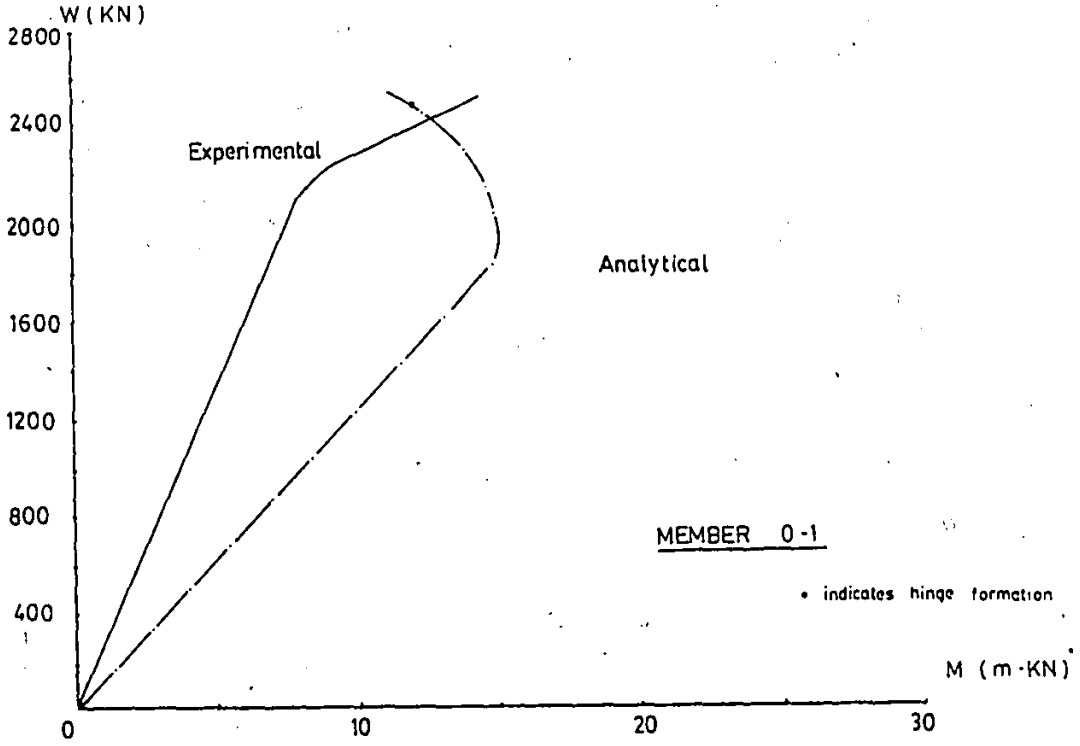

FIGURE 4.4 LOAD-MOMENT CURVES FOR DIAGONALS AT JOINT 0 OF TRUSS BBST

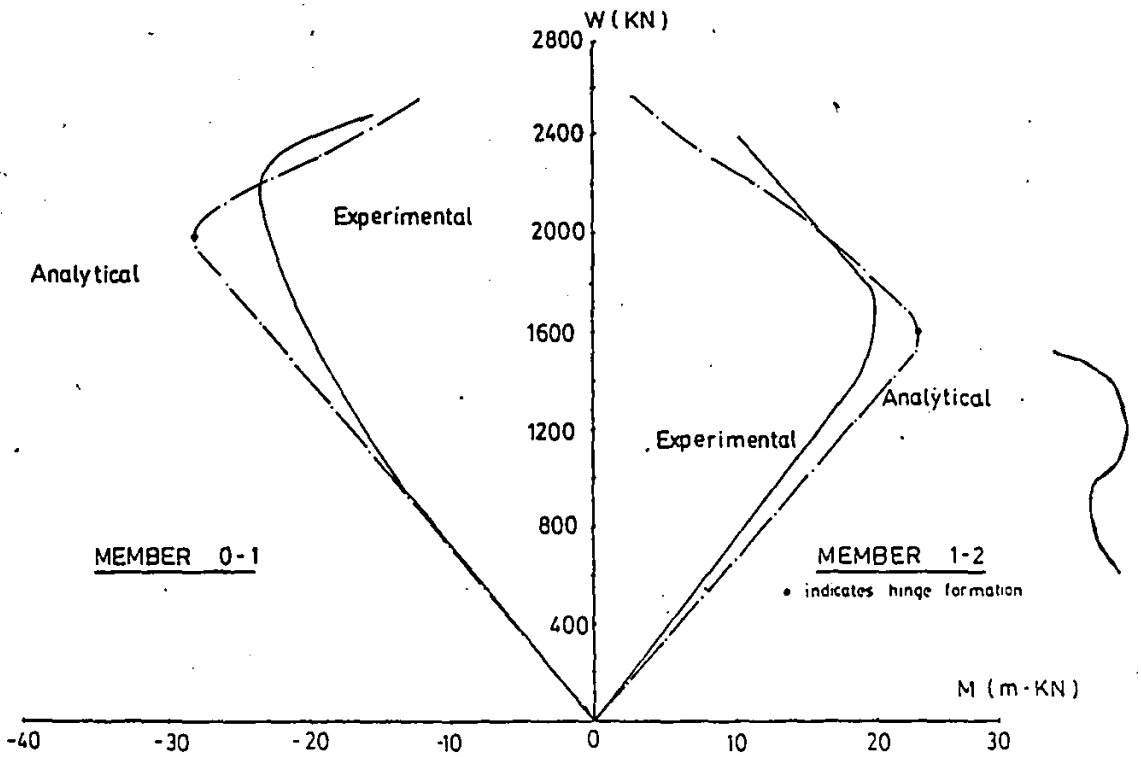

FIGURE 4.5 LOAD-MOMENT CURVES FOR DIAGONALS AT JOINT 1 OF TRUSS BBST

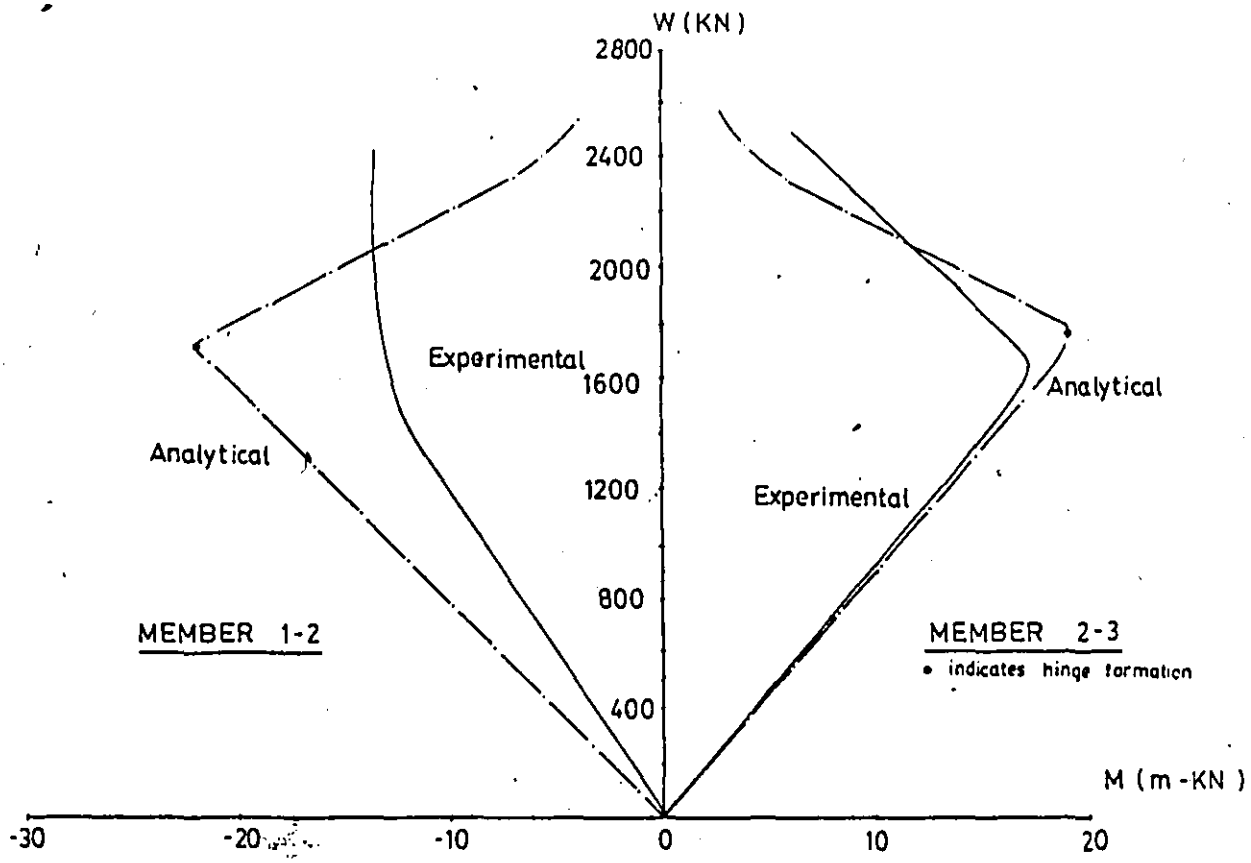

FIGURE 4.6 LOAD-MOMENT CURVES FOR DIAGONALS AT JOINT. 2 OF TRUSS BBST

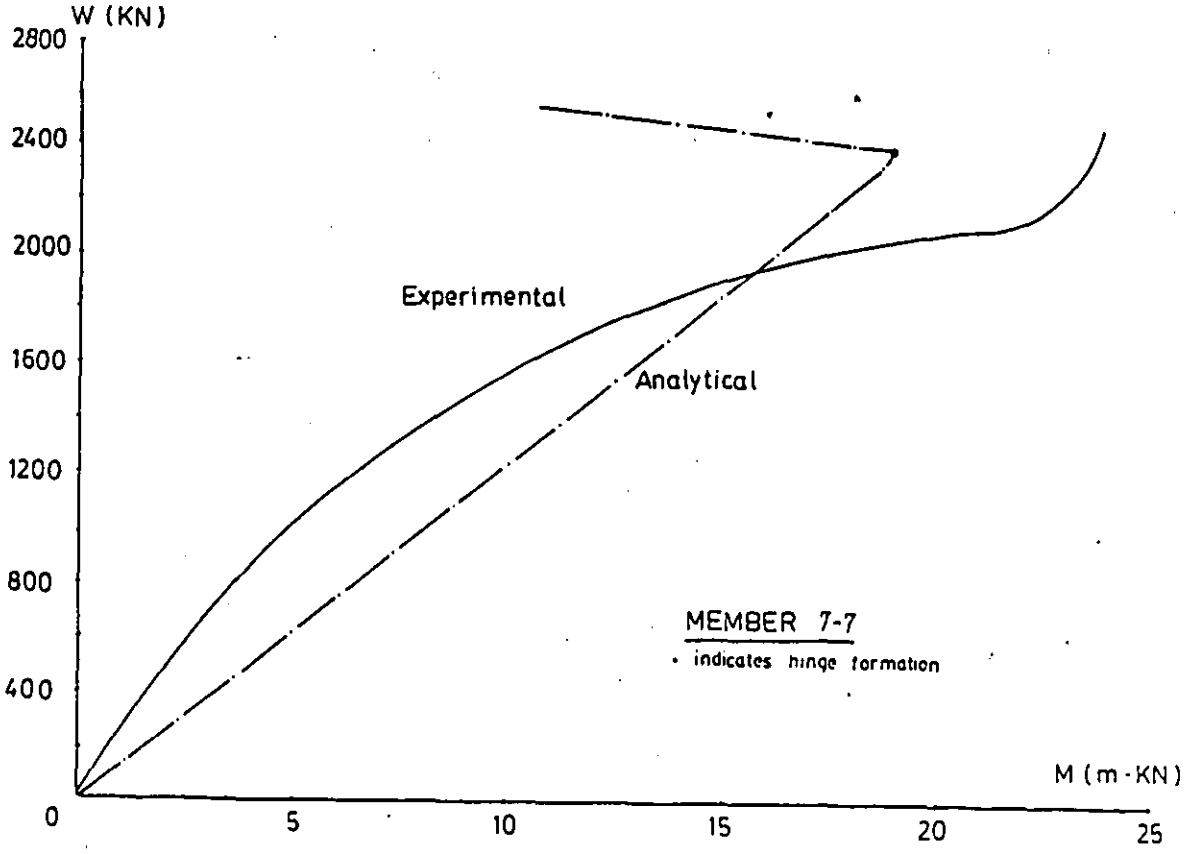

FIGURE 4.7 LOAD-MOMENT CURVES FOR TOP CHORD MEMBER OF TRUSS BBST

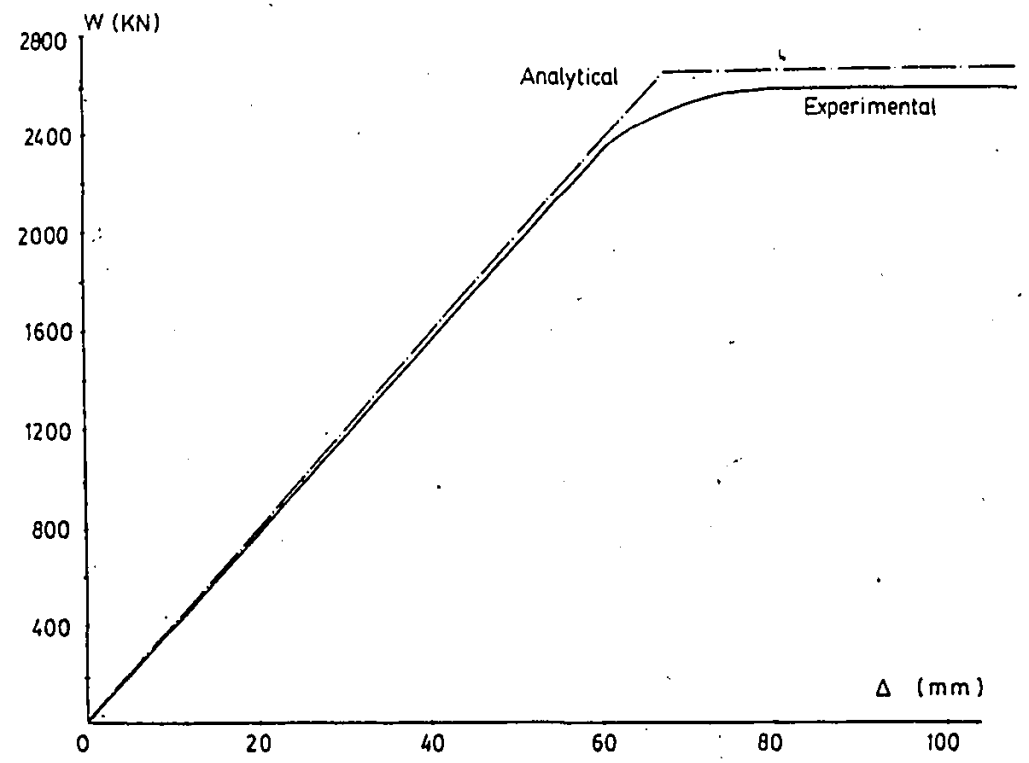

FIGURE 4.8 LOAD-DEFLECTION CURVES OF MID-SPAN FOR TRUSS BBOV

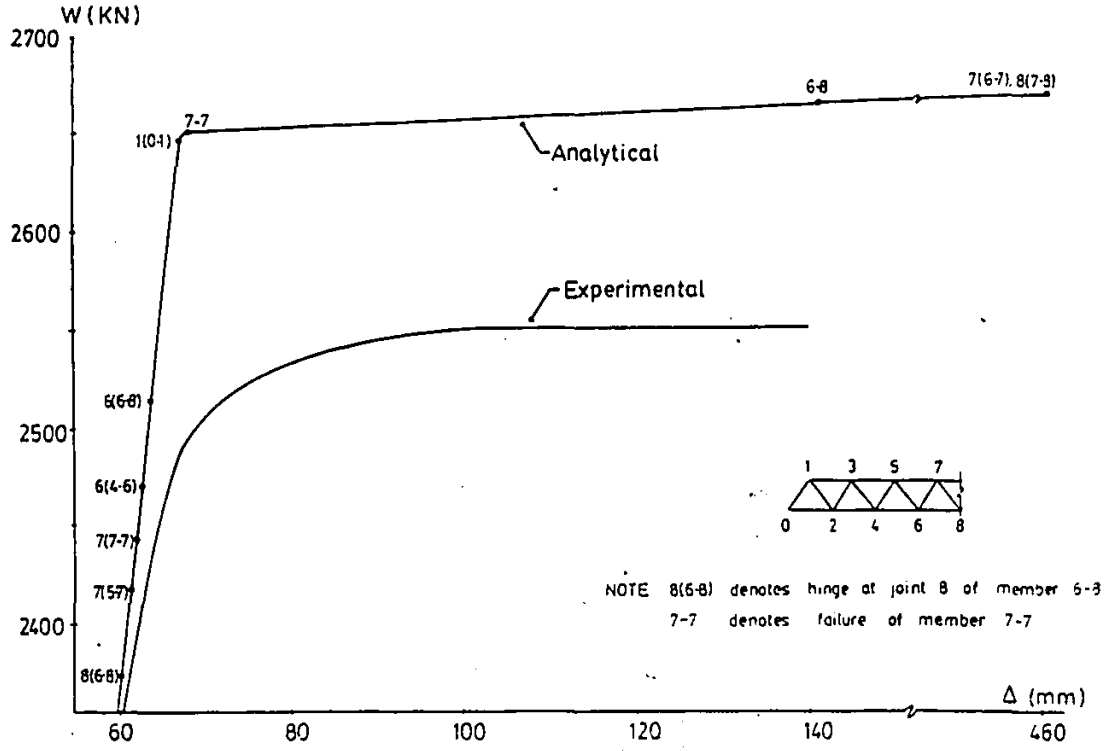

FIGURE 4.9 FAILURE SEQUENCE FOR TRUSS BBOV

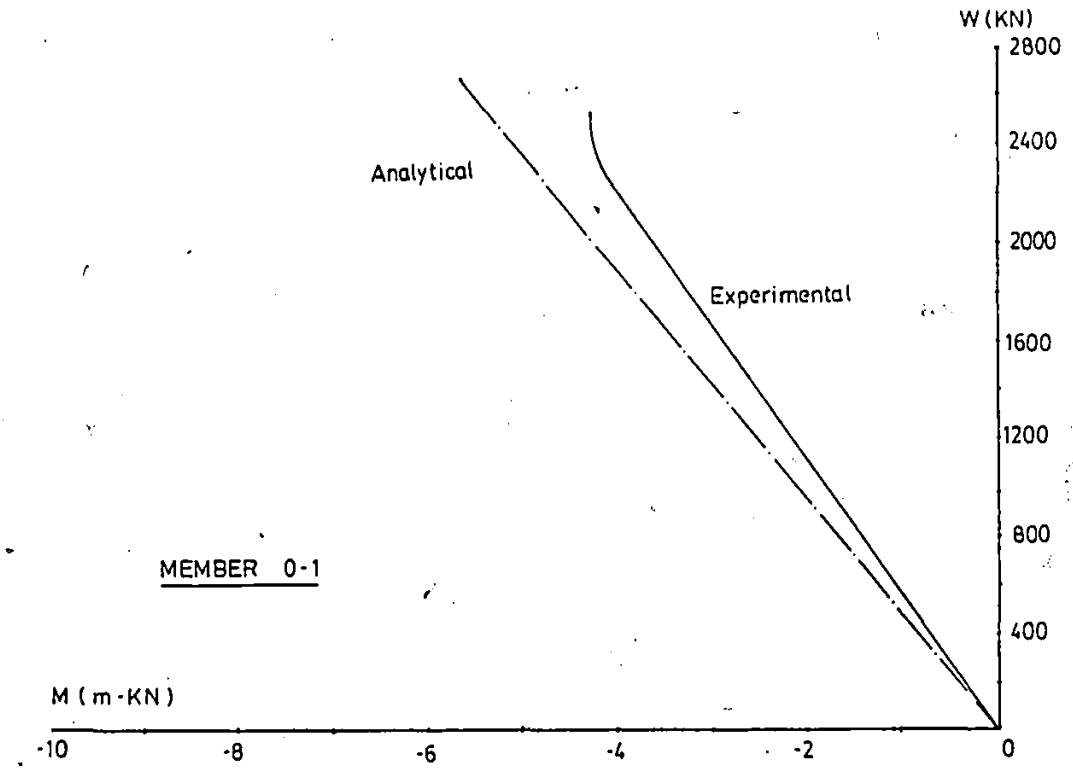

FIGURE 4.10 LOAD-MOMENT CURVES FOR DIAGONALS AT JOINT 0 OF TRUSS BBOV

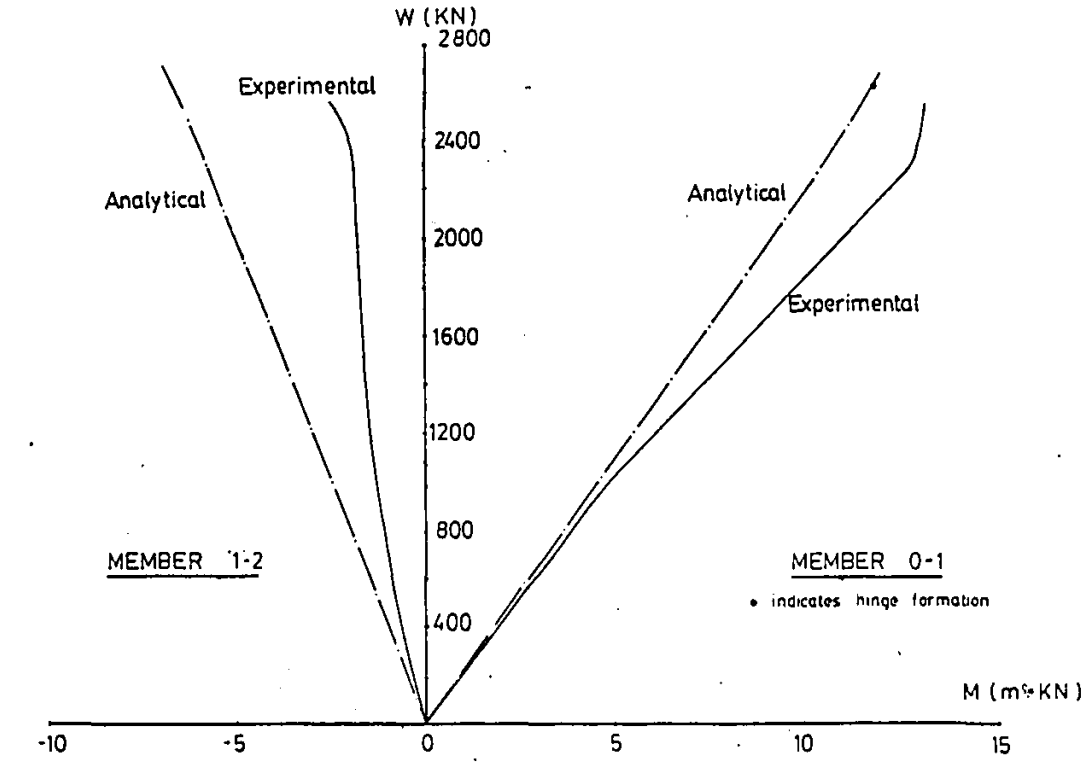

FIGURE 4.11 LOAD-MOMENT CURVES FOR DIAGONALS AT JOINT 1 OF TRUSS BBOV

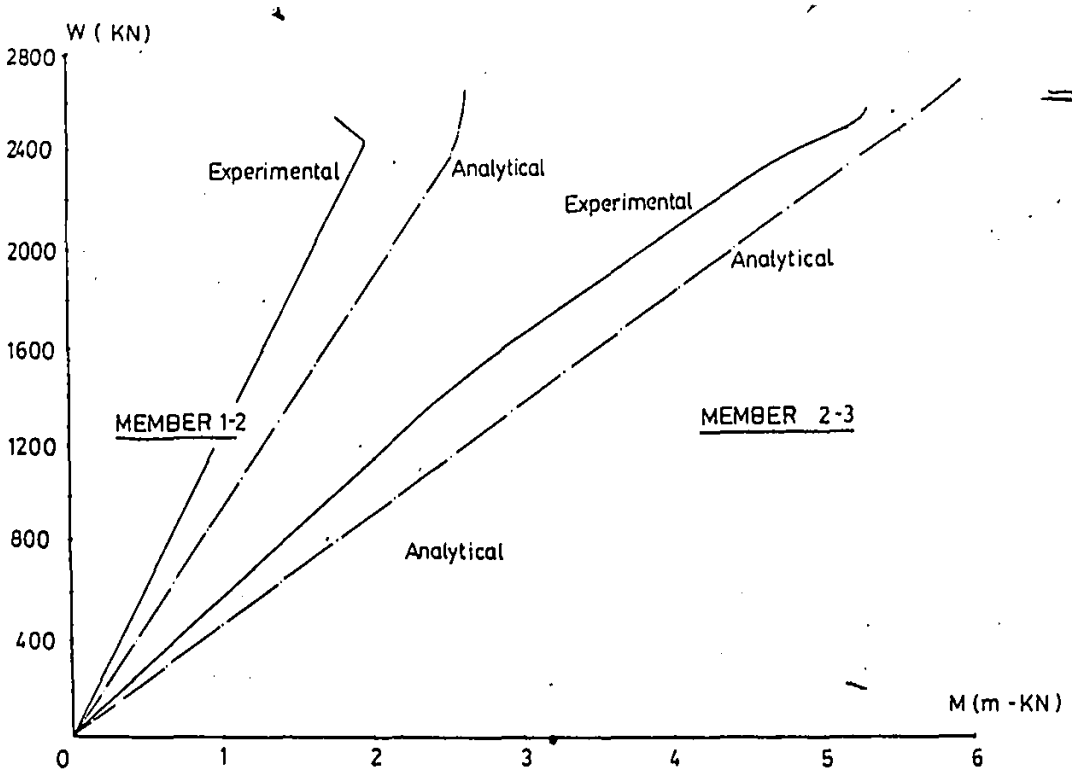

FIGURE 4.12 LOAD-MOMENT CURVES FOR DIAGONALS AT JOINT 2 OF TRUSS BBOV

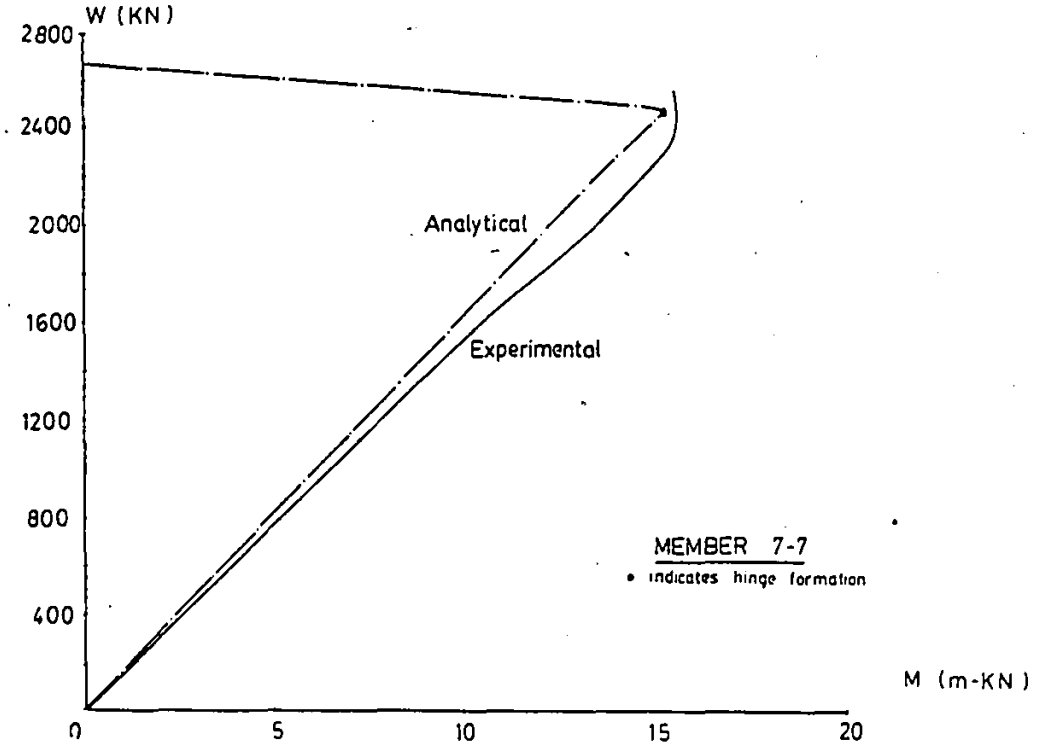

FIGURE 4.13 LOAD-MOMENT CURVES FOR TOP CHORD MEMBER OF TRUSS BBOV

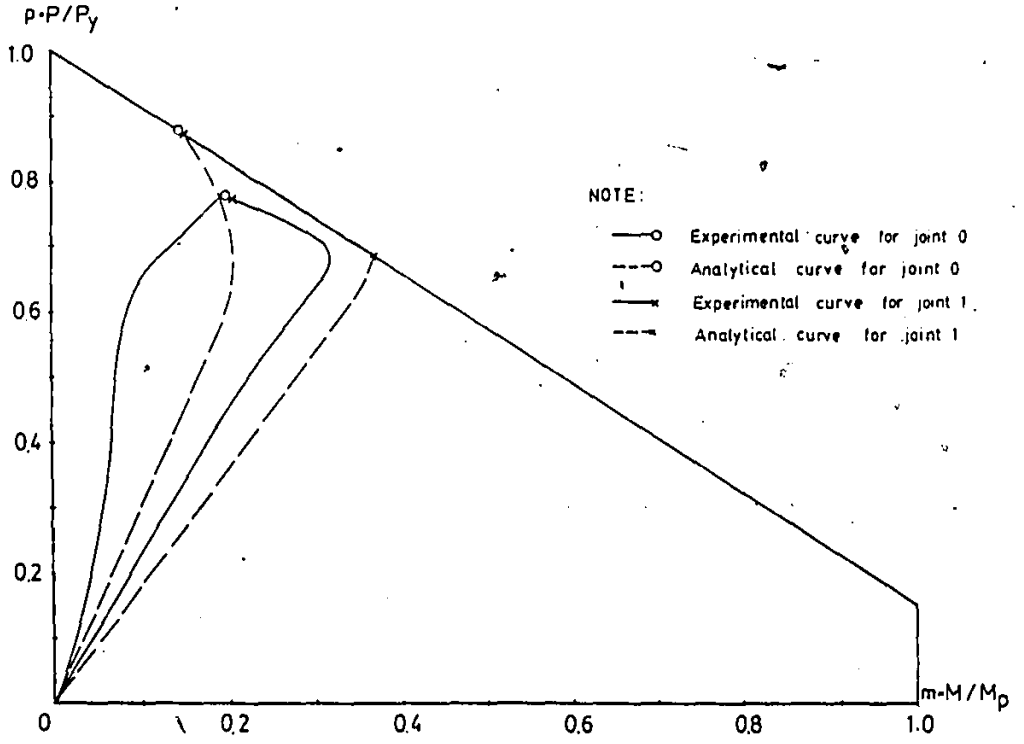

FIGURE 4.14 INTERACTION DIAGRAM FOR MEMBER 0-1 OF TRUSS BBST

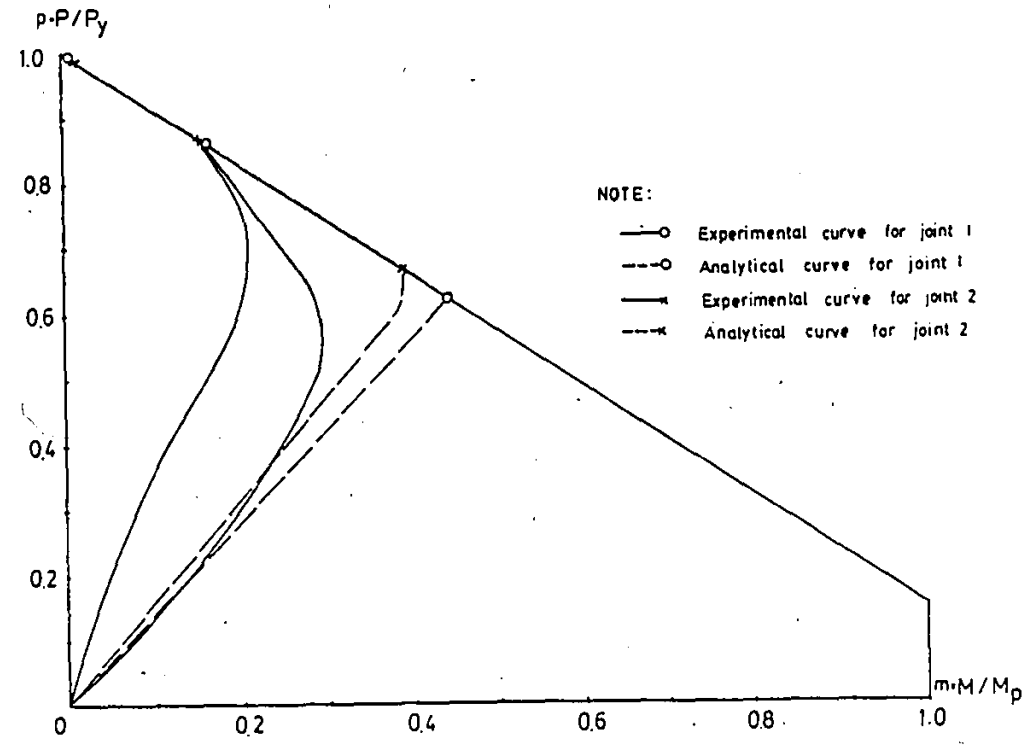

FIGURE 4.15 INTERACTION DIAGRAM FOR MEMBER 1-2 OF TRUSS BBST

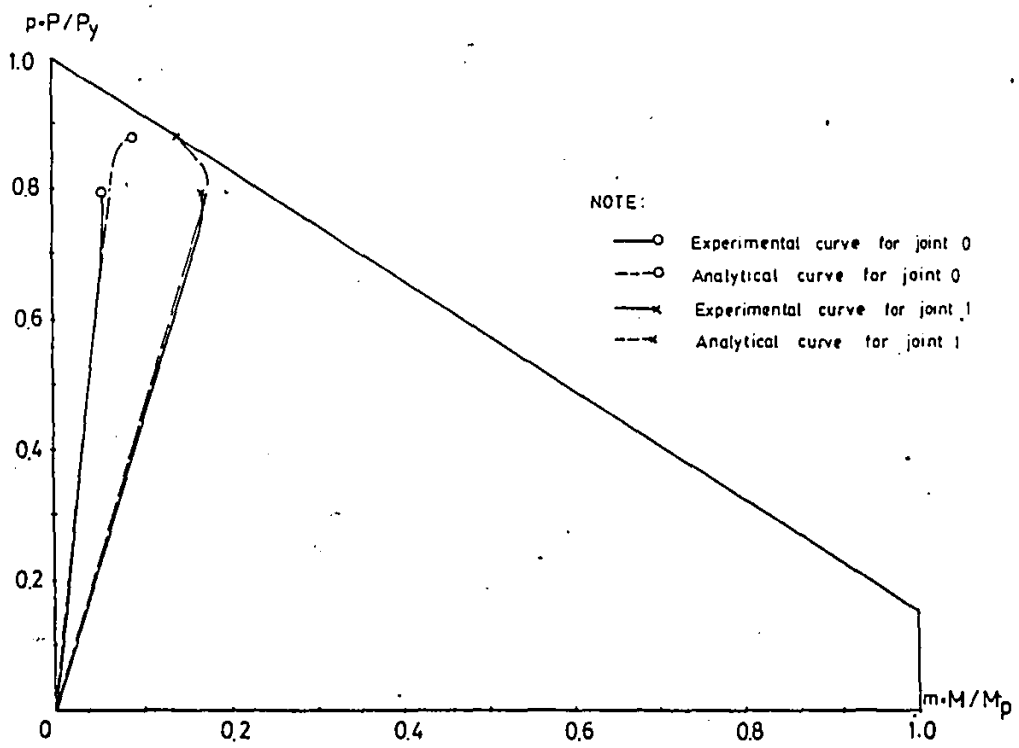

FIGURE 4.16 INTERACTION DIAGRAM FOR MEMBER 0-1 OF TRUSS BBOV

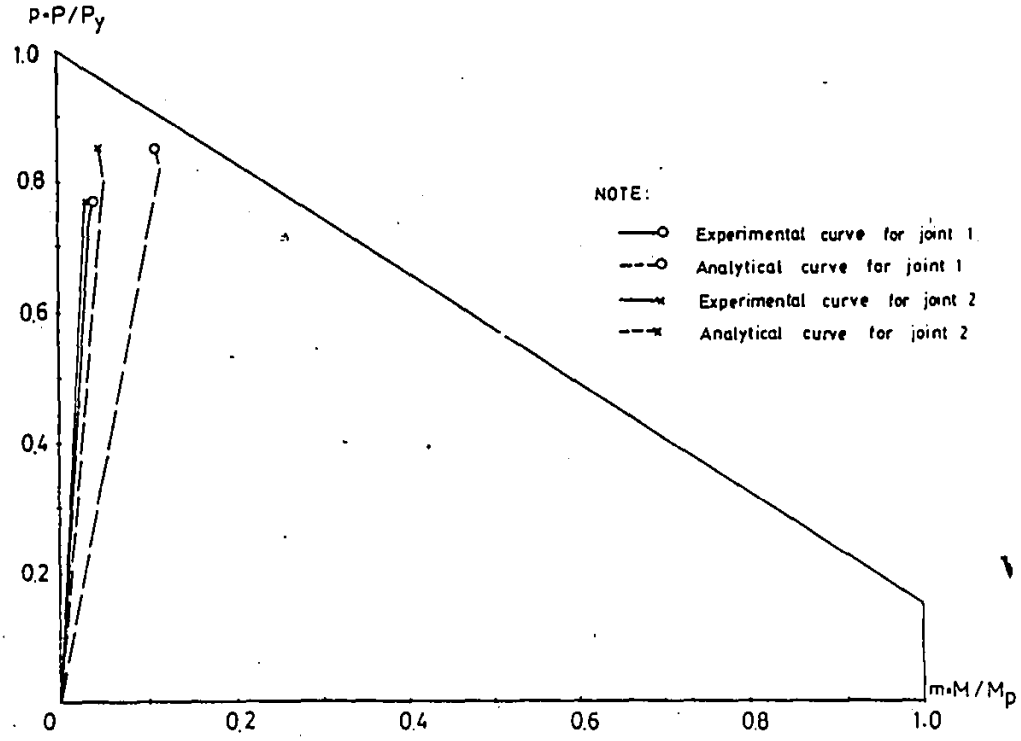

FIGURE 4.17 INTERACTION DIAGRAM FOR MEMBER 1-2 OF TRUSS BBOV

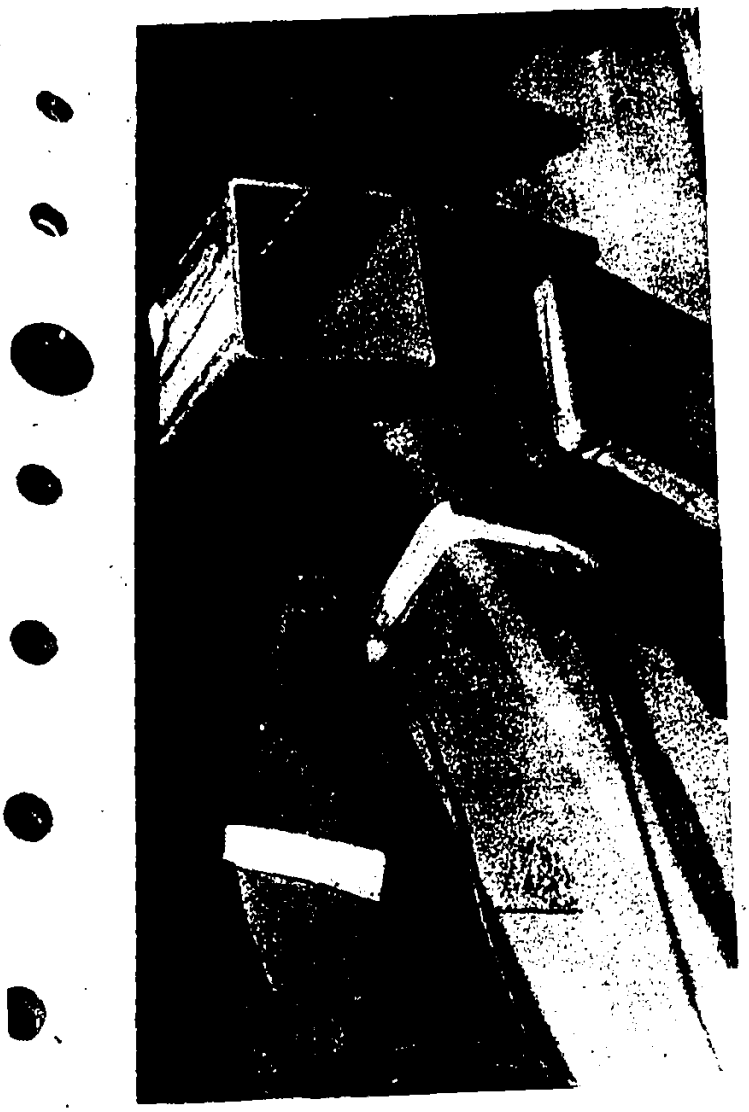

FIGURE 4.18 FAILURE MODE OF TRUSS S1

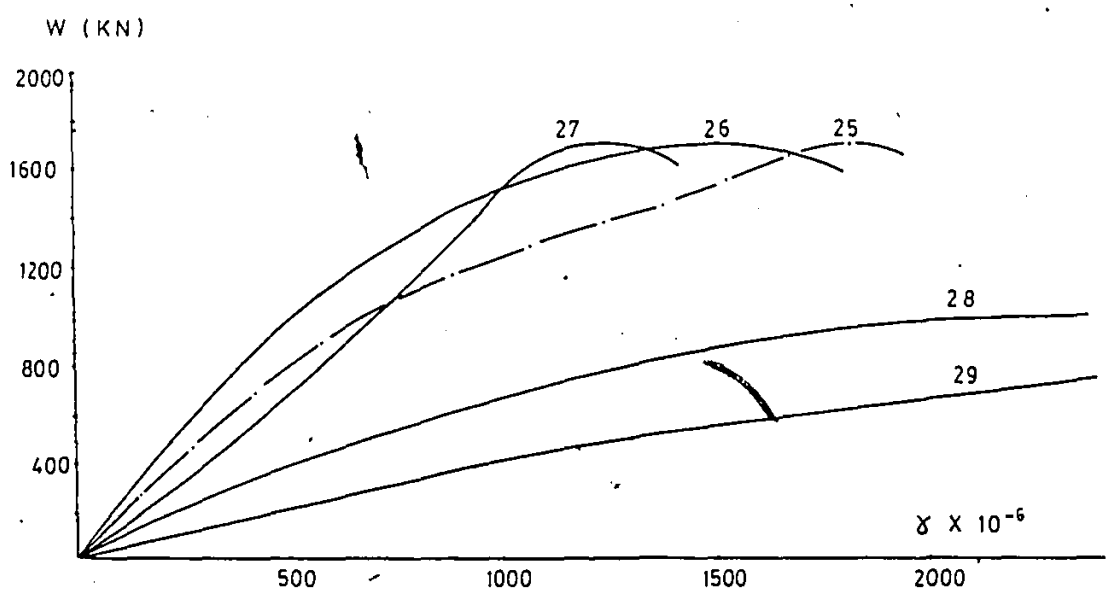

FIGURE 4.19 LOAD-SHEAR STRAIN CURVES FOR JOINT 1 OF TRUSS S1

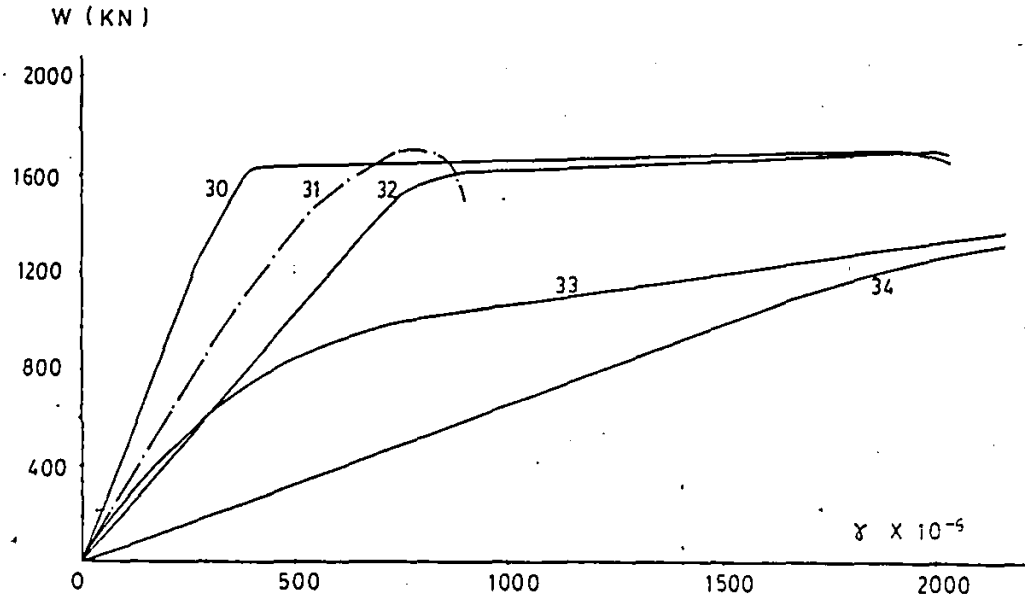

FIGURE 4.20 LOAD-SHEAR STRAIN CURVES FOR JOINT 2 OF TRUSS S1

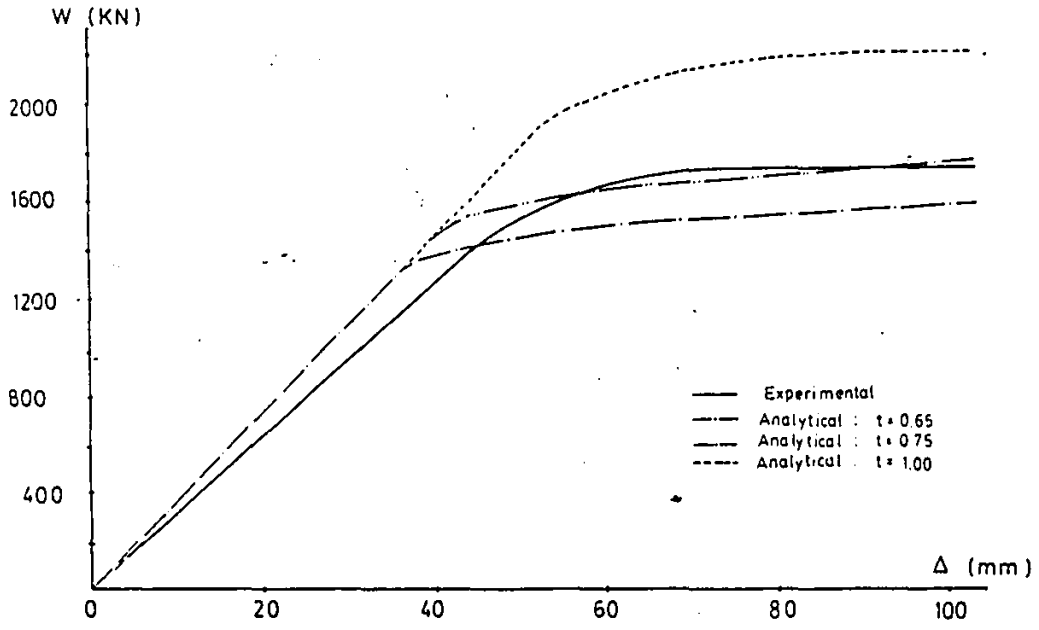

FIGURE 4.21 LOAD-DEFLECTION CURVES OF MID-SPAN FOR TRUSS S1

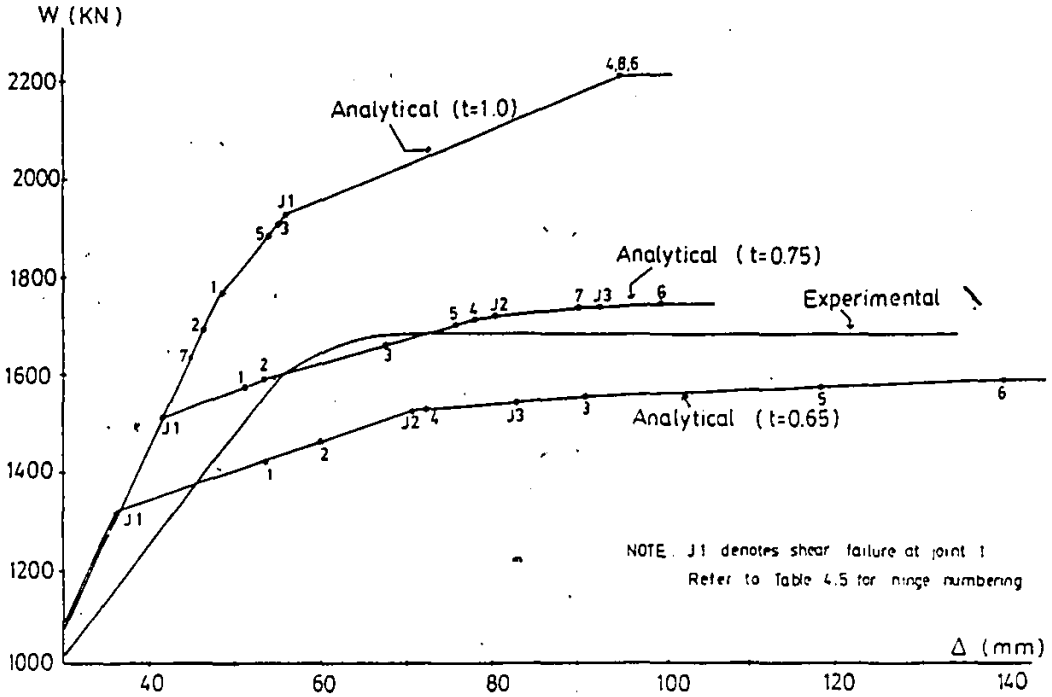

FIGURE 4.22 FAILURE SEQUENCE FOR TRUSS S1

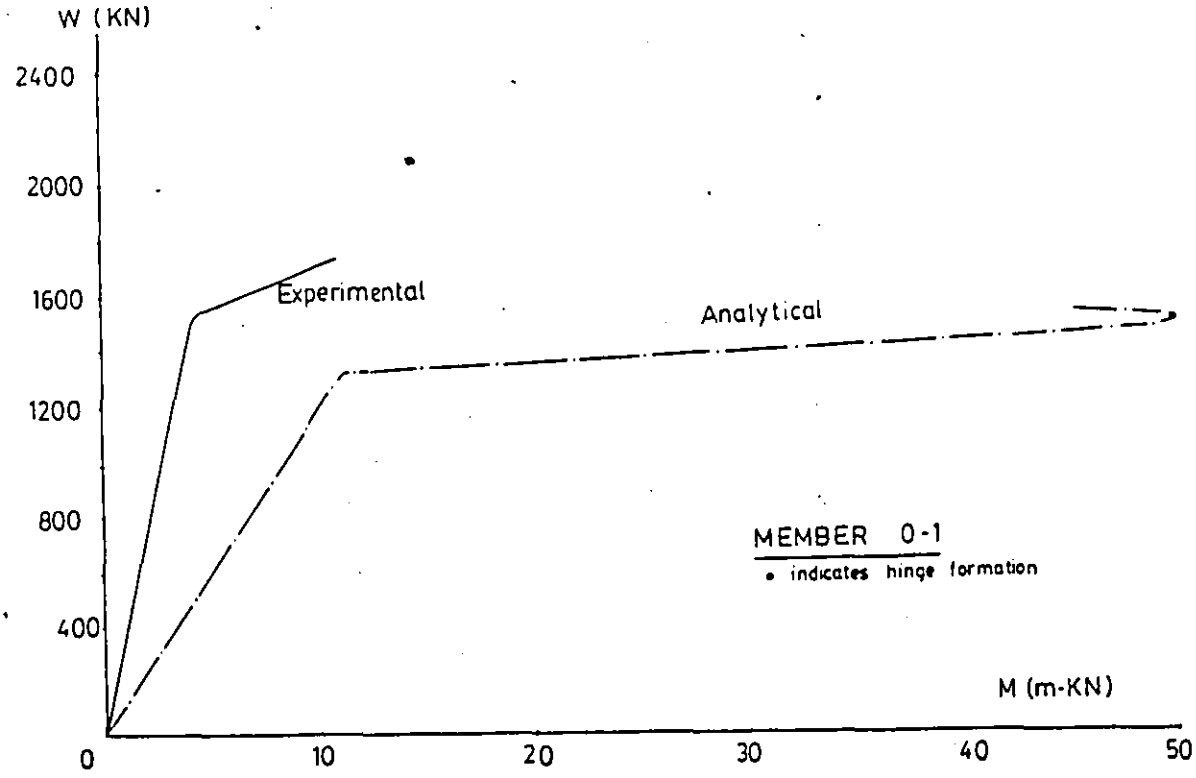

FIGURE 4.23 LOAD-MOMENT CURVES FOR DIAGONALS AT JOINT 0 OF TRUSS S1

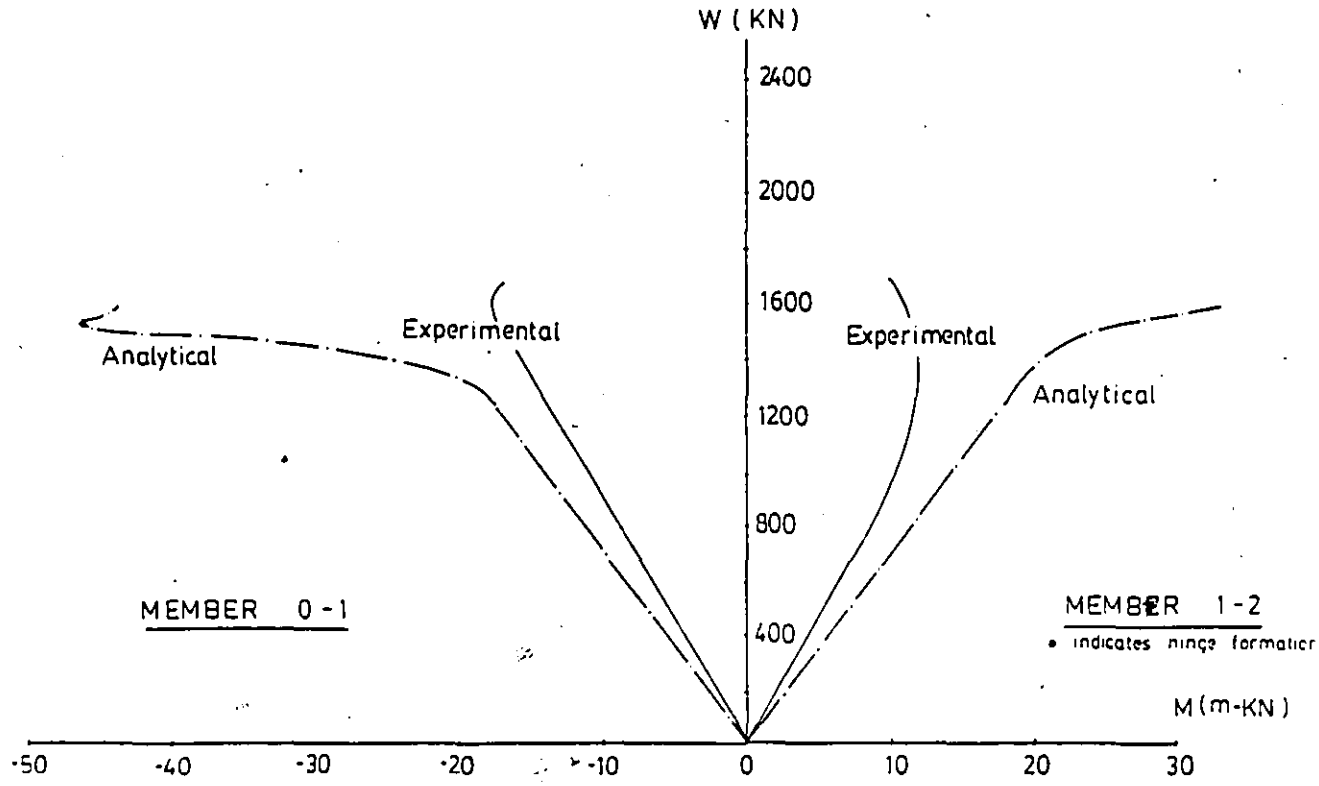

FIGURE 4.24 LOAD-MOMENT CURVES FOR DIAGONALS AT JOINT 1 OF TRUSS S1

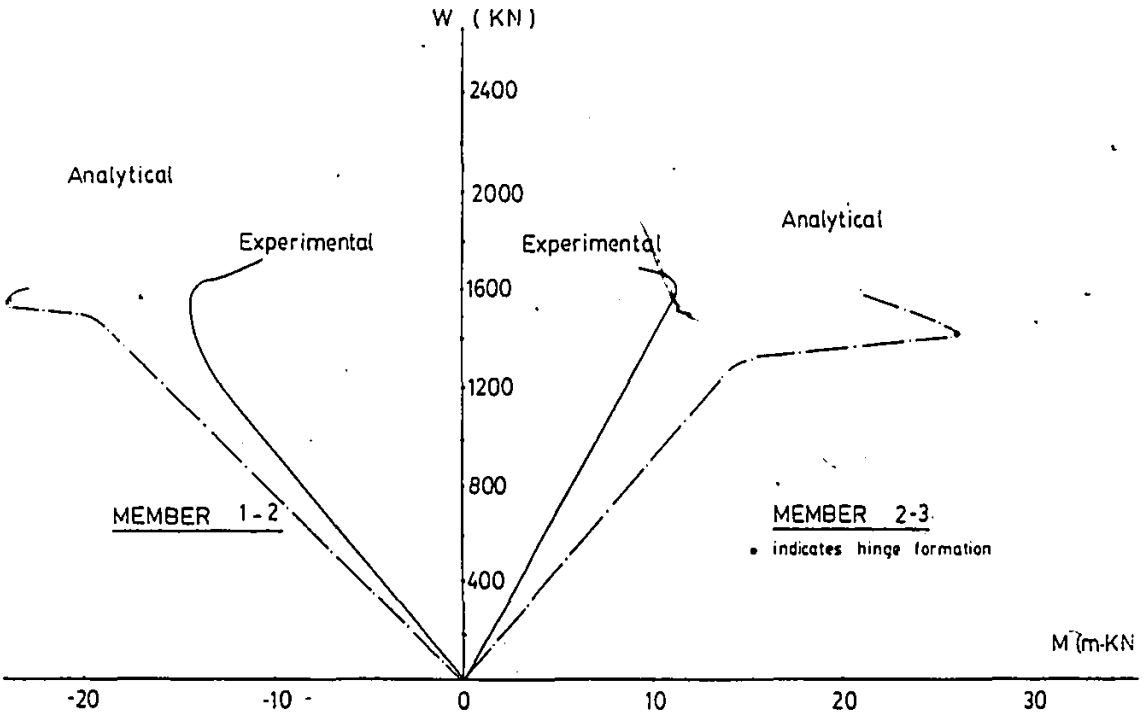

FIGURE 4.25 LOAD-MOMENT CURVES FOR DIAGONALS AT JOINT 2 OF TRUSS S1

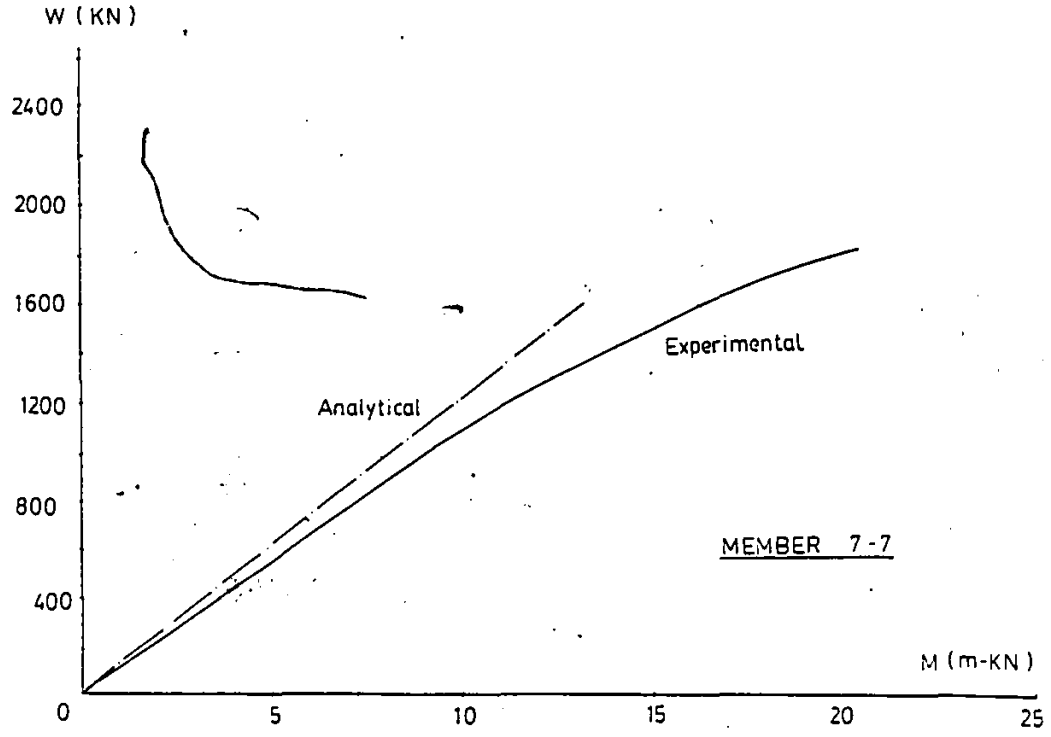

FIGURE 4.26 LOAD-MOMENT CURVES FOR TOP CHORD MEMBER OF TRUSS S1

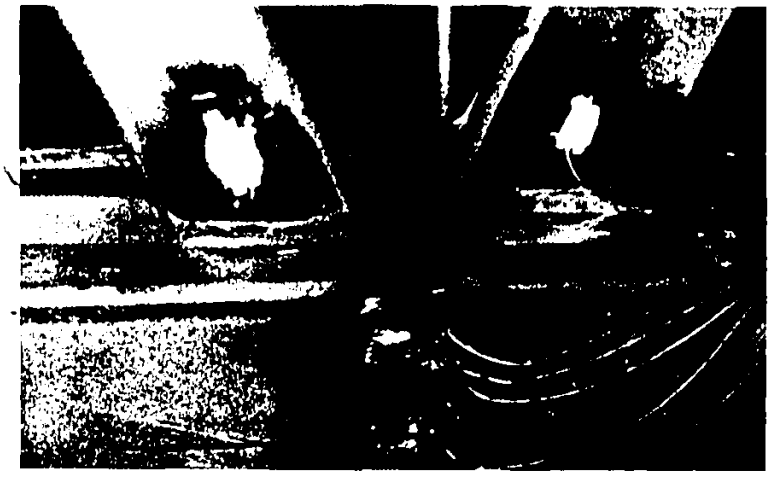

(a) Truss S1A

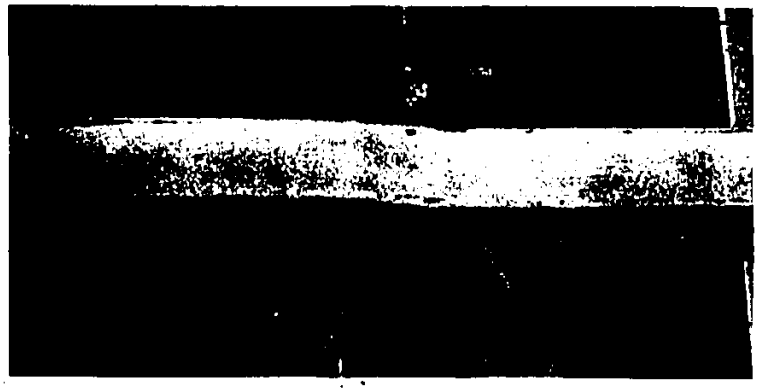

(b) Truss S1B

(c) Truss S1C

FIGURE 4.27 FAILURE MODE OF REINFORCED TRUSS S1

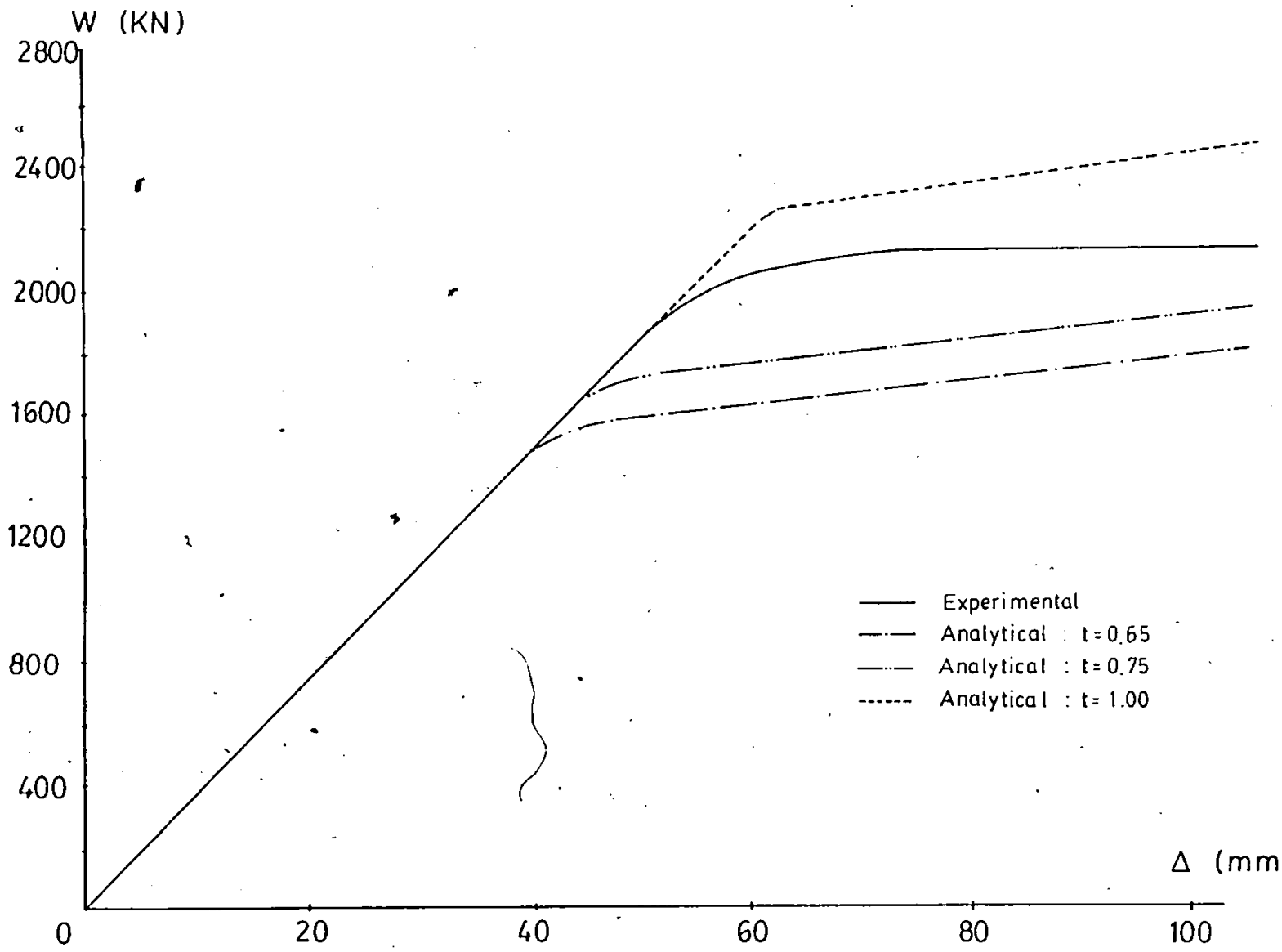

FIGURE 4.28 LOAD-DEFLECTION CURVES OF MID-SPAN FOR TRUSS S 1A

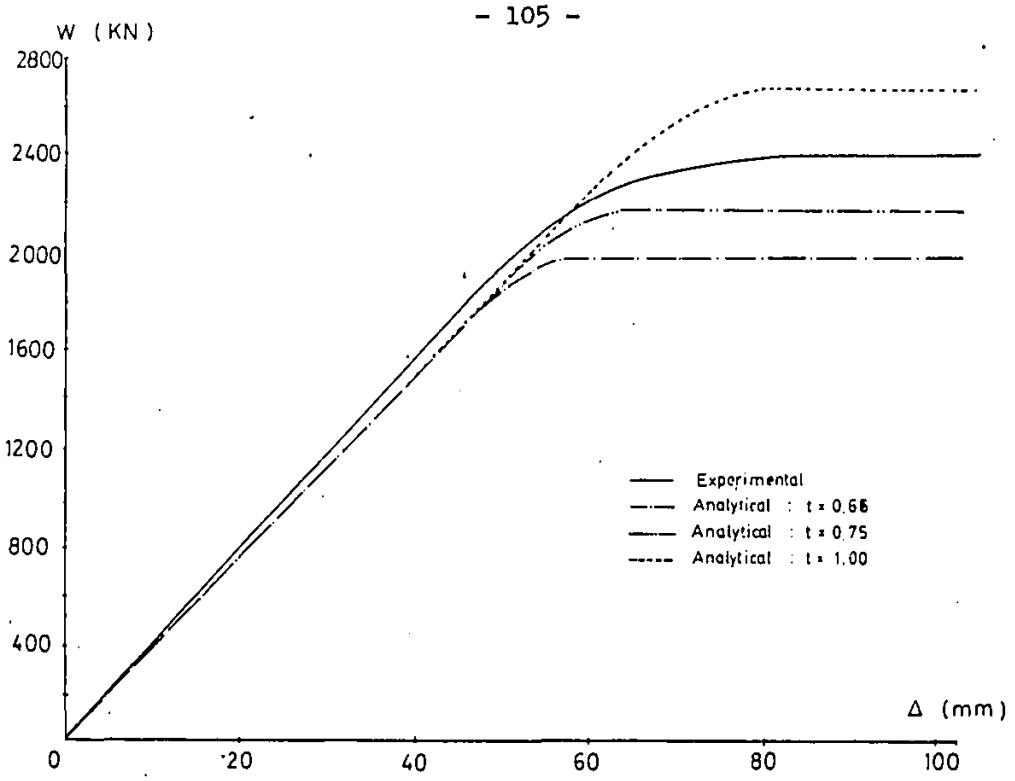

FIGURE 4.29 LOAD-DEFLECTION CURVES OF MID-SPAN FOR TRUSS S 1B

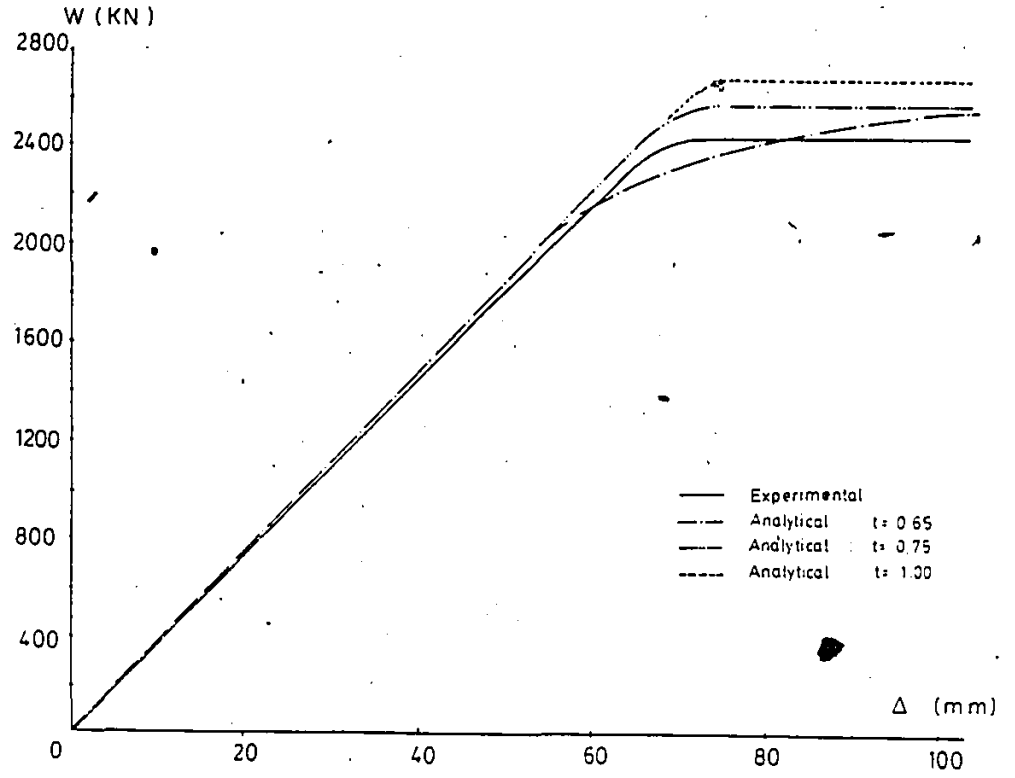

FIGURE 4.30 LOAD-DEFLECTION CURVES OF MID-SPAN FOR TRUSS S 1C

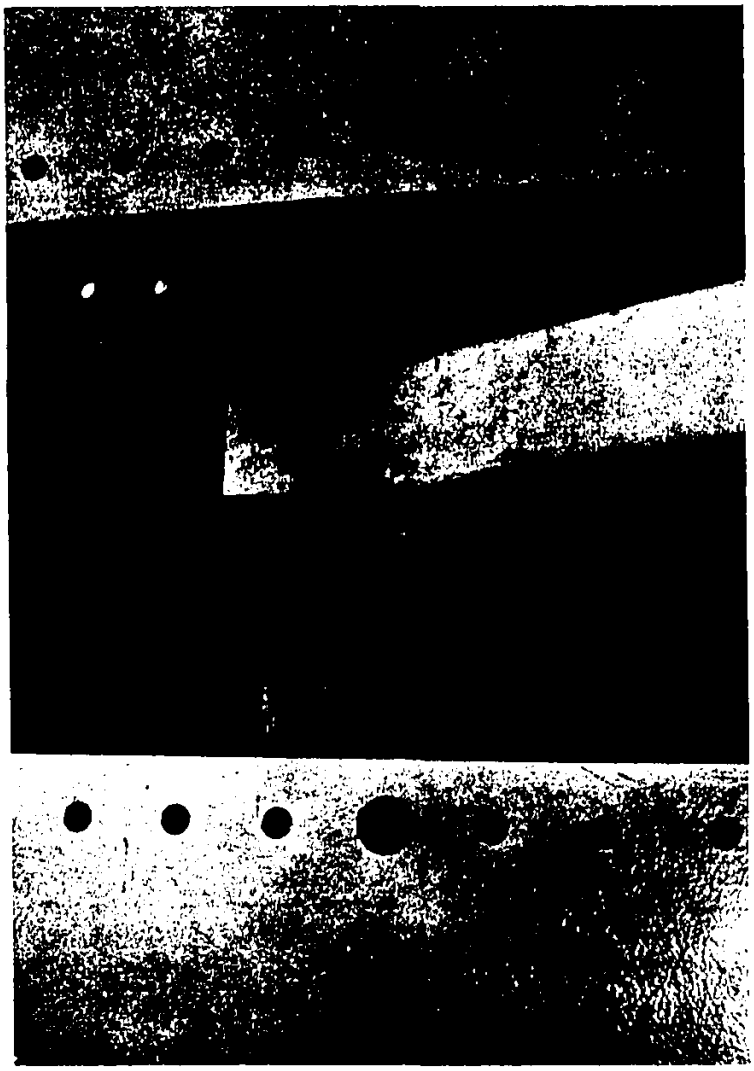

FIGURE 4.31 END-CAPPING OF TRUSS S2

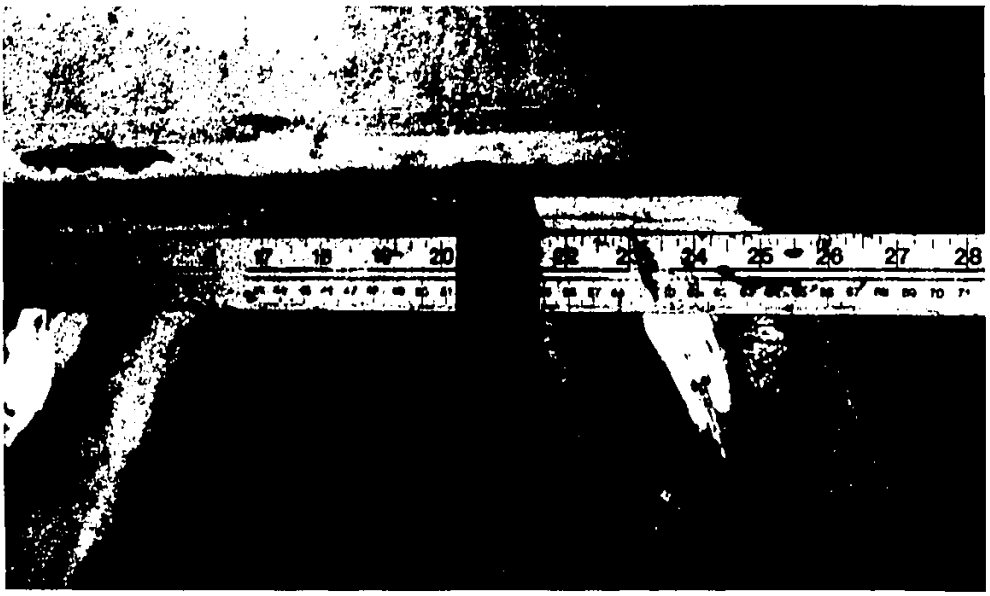

(a) Truss S2

(b) Truss S2A

FIGURE 4.32 FAILURE MODE OF STANDARD TYPE

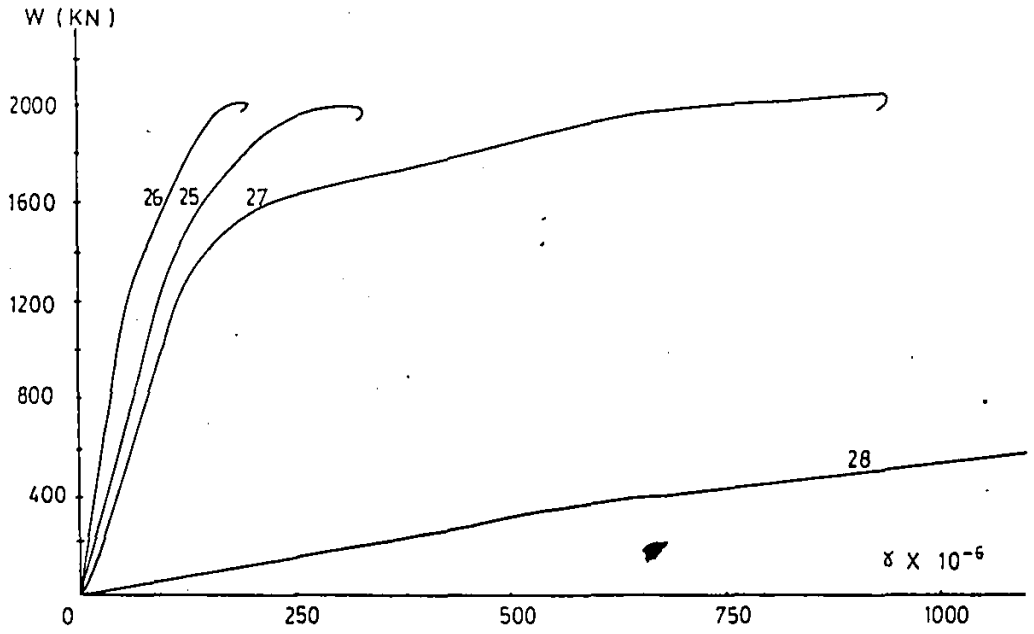

FIGURE 4.33 LOAD-SHEAR STRAIN CURVES FOR JOINT 1 OF TRUSS S2

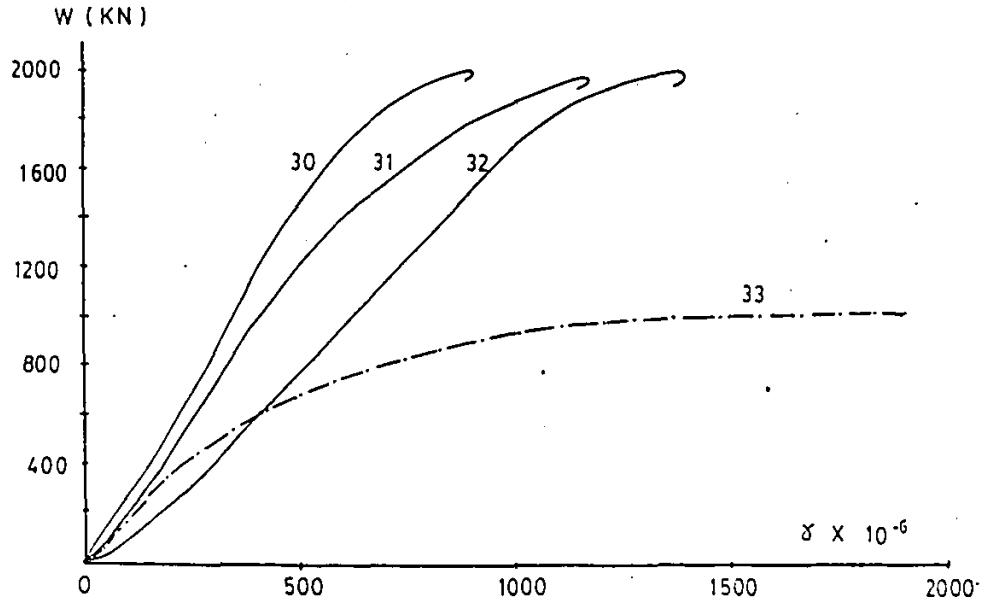

FIGURE 4.34 LOAD-SHEAR STRAIN CURVES FOR JOINT 2 OF TRUSS S2

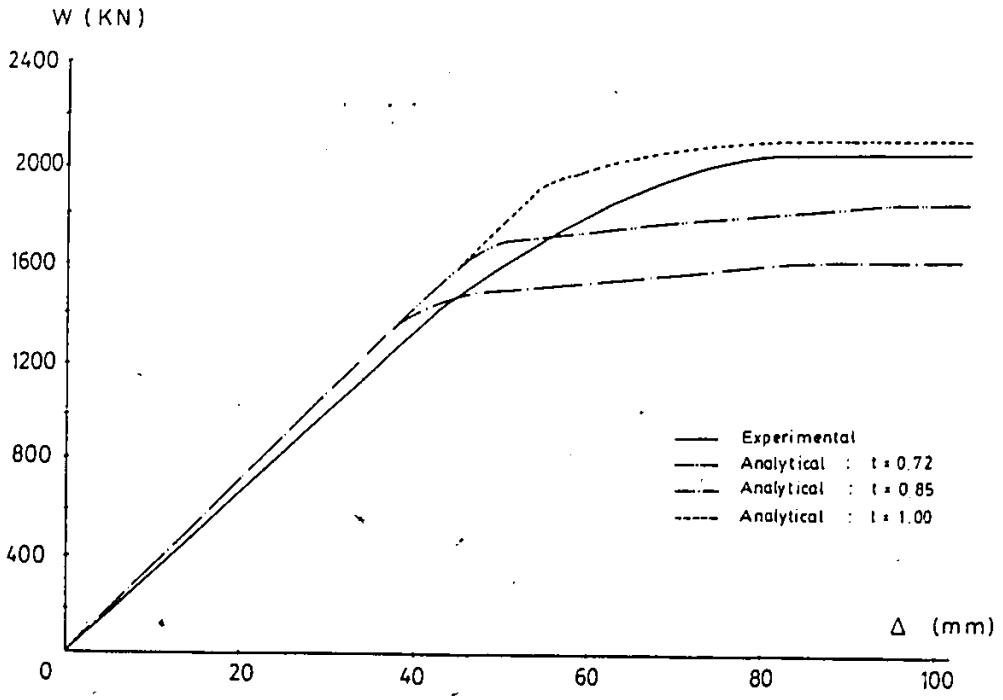

FIGURE 4.35 LOAD-DEFLECTION CURVES OF MID-SPAN FOR TRUSS S2

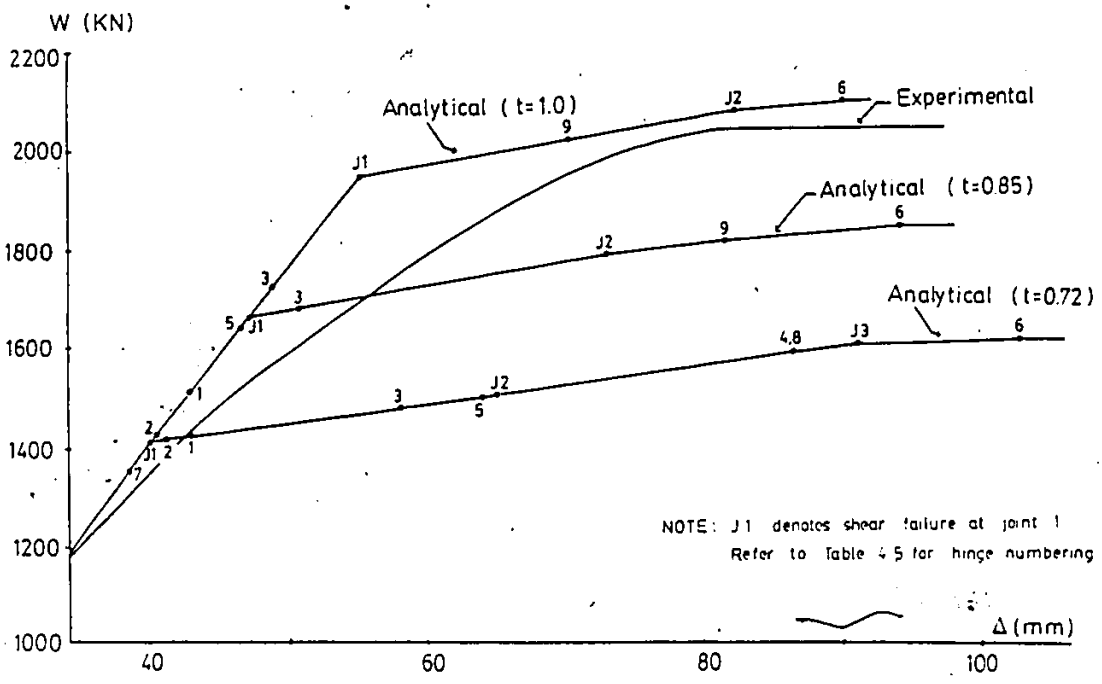

FIGURE 4.36 FAILURE SEQUENCE FOR TRUSS S2

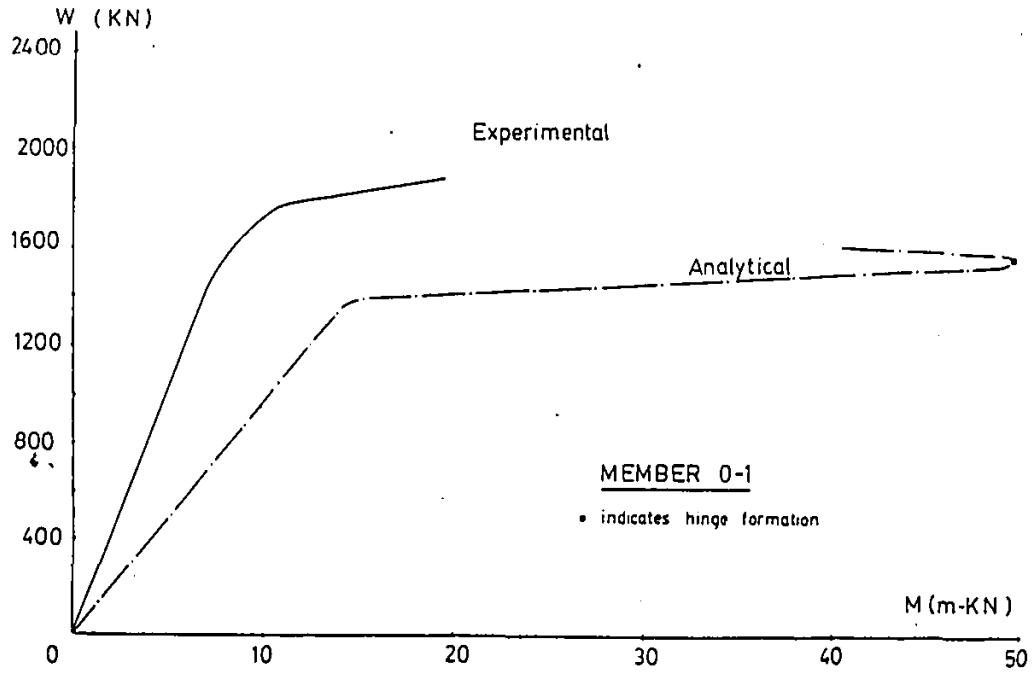

FIGURE 4.37 LOAD-MOMENT CURVES FOR DIAGONALS AT JOINT 0 OF TRUSS S2

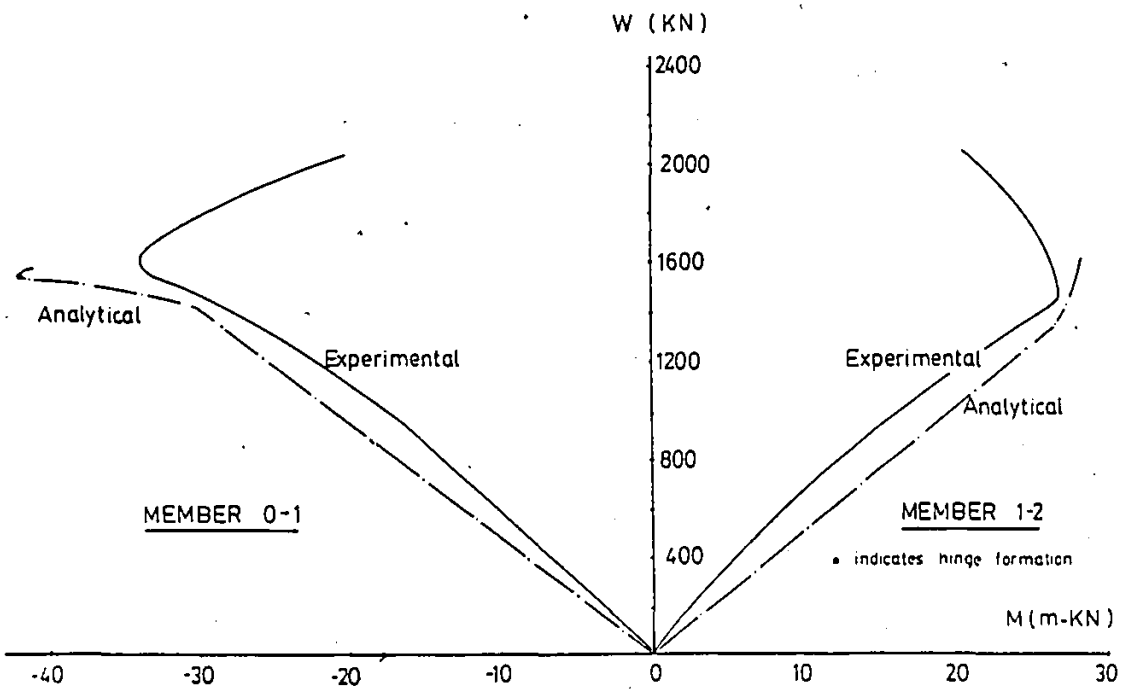

FIGURE 4.38 LOAD-MOMENT CURVES FOR DIAGONALS AT JOINT 1 OF TRUSS S2

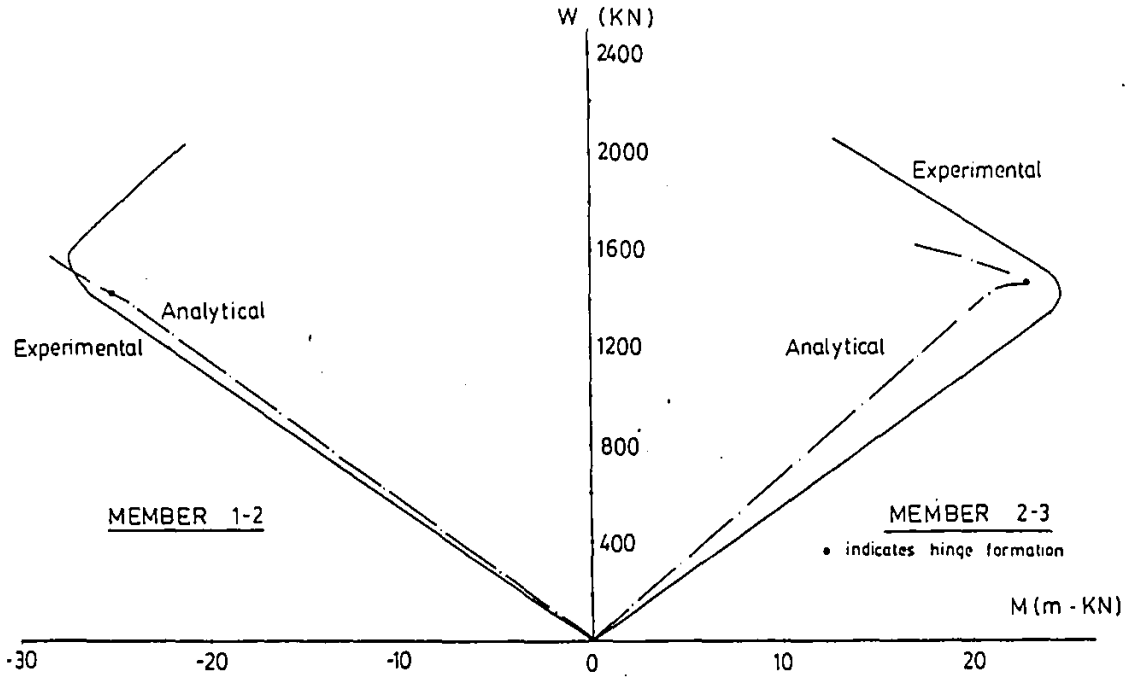

FIGURE 4.39 LOAD-MOMENT CURVES FOR DIAGONALS AT JOINT 2 OF TRUSS S2

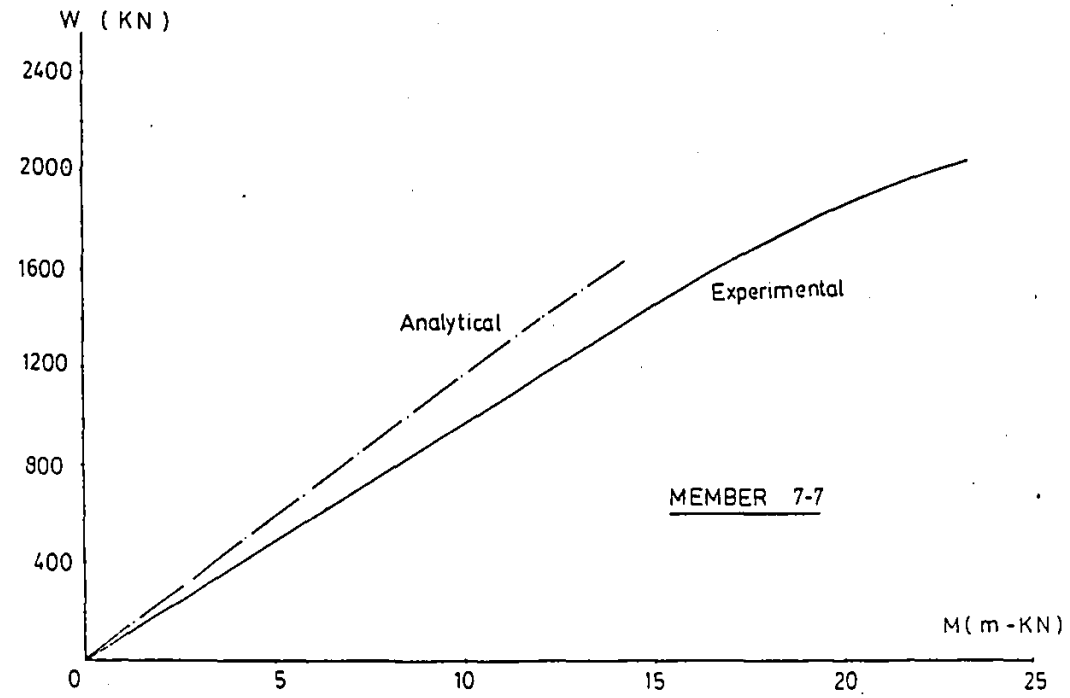

FIGURE 4.40 LOAD-MOMENT CURVES FOR TOP CHORD MEMBER OF TRUSS S2

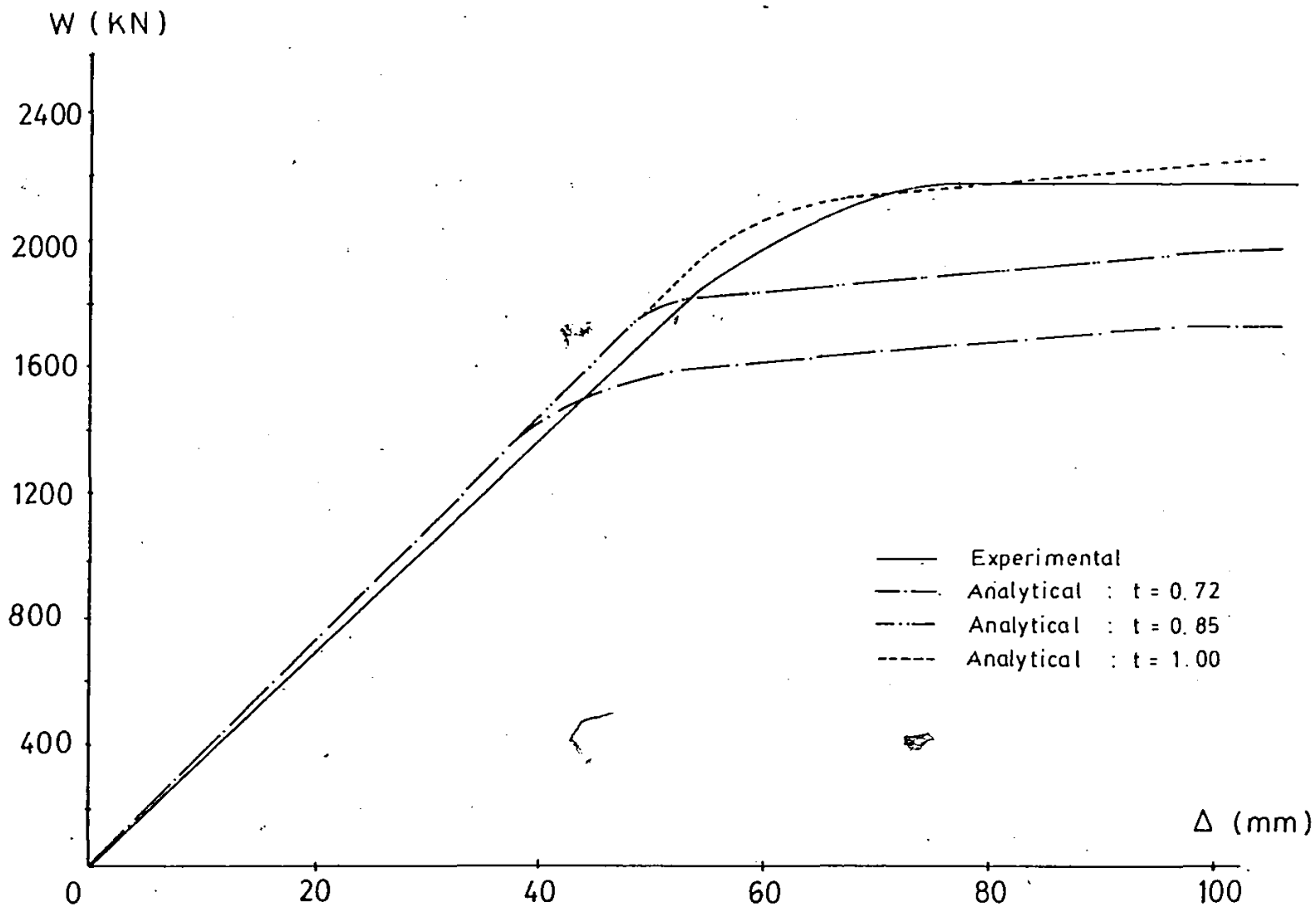

FIGURE 4.41 LOAD-DEFLECTION CURVES OF MID-SPAN FOR TRUSS S 2A

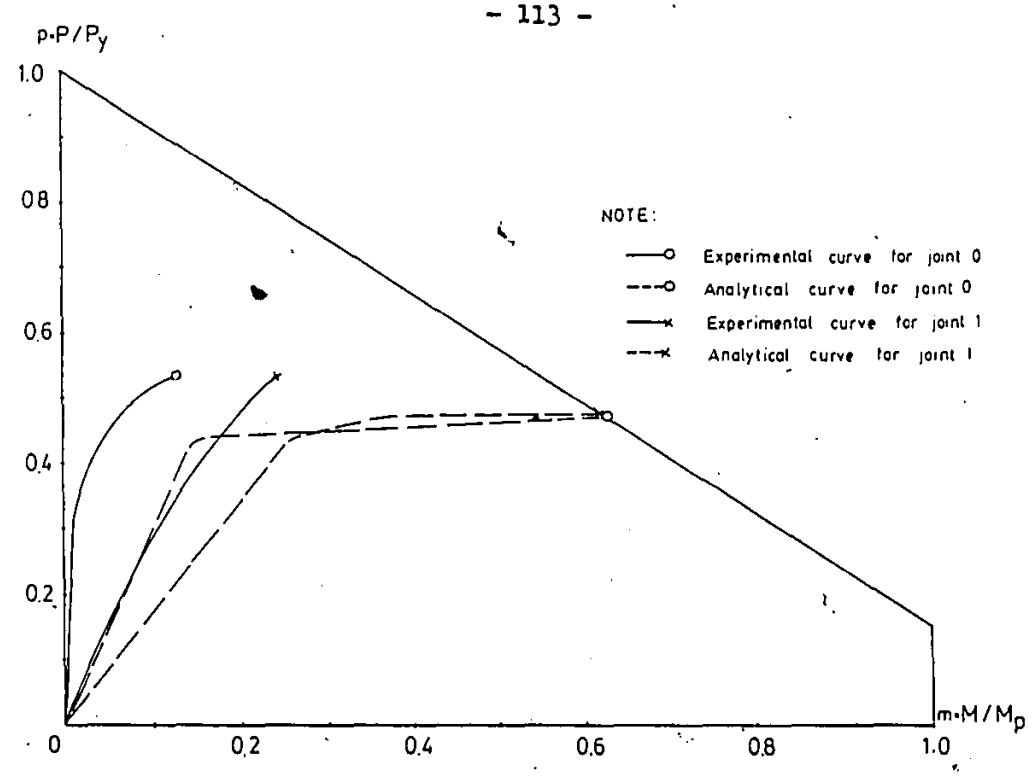

FIGURE 4.42 INTERACTION DIAGRAM FOR MEMBER 0-1 OF TRUSS S1

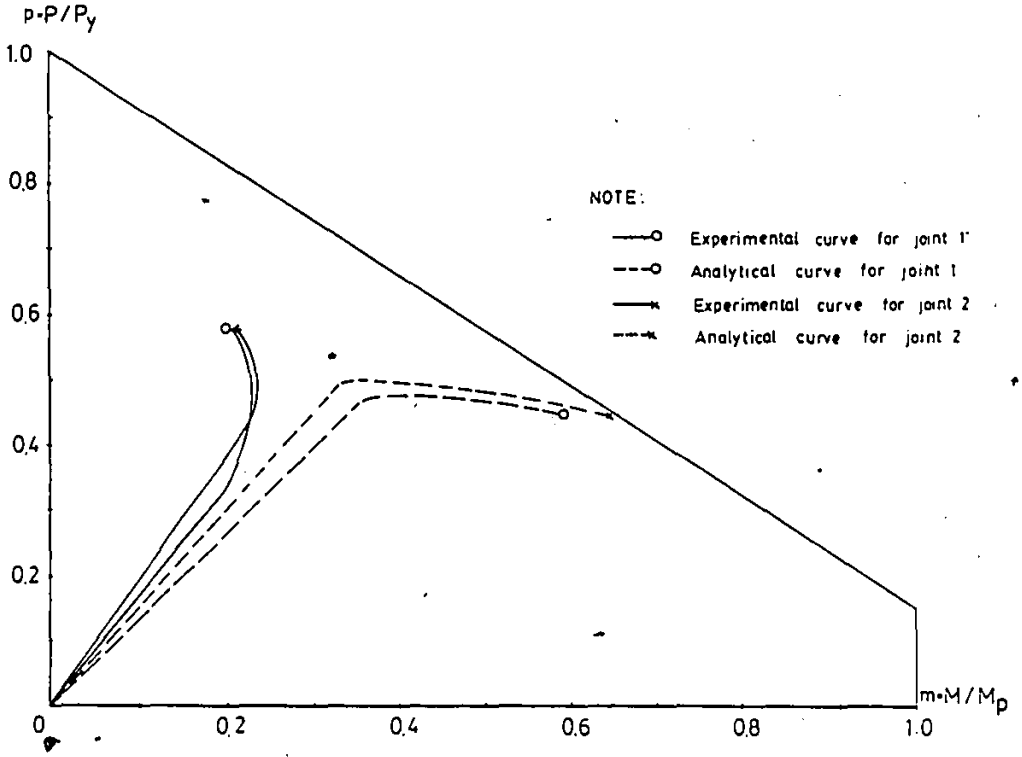

FIGURE 4.43 INTERACTION DIAGRAM FOR MEMBER 1-2 OF TRUSS S1

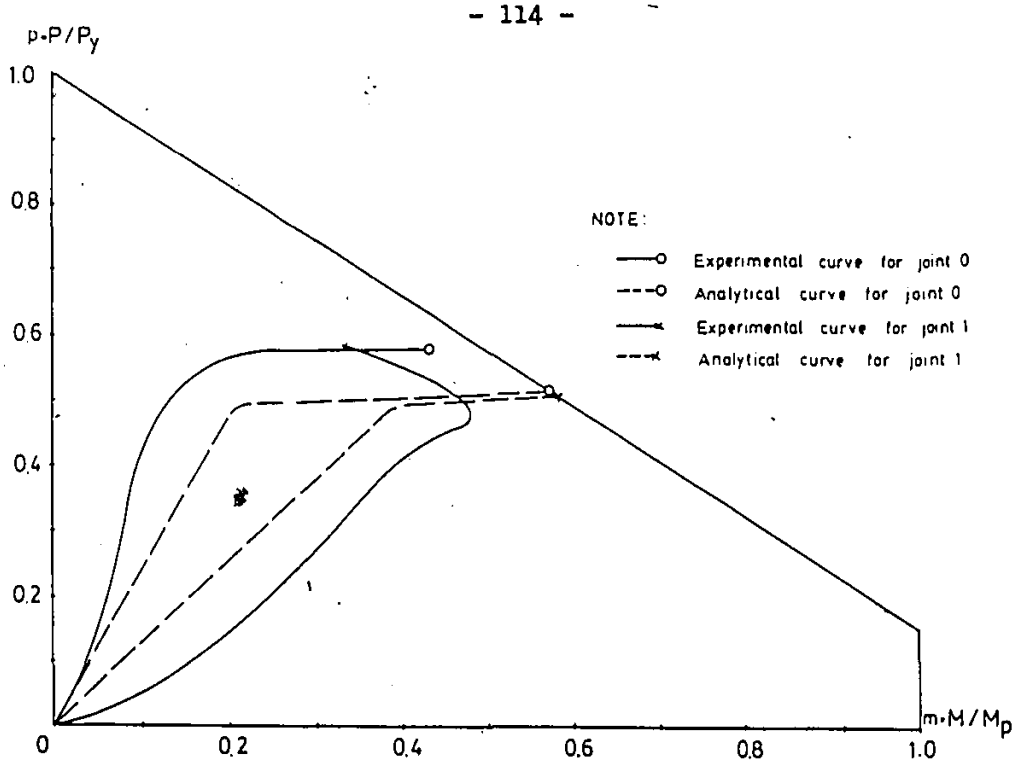

FIGURE 4.44 INTERACTION DIAGRAM FOR MEMBER 0-1 OF TRUSS S2

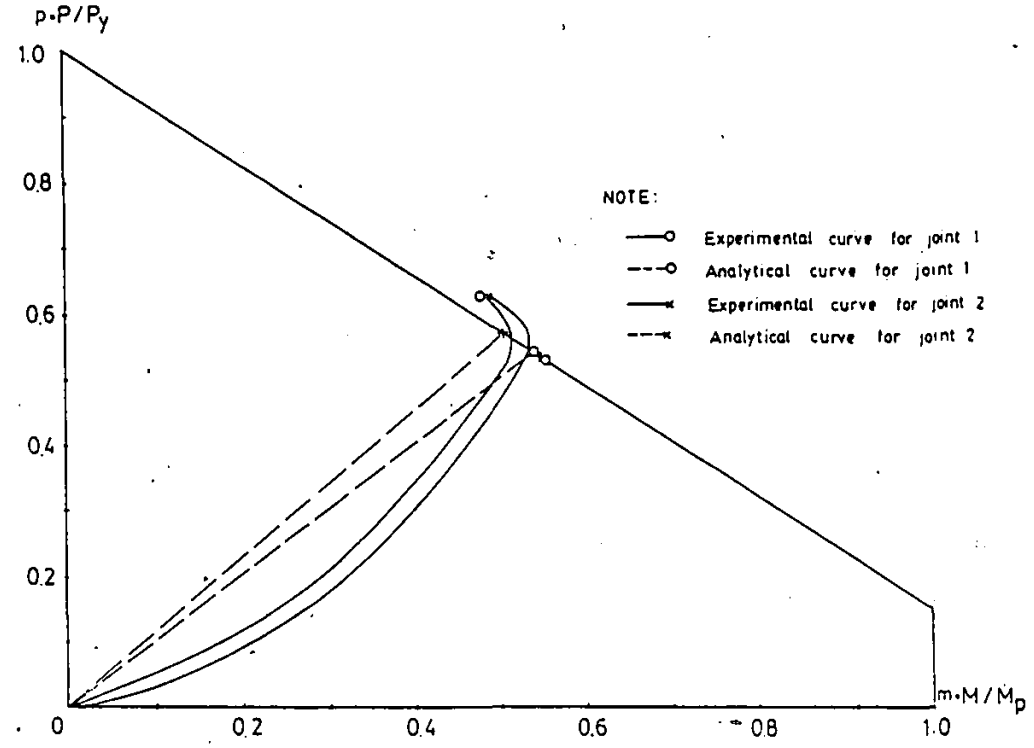

FIGURE 4.45 INTERACTION DIAGRAM FOR MEMBER 1-2 OF TRUSS S2

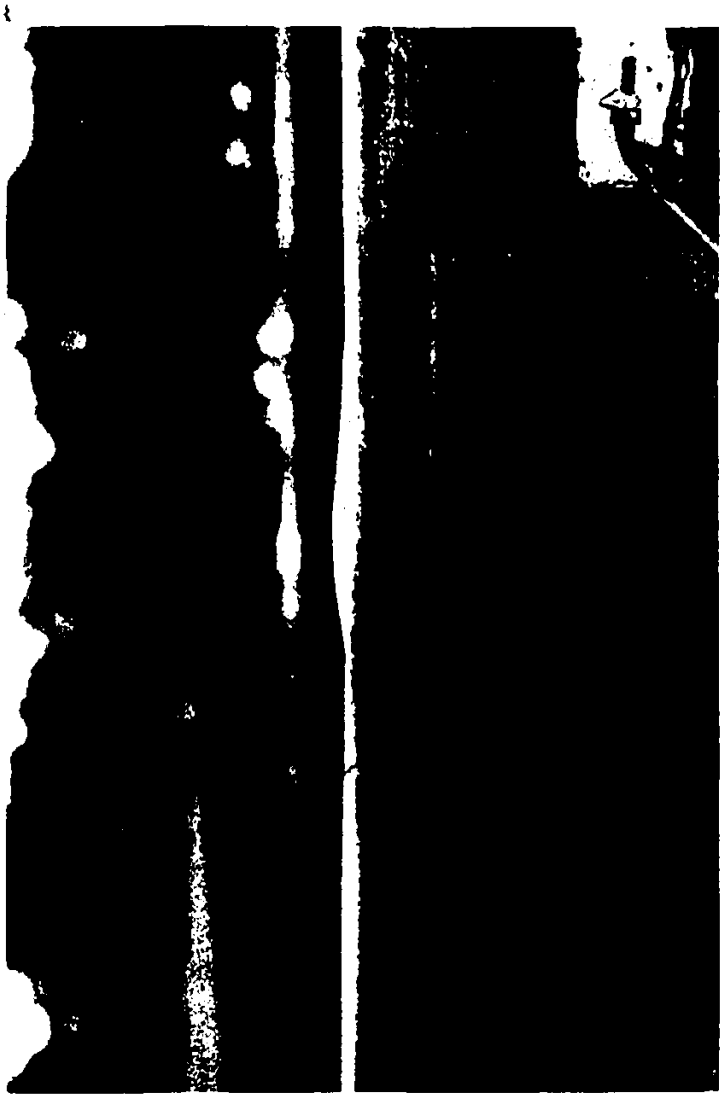

FIGURE 4.46 FAILURE MODE OF TRUSS B0

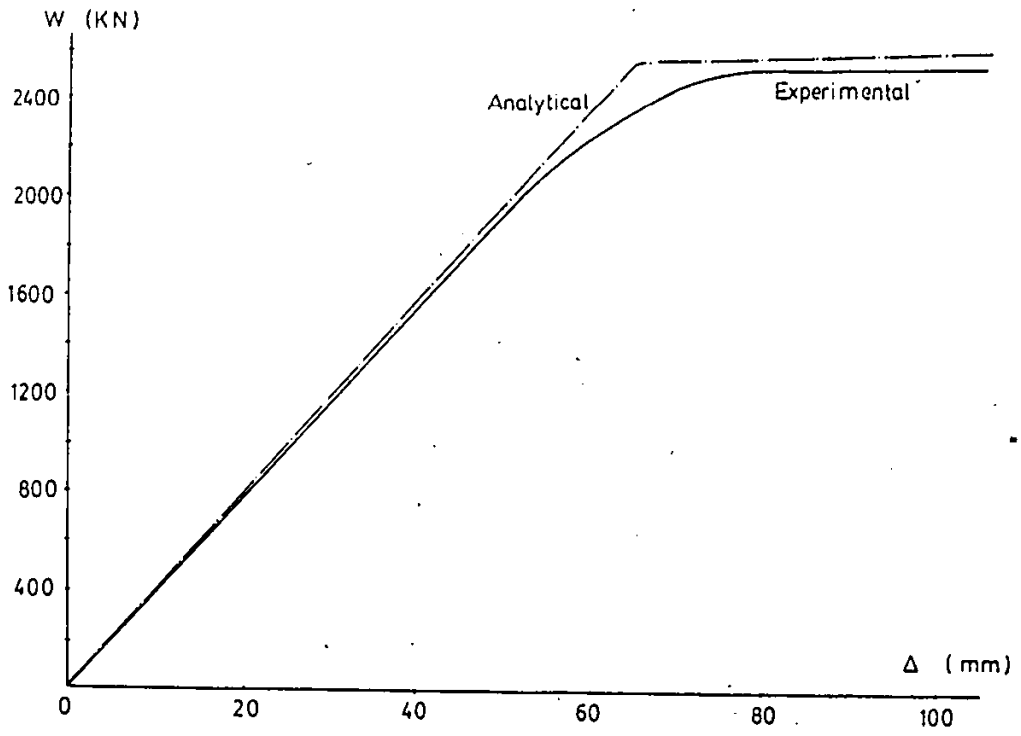

FIGURE 4.47 LOAD-DEFLECTION CURVES OF MID-SPAN FOR TRUSS B0

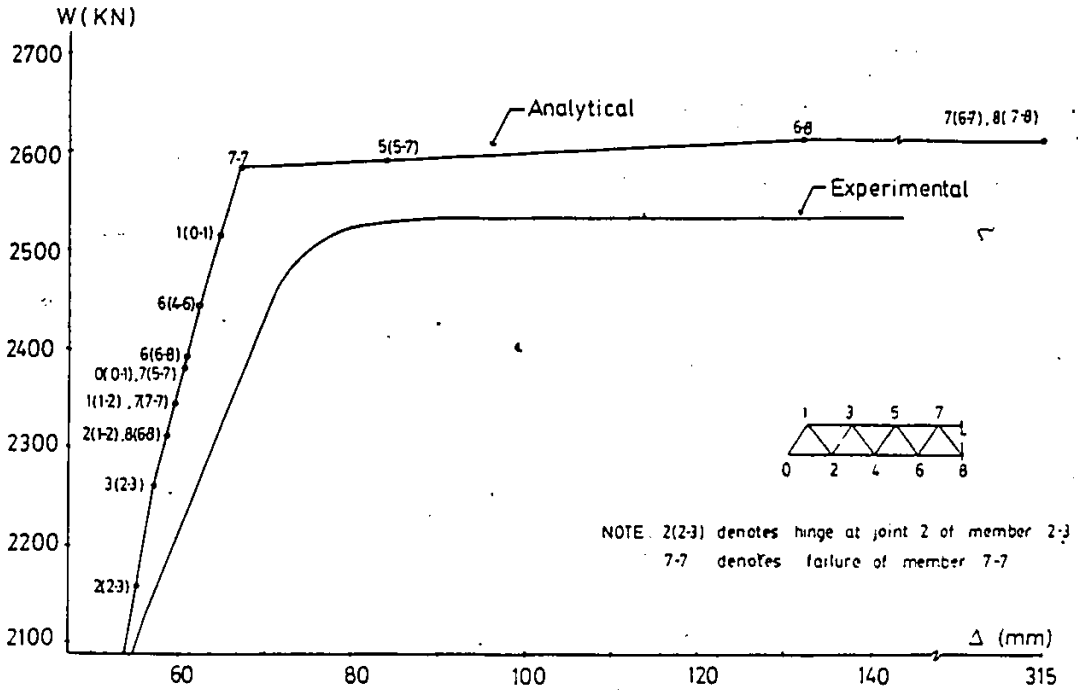

FIGURE 4.48 FAILURE SEQUENCE FOR TRUSS B0

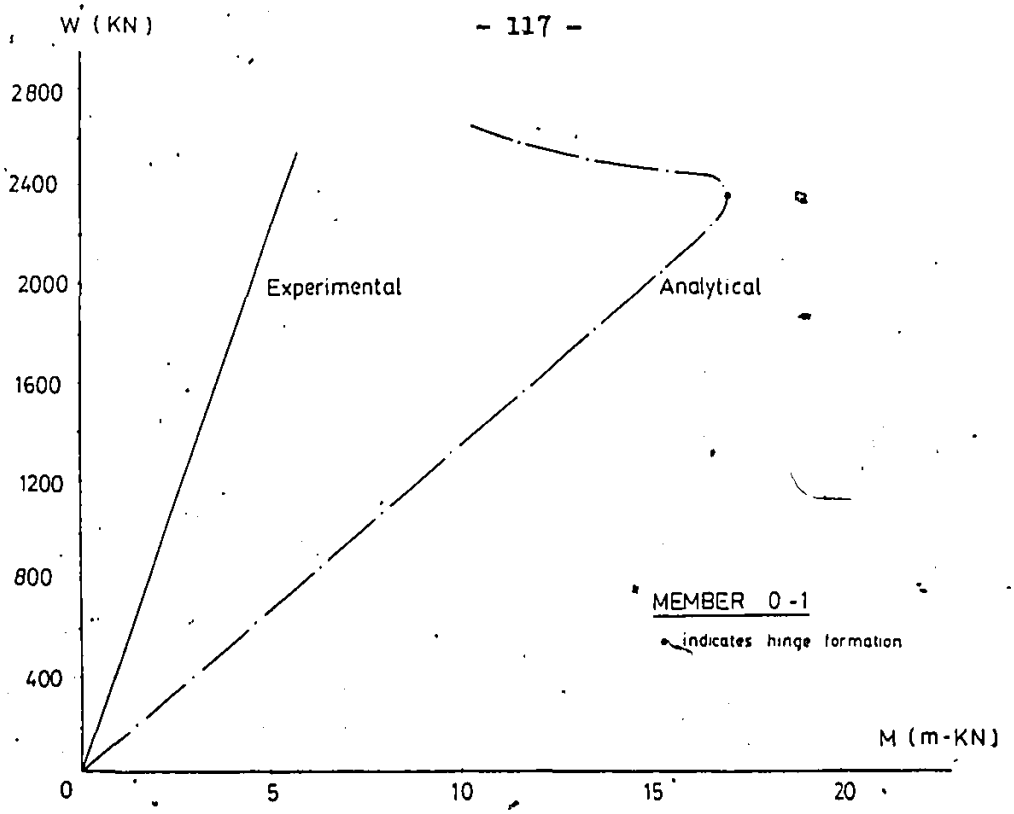

FIGURE 4.49 LOAD-MOMENT CURVES FOR DIAGONALS AT JOINT 0 OF TRUSS BO

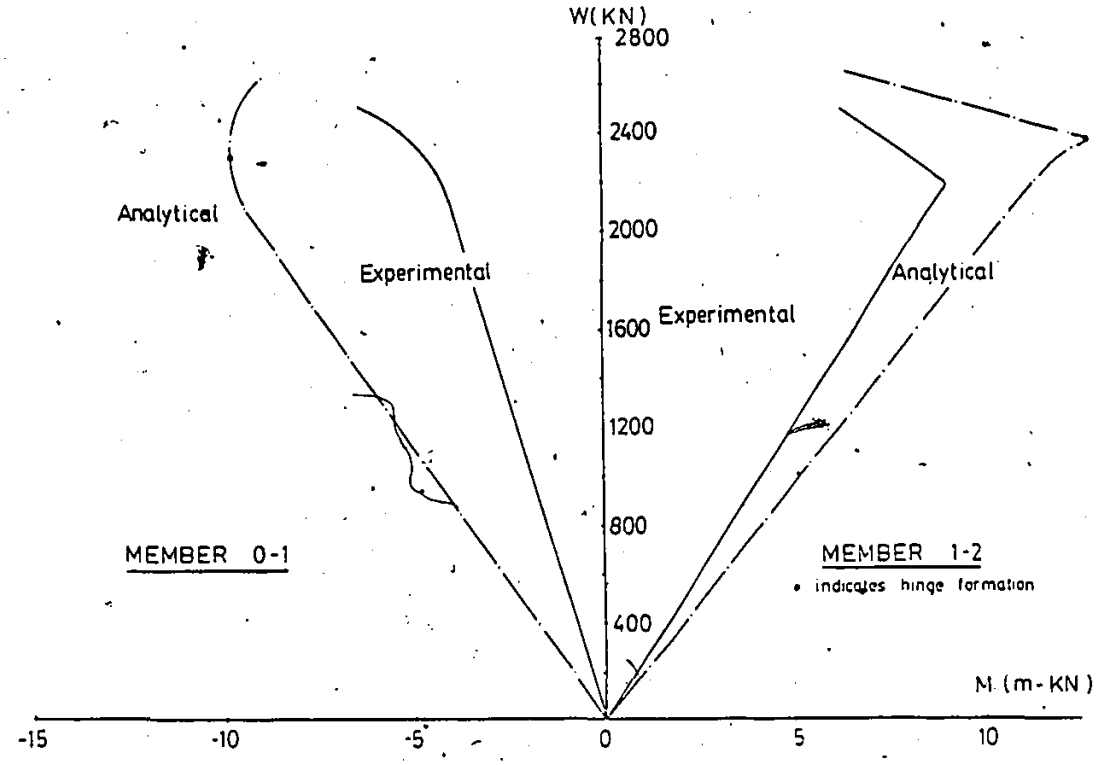

FIGURE 4.50 LOAD-MOMENT CURVES FOR DIAGONALS AT JOINT 1 OF TRUSS BO

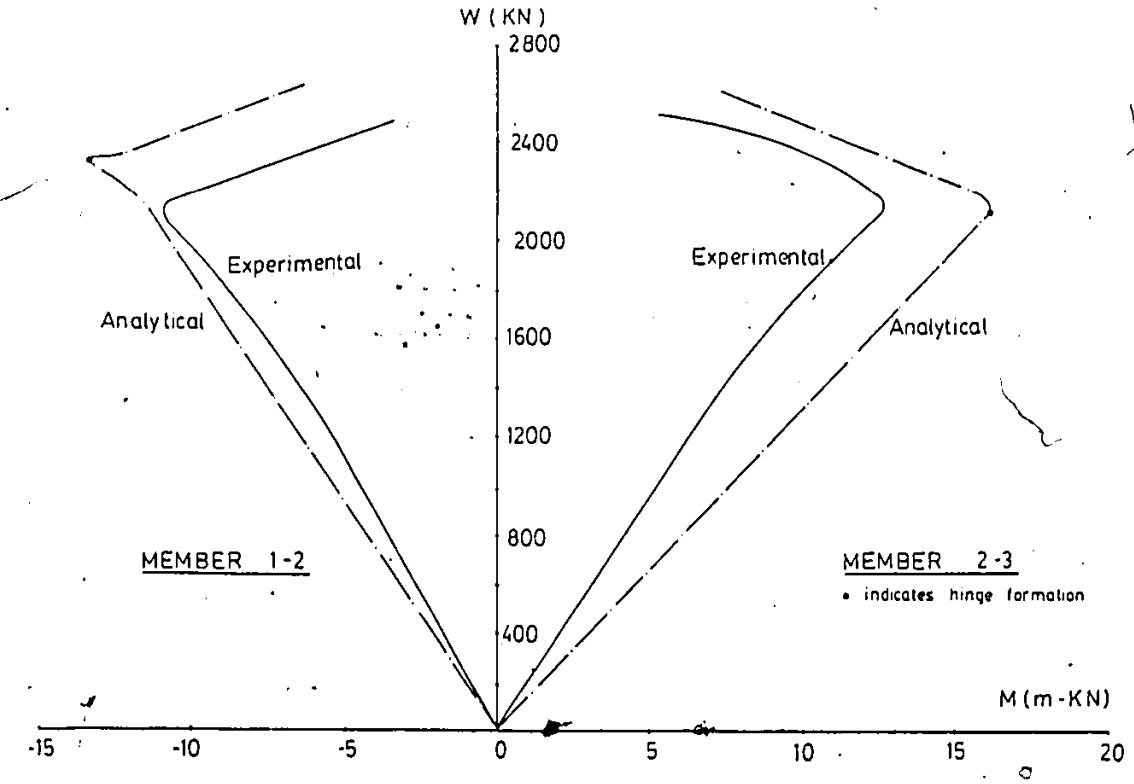

FIGURE 4.51 LOAD-MOMENT CURVES FOR DIAGONALS AT JOINT 2 OF TRUSS BO.

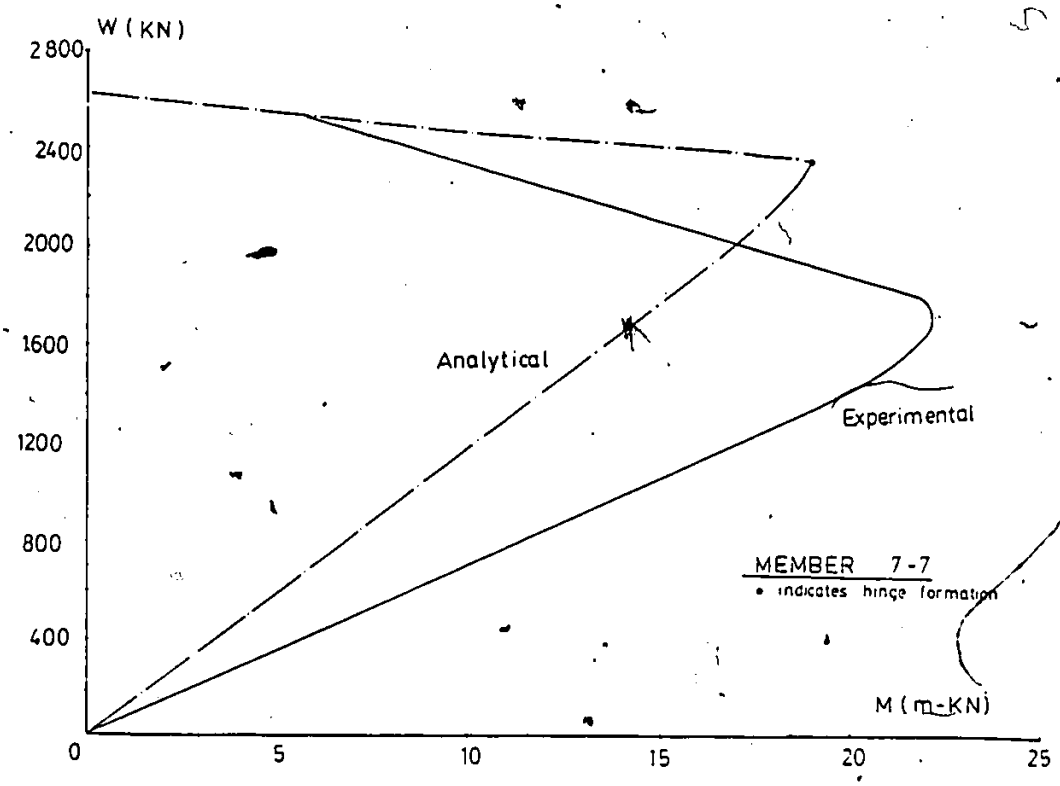

FIGURE 4.52 LOAD-MOMENT CURVES FOR TOP CHORD MEMBER OF TRUSS BO

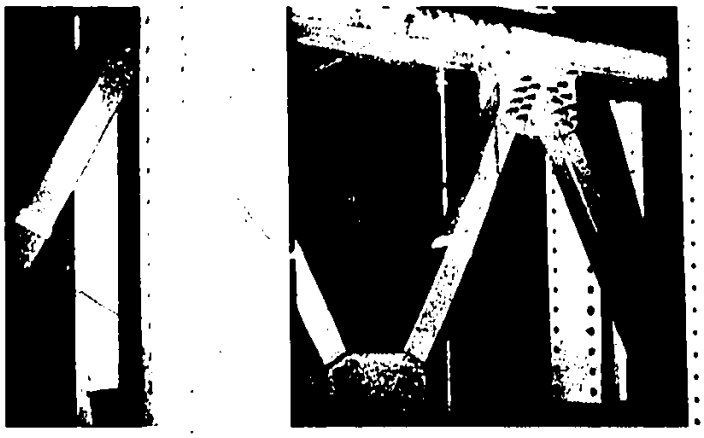

(a) Truss B0A

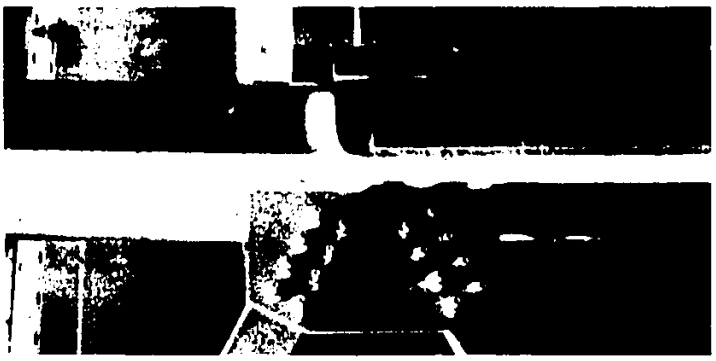

(b) Truss B0B

(c) Truss B0C

FIGURE 4.53 FAILURE MODE OF REINFORCED TRUSS B0

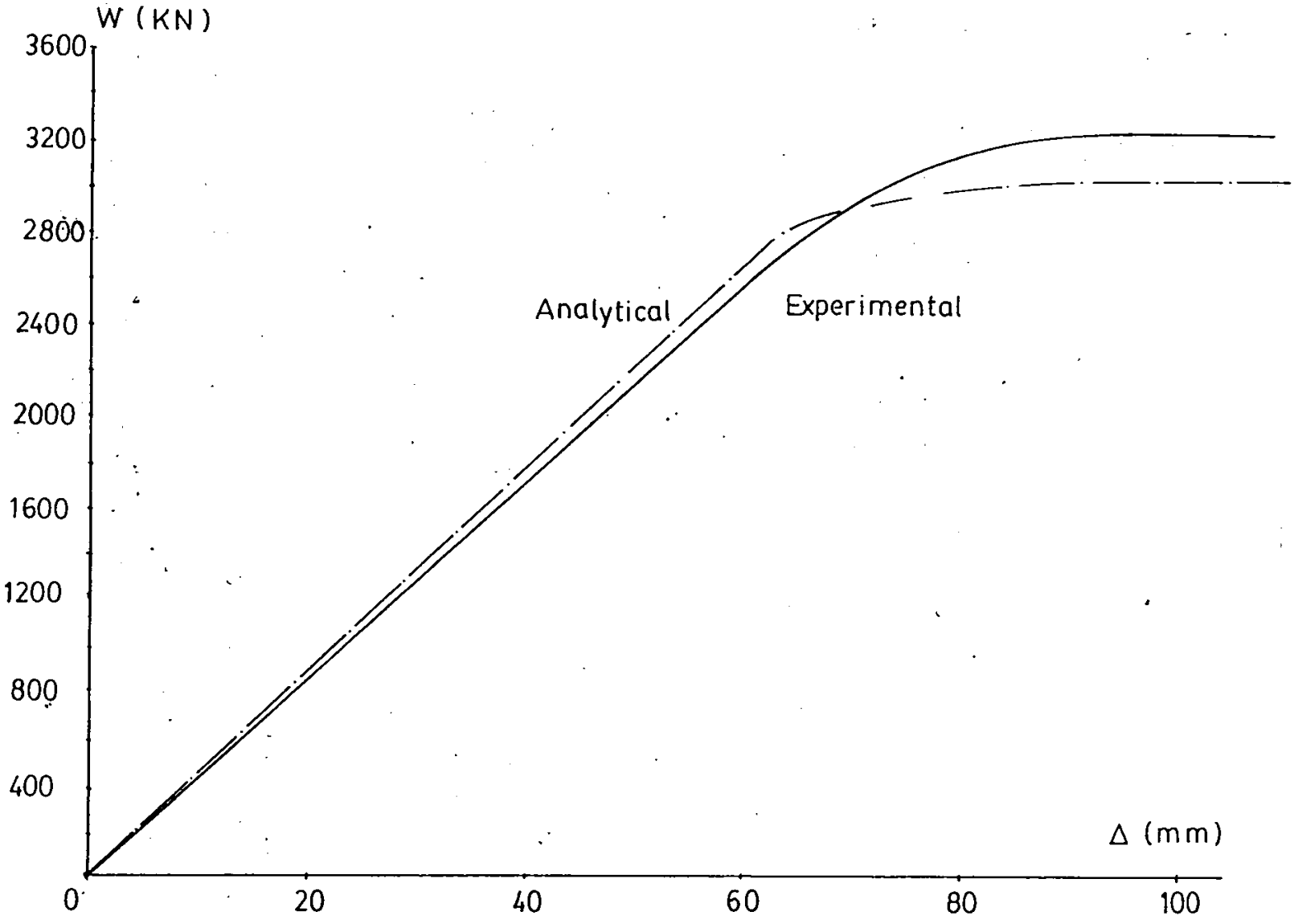

FIGURE 4.54 LOAD-DEFLECTION CURVES OF MID-SPAN FOR TRUSS B0A

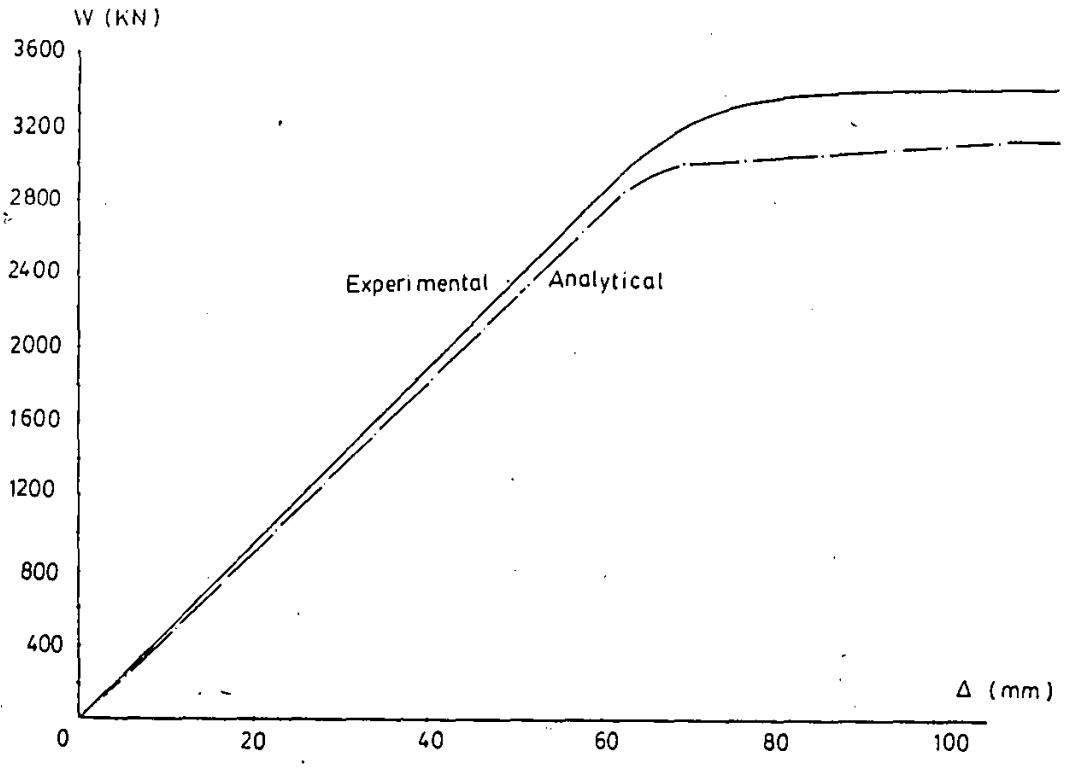

FIGURE 4.55 LOAD-DEFLECTION CURVES OF MID-SPAN FOR TRUSS B0B

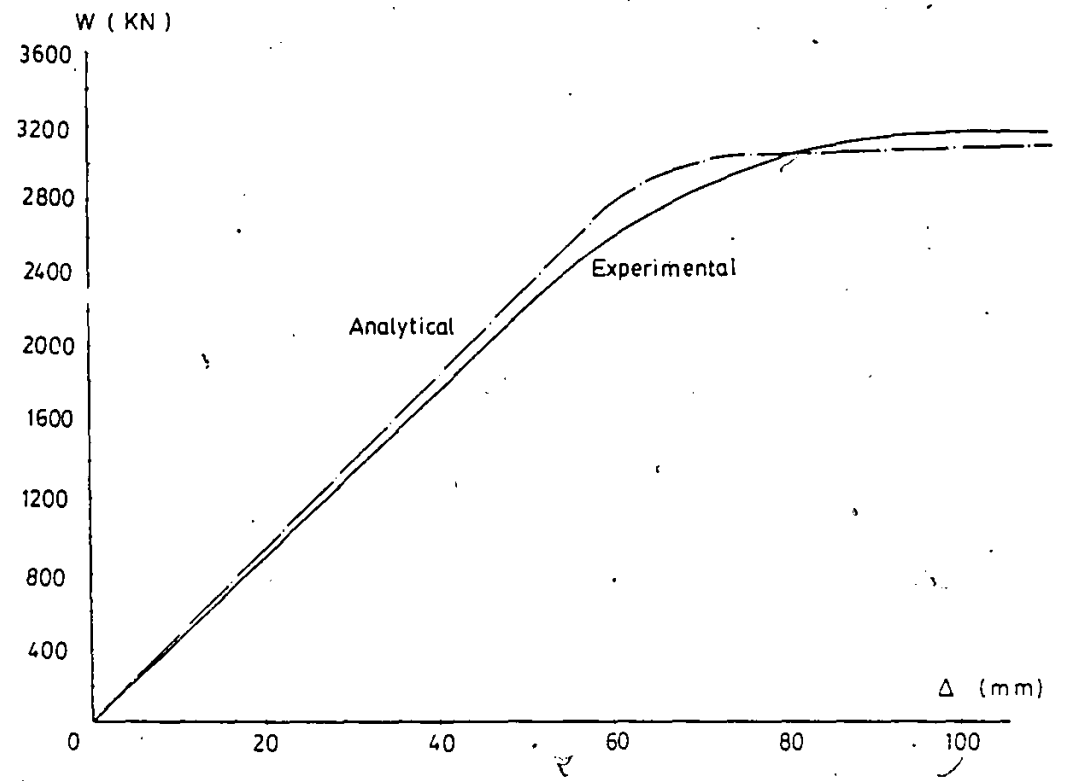

FIGURE 4.56 LOAD-DEFLECTION CURVES OF MID-SPAN FOR TRUSS B0C

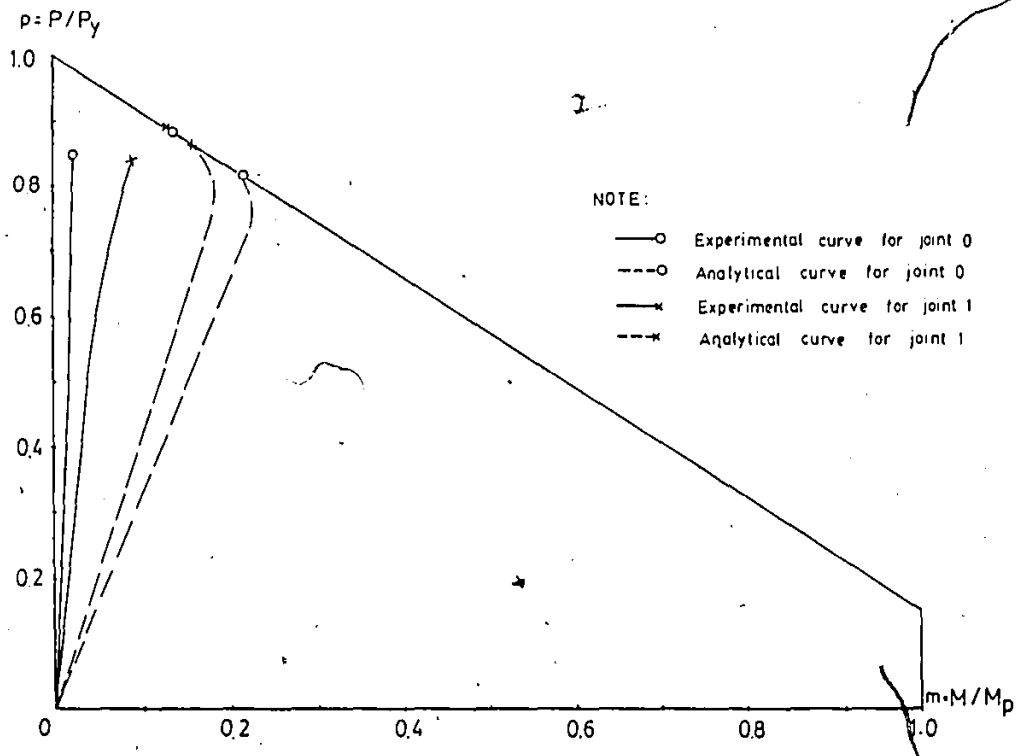

FIGURE 4.57 INTERACTION DIAGRAM FOR MEMBER 0-1 OF TRUSS B0

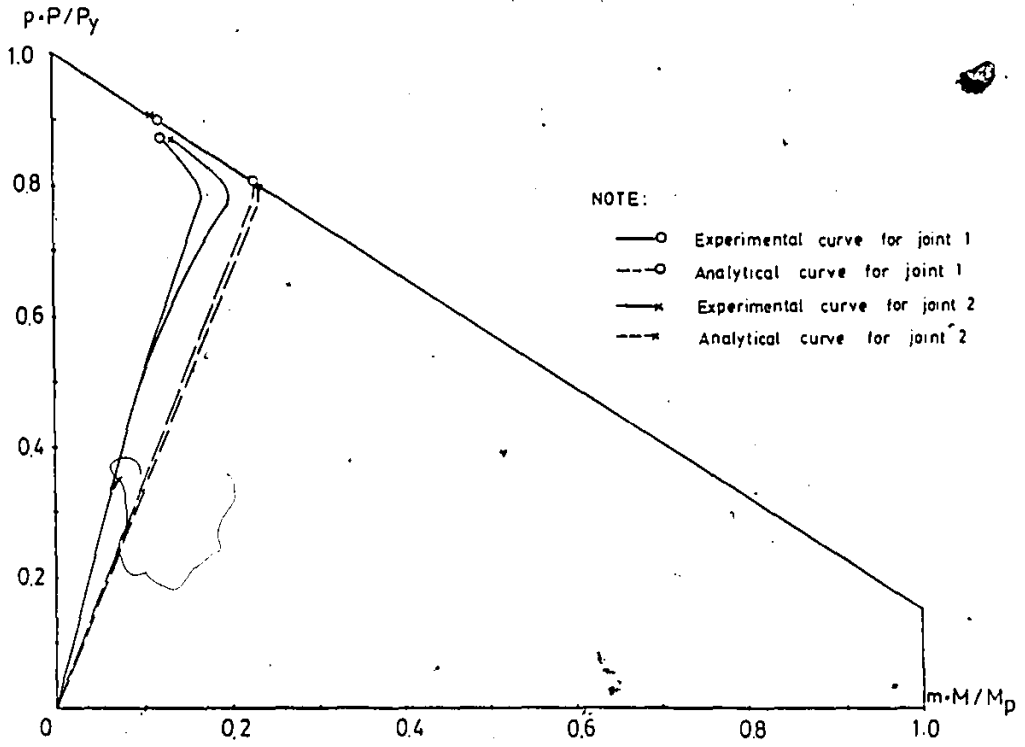

FIGURE 4.58 INTERACTION DIAGRAM FOR MEMBER 1-2 OF TRUSS B0

Member	Joint	Strain Gauge Number	W/W_{max}	
			Experimental	Analytical
0 - 1	0	1	0.93	0.92
		2	*	
	1	3	*	0.73
		4	0.85	
1 - 2	1	5	0.64	0.60
		6	*	
	2	7	*	0.62
		8	0.72	
2 - 3	2	9	0.52	0.64
		10	*	
7 - 7	7	20	1.00	0.85
		21	0.85	
	Centre	22	1.0	*
	Span	24	1.0	

Note: W = Total load on truss

W_{max} = Failure load of truss

Yielding is based on σ_y = 394.4 MPa

* indicates ratio exceeds 1.0

Table 4.1 Ratio of applied load to Truss BBST failure load for yielding at extreme fibres of members

Member	Joint	Strain Gauge Number	W/W_{max}	
			Experimental	Analytical
0 - 1	0	1	0.96	*
		2	*	
	1	3	0.94	0.93
		4	*	
1 - 2	1	5	*	*
		6	*	
	2	7	*	*
		8	*	
2 - 3	2	9	*	*
		10	*	
7 - 7	7	20	0.96	0.86
		21	*	
	Centre	22	0.87	0.93
	Span	24	*	

Note: W = Total load on truss

W_{max} = Failure load of truss

Yielding is based on σ_y = 403.3 MPa

* indicates ratio exceeds 1.0

Table 4.2 Ratio of applied load to Truss BBOV failure load for yielding at extreme fibres of members

Truss	Experimental		Analytical			
	W_{max} (kN)	Failure Mode	W_{max} (kN)	Failure Mode	No. of hinges formed	Failure Location (Member No.)
BBST	2535	Buckling of member 7-7	2575	Mechanism	28	2-3
BBOV	2553	Buckling of member 7-7	2687	Deflection	16	7-7

Table 4.3 Summary of Results for Back-to-Back Trusses

Member	Joint	Strain Gauge Number	W/W_{max}	
			Experimental	Analytical
0 - 1	0	1	0.97	0.91
		2	*	
	1	3	*	0.92
		4	*	
1 - 2	1	5	*	*
		6	*	
	2	7	*	0.87
		8	*	
2 - 3	2	9	*	0.85
		10	*	
7 - 7	3	20	*	*
		21	*	
	Centre	22	*	*
	Span	24	*	

Note: W = Total load on truss

W_{max} = Failure load of truss

Yielding is based on σ_y = 380.8 MPa

* indicates ratio exceeds 1.0

Table 4.4 Ratio of applied load to Truss S1 failure load for yielding at extreme fibres of members

Hinge No.	Plastic hinge formed at	
	Joint	Member
1	2	2-3
2	2	1-2
3	1	0-1
4	0	0-1
5	3	2-3
6	2	2-4
7	1	1-2
8	5	4-5

Note: Refer to Fig. 2.1 for joint numbering system.

Table 4.5 Plastic Hinge Progression for Standard Trusses

Member	Joint	Strain Gauge Number	W/W_{max}	
			Experimental	Analytical
0 - 1	0	1	*	0.92
		2	*	
	1	3	*	0.87
		4	0.78	
1 - 2	1	5	0.66	0.79
		6	*	
	2	7	*	0.83
		8	0.70	
2 - 3	2	9	0.69	0.83
		10	*	
7 - 7	7	20	*	*
		21	*	
	Centre	22	*	*
	Span	24	*	

Note: W = Total load on truss

W_{max} = Failure load of truss

Yielding is based on σ_y = 375.4 MPa

* indicates ratio exceeds 1.0

Table 4.6 Ratio of applied load to Truss S2 failure load for yielding at extreme fibres of members

Truss	Experimental		Analytical			
	W_{max} (kN)	Failure Mode	W_{max} (kN)	Failure Mode	No. of hinges formed	Failure Location (Joint No.)
S1	1727	Shear failure at joint 1	1581	Mechanism	12	1, 2 & 3
S1A	2108	Shear failure at joint 2	1762	Mechanism	12	2
S1B	2393	Shear failure at joint 3	1995	Mechanism	12	3
S1C	2420	Buckling of member 7-7	2539	Deflection	28	4
S2	2045	Shear failure at joint 1	1613	Mechanism	16	1, 2 & 3
S2A	2162	Shear failure at joint 2	1717	Mechanism	16	2

Table 4.7 Summary of Results for Standard Trusses

Member	Joint	Strain Gauge Number	W/W_{max}	
			Experimental	Analytical
0 - 1	0	1	*	0.86
		2	*	
	1	3	*	0.91
		4	*	
1 - 2	1	5	0.89	0.84
		6	*	
	2	7	*	0.83
		8	0.86	
2 - 3	2	9	0.83	0.78
		10	*	
7 - 7	7	30	0.75	0.84
		31	0.93	
	Centre	32	0.86	0.93
	Span	34	0.97	

Note: W = Total load on truss

W_{max} = Failure load of truss

Yielding is based on σ_y = 398.0 MPa

* indicates ratio exceeds 1.0

Table 4.8 Ratio of applied load to Truss BO failure load for yielding at extreme fibres of members

Truss	Experimental			Analytical		
	W_{max} (kN)	Failure Mode	W_{max} (kN)	Failure Mode	No. of hinges formed	Failure Location (Member No.)
BO	2528	Buckling of member 7-7	2624	Deflection	28	6-8 7-7
BOA	3176	Buckling of member 2-3	2980	Deflection	26	1-2 2-3 4-6
BOB	3327	Local buckling of member 5-7 at joint 5	3060	Deflection	26	1-2 4-6
BOC	3096	Local buckling of member 2-3 at joint 3	3123	Deflection	26	0-1 1-2 4-6

Table 4.9 Summary of Results for Bolted Trusses

CHAPTER 5

DISCUSSION AND COMPARISON OF TRUSS TYPES

With reference to the experimental and analytical results of the various trusses as presented in Chapter 4, a brief description of the original and reinforced trusses along with the corresponding failure loads is given in Table 5.1. Discussion and comparison of the various trusses are presented in the following sections.

5.1 Experimental Program

In the case of the Back-to-Back truss with gap joints (Truss BBST), the provision of 19.05 mm stiffening plates at connections was sufficient to prevent a joint failure despite the fact that there was visually apparent shear distortion at the end joints prior to the attainment of ultimate load. This result confirmed the findings by Chidiac on joints [2] which concluded that a stiffening plate of lesser thickness (12.7 mm) was inadequate while one of 31.75 mm was overly conservative. The analytical model confirmed that shear across the section of the connections of Truss BBST was not critical, but did predict a significant increase in the overall loading capacity of the truss as compared to the case where no stiffening plates were used. Therefore, stiffeners are essential for the gap joint type double chord configuration. However, by overlapping the web members at connections, stiffening plates are generally not required. From the test on Truss BBOV, there was an effective transfer of forces from one diagonal member to the other.

Therefore, the chord section and the junction where the diagonals met the chord face was largely spared of the high stresses which otherwise might greatly reduce the truss' capacity. One important design detail which needs to be emphasized is that high stressed generated at a reaction (joint 0 in the case of Truss BBOV) needs to be taken into account. It was observed that the inner webs of the double chord directly above the support were prone to web crippling. One possible solution is to provide stiffening plates at the end connections similar to Truss BBST. This would provide a more uniform distribution of stresses to all four webs thus alleviating the problem. As was evident from the analytical results, none of the web members reached its load carrying capacity. The diagonal member forces were therefore effectively transferred from one to the other thus maintaining integrity of the chord members. This resulted in a high load carrying capacity for the truss.

The two Standard trusses S1 and S2 with no reinforcements were shown to be susceptible to high shear forces developed at the connections. Particularly at the end joints of the top double chord where resistance was low due to two factors - the diagonal forces were the highest and a lack of continuity of the chord section past the joint. This latter deficiency was particuarly noticed in Truss S1. Both in-plane shear and shearing action on the chord members themselves combined to cause an unexpected failure at one of the end joints. It was clear that either end-capping the chord section or extending the chord beyond the joint would have provided additional strengthening. Therefore, prior to testing of Truss S2, the ends of the top chord members were

capped which resulted in 15.6% increase of total truss load carrying capacity as compared to Truss S1. The end caps transferred some of the shear force developed at the connection to both the inner and the outer webs of the chord members, thereby providing a higher shearing capacity than when only the inner webs were effective. For the interior joints where continuity is not a problem, it was found that the effectiveness of the outer chord webs in resisting shear for Truss S1 was only 30% as compared to 44% for Truss S2. Thus it is evident then that the effect of eccentricity on the behaviour of double chord Standard trusses needs further investigation. Recent studies at the University of New Brunswick [8] suggested that when two diagonal members meet a single chord T-section very near to each other, i.e. e is small, a high stress concentration or bridging action tends to occur. Furthermore, welding at the toes of the diagonals tends to introduce residual stresses across the gap between them. For the double chord configuration, assuming the same combination of effects may occur, and can consequently lead to a crack development in the inner webs and a lower ultimate failure load of the truss. This, in fact, was observed from the tests. By reinforcing the joints of Truss S1, after the joint failures had occurred, it was confirmed that the joints themselves without reinforcement were weak as they failed one after another moving progressively inwards until a top chord buckling failure prevented further testing.

Although end-cutting of the diagonal members can reduce the eccentricity (as in Truss S1), the facts mentioned above have to be carefully considered before the best design can be achieved. End preparations for the diagonal members of this type of truss is much less

expensive than for the Back-to-Back truss. Hence it is a viable option for the Standard type trusses.

The analytical load-deflection curves in Chapter 4 revealed that the shear capacity of the connections and, consequently, the truss failure load was relatively sensitive to the effectiveness of the outer webs in resisting shear. The model predicted that the systematic reinforcement of various critical connections would subsequently lead to failure of the next critical location which was also confirmed by the test results of Truss S1. It is clear that before this type of truss can be recommended for practice, a further study should be undertaken on the design of the connections. It would seem important to study two aspects of the problem -- the effect of eccentricity on sharing the joint shear force between inner and outer webs at a connection, and to determine the optimum angle cut to be used on diagonals for purposes of efficiently transferring diagonal member forces.

For the bolted truss, the number of bolts per connection, the provision of 9.5 mm thick gusset plates and the tie plates across the chord members were more than adequate in ensuring that the strength of the connections surpassed that of the individual members. Compression buckling of the top chord member was the failure mode for the original truss. Despite systematically reinforcing the chord and web members following the truss failures, joint failure did not occur. Minimal bolt slippage was observed while the gusset plates remained secure throughout the testing. With reference to the bolts, it is evident from Table 5.2 that their number per joint for Truss B0 was more than that required.

This number is based on the bolt resistance provisions of CSA S16.1 - 1974. It was therefore decided to remove one row of bolts from each connection after reparations were made to Truss BOB. After Truss BOC had been tested, it was observed that a local buckling failure had occurred in the flange of the end of the third diagonal adjacent to where the row bolts had been removed. The overall effect of adding side plates to chord and web members and, at the same time, removing the row of bolts at each connection was to increase the truss failure load by 18.3% over the original truss configuration. However, there was a loss of strength of 7.5% as compared to Truss BOB. Table 5.2 shows the number of bolts required to be slightly more than those provided for Truss BOC. The low performance factor (i.e. 0.67) used in the calculation suggests that an avoidance of bolt shear failure is likely. Nonetheless, it was evident in testing that a redistribution of stresses occurred locally with the removal of the bolts which caused failure before it was expected. Therefore, while no bolt failures occurred, a more conservative design of the connections had the effect of sustaining higher member forces. For the original truss, it is concluded that the connections were over designed.

As revealed by the dial gauges mounted on the side of the top chord member, minimal lateral deflection was observed during the testing of the above trusses. This is further confirmed by the lateral loading of Truss BO as explained in the preceeding chapter. It is, therefore, suggested that high lateral rigidity can be obtained from these double-chord trusses so as to minimize lateral bracings.

5.2 Analytical Model and Limitations

The overall gross behaviour of the trusses, as predicted by the analytical model, was presented in the form of load-deflection curves in the previous chapter. Good agreement with the experimental curves is noted throughout the loading process; especially in the elastic range where excellent correlation was obtained. In the testing of the Standard trusses, it is evident from the load-deflection curves that the overall behaviour of the truss is sensitive to the effectiveness of the webs in resisting shear at the connections. When comparing Truss S1 with assumed chord web efficiencies of 65% and 100% and Truss S2 with 72% and 100%, the truss failure loads increased by 28.7% and 23.1%, respectively. The model would predict the overall behaviour very well if the web efficiencies were increased. Whether the model needs refinement or that further tests on joints of this type ought to be conducted in order to determine web effectiveness more precisely is desirable.

When comparing the load-moment curves predicted by the analytical model with those obtained from the experiments, excellent correspondence is obtained in some cases (Fig. 4.5) while there is considerable disparity in other instances (Fig. 4.37). Nonetheless, the general shape of the curves is consistent. This phenomenon also occurs in various m-p curves. A possible explanation for this discrepancy is that the experimental results were limited by the data obtained from the strain gauges and rosettes — partcularly in placement of these devices. Unexpected localized stress distribution can significantly alter computed force resultants in the members. In addition, these readings

are always susceptible to possible experimental errors, for instance, instrumental defects or improper functioning of gauges. This is further complicated by the complex stress distributions due to different joint configurations. The analytical model which is based on idealized joint behaviour, does not take into account the effects of residual stresses, localized yield, strain hardening and large deformations. Considering the limitations, the model does appear to be capable of predicting the overall truss behaviour very well and to provide an incite into failure modes, hinge formation sequences, resultant member forces and joint displacements.

5.3 Performance and Cost Comparison

Previous joint test results [2] were used as a basis in comparing with those obtained from the truss tests. By examining the strain readings along the web and chord members framing into the failed connection, the failure load for joint 2 of Truss S1A was found to be 26% lower than the equivalent isolated joint failure load. A consistent discrepancy of 15% was also observed for Truss S2A where larger gap joints were used. The difference can be explained by the fact that both axial force and bending moments were introduced to the joints in the truss tests whereas only the former was present during the individual joint tests. This result also seems consistent with the tests conducted at the University of Nottingham [6], as revealed in Section 1.1.

The stiffnesses of the various trusses computed from their load-deflection curves in the elastic range are shown in Table 5.3. The

analytical solutions show a consistent trend of increase in stiffness when the various trusses were reinforced. Truss BBST with stiffening plates had a higher stiffness than Truss S1 which possessed similar joint eccentricity but a gap joint. This further confirmed that the total number of webs for a chord member in resisting shear had an effect on the truss' stiffness. As expected, Truss S2 which had a larger gap than Truss S1 yielded lower stiffness. The results of the bolted trusses indicated that reinforcing of the original truss could increase its stiffness by a significant amount. Nonetheless, good agreement with the experimental results was generally evident.

The load capacities of the various trusses and their ratios with respect to Truss S2 are also shown in Table 5.3. Truss S1, which experienced a premature joint failure, was the only truss that showed lesser capacity than Truss S2. The rest of the trusses all showed promising load capacities, in particular the reinforced bolted trusses.

From Table 5.1, the starred values indicate the capacities representative of the various truss types. It is evident that Trusses BBST, BBOV and BO all sustained about equal ultimate loads. On the other hand, the Standard trusses S1 and S2 were also quite close (perhaps even more so if end capping had been done for Truss S1 rather than the use of gusset plates) but their capacities suffered due to undesirable connection failures.

A comparison among the various trusses themselves would not be complete without considering the associated fabrication costs. Despite

efforts to convince fabricators to provide cost data, only the information provided by one firm and quoted in earlier work [2] has been obtained to date. This information related only to the joints and not the trusses themselves. The relative costs between joints will be presented to discount the effects of inflation since the time the data was procured.

The most economical truss to fabricate is Truss S2 -- straight end cuts and fillet welding. Assume its cost to be the bench mark for comparison. The Truss S1 is slightly more complicated because of angle cuts to the diagonal member ends. For the connection itself, Truss S1 was found to be 7% more costly than Truss S2 -- not an unreasonable additional cost for a better performance. However, it is difficult to draw conclusions from just two tests. It would seem that the end cuts ought to have been made to form parallel edges at the joint thus facilitating the transfer of diagonal forces. This may have resulted in significantly higher strength particularly if an optimum gap (or eccentricity) had been applied. If the gap is too small, the outer chord webs are not effective in carrying shear, while too large a gap causes undesirable relative displacements at the joints and causes non negligible secondary moments. Alternatively, snug fitting of the parallel end cuts of the diagonals before welding necessitates care to be taken in cutting and fitting up which results in somewhat higher costs. These aspects need further investigation.

Of the other three, Truss BBOV appears to be considerably less costly to fabricate than the other two. It is only 34% higher in cost

than Truss S2 while Trusses BBST and BO are 94% and 120% higher, respectively. However, the bolted truss could not be ruled out because of the other factors involved. It can be an economical alternative for large spans where field erection procedures must be followed. Constraints on transportation will often necessitate some form of on-site assembly hence making this type of truss viable. The Back-to-Back trusses are relatively costly due to the amount of end preparation for the diagonals required. This would involve the precise cutting at the ends of the diagonal members in order to ensure proper fitting. Further treatment of the ends for weldment is also necessary. In conclusion, it is necessary to consider the above factors in order to arrive at the best design from the point of view of both strength and economy.

Group	Truss	Description	W_{max}(kN)	% difference with analytical values
Back-to -Back	BBST	Original configuration with stiffening plates at joints	2535*	+ 1.6
	BBOV	Original configuration with overlapped diagonals	2553*	+ 5.2
Standard	S1	Original configuration with e = 108 mm	1727	- 8.5
	S1A	Gusset plates welded to joint 1	2108*	-16.4
	S1B	Gusset plates welded to joints 1 and 2	2393	-16.6
	S1C	Gusset plates welded to joints 1, 2 and 3	2420	+ 4.9
	S2	Original configuration with e = 178 mm and top chords end-capped	2045*	-21.1
	S2A	Gusset plates welded to joint 1	2162	-20.6
Bolted	BO	Original configuration with all joints bolted	2528*	+ 3.8
	BOA	Side plates welded to members 5-7, 7-7 and 6-8	3176	- 6.2
	BOB	Side plates welded to members 5-7, 7-7, 6-8 and 2-3	3327	- 8.0
	BOC	Side plates welded to members 5-7, 7-7, 6-8, 2-3 and 3-5	3095	+ 0.9

Note: W_{max} denotes experimental truss failure load.
Truss designations A, B or C indicate progressive reinforcing before testing.
Refer to Section 2.1 for details of trusses.
Refer to Figure 2.1 for joint numbering system.

* Capacities representative of truss types.

Table 5.1 Experimental Program for Original and Reinforced Trusses

Joint	Member	A(mm^2)	F_v(kN)	Bolt Details			Number of bolts		
				Grade	F_u(MPa)	V_r(kN)	Required*	Provided by BO	Provided by BOC
0	0-1	4265	1668	A490	1034	118.8	14	16	12
1	1-0	4265	1668	A490	1034	118.6	14	16	12
	1-2	2961	1165				10	16	12
2	2-1	2961	1165	A325	827	94.8	13	16	12
	2-3	2961	1165				13	16	12
3	3-2	2961	1165	A325	827	94.8	13	16	12
	3-4	2961	1165				13	16	12
4	4-3	2961	1165	A325	827	94.8	13	16	12
	4-5	2961	1165				13	16	12
5	5-4	2961	1165	A325	827	94.8	13	16	12
	5-6	2277	894				10	16	12
6	6-5	2277	894	A325	827	94.8	10	12	8
	6-7	2277	894				10	12	8
7	7-6	2277	894	A325	827	94.8	10	12	8
							10	12	8

Note: A = Cross-sectional area of member
F_v = Maximum axial force based on σ_y = 392.7 MPa
A_b = Area of bolt = 285 mm^2
F_u = Tensile strength of bolt
V_r = shear strength of bolt = $0.6 \times 0.67 \times A_b \times F_u$ [22]
* based on CSA S16.1 (1974)

Table 5.2 Comparison of Bolt Requirements with Bolts Provided for Truss BO and Truss BOC

Group	Truss	Stiffness† (kN/mm)		Capacity	
		Experimental	Analytical	W_{max} (kN)	Strength Ratio*
Back-to-Back	BBST	34.8	36.2	2535	1.240
	BBOV	38.8	39.3	2553	1.248
Standard	S1	32.1	35.7	1727	0.844
	S1A	37.3	35.9	2108	1.031
	S1B	39.3	36.1	2393	1.170
	S1C	35.9	36.3	2420	1.183
	S2	32.8	34.5	2045	1.000
	S2A	33.7	34.7	2162	1.057
Bolted	BO	38.8	38.9	2528	1.236
	BOA	42.3	44.4	3176	1.553
	BOB	47.0	45.1	3327	1.627
	BOC	45.2	46.8	3096	1.514

Note: † Based on truss load and mid-span deflection in the elastic range

* Based on W_{max} of Truss S2

Table 5.3 Comparison of Truss Strength and Stiffness

CHAPTER 6

SUMMARY AND CONCLUSIONS

6.1 Summary

The purpose of this investigation was to study the behaviour of HSS double chord trusses under in-plane static loading. Such a concept has been shown to offer great potential in long span Warren truss applications. The experimental program consisted of a study on these trusses with different joint arrangements, namely Back-to-Back, Standard and Bolted. Of the two Back-to-Back trusses, one represented the type in which the diagonals were fully overlapped at the joints. The other modelled a stiffened gap joint type configuration. The two Standard trusses possessed different joint eccentricities, one with straight diagonal end cuts, the other having skewed ends to permit a snugger fit so as to reduce eccentricity. Finally, a Bolted truss was tested which can be assembled on-site. These trusses were incrementally loaded until failure. In the event of localized failures at a connection, reinforcing was undertaken when possible and the tests resumed thus providing a maximum amount of information on the trusses themselves and their connections. In total, twelve tests were undertaken for the five trusses. It was found that the joints that failed in the truss tests had lower failure loads than the isolated joint failure loads obtained from previous tests [2].

An analytical model was developed which incorporated the m-p

interaction diagrams and yielding of connections in shear. An existing elastic, plane frame analysis program was extended to include the analytical model and allows one to perform an elastic-plastic analysis of plane frames under incremental loads. Three types of yield mechanisms were introduced to predict individual member end and connection behaviour; these are plastic hinge formation at an end of a member, localized failure due to plastic limit load of a member with plastic hinges at both ends and shear yielding at a connection. Various simulation models for m-p interaction and shear springs at the connections were chosen for the different types of trusses tested so as to more accurately model their behaviour. The analytical model did not include localized buckling of individual members as this would be avoided in design of the trusses discussed. Furthermore, the individual members are assumed stocky enough not to undergo buckling.

The comparison between the experimental and analytical results led to a reasonably good agreement in general. Finally, some design recommendations are proposed and the need for further work identified.

6.2 Conclusions

It is evident from the results that the double chord concept provides higher overall load capacity of the trusses as well as a high lateral rigidity, thus minimizing the use of bracing. However, the performance of a double chord truss does depend on the truss type and joint arrangement. For example, the Back-to-Back trusses showed good strength and stiffness characteristics. By providing stiffening plates

(Truss BBST) or overlapping the diagonal members at the connections (Truss BBOV), the chord members were largely relieved of high stresses at the joints thus achieving a high stiffness and an overall truss load carrying capacity.

The failure mode of both trusses (BBST and BBOV) was combined local and overall buckling of the top chord which confirmed the adequate strength inherent in the connections. In the case of Truss BBOV, web crippling of the chord members over the supports may occur unless some form of reinforcing is used to prevent a possible localized failure. In general there was very good agreement between the experimental results and the analytical solutions for both trusses.

The mode of failure for both Standard trusses (S1 and S2) with original configuration was shear distortion of the chord member at the critical connnection (Joint 1). This was due to a number of reasons: (1) diagonal forces were the highest at this location; (2) there was a lack of continuity of the chord member, and (3) only the inner webs of the chord section were fully effective in transferring shear. By end-capping the ends of the top chord members (Truss S2) a higher capacity was achieved. This design detail tended to prevent shear distortion of the square cross sections, thus offering more joint resistance. Furthermore the outer webs of the chord members were used more effectively in transferring the diagonal forces. For the case with no end capping, only the inner webs were effective. The shear capacity of the connection and thus the total truss capacity was shown to be sensitive to the effectiveness with which the diagonal forces are partitioned to

the four chord webs. End-cutting of the diagonal members permits a reduction in the eccentricity at the connection but appears to have the effect of concentrating the shear forces in the inner webs of the double chords. A further complication is the stress concentration occurring at the toes of diagonals which would be compounded by the welding residual stresses in the gap. A detailed study of the above factors is necessary to fully understand their effects on the behaviour of the trusses. Further retesting of the Standard trusses, after progressively reinforcing the failed joints, confirmed that these joints were under-designed. Therefore, these should be reinforced so that the final failure would be the result of progressive hinge formations in the members themselves thus leading to a collapse mechanism or the predicted plastic buckling of the top chord member at mid span. Indeed, a higher truss stiffness was obtained from both the analytical and experimental results when these joints were reinforced.

The Bolted truss also showed promising results while large joint stiffness was obtained by employing gusset plates and tie plates. The mode of failure was combined local and overall buckling of the top chord member. Systematically reinforcing the failed members transferred the failure to the next critical member and resulted in higher truss stiffness. The failure mode for Truss BOC, with one row of bolts removed from each connection, was local buckling of a diagonal member adjacent to where the bolts were removed. No joint failure was observed throughout the testing of the original and reinforced trusses. Again, it was revealed that the connections for the original truss were over-designed. It still remains at the discretion of the designer to determine whether

the number of bolts and the thickness of the gusset plates used are economically viable.

6.3 Suggestions for Future Research

Based on the promising results from the preceeding sections, the following suggestions are made for future research in order to achieve a better understanding into the behaviour of individual connections as well as the overall truss.

Further investigation into the fully-overlapped end gap joint with stiffening plates of Back-to-Back trusses should be performed, possibly by using finite element techniques. For the Standard truss, where the gap joints are under high shear forces, the effectiveness of the outer and inner webs in resisting shear as well as behaviour of flanges of the chord members should be further investigated. The stress concentrations and residual stresses due to welding at the connections should also be studied so that an improved joint model and consequently a better design could be achieved. Also, more information regarding the optimum number of bolts per connection and the thickness of the gusset plates should be acquired for use in designing a bolted truss to achieve maximum capacity at a minimum cost.

Finally, it is proposed that further refinements be made to the analytical model and the computer program developed in this investigation for application to standard connections. In lieu of the simple shear spring mechanism used it would be desirable to include the inter-

action of shear force, axial force and moment and their influence on the joint stiffness at a typical connection would help simulate a better model to predict behaviour of joints at interior supports for multi-span trusses. It is also possible to extend the model to incorporate curved interaction (m-p) diagrams and checks on localized or overall member buckling. Once the above has been accomplished, this will form a comprehensive computer program for analysis of large span, double chord Warren trusses.

APPENDIX I

LISTING OF ELASTIC-PLASTIC COMPUTER PROGRAM

The program was written in Fortran IV language for use on the CYBER 170 computer at McMaster University. The basic logic and general analysis procedures for the computer program have been presented in Chapter 3. A listing of subroutines and a brief description of their functions are presented below.

1) ASSIGN — Assigns values of axial force increments obtained from the case where $\beta_k = 1.0$ and the case where unit moments are applied at the various hinges formed which are then placed in the appropriate matrices.

2) BANDWH — Computes the half bandwidth of the stiffness matrix.

3) CHANGE — Adds a rotational degree of freedom at the joint where a plastic hinge has formed and subsequently changes the degrees of freedom at the rest of the joints.

4) CLOAD — Reads the values for the loads at the joints and computes the load vector.

5) CONFOR — Converts forces into their absolute values.

6) ESORT — Sorts out the minimum load factor β_k and the locations where either a shear failure or a plastic hinge formation or a member removal occurs.

7) EXPAND — Points out nodal displacements according to the joint numbers.

8) EXTRACT — Extracts the local degrees of freedom from the global degrees of freedom for a member.

9) FBAND — Carries out the Cholesky decomposition of the stiffness matrix.

10) IMTER — Uses the axial forces, shear forces, and bending moments of each member end after the previous load increment and the present load increment to compute the ratio β_k for all members.

11) INFORC — Computes member forces from joint displacements and puts into storage for subsequent computations.

12) INTER — Computes the ratio β_0 for each member to determine the elastic limit load.

13) LAYOUT — Reads all data for joints and member properties of the structure.

14) MSTIFF — Computes the global stiffness matrix.

15) PRESET — Initializes two-dimensional array.

16) PSET — Initializes one-dimensional array.

17) SBAND — Performs forward and backward substitution to solve for the displacements called from FBAND.

18) SETUP — Groups all member stiffness matrices into the one-dimensional global stiffness matrix.

19) SOLVE — Solves various incremental limit moments at the hinges by employing the Gaussian Elimination method.

20) STIFF — Computes member stiffness matrices.

21) SUMF — Computes joint displacements and member forces in the plastic range by adding the incremental values to the preceeding values.

22) SUMI — Sums up forces in members due to the case where $\beta_k = 1.0$ and the case where incremental limit moments are applied at the various hinges.

```
C
C                    PROGRAM MUG
C                    ***********
C
C                                        WRITTEN BY E. CHIU
C                                        AT MCMASTER UNIVERSITY
C                                        M. ENG. THESIS (1982)
C
C
C     THIS PROGRAM EXTENDS AN ELASTIC PLANE FRAME PROGRAM (DEVELOPED
C     BY DR. MIRZA) INTO THE PLASTIC RANGE WHERE STEP-BY-STEP
C     COMPUTATION IS EMPLOYED TO PROPORTION THE TRUSS TO FAILURE,
C     EITHER DUE TO EXCESSIVE DEFLECTION OR MECHANISM FORMATION.
C     THREE TYPES OF YIELD MECHANISM ARE INTRODUCED, NAMELY HINGE
C     FORMATION AT THE END OF A MEMBER, MEMBER REACHING ITS PLASTIC LIMIT
C     LOAD AND SHEAR YIELD AT A CONNECTION.
C
C
C     NOMENCLATURE
C     ************
C
C     ALD     ALLOWABLE DISPLACEMENT AT CONNECTION
C     AREA    CROSS SECTIONAL AREA OF I MEMBER
C             EQUALS 0 IF SAME AS PREVIOUS MEMBER
C             EQUALS 10.0 FOR SMALL MEMBERS
C     AV      SHEAR AREA OF CHORD AT CONNECTION
C     BI      MOMENT OF INERTIA OF I MEMBER
C             EQUALS 0 IF SAME AS PREVIOUS MEMBER
C             EQUALS 1000.0 FOR SMALL MEMBERS
C     BF      WIDTH OF FLANGE AT CONNECTION
C     C       RATIO OF AXIAL FORCE TO PY WHEN MOMENT EQUALS PM
C     E       MODULUS OF ELASTICITY
C     EAD     ALLOWABLE MID-SPAN DEFLECTION
C     FFX(I)  FORCE IN X-DIRECTION
C     FFY(I)  FORCE IN Y-DIRECTION
C     GM      SHEAR MODULUS OF ELASTICITY
C     HS      HEIGHT OF SECTION
C     IX(J)   DEGREE OF FREEDOM ALLOWED AT EACH JOINT
C             EQUALS 0 IF DISPLACEMENT NOT ALLOWED
C             EQUALS 1 IF DISPLACEMENT IS ALLOWED IN X,Y AND Z DIRECTION.
C             EQUALS JOINT NUMBER FOR SAME DEGREE OF FREEDOM
C     JN(I)   JOINT NUMBER AT WHICH LOAD IS APPLIED
C     JNG(I)  GREATER JOINT NUMBER OF I MEMBER
C     JNL(I)  LESSER JOINT NUMBER OF I MEMBER
C     LF1     JOINT NUMBER FOR DEFLECTION CALCULATION
C     LF2     JOINT NUMBER FOR DEFLECTION CALCULATION
C     MEMTYP  MEMBER TYPE OF I MEMBER
C             EQUALS 0 IF SAME AS PREVIOUS MEMBER
C             EQUALS 1 FOR PIN-PIN ENDS
C             EQUALS 2 FOR FIX-FIX ENDS
C             EQUALS 3 FOR PIN-FIX ENDS
C             EQUALS 4 FOR FIX-PIN ENDS
C             EQUALS 6 FOR SHEAR SPRING
C     NJ      NUMBER OF JOINTS
C     NM      NUMBER OF MEMBERS
C     NS      NUMBER OF SMALL MEMBERS WITH BI=1000.0
C     NLJ     NUMBER OF JOINTS LOADED
C     NRS     STRUCTURE NUMBER
C     PM      PLASTIC YIELD MOMENT
C     PS      PLASTIC SECTIONAL MODULUS OF I MEMBER
C             EQUALS 0 IF SAME AS PREVIOUS MEMBER
```

```
C      FV      ALLOWABLE PLASTIC SHEAR FORCE AT CONNECTION
C      FY      PLASTIC AXIAL FORCE
C      TF      THICKNESS OF STIFFENING PLATE
C      TS      TOTAL THICKNESS OF SECTION IN RESISTING SHEAR
C      TITLE   PROJECT NAME
C      X(I)    X COORDINATE OF THE I JOINT
C      Y(I)    Y COORDINATE OF THE I JOINT
C      YS      YIELD STRESS
C
C
      PROGRAM MLG(INPUT,OUTPUT,TAPE5=INPUT,TAPE6=OUTPUT,TAPE11,TAPE13,TA
     1PE14,TAPE15,TAPE16,TAPE17)
C
C
      DIMENSION A(8580), E(480),IX(480),JX(480),XM(120),YM(120),AL(120),
     1JNL(120),MEMTYP(120),AREA(120),BI(120),X(160),Y(160),FFY(20),
     2FFX(20),BY(120),BM(120),LJ(6),S(6,6),FL(6),QS(20),U(6),JNG(120),
     3TITLE(8),IC(40),FI(10416),CI(11844),MF(10),NNH(30),ME(30),BF(30),
     4AF(30,30),DM(30),JT(160),MI(10),JI(10),MPI(10),MSI(10),LLF(120)
C
C  READ IN AND WRITE OUT CONSTRAINTS OF PROBLEM
C
      READ (5,3) NPS,NJ,NM,E,C,YS
      READ(5,17)LP1,LP2,NS,FS,TS,TF,BF
      READ(5,2)TITLE
      READ(5,9)AV,GM,ALD
      FV=(HS*TS+2.0*TF*BF/3.0)*YS/(SQRT(3.0))
      WRITE(6,1)
      WRITE(6,5)NPS,TITLE,NJ,NM,E,GM,C,YS,FV,AV,TS,ALD
C
C  LAYOUT ALL THE MEMBER PROPERTIES
C
      CALL LAYOUT(X,Y,I),JX,JNL,JNG,MEMTYP,AREA,BI,AL,XM,YM,LJ,
     1NDEG,NMAT,NJ,NM,FY,FM,YS,NS,IC,JT,LK)
C
C  INITIALIZE VALUES
C
      LF=0
      LZ=0
      YZ=0.0
      Z=0.0
      IR=0
      JK=0
      NH=0
      CAB=2.0
      CAC=2.0
      NCOR=NDEG
      CALL PSET(LLF,NM)
      CALL PSET(MPI,10)
      CALL PSET(MF,10)
      CALL PSET(JI,10)
      CALL PSET(MI,10)
C
C  COMPUTE THE SIZE OF THE PROBLEM
C
      IF(LZ.EQ.1)GO TO 502
  500 CALL CHANGE(NNH,JJ),NJ,NM,JT,LK,KC)
  502 NDEG=NCOR+NH
      LZ=LZ+1
      WRITE(6,142)LZ
      IF(LZ.EQ.20) GO TO 997
      GO TO 506
  505 LT=1
      WRITE(6,40)LZ
  506 CALL BANDWH(JNL,JNG,JJ,LJ,NM,NE)
      LBAND=NE-1
      NV=NDEG*NJ
      WRITE(6,6) NDEG,NE,NV
```

```
C
C   COMPUTE STIFFNESS MATRIX
C
      REWIND 11
      CALL PSET(A,NV)
      DO 13 JM=1,NM
      IF(JK.EQ.0) GO TO 18
      DO 14 JG=1,JK
      IF(IM.NE.MF(IG)) GO TO 14
      AREA(TH)=0.0
      VF=0.0
      GO TO 16
 14   CONTINUE
 18   VF=PV
 16   CALL MSTIFF(LJ,JX,E,NV,LBAND,A,IM,JNL,JNG,MEMTYP,AL,XM,YM,BI,AREA,
     1S,AV,GM,VF,ALG)
      WRITE(11)(LJ(I),I=1,6),((S(I,J),I=1,6),J=1,6)
   13 CONTINUE
C
C   COMPUTE AND WRITE OUT LOAD MATRIX
C
      IF(LZ.NE.1) GO TO 507
      READ(5,17)NLJ
      WRITE(6,21)NLJ
 507  CALL PSET(B,NDEG)
      GM=0.0
      CALL CLOAD(B,JX,NLJ,YZ,FFY,FFX,GM,NNM,IR,JT,LK)
      WRITE(6,22) (B(J),J=1,NDEG)
      IF(LZ.NE.1) GO TO 138
      WRITE(6,38)FFX(1),FFY(1)
      WRITE (6,39)
C
C   SOLVE FOR JOINT DISPLACEMENTS
C
 138  RATIO=0.1E-12
      LT=1
      CALL FBAND(A,B,NDEG,NE,LT,RATIO,DET,NCN,Z)
      IF(Z.EQ.1.0)GO TO 557
      WRITE (6,25) DET,NCN
      IF(DET.LE.0.0) WRITE(6,26)
      IF(DET.LE.0.0) GO TO 999
C
C   WRITE OUT JOINT DISPLACEMENTS
C
      CALL EXPAND(B,NMAT,JX,U,NJ,3,LF1,LF2,D1,D2,LZ,IG,DS,NM,CAC,DI,IR,
     1LF)
      IF(LZ.NE.1) GO TO 131
      D=(D1+D2)/2.0
      WRITE(6,143)D
C
C   COMPUTE AND WRITE OUT MEMBER FORCES
C
 131  CALL INFORC(B,U,FL,S,LJ,XM,YM,AL,JX,NM,C,FY,PM,BI,FV,LZ,FFX,FFY,ME
     1MTYP,DS,ALD,TS,JNL,JNG,NJ,FI,NM,NC,CAE,NNM,D,ME,FAC,NLJ,IR,JK,M1,M.
     22,KP,KC,MI,JI,MF,LF1,LF2,LF,LLF)
      IF(D.LT.FAC) GO TO 504
      IF(LF.NE.1) GO TO 7
      YZ=1.0
      GO TO 500
 7    IF(LZ.NE.1.AND.NM.NE.0) GO TO 600
 601  YZ=1.0
      IF(NM.EQ.0) GO TO 502
      GO TO 500
 600  IF(IF.EQ.100) GO TO 601
```

```
C
C    APPLY UNIT MOMENT TO PLASTIC HINGES
C
 79    DO 41 IR=1,NH
       CALL PSET(B,NDEG)
       CALL CLOAD(B,JX,2,2.0,0.0,0.0,0.0,CM,NNH,IR,JT,LK)
       CALL FBAND(A,B,NDEG,NE,2,RATIO,DET,NCA,7)
      >CALL BKBAND(B,NMAT,JX,U,NJ,3,LF1,LF2,D1,D2,LZ,IQ,BS,NF,CAC,DI,IR,
      1LF)
       CALL INFORC(B,U,FL,S,LJ,XM,YM,AL,JX,NM,C,FY,PM,BI,PV,LZ,FFX,FFY,ME
      1MTYP,DS,ALD,TS,JAL,JNC,NJ,FI,NM,KC,CAE,NNF,D,ME,FAC,NLJ,IR,JK,M1,M
      22,KP,KC,MI,JI,MF,LF1,LF2,LF,LLF)
 41    CONTINUE
       YZ=1.0
       CALL PRESET(AF,NH,NH)
       CALL PSET(BF,NH)
       CALL PSET(DM,NH)
       CALL ASSIGN(NH,PY,FI,ME,FI,AF,BF,NJ,NM)
       CALL SOLVE(AF,BF,DM,NH)
       CALL SUPI(DM,FI,KF,NJ,NH,MS)
C
C    COMPUTE TYPE OF YIELD MECHANISM IN THE PLASTIC RANGE
C
       REWIND M1
       REWIND MS
       CALL INTER(C,PY,PM,NJ,NM,M1,JAL,JNC,BI,KC,MI,JI,MEMTYP,PV,MF,
      1PMIN,PBUC,PSHE,JF,JK,NH,NNH,MFI,MS,MSI,LLF)
       CALL SUPE(DI,U,JNC,NH,NJ,DM,LF1,LF2,D,FI,NM,NLJ,JK,MF,PY,M1,M2,FFX
      1,FFY,MEMTYP,PM,JAL,BI,KP,KC,MI,JI,ME,NS,C,NNH,PMIN,PSHE,PBUC,BAT,
      2JF,MFI,IR,PV,MSI,LLF)
       IF(D.LT.FAD) GO TO 504
       WRITE(6,78)NH
       IF(PMIN.NE.BAT) GO TO 502
       GO TO 500
 504   WRITE(6,77)FFX(1),FFY(1)
 502   WRITE(6,998)NM
 999   WRITE(6,996)
C
     1 FORMAT("1",10X,"**********PLANE FRAME ANALYSIS**********",///)
     2 FORMAT(8A8)
     3 FORMAT(3I10,F10.0,2F8.4)
     5 FORMAT(5X,"PLANE FRAME PROBLEM NUMBER=",I5,//,5X,"***",8A8,"***",//
      1,5X,
      1"NUMBER OF JOINTS=",I5,/ ,5X,"NUMBER OF MEMBERS=",
      2I5,/ ,5X,"MODULUS OF ELASTICITY=E=",F15.2,/ ,5X,
      3"SHEAR MODULUS OF ELASTICITY=",F15.2,/,5X,
      3"RATIO OF LOAD TO PLASTIC LOAD=",F8.4,/,5X,
      4"YIELD STRESS=",F8.4,/,5X,"PLASTIC SHEAR FORCE=",F8.4,/,5X,
      5"SHEAR AREA=",F8.4,/,5X,"THICKNESS OF SECTION IN SHEAR=",F8.4,/,
      65X,"ALLOWABLE DISPLACEMENT AT CONNECTIONS=",F8.4)
     6 FORMAT(//,5X,"TOTAL DEGREES OF FREEDOM=",I6,5X,
      1"HALF BANDWIDTH INCLUDING THE DIAGONAL=",I4,//,5X,
      2"SIZE OF THE SINGLE DIMENSIONED ARRAY FOR THE MASTER",
      3" STIFFNESS MATRIX=",I7,/)
     9 FORMAT(8F10.4)
    17 FORMAT (3I10,5F10.4)
    21 FORMAT(//,5X,"NO. OF JOINTS LOADED",I4)
    22 FORMAT(5X,8E15.6)
    25 FORMAT(//,5X,"DETERMINANT OF THE STIFFNESS MATRIX=",
      1E20.8,"*10**",I3,/)
    26 FORMAT(/,5X,"THE STIFFNESS MATRIX IS SINGULAR",/)
    38 FORMAT(//,5X,"***LOAD VECTOR FOR HORIZONTAL LOAD OF",F8.4,3X,"AND
      1VERTICAL LOAD OF ",F8.4,1X," AS FOLLOWS***",//)
    39 FORMAT (//,5X,"********* SOLUTION FOR THE ABOVE LOADING *********",/
      1/)
```

```
 40   FORMAT(/////,5X,"LOADING SEQUENCE NUMBER",I5,4X,"***ELASTIC RANGE*
     1**")
 77   FORMAT(/,5X,"TRUSS FAILED AT HORIZONTAL LOAD OF",F8.4,
     2 5X,"AND VERTICAL LOAD OF",F8.4,/,7X,"DUE TO EXCESSIVE DEFLECTION")
 78   FORMAT(/,5X,"TRUSS IS IN PLASTIC RANGE AND STILL CAN HOLD",
     1/,5X,"TOTAL NUMBER OF HINGES FORMED IS",I7)
 142  FORMAT(///,5X,"LOADING SEQUENCE NUMBER",I5,4X,"***ADDITIONAL LO
     1ADING AFTER ELASTIC RANGE ***")
 143  FORMAT(//,5X,"TOTAL MID SPAN DEFLECTION IS",E23.6)
 996  FORMAT(//,5X,"****** END OF PLANE FRAME ANALYSIS ******",/)
 998  FORMAT(//,5X,"MECHANISM IS FORMED WITH TOTAL NUMBER OF PLASTIC HIN
     1GES EQUALS TO",I6)
C
 1000 STOP
      END
C
C
C
      SUBROUTINE ASSIGN(NH,PY,PM,ME,FI,AF,BF,NJ,NM)
      DIMENSION BF(30),PY(1),PM(1),ME(1),FI(1),AF(30,30),BF(1),TU(4)
      REWIND 16
      DO 1 I=1,NH
      BF(I)=(.85*PY(ME(I)))/PM(ME(I))
 1    CONTINUE
      DO 2 I=1,NH
      DO 3 J=1,NH
      IA=(4*ME(I)-3)+(4*(J-1)*NM)
      AF(I,J)=FI(IA)
      IF(I.NE.J) GO TO 3
      AF(I,J)=AF(I,J)+BF(I)
 3    CONTINUE
 2    CONTINUE
      DO 4 K=1,NH
      DO 5 IG=1,NJ
      READ(16)A,B,C
 5    CONTINUE
      DO 6 J=1,NM
      READ(16)(TU(N),N=1,4)
      IF(ME(K).NE.J) GO TO 6
      BF(K)=-TU(1)
      GO TO 7
 6    CONTINUE
 7    REWIND 16
 4    CONTINUE
      RETURN
      END
C
C
      SUBROUTINE BANDWH(JNL,JNG,JX,LJ,NM,NE)
      DIMENSION JNL(1),JNG(1),JX(1),LJ(1)
      NE=0
      DO 1 I=1,NM
      N1=JNL(I)
      N2=JNG(I)
      CALL EXTRAC(LJ,JX,N1,N2)
      MAX=0
      MIN=10000
      DO 2 J=1,6
      IF(LJ(J).EQ.0) GO TO 2
      IF(LJ(J)-MAX) 3,3,4
 4    MAX=LJ(J)
 3    IF(LJ(J)-MIN) 5,2,2
 5    MIN=LJ(J)
 2    CONTINUE
      NE1=MAX-MIN
      IF(NE1.GT.NE) NE=NE1
```

```
    1 CONTINUE
      NE=NP+1
      RETURN
      END
C
C
      SUBROUTINE CHANGE(NNH,JX,NJ,NP,JT,LK,KC)
      DIMENSION NNH(1),JX(1),JT(1)
      KP=KC-1
      KT=0
      NMAT=3*NJ
      DO 15 JZ=1,KP
      NC=NH-KP+JZ
    3 NC=NNH(NC)*3
      NDE=NC-1
      NDS=NC+9
      NCD=JX(NDS)-JX(NC)
      NE1=NNH(NC)*3-11
      NE2=NNH(NC)*3-2
      IF(JX(ND).NE.0) GO TO 8
      ND1=NC-1
      DO 10 LE=1,ND1
      IF(JX(LE).GT.KT) GO TO 11
      GO TO 10
   11 KT=JX(LE)
   10 CONTINUE
      JX(NC)=KT+1
      GO TO 9
    8 JX(ND)=JX(ND)+1
      IF(NC.EQ.1) GO TO 9
      NZ=NC-1
      DO 40 IK=1,NZ
      NY=NNH(IK)*3
      YYY=JX(ND)-JX(NY)
      IF(ABS(YYY).LE.1.E-6.AND.JX(NY-2).NE.0) GO TO 41
   40 CONTINUE
      GO TO 9
   41 JX(ND)=JX(ND)+1
    9 IE=LK-1
      IF(IE.EQ.0) GO TO 7
      DO 5 IS=1,IE
      IF(NNH(NC).NE.JT(IS)) GO TO 5
      NNN=NC+4
      GO TO 6
    5 CONTINUE
    7 NNN=NC+1
    6 IF(NNN.GE.NMAT) GO TO 2
      NC=NNN-3
      IG=NNN
   27 IF(JX(IG).NE.JX(NC)) GO TO 25
      IG=IG+3
      GO TO 27
   25 DO 13 JJ=IG,NMAT
      IF(JX(JJ).EQ.0) GO TO 13
      JX(JJ)=JX(JJ)+1
   13 CONTINUE
   15 CONTINUE
    2 RETURN
      END
C
C
      SUBROUTINE CLOAD(E,JX,NLJ,YZ,FFY,FFX,CM,NNH,IF,JT,LK)
      DIMENSION B(1),JX(1),FFY(1),FFX(1),JN(20),NNH(1),JF(20),JT(1)
      RA=((IF+1)/(IF/2+1))-1
      DO 1 I=1,NLJ
      IF(YZ.EQ.0.0)GO TO 5
      IF(Y).EQ.0.0) GO TO 8
```

```
      IE=LK-1
      IF(IE.EQ.0) GO TO 13
      DO 11 IS=1,IE
      LC=JT(IS)+1
      IF(NNH(IE).NE.LC) GO TO 11
      IF(I.EQ.2) GO TO 14
      JF(I)=NNH(IR)-2
      GO TO 12
 14   JF(I)=NNH(IR)
      GO TO 12
 11   CONTINUE
 13   JF(I)=NNH(IR)-2+I
 12   IF(RA)20,21,20
 20   RT=1.0
      GO TO 22
 21   RT=-1.0
 22   IF(I.EQ.1) GO TO 6
      CM=RT
      GO TO 9
 6    CM=-RT
 9    NN=3*(JF(I)-1)
      GO TO 4
 8    READ(5,2)JN(I),FFX(I),FFY(I)
 5    NN=3*(JN(I)-1)
 7    N1=JX(NN+1)
      IF(N1.EQ.0) GO TO 3
      E(N1)=E(N1)+FFX(I)
 3    N2=JX(NN+2)
      IF(N2.EQ.0) GO TO 4
      E(N2)=E(N2)+FFY(I)
 4    N3=JX(NN+3)
      IF(N3.EQ.0) GO TO 1
      E(N3)=E(N3)+CM
 1    CONTINUE
 2    FORMAT(I3,5X,F5.1,7X,F5.1)
      RETURN
      END

C
C
      SUBROUTINE CONFOR(A,BA,BB)
      IF(A)1,2,2
 1    A=-A
 2    IF(BA)3,4,4
 3    BA=-BA
 4    IF(BB)5,6,6
 5    BB=-BB
 6    RETURN
      END
C
C
      SUBROUTINE ESCRT(PE,I,PMIN,NL,KC,MI,JI)
      DIMENSION JI(1),MI(1),PE(1)
      IF(PE(I).LE.0.0) GO TO 2
      R=PE(I)-PMIN
      IF(R)5,6,6
 5    R=-R
 6    IF(R.LE.0.002) GO TO 3
      IF(PE(I).LT.PMIN) GO TO 1
      GO TO 2
 1    KC=1
      PMIN=PE(I)
 3    MI(KC)=I
      JI(KC)=NL
      KC=KC+1
 2    RETURN
      END
C
```

```
C
      SUBROUTINE EXPAND (B,NMAT,JX,U,NJ,NVAR,LF1,LF2,D1,D2,LZ,IC,DS,
     1NH,CAC,DI,IP,LF)
      DIMENSION B(1),JX(1),U(3),IC(1),DS(1),DI(1)
      IF(LF.EQ.1) GO TO 20
      IF(LZ.EQ.1) GO TO 18
      IF(NH.EQ.0) GO TO 20
      IF(CAC.EQ.1.0) GO TO 19
      REWIND 16
      GO TO 19
   18 WRITE (6,2)
   20 REWIND 14
   19 JP=0
      KY=1
      KK=1
      DO 1 I=1,NJ
      I2=NVAR*I
      I1=I2-NVAR+1
      II=1
      DO 3 J=I1,I2
      U(II)=0.0
      IF (JX(J).NE.0) U(II)=B(JX(J))
      II=II+1
    3 CONTINUE
      IF(I.EQ.LF1)D1=U(2)
      IF(I.EQ.LF2)D2=U(2)
      IF(I.NE.IC(KY)) GO TO 10
      IF(JP.EQ.1) GO TO 6
      DS1=U(2)
      KY=KY+1
      JP=1
      GO TO 10
    6 IF(U(2)-DS1)7,8,8
    7 DS(KK)=DS1-U(2)
      GO TO 9

    8 DS(KK)=U(2)-DS1
    9 KK=KK+1
      JP=0
      KY=KY+1
   10 IF(LZ.EQ.1) GO TO 21
      IF(LF.EQ.1) GO TO 11
      IF(LZ.NE.1.AND.NH.NE.0) GO TO 13
      GO TO 11
   21 WRITE(6,4)I,(U(N),N=1,3)
      GO TO 11
   13 IF(CAC.NE.1.0) GO TO 16
      GO TO 12
   11 WRITE(14)U(1),U(2),U(3)
      GO TO 1
   16 WRITE(16)U(1),U(2),U(3)
      IF(I.EQ.NJ)CAC=1.0
      GO TO 1
   12 KT=(3*I)+(IP-1)*NJ*3
      KT1=KT-2
      KT2=KT-1
      DI(KT1)=U(1)
      DI(KT2)=U(2)
      DI(KT)=U(3)
    1 CONTINUE
      IF(IP.EQ.NH.AND.CAC.EQ.1.0)CAC=2.0
    2 FORMAT(///,5X,"JOINTS",19X,"DISPL.-X",15X,"DISPL.-Y",
     115X,"ROTATION",//)
    4 FORMAT (I10,1X,3E23.6)
      RETURN
      END
C
```

```
C
      SUBROUTINE EXTRAC(LJ,JX,N1,N2)
      DIMENSION LJ(1),JX(1)
      K=1
      N=N1
    1 J1=3*(K-1)
      J2=3*(N-1)
      DO 2 I=1,3
    2 LJ(I+J1)=JX(I+J2)
      K=K+1
      N=N2
      IF(K.LE.2) GO TO 1
      RETURN
      END
C
C
      SUBROUTINE FRANDI(A,B,N,M,LT,RATIO,DET,NCN,Z)
      DIMENSION A(1),B(1)
C
CCC   THIS ROUTINE SOLVES SYSTEM OF EQNS. AX=B WHERE A IS +IVE DEFINITE
CCC   SYMMETRIC BAND MATRIX, BY CHOLESKY'S METHOD.
CCC   LOWER HALF BAND ONLY (INCLUDING THE DIAGONAL) OF A IS STORED
CCC   COLUMN BY COLUMN IN A 1 DIMENSIONAL ARRAY.
CCC   SOLUTIONS X ARE RETURNED IN ARRAY B.
CCC   N - ORDER OF MATRIX A.
CCC   M - LENGTH OF LOWER HALF BAND.
CCC   DETERMINANT OF A = DET*(10**NCN), 1.E-15<!DET!<1.E15
CCC   LT=1 IF ONLY 1 B VECTOR OR IF FIRST OF SEVERAL. LT NOT = 1 FOR
CCC   SUBSEQUENT B VECTORS.
CCC   RATIO = SMALLEST RATIO OF 2 ELEMENTS ON MAIN DIAGONAL OF
CCC   TRANSFORMED A >1.E-7.
C
      IF(M.EQ.1) GO TO 101
      MM=M-1
      NM=N*M
      NM1=NM-MM
71    IF(LT.NE.1) GO TO 55
 3001 MP=M+1
C
C       TRANSFORMATION OF A.
CCC   A IS TRANSFORMED INTO A LOWER TRIANGULAR MATRIX L SUCH THAT A=L.LT
CCC   (LT=TRANSPOSE OF L.). IF Y=LT.X THEN L.Y=B.
CCC   ERROR RETURN TAKEN IF RATIO<1.E-7
C
      KK=2
      NCN=0
      DET=0.
      FAC=RATIO
      IF(A(1).GT.0.) GO TO 15
      NROW=1
      RATIO=A(1)
      GO TO 60
15    DET=A(1)
      A(1)=1./SQRT(A(1))
      BIGL=A(1)
      SML=A(1)
      A(2)=A(2)*A(1)
      TEMP=A(MP)-A(2)*A(2)
      IF(TEMP.LT.0.0) RATIO=TEMP
      IF(TEMP.EQ.0.0) RATIO=0.0
      IF(TEMP.GT.0.0) GO TO 21
      NROW=2
      GO TO 60
101   DET=1.
      NCN=0
      DO 102 I=1,N
```

```
      DET=DET*A(I)
      IF(A(I).EQ.0.0) GO TO 104
      IF(DET.GT.1.E-15) GO TO 1144
      DET=DET*1.E+15
      NCN=NCN-15
      GO TO 1145
1144   IF(DET.LT.1.E+15) GO TO 1145
      DET=DET*1.E-15
      NCN=NCN+15
1145   CONTINUE
102   B(I)=B(I)/A(I)
      RETURN
104   RATIO=A(I)
103   NROW=I
      GO TO 60
21    AMP=1.0/SQRT(TEMP)
      DET=DET*TEMP
      IF(A(MP).GT.BIGL)BIGL=A(MP)
      IF(A(MP).LT.SML)SML=A(MP)
      IF(N.EQ.2) GO TO 62
      MP=MP+M
      DO 62 J=MP,NM1,M
      JP=J-MP
      MZC=0

      IF(KK.GE.M) GO TO 1
      KK=KK+1
      II=1
      JC=1
      GO TO 2
1     KK=KK+M

      II=KK-MM
      JC=KK-MM
2     DO 65 I=KK,JP,MM
      IF(A(I).EQ.0.0) GO TO 64
      GO TO 66
64    JC=JC+M
65    MZC=MZC+1
      ASUM1=0.00
      GO TO 61
66    MMZC=MM*MZC
      II=II+MZC
      KM=KK+MMZC
      A(KM)=A(KM)*A(JC)
      IF(KM.GE.JP) GO TO 6
      KJ=KM+MM
      DO 5 I=KJ,JP,MM
      ASUM2=0.00
      IM=I-MP
      II=II+1
      KI=II+MMZC
      DO 7 K=KM,IM,MM
      ASUM2=ASUM2+A(KI)*A(K)
7     KI=KI+MM
5     A(I)=(A(I)-ASUM2)*A(KI)
6     CONTINUE
      ASUM1=0.00
      DO 4 K=KM,JP,MM
4     ASUM1=ASUM1+A(K)*A(K)
61    S=A(J)-ASUM1
      IF(S.LT.0.)RATIO=S
      IF(S.EQ.0.)RATIO=0.
      IF(S.GT.0.)GO TO 63
      NROW=(J+MM)/M
      GO TO 60
63    AIJ=1./SQRT(S)
      DET=DET*S
      IF(DET.GT.1.E-15) GO TO 144
      DET=DET*1.E+15
      NCN=NCN-15
      GO TO 145
144   IF(DET.LT.1.E+15) GO TO 145
```

```
      DET=DET*1.E-15
      NCN=NCN+15
  145 CONTINUE
      IF(A(J).GT.BIGL)BIGL=A(J)
      IF(A(J).LT.SML)SML=A(J)
   62 CONTINUE
   52 IF(SML.LE.FAC*BIGL) GO TO 54
      GO TO 53
   54 RATIO=0.
      RETURN
   60 WRITE(6,99) NROW
      Z=1.0
   99 FORMAT("0***SYSTEM IS NOT POSITIVE DEFINITE",5X,
     1"ERROR CONDITION OCCURRED IN ROW",I4)
      RETURN
   53 RATIO=SML/BIGL
   55 CALL SBAND (A,B,N,M)
      RETURN
      END
C
C
      SUBROUTINE INTER(C,FY,FM,NJ,NM,M1,JNL,JNG,BI,KC,MI,JI,
     1MEMTYP,PV,MF,PMIN,PEUC,PSHE,JF,JR,NH,NNH,MPI,ME,MSI,LLF)
      DIMENSION FY(1),FM(1),MEMTYP(1),MF(1),OV(10),NNH(1),
     1JNL(1),JNG(1),BI(1),MI(1),JI(1),MPI(10),MSI(10),
     2PE(120),PL(120),FC(120),SF(120),EU(120),LLF(1)
      CALL PSET(JI,10)
      CALL PSET(MI,10)
      CALL PSET(MPI,10)
      CALL PSET(MSI,10)
      PEUC=10.0
      PSHE=10.0
      PMIN=500.0
      CALL PSET(PE,NM)
      CALL PSET(PL,NM)
      CALL PSET(FC,NM)
      CALL PSET(SF,NM)
      CALL PSET(EU,NM)
      CALL PSET(LLF,NM)
      DO 20 J=1,NJ
      READ(M1)E,F,G
   20 CONTINUE
C
C     COMPUTE LOAD FACTOR FOR EACH MEMBER
C
      DO 21 I=1,NM
      READ(M1)AF1,VF1,BM1,BM2
      READ(M2)AF3,VF3,BM3,BM4
      IF(BM1.EQ.FM(I)) GO TO 21
      IF(BM2.EQ.FM(I)) GO TO 21
      IF(JK.EQ.0) GO TO 4
      DO 3 IE=1,JK
      IF(I.EQ.MF(IE)) GO TO 21
    3 CONTINUE
    4 IF(MEMTYP(I).EQ.6) GO TO 42
      IF(BI(I).EQ.1000.0) GO TO 21
C
C     CHECK FOR HINGE FORMATION
C
      CALL CONFOR(AF1,BM1,BM2)
      CALL CONFOR(AF3,BM3,BM4)
      AF3=AF3+AF1
      BM3=BM3+BM1
      BM4=BM4+BM2
      IF(I.EQ.IZ) GO TO 28
      DO 60 IZ=1,NH
      IF(JNL(I).EQ.NNH(IZ)) GO TO 28
   60 CONTINUE
      BMC=BM3
      BMO=BM1
   22 E1=BMC-BMO
      E2=AF3-AF1
```

```
      IF(BC.LE.0.0) GO TO 28
      IF(B7.LE.0.0) GO TO 28
      AF=C*PY(I)
      CS=(AF3-AF1)/(BMC-BMD)
      CU=AF3/BMC
      CW=AF/FM(I)
      IF(CU.LE.CW) GO TO 80
      CT=((1.0-C)*PY(I))/FM(I)
      B=(PY(I)+CS*BMC-AF3)/(CS+CT)
81    A=CS*(B-BMC)+AF3
      GO TO 2
80    B=FM(I)
      LLF(I)=1
      GO TO 81
2     TT=SQRT((AF3-AF1)**2+(BMC-BMC)**2)
      TB=SQRT((A-AF1)**2+(B-BMC)**2)
      DB=BM3-BM4
      IF(DB)40,41,41
40    DB=-DB
41    IF(DB.LE.1.0) GO TO 7
      IF(BMC.EQ.BM4) GO TO 23
      IF(TB.GT.TT) GO TO 26
      PL(I)=TB/TT
62    DO 61 IY=1,NH
      IF(JNG(I).EQ.NNH(IY)) GO TO 30
61    CONTINUE
26    BMC=BM4
      BMD=BM2
      DO 63 IW=1,NH
      IF(JNG(I).EQ.NNH(IW)) GO TO 28
63    CONTINUE
      GO TO 22
23    IF(TB.GT.TT) GO TO 28
      PG(I)=TB/TT
      IF(PL(I).EQ.0.0) GO TO 24
      IF(PG(I).EQ.0.0) GO TO 30
70    IF(PL(I).GT.PG(I)) GO TO 24
30    PE(I)=PL(I)
      NL=JNL(I)
      GO TO 25
24    PE(I)=PG(I)
      NL=JNG(I)
25    IF(PE(I).EQ.0.0) GO TO 28
      CALL ESCRT(PE,I,PMIN,NL,KC,MI,JI)
      GO TO 28
7     PE(I)=TB/TT
      NL=JNL(I)
31    CALL ESCRT(PE,I,PMIN,NL,KC,MI,JI)
      IF(NL.EQ.JNG(I)) GO TO 27
      NL=JNG(I)
      GO TO 31
27    IF(PE(I).EQ.PMIN)IA=I
C
C  CHECK FOR PLASTIC LIMIT LOAD FAILURE
C
28    IF(AF3.LT.PY(I)) GO TO 21
      PU(I)=(PY(I)-AF1)/(AF3-AF1)
      IF(PU(I).EQ.0.0) GO TO 21
      CALL ESCRT(PU,I,PULC,C,JF,MPI,CV)
      GO TO 21
C
C   CHECK FOR SHEAR FAILURE
C
42    VF3=VF3+VF1
      SF(I)=(FV-VF1)/(VF3-VF1)
      IF(SF(I).EQ.0.0) GO TO 21
      CALL ESCRT(SF,I,PSHE,C,JF,MSI,CV)
21    CONTINUE
29    RETURN
      END
C
C
```

```
      SUBROUTINE INFORCE(U,FL,S,LJ,XM,YM,AL,JX,NM,C,PY,PM,BI,FV,LZ,
     1FFX,FFY,MEMTYP,DS,ALC,TS,JNL,JNG,NJ,FI,NH,NO,CAB,NNH,D,ME,FAC,NLJ,
     2IE,JK,M1,M2,KF,KC,MI,JI,MF,LP1,LF2,LF,LLF)
      DIMENSION A(1),U(1),FL(1),S(6,6),LJ(1),XM(1),YM(1),PY(1),PM(1),BI(
     11),FFY(1),MEMTYP(1),AL(1),JX(1),FFX(1),DS(1),MPI(10),CV(10),MF(1),
     2JNL(1),JNG(1),FI(1),NNH(1),ME(1),MI(1),JI(1),PE(120),MSI(10),LLA(
     31)
      CALL PSET(PE,NM)
      REWIND 11
      IF(LZ.NE.1) GO TO 73
      M1=13
      M2=14
      WRITE(6,1)
   73 IF(NH.NE.0) GO TO 90
      REWIND M1
   90 KK=1
      PMIN=5C0.0
      PMON=5C0.0
      DO 2 I=1,NM
      READ(11)(LJ(J),J=1,6),((S(L,J),L=1,6),J=1,6)
      IF(MEMTYP(I).EQ.6) GO TO 182
      DO 3 J=1,6
      IKK=LJ(J)
      IF(IKK) 4,5,4
    5 U(J)=0.00
      GO TO 3
    4 U(J)=B(IKK)
    3 CONTINUE
      DO 6 J=1,3
      FL(J)=0.00
      DO 6 K=1,6
      FL(J)=FL(J)+S(J,K)*U(K)
    6 CONTINUE
      GO TO 184
  182 AF1=0.0
      AF2=0.0
      BM1=0.0
      BM2=0.0
      VF1=PV*DS(KK)/ALC
      VF2=VF1
      KK=KK+1
      GO TO 183
  184 VF1=(-FL(1)*YM(I)+FL(2)*XM(I))/AL(I)
      AF1=(-FL(1)*XM(I)-FL(2)*YM(I))/AL(I)
      VF2=VF1
      AF2=AF1
      BM1=-FL(3)
      BM2=BM1+VF1*AL(I)
  183 IF(LZ.EQ.1) GO TO 181
      IF(LF.EQ.1) GO TO 45
      IF(LZ.NE.1.AND.NF.NE.0) GO TO 43
      GO TO 45
  181 WRITE(6,9)I,AF1,VF1,BM1,AF2,VF2,BM2
      GO TO 45
   43 IF(CAB.NE.1.0) GO TO 49
      GO TO 44
   45 WRITE(M2)AF1,VF1,BM1,BM2
      GO TO 48
   49 WRITE(16)AF1,VF1,BM1,BM2
      IP=50
      IF(I.EQ.NM)CAB=1.0
      GO TO 2
   44 KT=(4*I)+(IP-1)*NM*4
      KT1=KT-3
      KT2=KT-2
      KT3=KT-1
      FI(KT1)=AF1
      FI(KT2)=VF1
      FI(KT3)=BM1
      FI(KT)=BM2
      GO TO 2
```

```
 48   IF(IF.EC.100) GO TC 2
      IF(MEMTYP(I).EC.6) GC TC 185
      IF(BI(I).EC.1000.0) GC TC 2

      IF(AF1.EC.0.0) GC TC 2
      CALL CCNFCR(AF1,EM1,BM2)
      IF(LF.EC.1) GC TC 2
C
CC    CHECK FCR HINGE FORMATION
C
      CALL INTER(I,C,PY,PM,AF1,EM1,BM2,JNL,JNG,NE,NL,LF,LLF)
      CALL ESCRT(PE,I,PMIN,NL,KC,MI,JI)
      GC TC 5
C
CC    CHECK FCR SHEAR FAILURE
C
 185  IF(VF1.EC.PV) GO TC 2
      PE(I)=PV/VF1
      IF(PE(I).EC.1.0) GC TC 2
      CC 39 JC=1,10
      IF(I.EC.MF(JC)) GC TO 2
 39   CCNTINLE
      CALL ESCRT(PE,I,PMCN,0,JF,MSI,CV)
 2    CCNTINLE
      IF(LF.NE.1) GO TC 132
      REWINC 17
      REWINC 13
      CC 168 NJT=1,NJ
      READ(13)B1,B2,B3
      WRITE(17)B1,B2,B3
 168  CCNTINLE
      CC 169 NMT=1,NM
      READ(13)B4,B5,B6,B7
      WRITE(17)B4,B5,B6,B7
 169  CCNTINLE
      REWINC M1
      GC TC 133
 132  IF(IR.NE.100) GO TC 60
 133  REWINC M2
      REWINC 17
      CC 61 MZ=1,NJ
      READ(M2)A1,A2,A3
 61   CCNTINLE
      CALL INTER(C,PY,PM,NJ,NM,17,JNL,JNG,EI,KC,MI,JI,
     1MEMTYP,PV,MF,PMIN,PEUC,PMCN,JF,JK,NH,NNH,MPI,14,MSI,LLF)
      REWINC 17
      IF(LF.NE.1) GO TC 60
      REWINC M1
      GC TC 30
 60   IF(LZ.EC.1) GC TC 52
      IF(NH.EC.0) GC TC 31
      IF(IR.EC.NH.AND.CAE.EC.1.0)CAE=2.0
      GC TC 82
 52   WRITE(6,51)
 30   JF=JF-1
      KF=KC-1
      IF(PMIN.LT.PMON) GC TC 74
      REWINC 17
      BAT=PMCN
      CC 76 LC=1,JF
      MF(JK+LC)=MSI(LC)
 76   CCNTINLE
      KF=0
      IF=100
      JK=JK+JF
      CALL PSET(MT,KP)
      CALL PSET(JI,KP)
      GC TC 77
 74   BAT=PMIN
```

```
      NH=NH+KP
      CALL PSET(MSI,JF)

      CALL PSET(MPI,JF)
      DO 16 ICC=1,KP
      MP(NH-KP+ICC)=MI(ICC)
      NRA(NH-KP+ICC)=JJ(ICC)
      IF(LLF(MP(NH-KP+ICC)).NE.1) GO TO 310
      LF=1
      GO TO 16
  310 LF=0
      IR=100
   16 CONTINUE

   77 REWIND M2
C
C     APPLY LOAD FACTOR TO COMPUTE JOINT DISPLACEMENTS
C
      WRITE(6,47)
      DO 23 IC=1,NJ
      IF(LZ.EQ.1) GO TO 55
      IF(NH.EQ.0) GO TO 55
      READ(17)U(1),U(2),U(3)
   55 READ(M2)U(4),U(5),U(6)
      IF(LZ.EQ.1) GO TO 91
      IF(NH.EQ.0) GO TO 91
      U(1)=BAT*U(4)+U(1)
      U(2)=BAT*U(5)+U(2)
      U(3)=BAT*U(6)+U(3)
      IF(IC.EQ.LP1)D3=U(2)
      IF(IC.EQ.LP2)D4=U(2)
      GO TO 92
   91 U(1)=BAT*U(4)
      U(2)=BAT*U(5)
      U(3)=BAT*U(6)

   92 WRITE(6,42)IC,U(1),U(2),U(3)
      IF(NP.NE.0) GO TO 53
      WRITE(17)U(1),U(2),U(3)
      GO TO 23
   53 WRITE(M1)U(1),U(2),U(3)
   23 CONTINUE
      IF(LZ.EQ.1) GO TO 96
      IF(NP.EQ.0) GO TO 96
      C=(D3+D4)/2.0
      GO TO 97
   96 C=BAT*C
      EAD=5.0*D
   98 WRITE(6,144)EAD
   97 WRITE(6,143)C
C
C     APPLY LOAD FACTOR TO COMPUTE MEMBER FORCES
C
      WRITE(6,1)
      DO 22 IA=1,NM
      IF(LZ.EQ.1) GO TO 56
      IF(NH.EQ.0) GO TO 56
      READ(17)AF1,VF1,BM1,BM2
   56 READ(M2)AF3,VF3,BM3,BM4
      IF(LZ.EQ.1) GO TO 93
      IF(NH.EQ.0) GO TO 93
      AF1=BAT*AF3+AF1
      VF1=BAT*VF3+VF1
      BM2=BAT*BM4+BM2
      BM1=BAT*BM3+BM1
      GO TO 94
   93 AF1=BAT*AF3
      VF1=BAT*VF3
      BM1=BAT*BM3
      BM2=BAT*BM4
   94 AF2=AF1
```

```
      VF2=VF1
      IF(MEMTYP(IA).NE.6) GO TO 187
      DO 186 IY=1,JK
      IF(IA.NE.MF(IY)) GO TO 186
      VF1=PV
      VF2=PV
      GO TO 187
  186 CONTINUE
  187 WRITE(6,9)IA,AF1,VF1,BM1,AF2,VF2,BM2
      IF(NH.NE.0) GO TO 54
      WRITE(17)AF1,VF1,BM1,BM2
      GO TO 22
   54 WRITE(11)AF1,VF1,BM1,BM2
   22 CONTINUE
      IF(BAT.EQ.PMIN) GO TO 13
      WRITE(6,123)BAT
      GO TO 14
   13 WRITE(6,124)BAT
C
C     APPLY LOAD FACTOR TO COMPUTE NEW LOADINGS
C
   14 DO 140 IB=1,NLJ
      IF(LZ.EQ.1) GO TO 95
      IF(NH.EQ.1) GO TO 95
      FFX(IB)=BAT*FFX(IB)+FFX(IB)
      FFY(IB)=BAT*FFY(IB)+FFY(IB)
      GO TO 140
   95 FFX(IB)=BAT*FFX(IB)
      FFY(IB)=BAT*FFY(IB)
  140 CONTINUE
      WRITE(6,141)FFX(1),FFY(1)
      IF(BAT.EQ.PMIN) GO TO 78
      DO 79 LE=1,JF
      WRITE(6,38)MF(LE)
   79 CONTINUE
      GO TO 82
   78 DO 190 LU=1,KP
      WRITE(6,151)JI(LU),MI(LU)
  190 CONTINUE
    1 FORMAT(//,4X,"MEMBER",5X,"A.F. AT JNL",3X,"V.F. AT JNL",
     13X,"B.M. AT JNL",3),"A.F. AT JNG",3X,"V.F. AT JNG",
     23X,"B.M. AT JNG",//)
    9 FORMAT(I10,6F14.6)
   38 FORMAT(7X,"MEMBER",I6,"  HAS REACHED ITS LOAD CAPACITY")
   42 FORMAT (I10,1X,3E23.6)
   47 FORMAT(///,5X,"JOINTS",15X,"DISPL.-X",15),"DISPL.-Y",
     115X,"ROTATION",//)
   51 FORMAT(///////,5X,"****ELASTIC LIMIT****")
  123 FORMAT(//,5X,"FAILURE IS CONTROLLED BY SHEAR AT CONNECTIONS",/,
     15X,"WITH RATIO OF FAILURE EQUALS TO ",F10.4)
  124 FORMAT(//,5X,"FAILURE IS CONTROLLED BY PLASTIC HINGE  FORMATION ON
     1 MEMBERS",/,2X,"WITH RATIO OF FAILURE EQUALS TO",F10.4)
  131 FORMAT(/,5X,"RATIO OF P OVER PY FOR FAILED MEMBER IS LESS THAN C")
  141 FORMAT(/,5X,"AT HORIZONTAL LOAD OF",F8.4,5X,"AND VERTICAL LOAD OF"
     1,F9.4)
  143 FORMAT(//,5X,"TOTAL MID SPAN DEFLECTION IS",E23.6)
  144 FORMAT(//,5X,"MAXIMUM MID-SPAN DISPLACEMENT ALLOWED IS",F15.6,/)
  151 FORMAT(7X,"HINGE IS FORMED AT JOINT",I5,2),"OF MEMBER",I5)
   82 IF(LF.EQ.1) WRITE(6,131)
      RETURN
      END
C
C
      SUBROUTINE INTER(I,C,FY,PM,AF1,BM1,BM2,JNL,JNG,PE,NL,LF,LLF)
      DIMENSION FY(1),PM(1),JNL(1),JNG(1),PE(1),LLF(1)
      IF(BM2.GT.BM1) GO TO 3
      BMC=BM1
      NL=JNL(I)
      GO TO 4
    3 BMC=BM2
      NL=JNG(I)
```

```
4     AF=C*PY(I)
      ES=AF1/EMC
      SK=ES/(1.0-C)
      SLY=AF/PM(I)
      IF(ES.LT.SLY) GO TO 1
      AE=(SK*PM(I))/(1.0+SK*PM(I)/PY(I))

      GO TO 2
1     AE=ES*PM(I)
      LLF(I)=1
2     PE(I)=AE/AF1
      RETURN
      END
C
C
      SUBROUTINE LAYOUT(X,Y,IX,JX,JNL,JNG,MEMTYP,AREA,BI,AL,XM,YM,LJ,
     1KDEG,KMAT,NJ,NM,PY,PM,NS,KS,IC,JT,LK)
      DIMENSION X(1),Y(1),IX(1),JX(1),JNL(1),JNG(1),MEMTYP(1),AREA(1),
     1BI(1),AL(1),XM(1),YM(1),LJ(1),PY(1),PM(1),PS(120),IC(1),JT(1)
      LK=1
      K=1
      DO 1 I=1,NJ

      I2=3*I
      I1=I2-3+1
      READ(5,2) X(I),Y(I),(IX(J),J=I1,I2)
      IF(IX(I1).EQ.0) GO TO 1
      IF(IX(I1).EQ.1) GO TO 1
      IF(I.EQ.1) GO TO 30
      LK1=I1-3
      IF(IX(LK1).EQ.IX(I1)) GO TO 31
      GO TO 30
31    JT(LK)=I-1
      LK=LK+1
      GO TO 1
30    I3=I1+1
      IF(IX(I3).EQ.IX(I1)) GO TO 1
      JA=K+1
      IC(K)=I-1
      IC(JA)=I
      K=K+2
    1 CONTINUE
      NMAT=3*NJ
      NDEG=0
      DO 7 I=1,NMAT
      IF(IX(I)-1) 8,9,10
    8 JX(I)=0
      GO TO 7
    9 NDEG=NDEG+1
      JX(I)=NDEG
      GO TO 7
   10 NJ1=(I-1)/3
      NL=IX(I)-1
      NJ2=I-3*NJ1
      JX(I)=JX(3*NL+NJ2)
    7 CONTINUE
      WRITE(6,6)
      NE=NM-NS
      DO 3 I=1,NM
      IF(I.GT.NE) GO TO 20
      READ(5,21)JNL(I),JNG(I),MEMTYP(I),AREA(I),BI(I),PS(I)
      IF(PS(I).EQ.0.0) PS(I)=PS(I-1)
      GO TO 22
20    READ(5,4) JNL(I),JNG(I),MEMTYP(I),AREA(I),BI(I)
22    IF(MEMTYP(I).EQ.0) MEMTYP(I)=MEMTYP(I-1)

      IF(AREA(I).EQ.0) AREA(I)=AREA(I-1)
      IF(BI(I).EQ.0) BI(I)=BI(I-1)
      N1=JNL(I)
      N2=JNG(I)
      CALL STRAC(LJ,J,N1,N2)
      XM(I)=X(N2)-X(N1)
```

```
      YM(I)=Y(N2)-Y(N1)
      AL(I)=SQRT(XM(I)**2+YM(I)**2)
      IF(BI(I).EQ.1000.0) GO TO 11
      FY(I)=YS*AREA(I)
      PM(I)=YS*FS(I)
      WRITE(6,5) I,JNL(I),JNG(I),MEMTYP(I),(LJ(K),K=1,6),AREA(I),
     1BI(I),AL(I),X(JNL(I)),Y(JNL(I)),X(JNG(I)),Y(JNG(I)),FY(I),PM(I)
      GO TO 3
   11 WRITE(6,12)I,JNL(I),JNG(I),MEMTYP(I),(LJ(K),K=1,6),AREA(I),
     1BI(I),AL(I),X(JNL(I)),Y(JNL(I)),X(JNG(I)),Y(JNG(I))
    3 CONTINUE
    2 FORMAT(F5.1,4X,F5.1,2X,3I5)
    4 FORMAT(I3,2X,I3,2),I1,F8.2,F9.1)
    5 FORMAT(5X,I5,1X,2I4,I4,1X,6I4,F12.2,F16.2,2X,F9.2,6F8.2)
    6 FORMAT(//,5X,"MEMBER",1X,"JNL",1X,"JNG",1X,"TYPE",1X,
     1"C-O-D-E--N-U-M-B-E-R-S",8X,"AREA",4X,"MOMENT OF INERTIA",
     22X,"LENGTH",3X,"X-JNL",3X,"Y-JNL",3X,"X-JNG",3X,"Y-JNG",  FY      PM
     3",//)
   12 FORMAT(5X,I5,1X,2I4,I4,1X,6I4,F12.2,F16.2,2X,F9.2,4F8.2,
     1"   NOT APPLICABLE")
   21 FORMAT(I3,2X,I3,2),I1,F8.2,F9.1,F9.2)
      RETURN
      END
C
C
      SUBROUTINE MSTIFF(LJ,JX,E,NV,LEAND,A,IM,JNL,JNG,MEMTYP,AL,XM,YM,BI
     1,AREA,S,AV,GM,PV,ALD)
      DIMENSION LJ(1),JX(1),A(1),JNL(1),JNG(1),MEMTYP(1),AL(1),XM(1),YM(
     11),BI(1),AREA(1),S(6,6)
      N1=JNL(IM)
      N2=JNG(IM)
      CALL EXTRAC(LJ,JX,N1,N2)
      XL=AL(IM)
      AX=XM(IM)
      AY=YM(IM)
      AR=AREA(IM)
      CI=BI(IM)
      MT=MEMTYP(IM)
      CALL PRESET(S,6,6)
      CALL STIFF(S,XL,AX,AY,E,AR,CI,MT,AV,GM,PV,ALD)
      CALL SETUP(A,S,LJ,LEAND)
      RETURN
      END
C
C
      SUBROUTINE PRESET(A,M,N)
      DIMENSION A(M,1)
      DO 1 I=1,M
      DO 2 J=1,N
    2 A(I,J)=0.00
    1 CONTINUE
      RETURN
      END
C
C
      SUBROUTINE PSET(A,M)
      DIMENSION A(1)
      DO 1 I=1,M
    1 A(I)=0.00
      RETURN
      END
C
C
      SUBROUTINE SBAND(A,E,N,M)
      DIMENSION A(1),B(1)
C
C  THIS ROUTINE SOLVES FOR L.Y=E BY A FORWARDS SUBSTITUTION, AND
C  HENCE FOR X FROM LT.)=Y BY A BACKWARDS SUBSTITUTION.
C
      MP=M-1
      NP=N*M
```

```
      NM1=NM-MM
   55 SUM=0.00
    5 B(1)=B(1)*A(1)
      KK=1
      K1=1
      J=1
      DO 8 L=2,N
      BSUM1=0.00
      LM=L-1
      J=J+M
      IF(KK.GE.M)GO TO 12
      KK=KK+1
      GO TO 13
   12 KK=KK+M
      K1=K1+1
   13 JK=KK
      DO 9 K=K1,LM
      BSUM1=BSUM1+A(JK)*B(K)
      JK=JK+MM
    9 CONTINUE
    8 B(L)=(B(L)-BSUM1)*A(J)
  100 B(N)=B(N)*A(NM1)
      NMM=NM1
      NN=N-1
      ND=N
      DO 10 L=1,NN
      BSUM2=0.00
      NL=N-L
      NL1=N-L+1
      NMM=NMM-M
      NJ1=NMM
      IF(L.GE.M)ND=ND-1
      DO 11 K=NL1,ND
      NJ1=NJ1+1
      BSUM2=BSUM2+A(NJ1)*B(K)
   11 CONTINUE
   10 B(NL)=(B(NL)-BSUM2)*A(NMM)
    6 RETURN
      END
C
C
      SUBROUTINE SETUP(A,S,LJ,LBAND)
      DIMENSION A(1),S(6,1),LJ(1)
      DO 1 I=1,6
      LJR=LJ(I)
      IF(LJR.EQ.0) GO TO 1
      DO 2 J=I,6
      LJC=LJ(J)
      IF(LJC.EQ.0) GO TO 2
      IF(LJR-LJC) 2,5,4
    6 IF(J-I) 7,4,7
    7 K=(LJC-1)*LBAND+LJR
      A(K)=A(K)+2.0*S(I,J)
      GO TO 2
    4 K=(LJC-1)*LBAND+LJR
      GO TO 5
    3 K=(LJR-1)*LBAND+LJC
    5 A(K)=A(K)+S(I,J)
    2 CONTINUE
    1 CONTINUE
      RETURN
      END
C
C
      SUBROUTINE SOLVE1(C,E,Y,N)
      DIMENSION A(30,30),E(30),Y(30),C(30,30),C(30)
      CALL PRESET(C,N,N)
      DO 11 I=1,N
      DO 11 J=1,N
      C(I)=B(I)
   11 C(I,J)=A(I,J)
```

```
      M=1
   13 DO 7 K=1,N
      IF(A(K,K).EQ.0.0) GO TO 24
      A(K,K)=1.00/A(K,K)
      I=K
      DO 2 J=1,N

      IF(I.EQ.J) GO TO 2
      A(I,J)=-A(I,J)*A(K,K)
    2 CONTINUE
      DO 3 I=1,N
      DO 3 J=1,N
      IF(I.EQ.K) GO TO 3
      IF(J.EQ.K) GO TO 3
      A(I,J)=A(I,J)+A(K,J)*A(I,K)
    3 CONTINUE
      DO 4 I=1,N
      IF(I.EQ.K) GO TO 4
      J=K
      A(I,J)=A(I,K)*A(K,K)
    4 CONTINUE
    7 CONTINUE
C       MATRIX MULT
      DO 5 I=1,N
      Y(I)=0
      DO 5 J=1,N
    5 Y(I)=Y(I)+A(I,J)*B(J)
      GO TO 20
   24 DO 6 I=1,N
      DO 6 J=1,N
      A(I,J)=C(I,J)
    6 B(I)=D(I)
   30 M=M+1
      IF(A(M,1)) 28,30,28
   28 I=M
      IF(M.EQ.N) GO TO 20
      B(1)=D(M)
      B(M)=D(1)
      DO 40 J=1,N
      A(M,J)=C(1,J)
   40 A(1,J)=C(I,J)
      GO TO 13
   20 RETURN
      END
C
C
      SUBROUTINE STIFF(S,XL,AX,AY,E,AR,CI,MT,AV,GM,PV,ALD)
      DIMENSION S(6,6)
      IF(MT.EQ.6) GO TO 42
      AA=AR*E/XL**3
      CC=AX**2
      DD=AY**2
      EE=AX*AY
      S(1,1)=AA*CC
      S(2,1)=AA*EE
      S(2,2)=AA*DD
      S(4,1)=-S(1,1)
      S(4,2)=-S(2,1)
      S(4,4)=S(1,1)
      S(5,1)=S(4,2)
      S(5,2)=-S(2,2)
      S(5,4)=S(2,1)
      S(5,5)=S(2,2)
      GO TO (23,24,25,25,27),MT
   27 G=12.0*E*CI/AV*GM*)L**2
      BB=(12.0*E*CI/XL**3)/(1.0+G)
      GO TO 26
   24 BB=12.00*E*CI/XL**3
      GO TO 26
   25 BB=3.00*E*CI/XL**3
   26 FF=BB*DD
      GG=BB*EE
```

```
      TT=BB*CC
      YY=AY*BB*XL**2/2.DC
      XX=AX*BB*XL**2/2.DC
      ALL=BB*XL**4/3.DC
      ALA=BB*XL**4/3.DC
      S(1,1)=S(1,1)+FF
      S(2,1)=S(2,1)-GG
      S(2,2)=S(2,2)+HH
      S(4,1)=S(4,1)-FF
      S(4,2)=S(4,2)+GG
      S(4,4)=S(4,4)+FF

      S(5,1)=S(5,1)+GG
      S(5,2)=S(5,2)-HH
      S(5,4)=S(5,4)-GG
      S(5,5)=S(5,5)+HH
      GO TO (27,28,29,31,30),MT
   30 ALL=ALL*(1.0+G/4.0)
      ALA=ALA*(1.0-G/2.0)
   28 S(3,1)=S(3,1)-YY
      S(3,2)=S(3,2)+XX
      S(3,3)=S(3,3)+ALL
      S(4,3)=S(4,3)+YY
      S(5,3)=S(5,3)-XX
      S(6,1)=S(6,1)-YY
      S(6,2)=S(6,2)+XX
      S(6,3)=S(6,3)+ALA/2.DC
      S(6,4)=S(6,4)+YY
      S(6,5)=S(6,5)-XX
      S(6,6)=S(6,6)+ALL
      GO TO 23
   29 S(6,1)=S(6,1)-2.DC*YY
      S(6,2)=S(6,2)+2.DC*XX
      S(6,4)=S(6,4)+2.DC*YY
      S(6,5)=S(6,5)-2.DC*XX
      S(6,6)=S(6,6)+3.DC*ALL
      GO TO 23
   31 S(3,1)=S(3,1)-2.DC*YY

      S(3,2)=S(3,2)+2.DC*XX
      S(3,3)=S(3,3)+3.DC*ALL
      S(4,3)=S(4,3)+2.DC*YY
      S(5,3)=S(5,3)-2.DC*XX
      GO TO 23
   42 SC=PV/ALD
   43 S(2,2)=SC
      S(5,2)=-SC
      S(5,5)=SC
   23 DO 32 I=1,6
      DO 32 J=I,6
   32 S(I,J)=S(J,I)
      RETURN
      END
C
C
      SUBROUTINE SUMFIC(L,JNG,NH,NJ,DM,LP1,LP2,D,FI,NM,NLJ,
     1JK,MF,FY,M1,M2,FF),FFY,MEMTYP,PM,JNL,BI,MI,KO,MI,JI,ME,NS,C,
     2NNH,PMIN,PSHE,PBUC,EAT,JF,MPI,IR,PV,MSI,LLF)
      DIMENSION DI(1),U(1),DM(10),C(3),FT(4),FS(P),FI(1),MF(1),FY(1),
     1FFX(1),FFY(1),MEMTYP(1),NNH(1) ,JNL(1),BI(1),MI(1),JI(1),ME(1),
     2PM(1),JNG(1),MPI(10),MSI(10),LLF(1)
      NT=NH-NS
      JE=JF-1
      KE=KC-1
C
C   DETERMINE TYPE OF YIELD MECHANISM
C
      IF(PSHE.EQ.10.0) GO TO 23
      IF(PBUC.LT.PSHE) GO TO 23
      IF(PMIN.LT.PSHE) GO TO 23
```

```
      BAT=PSHE
      DO 12 JS=1,JF
      MF(JK+JS)=MSI(JS)
12    CONTINUE
      GO TO 13
23    IF(PMIN.LT.PBUC) GO TO 25
      BAT=PBUC
27    DO 11 JZ=1,JF
      MF(JK+JZ)=MPI(JZ)
11    CONTINUE
13    JK=JF+JK
      CALL PSET(MI,KP)
      CALL PSET(JI,KP)
      IR=100
      KF=0
      GO TO 26
25    BAT=PMIN
      CALL PSET(MPI,JF)
      CALL PSET(MSI,JF)
      NHH=NH+KP
      DO 160 LV=1,KP
      ME(NH+LV)=MI(LV)
      NNH(NH+LV)=JI(LV)
160   CONTINUE
26    IF(M1-M2)40,42,41
40    M1=14
      M2=13
      GO TO 42
41    M1=13
      M2=14
42    REWIND 16
      REWIND M1
      REWIND M2
C
C     APPLY LOAD FACTOR TO COMPUTE JOINT DISPLACEMENTS
C
      WRITE(6,1)
      DO 2 J=1,NJ
      READ(16)U(1),U(2),U(3)
      READ(M2)U(4),U(5),U(6)
      DO 3 IG=1,3
      F=0.0
      DO 4 I=1,NH
      G(IG)=DM(I)*DI(3*(I-1)*NJ+(3*J)-(3-IG))+G
      F=G(IG)
4     CONTINUE
      G(IG)=(U(IG)+G(IG))*BAT+U(IG+3)
3     CONTINUE
      WRITE(6,5)J,(G(IG),IG=1,3)
      IF(J.EQ.LP1)D1=G(2)
      IF(J.EQ.LP2)D2=G(2)
      WRITE(M1)(G(N),N=1,3)
2     CONTINUE
      D=(D1+D2)/2.0
      WRITE(6,143)D
C
C     APPLY LOAD FACTOR TO COMPUTE MEMBER FORCES
C
      WRITE(6,9)
      DO 6 J=1,NM
      READ(16)(FS(K),K=1,4)
      READ(M2)(FS(K),K=5,8)
      DO 7 IG=1,4
      X=0.0
```

```
      DO 8 I=1,NH
      FT(IC)=PM(I)*FI(4*(I-1)*NP+(4*J)-(4-IC))+X
      X=FT(IC)
8     CONTINUE
      FT(IC)=(FS(IC)+FT(IC))*BAT+FS(IC+4)
      IF(MEMTYP(J).NE.6) GO TO 43
      DO 44 IL=1,JK
      IF(J.NE.MF(IL)) GO TO 44
      FT(2)=FV
      GO TO 7
44    CONTINUE
43    IF(IC.EQ.1) GO TO 66
      IF(IC.EQ.2) GO TO 7
      IF(J.GT.NT) GO TO 7

      DO 650 IT=1,NHH
      IF(J.NE.ME(IT)) GO TO 650
      IF(IC.EQ.3) GO TO 80
      GO TO 81
 80   IF(JNL(J).EQ.NNH(IT)) GO TO 82
      GO TO 650
 81   IF(JNG(J).NE.NNH(IT))GO TO 650
82    RA=FT(1)
      IF(RA)60,61,61
60    RA=-RA
61    RT=(PM(J)/(1.0-C))*(1.0-RA/PY(J))
      IF(FT(IC))64,65,65
64    FT(IC)=-RT
      GO TO 650
65    FT(IC)=RT
650   CONTINUE
      GO TO 7
66    IF(MEMTYP(J).EQ.6) GO TO 7

      DO 70 MC=1,JK
      IF(J.NE.MF(MC)) GO TO 70
      IF(FT(1))68,69,69
68    FT(1)=-PY(J)
      GO TO 71
69    FT(1)=PY(J)
71    FT(3)=0.0
      FT(4)=0.0
      FT(2)=0.0
      GO TO 14
70    CONTINUE
7     CONTINUE
      IF(LLF(J).NE.1) GO TO 14
      DO 18 JC=3,4
      IF(ABS(FT(JC)).LT.PM(J)) GO TO 18
      IF(FT(JC))21,22,22
21    FT(JC)=-PM(J)
      GO TO 18
22    FT(JC)=PM(JC)
18    CONTINUE
14    WRITE(6,10)J,FT(1),FT(2),FT(3),FT(1),FT(2),FT(4)
      WRITE(61)(FT(N),N=1,4)
6     CONTINUE
      IF(BAT.EQ.PMIN) GO TO 171
      IF(BAT.EQ.PRUC)WRITE(6,122)BAT
      IF(BAT.EQ.PSHE)WRITE(6,123)BAT
      GO TO 16
171   WRITE(6,124)BAT
      NH=NH+NP
C
C     APPLY LOAD FACTOR TO COMPUTE NEW LOADINGS
C
```

```
      DO 20 IA=1,NLJ
      FFX(IA)=BAT*FFX(IA)+FFX(IA)
      FFY(IA)=BAT*FFY(IA)+FFY(IA)
   20 CONTINUE
      WRITE(6,141)FFX(1),FFY(1)
      IF(BAT.NE.BMIN) GO TO 152
      DO 180 LU=1,KF
      WRITE(6,151)JI(LU),MI(LU)
  180 CONTINUE
      GO TO 34
  152 IF(JF.EQ.JK) GO TO 36
      JG=JK-JF+1
      GO TO 37
   36 JG=1
   37 DO 35 IG=JG,JK
      WRITE(6,38)MF(IG)
   35 CONTINUE
    1 FORMAT(///,5X,"JOINTS",15X,"DISPL.-X",15X,"DISPL.-Y",
     115X,"ROTATION",//)
    5 FORMAT (I10,1X,3E23.6)
    9 FORMAT(//,4X,"MEMBER",5X,"A.F. AT JNL",3X,"V.F. AT JNL",
     13X,"B.M. AT JNL",3X,"A.F. AT JNG",3X,"V.F. AT JNG",
     23X,"B.M. AT JNG",//)
   10 FORMAT(I10,6F14.5)
   38 FORMAT(7X,"MEMBER",I6," HAS REACHED ITS LOAD CAPACITY")
  122 FORMAT(///,5X,"FAILURE IS CONTROLLED BY MEMBER REACHING PLASTIC LOA
     1D LIMIT",/,
     15X,"WITH RATIO OF FAILURE EQUALS TO ",F10.4)
  123 FORMAT(///,5X,"FAILURE IS CONTROLLED BY SHEAR AT CONNECTIONS",/,
     15X,"WITH RATIO OF FAILURE EQUALS TO ",F10.4)
  124 FORMAT(//,5X,"FAILURE IS CONTROLLED BY PLASTIC HINGE FORMATION ON
     1 MEMBERS",/,7X,"WITH RATIO OF FAILURE EQUALS TO",F10.4)
  141 FORMAT(/,5X,"AT HORIZONTAL LOAD OF",F8.4,5X,"AND VERTICAL LOAD OF"
     1,F9.4)
  143 FORMAT(//,5X,"TOTAL MID SPAN DEFLECTION IS",E23.6)
  151 FORMAT(7X,"HINGE IS FORMED AT JOINT",I5,2),"OF MEMBER",I5)
   34 RETURN
      END
C
C
      SUBROUTINE SUMI(DM,FI,NM,NJ,NH,ME)
      DIMENSION AS(4),FC(4),DM(1),FI(1)
      ME=15
      REWIND 15
      REWIND 16
      DO 30 J=1,NJ
      READ(16)A,B,C
   30 CONTINUE
      DO 31 J=1,NM
      READ(16)(AS(M),M=1,4)
      DO 32 IG=1,4
      D=0.0
      DO 33 I=1,NH
      MA=4*(I-1)*NM+(4*J)-(4-IG)
      FC(IG)=DM(I)*FI(MA)+D
      D=FC(IG)
   33 CONTINUE
      FC(IG)=FC(IG)+AS(IG)
   32 CONTINUE
      WRITE(ME)(FC(N),N=1,4)
   31 CONTINUE
      RETURN
      END
C
C
```

INPUT SEQUENCE
****

	FORMAT	LOCATION	NO. OF CARDS
1.	READ(5,3)NPS,NJ,NM,E,C,YS 3 FORMAT(3I10,F10.0,2F8.4)	MAIN	1
2.	READ(5,17)LP1,LP2,NS,MS,TS,TF,BP 17 FORMAT(3I10,5F10.4)	MAIN	1
3.	READ(5,2)TITLE 2 FORMAT(8A8)	MAIN	1
4.	READ(5,9)AV,GM,ALO 9 FORMAT(8F10.4)	MAIN	1
5.	READ(5,2)X(I),Y(I),(IX(J),J=I1,I2) 2 FORMAT(F5.1,4X,F5.1,2X,3I5)	LAYOUT	NJ
	IF NS=0,GO TO 8		
6.	READ(5,21)JNL(I),JNG(I),MEMTYP(I), AREA(I),BI(I),PS(I) 21 FORMAT(I3,2X,I3,2X,I1,F8.2,F9.1,F9.2)	LAYOUT	NM-NS
7.	READ(5,4)JNL(I),JNG(I),MEMTYP(I), AREA(I),BI(I) 4 FORMAT(I3,2X,I3,2X,I1,F8.2,F9.1)	LAYOUT	NS
	GO TO 9		
8.	READ(5,21)JNL(I),JNG(I),MEMTYP(I), AREA(I),BI(I),PS(I) 21 FORMAT(I3,2X,I3,2X,I1,F8.2,F9.1,F9.2)	LAYOUT	NM
9.	READ(5,17)NLJ 17 FORMAT(3I10,5F10.4)	MAIN	1
10.	READ(5,2)JN(I),FFX(I),FFY(I) 2 FORMAT(I3,5X,F5.1,7X,F5.1)	CLOAD	NLJ

APPENDIX II

LOAD-STRAIN CURVES FOR VARIOUS TRUSSES

The experimental load-strain curves for the testing of the five trusses BBST, BBOV, S1, S2 and BO are presented in the following figures. The arrangements of strain gauges and rosettes for the above trusses have been described in Chapter 2.

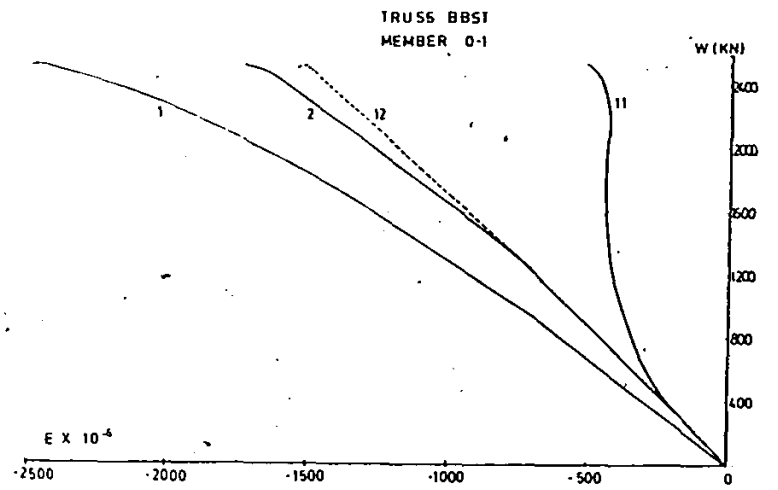
TRUSS BBST
MEMBER 0-1
W (KN)
2400
2000
1600
1200
800
400
1
2
12
11
E X 10⁻⁶
-2500
-2000
-1500
-1000
-500
0

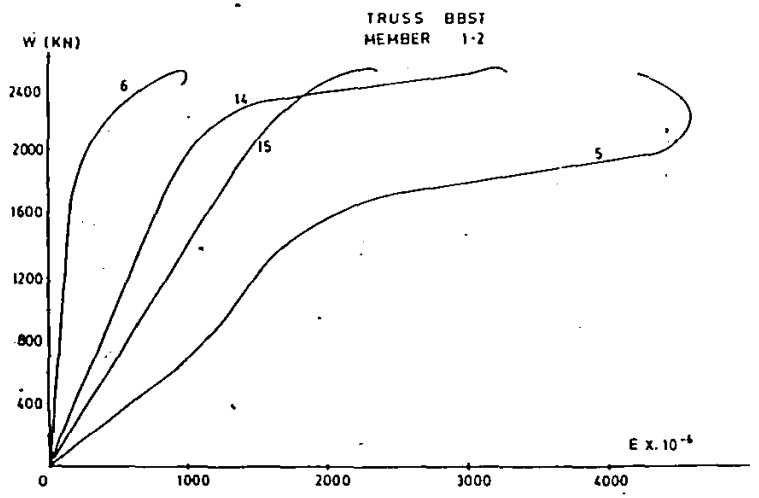
TRUSS BBST
MEMBER 1-2
W (KN)
2400
2000
1600
1200
800
400
6
14
15
5
E x.10⁻⁶
0
1000
2000
3000
4000

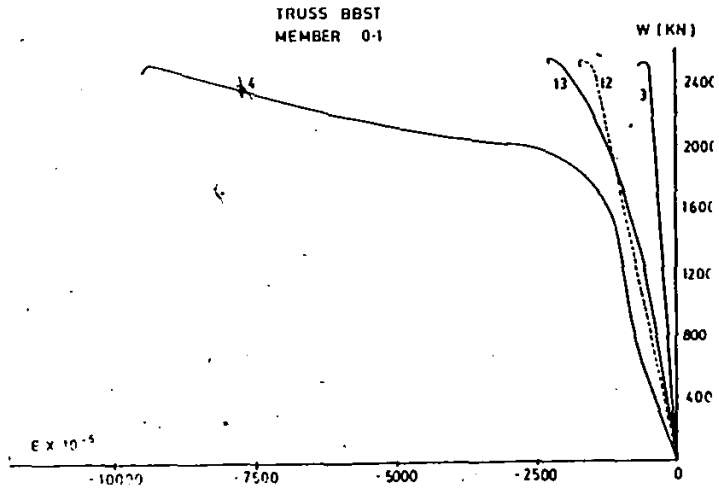
TRUSS BBST
MEMBER 0-1
W (KN)
4
13
12
3
E x 10⁻⁶
-10000
-7500
-5000
-2500
0

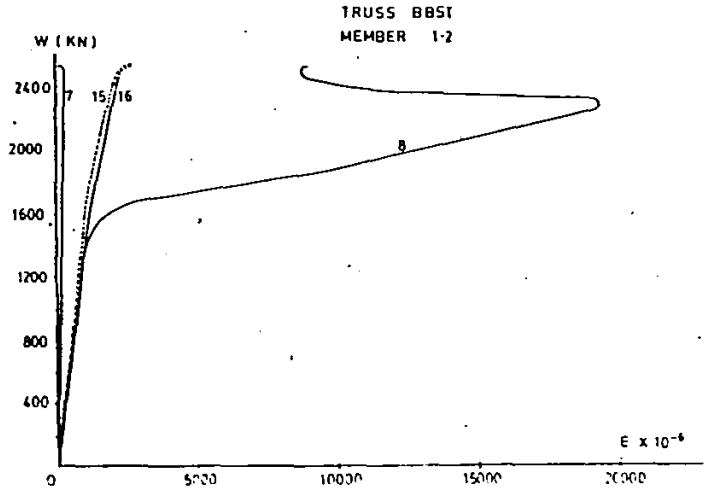
TRUSS BBST
MEMBER 1-2
W (KN)
2400
2000
1600
1200
800
400
7
15
16
8
E x 10⁻⁶
0
5000
10000
15000
20000

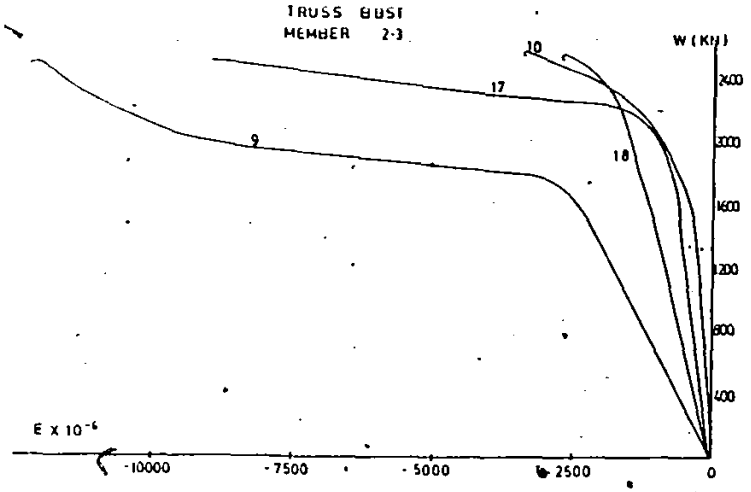
TRUSS BBST
MEMBER 2-3
W (KN)
2400
2000
1600
1200
800
400
10
17
9
18
E X 10⁻⁶
-10000
-7500
-5000
-2500
0

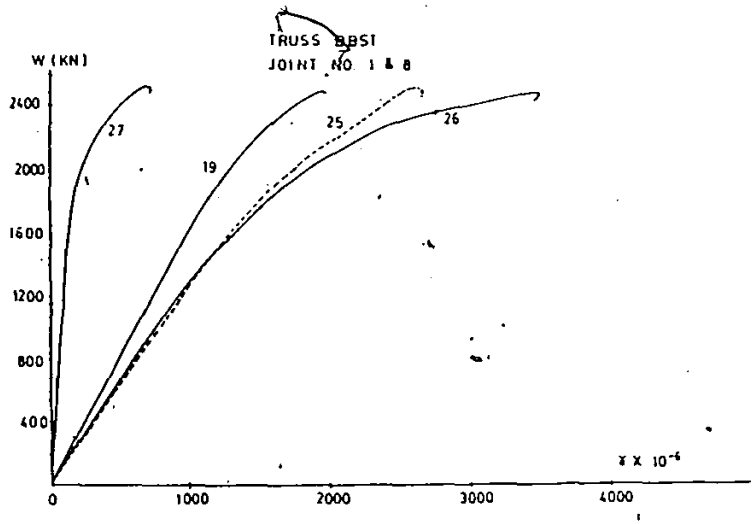
TRUSS BBST
JOINT NO. 1 & 8
W (KN)
2400
2000
1600
1200
800
400
27
19
25
26
X X 10⁻⁶
0
1000
2000
3000
4000

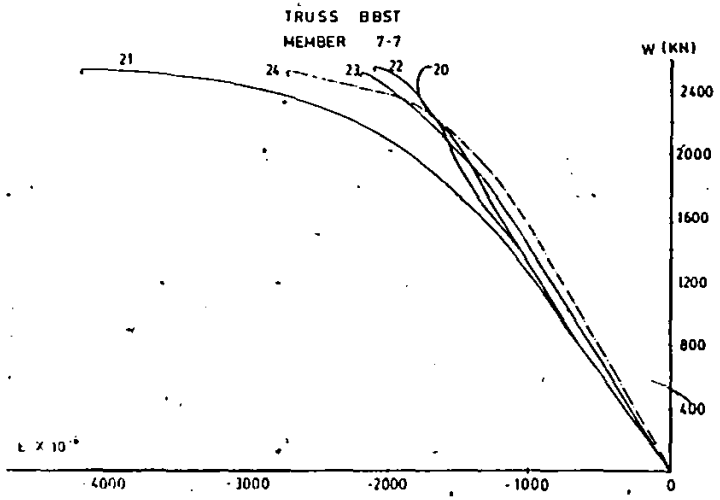
TRUSS BBST
MEMBER 7-7
W (KN)
2400
2000
1600
1200
800
400
21
24
23
22
20
E X 10⁻⁶
-4000
-3000
-2000
-1000
0

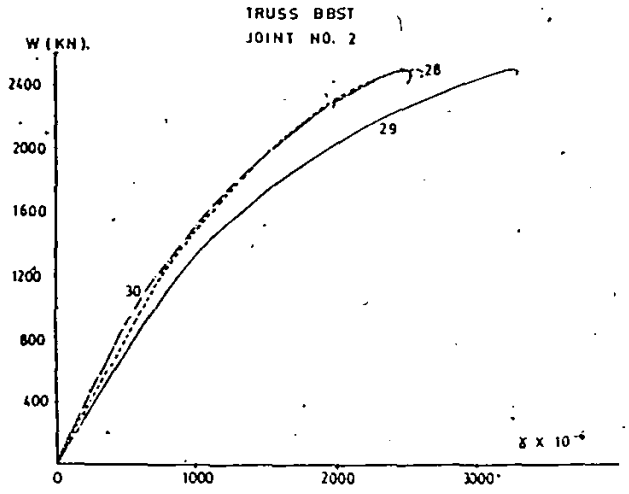
TRUSS BBST
JOINT NO. 2
W (KN).
2400
2000
1600
1200
800
400
28
29
30
X X 10⁻⁶
0
1000
2000
3000

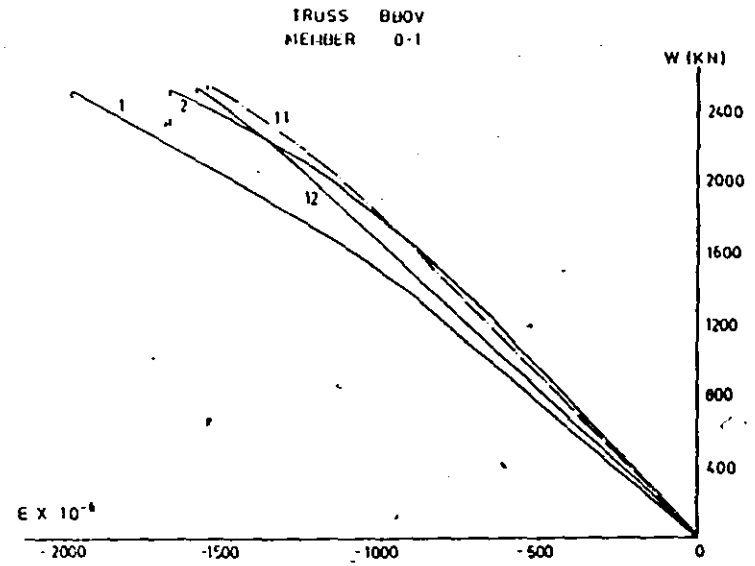
TRUSS BBOV
MEMBER 0-1
W (KN)
2400
2000
1600
1200
800
400
E X 10⁻⁶
-2000
-1500
-1000
-500
0
1
2
11
12

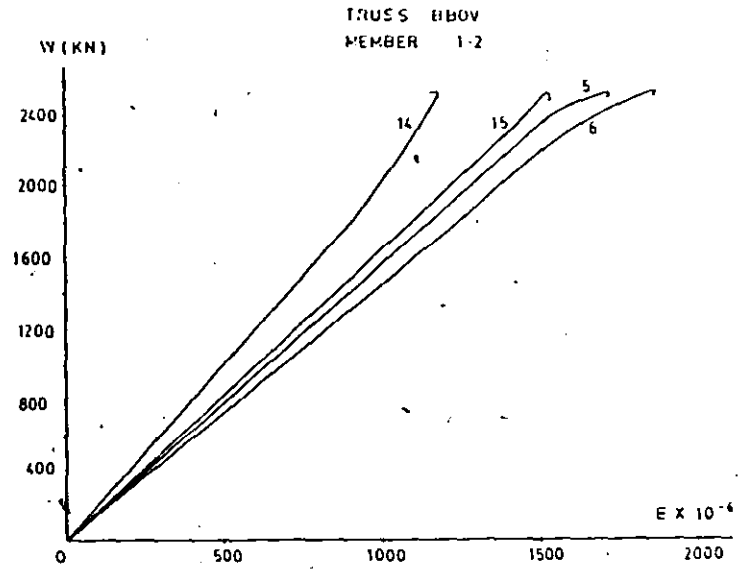
TRUSS BBOV
MEMBER 1-2
W (KN)
2400
2000
1600
1200
800
400
E X 10⁻⁶
0
500
1000
1500
2000
14
15
5
6

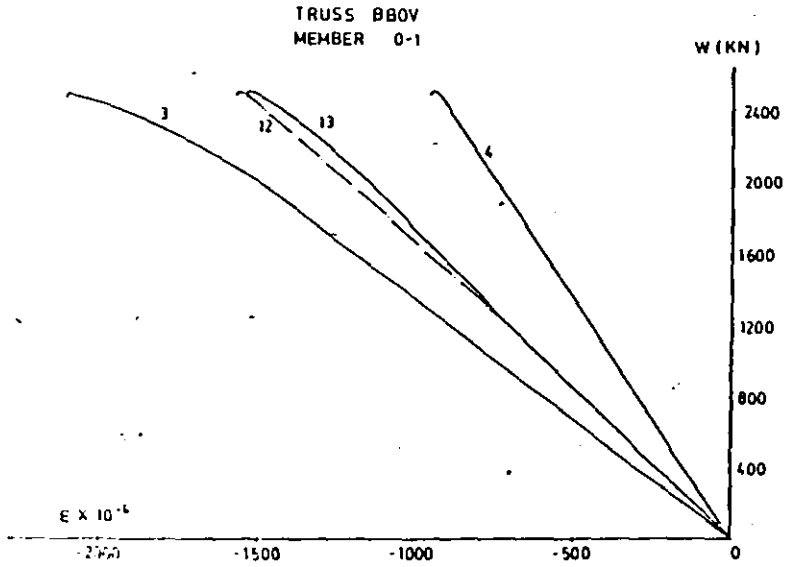
TRUSS BBOV
MEMBER 0-1
W (KN)
2400
2000
1600
1200
800
400
E X 10⁻⁶
-1500
-1000
-500
0
3
12
13
4

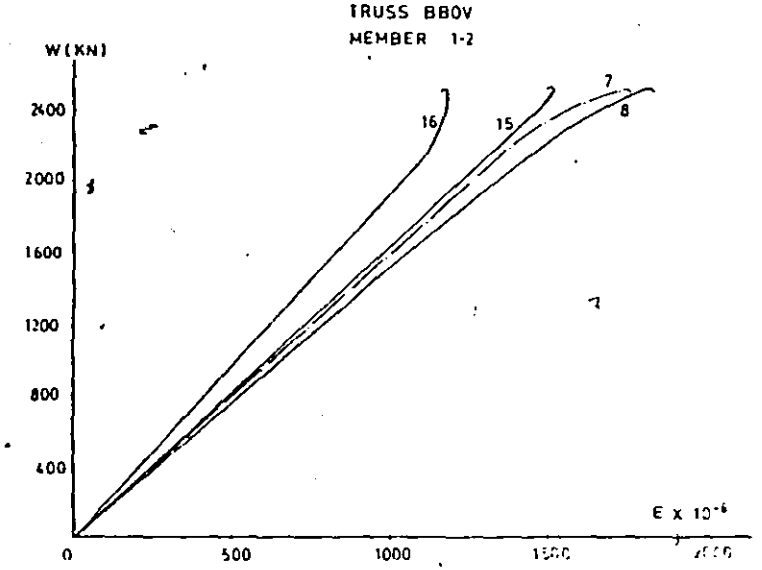
TRUSS BBOV
MEMBER 1-2
W (KN)
2400
2000
1600
1200
800
400
E X 10⁻⁶
0
500
1000
16
15
7
8

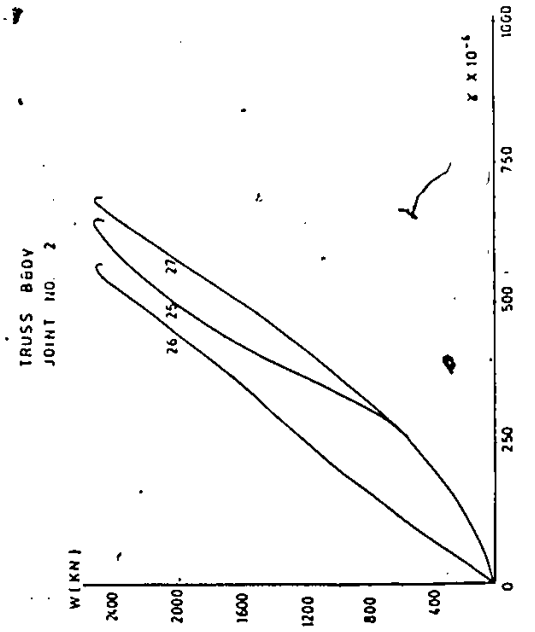
TRUSS BBOV
JOINT NO. 2
W (KN)
2400
2000
1600
1200
800
400
0
250
500
750
1000
x x 10⁻⁶
26
25
27

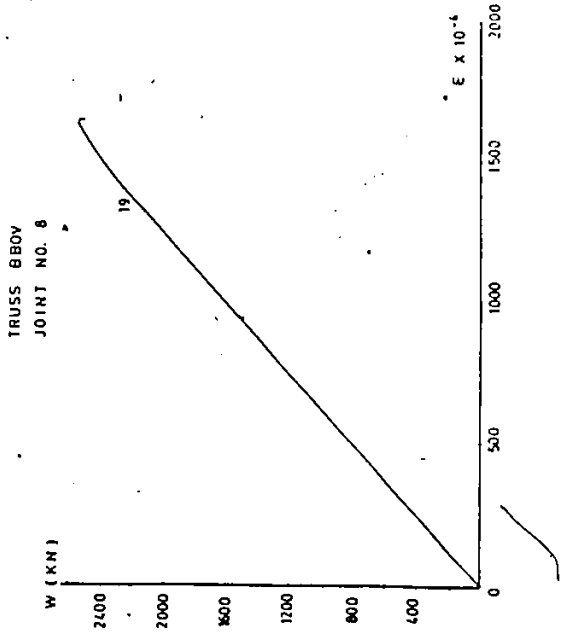
TRUSS BBOV
JOINT NO. 8
W (KN)
2400
2000
1600
1200
800
400
0
500
1000
1500
2000
ε x 10⁻⁶
19

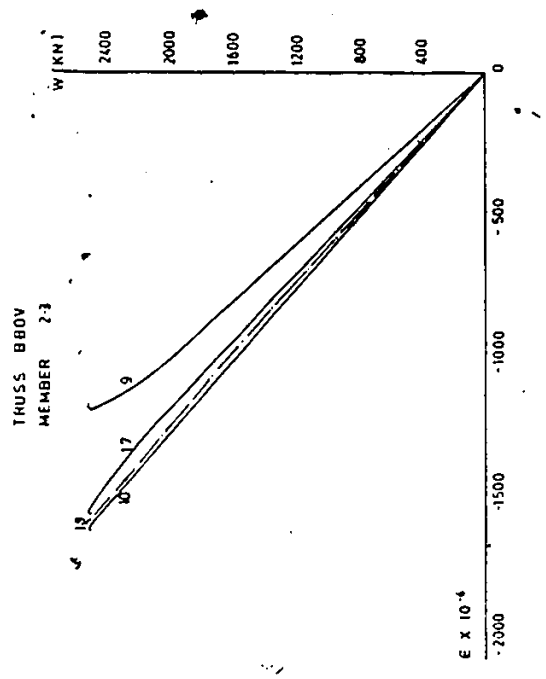
TRUSS BBOV
MEMBER 2-3
W (KN)
2400
2000
1600
1200
800
400
0
-500
-1000
-1500
-2000
ε x 10⁻⁶
9
17
18

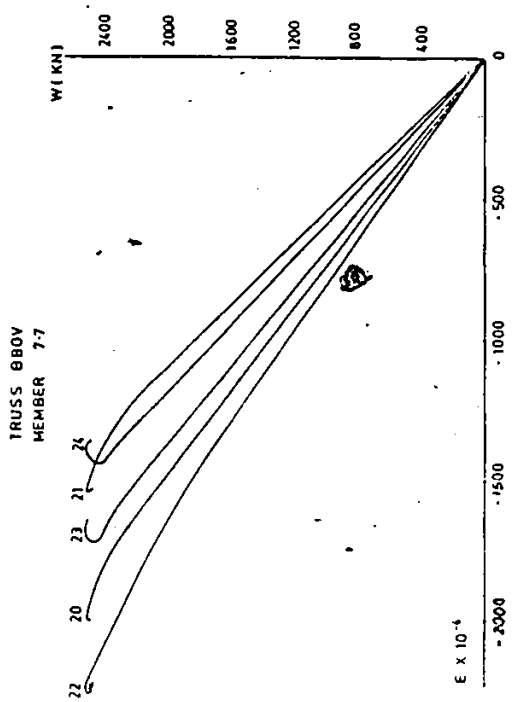
TRUSS BBOV
MEMBER 7-7
W (KN)
2400
2000
1600
1200
800
400
0
-500
-1000
-1500
-2000
ε x 10⁻⁶
24
21
23
20
22

TRUSS S1
MEMBER 0-1

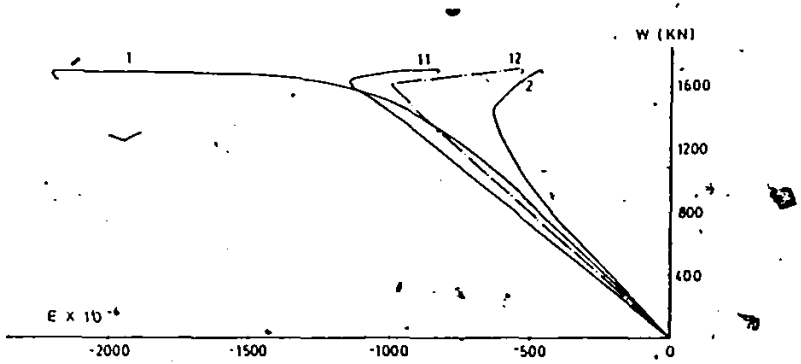

TRUSS S1
MEMBER 1-2

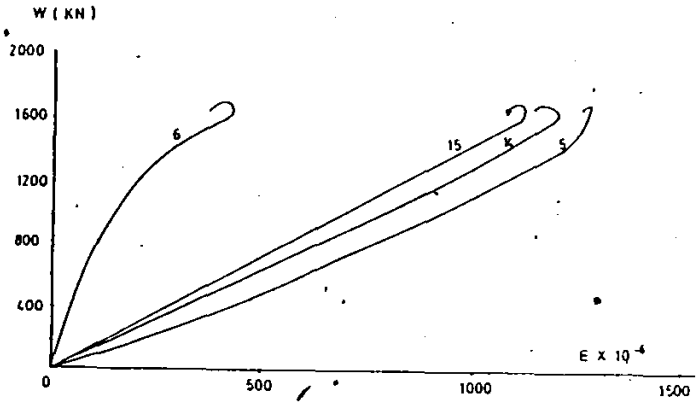

TRUSS S1
MEMBER 0-1

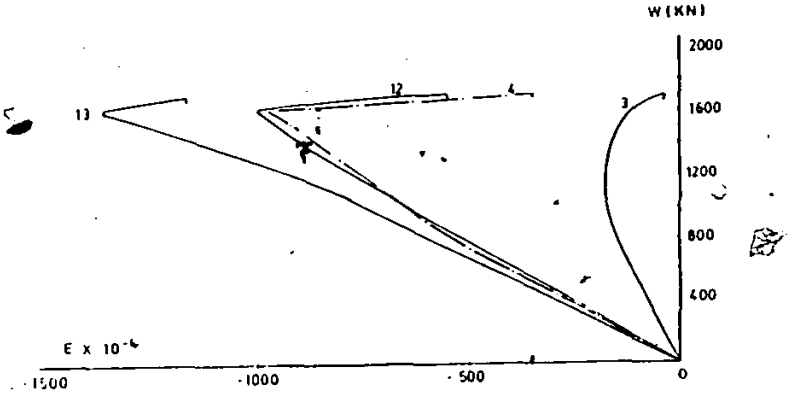

TRUSS S1
MEMBER 1-2

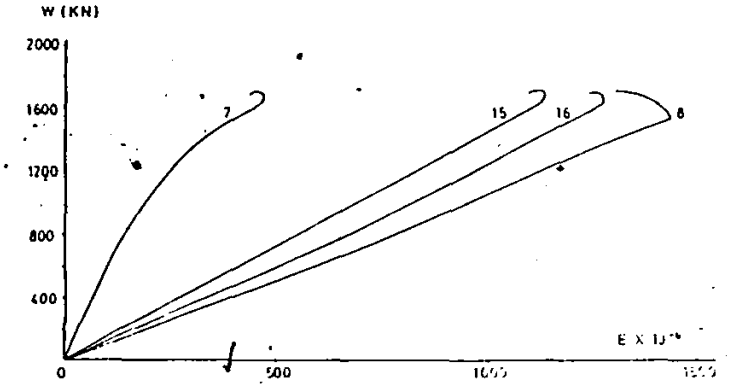

TRUSS S 1
MEMBER 2-3

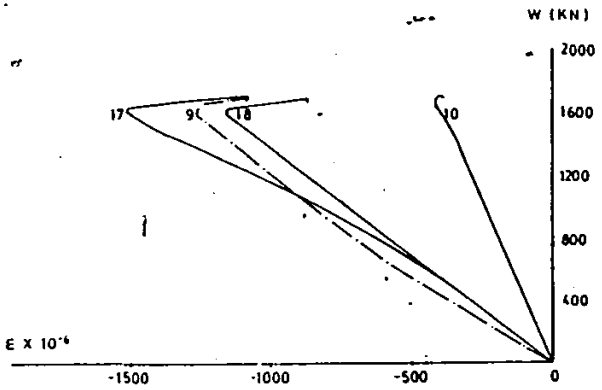

TRUSS S 1
JOINT NO 8

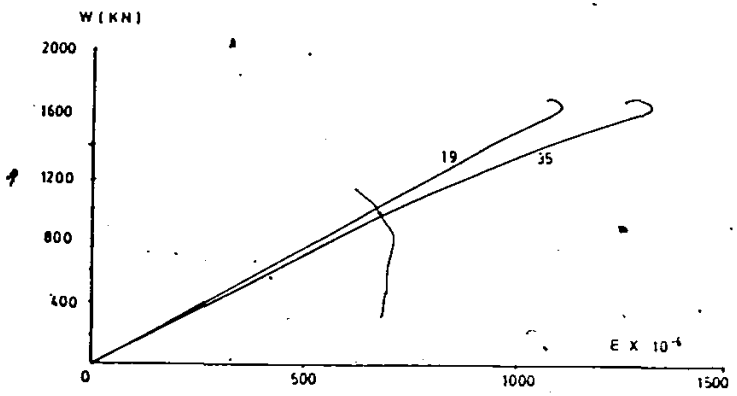

TRUSS S 1
MEMBER 7-7

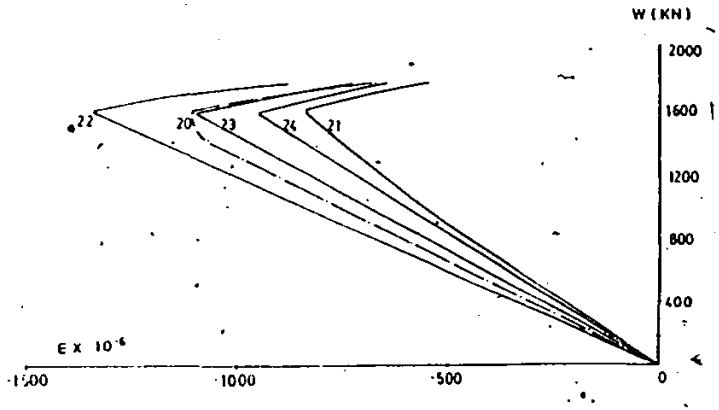

TRUSS S 2
MEMBER 0-1

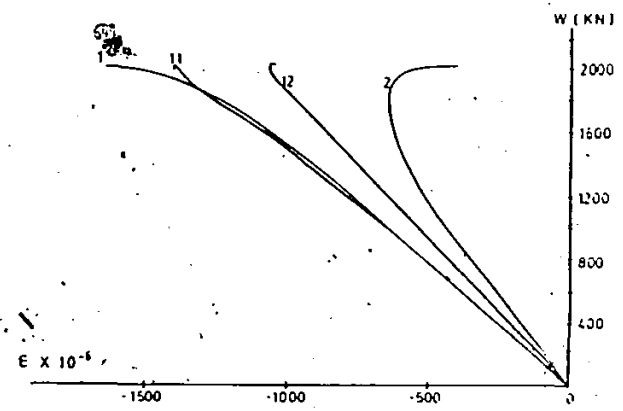

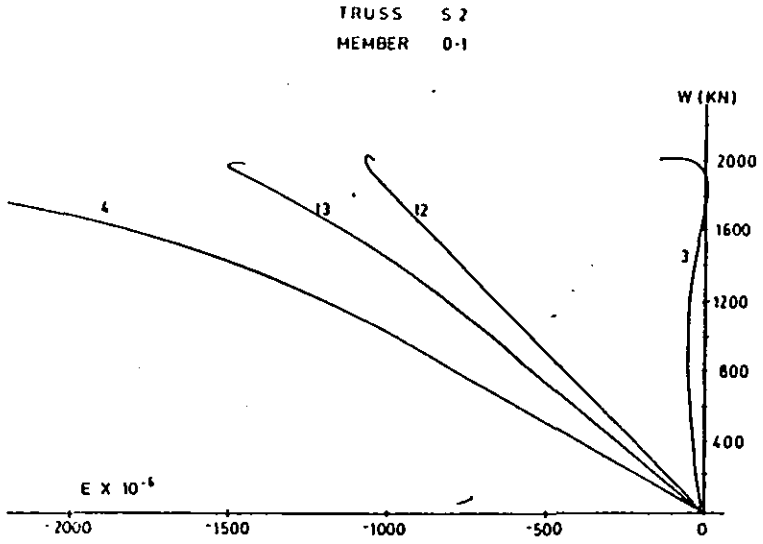
TRUSS S 2
MEMBER 0-1
W (KN)
2000
1600
1200
800
400
4
13
12
3
E X 10⁻⁶
-2000
-1500
-1000
-500
0

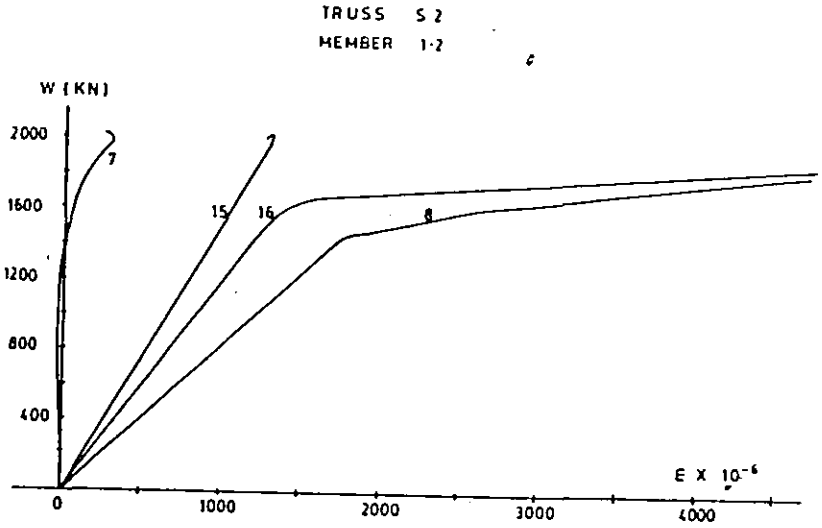
TRUSS S 2
MEMBER 1-2
W (KN)
2000
1600
1200
800
400
7
15
16
8
E X 10⁻⁶
0
1000
2000
3000
4000

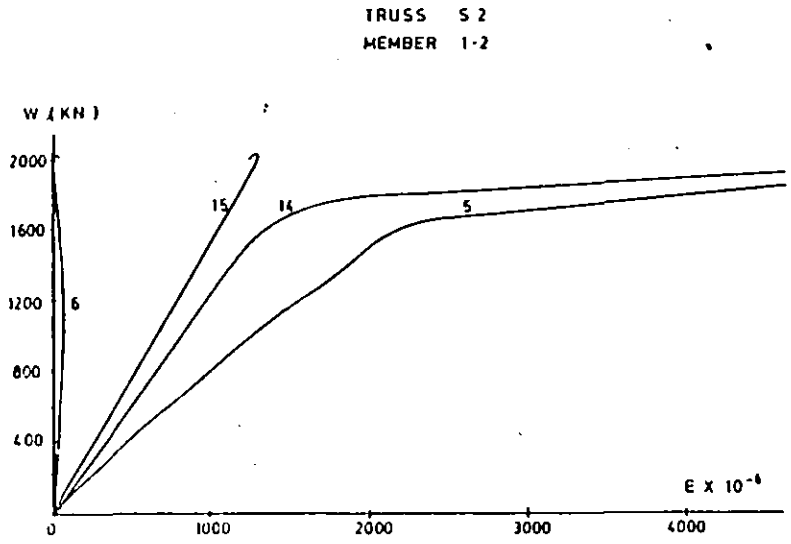
TRUSS S 2
MEMBER 1-2
W (KN)
2000
1600
1200
800
400
15
14
5
6
E X 10⁻⁶
0
1000
2000
3000
4000

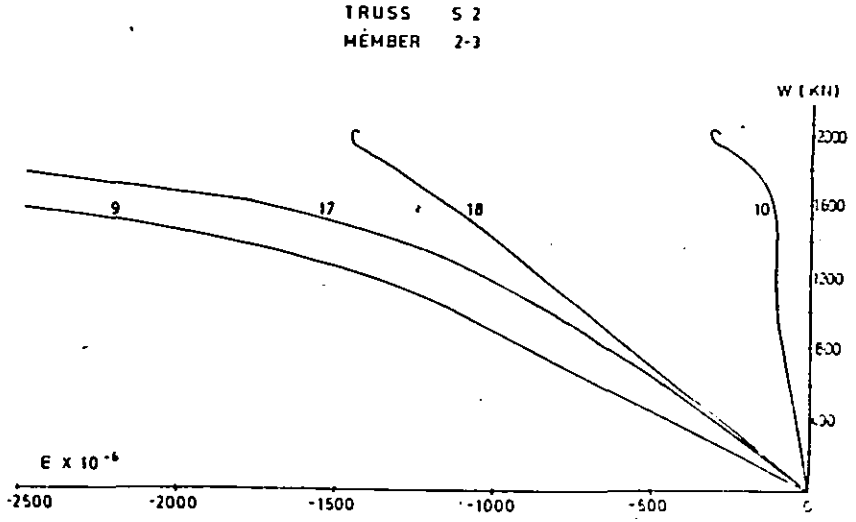
TRUSS S 2
MEMBER 2-3
W (KN)
2000
1600
1200
800
400
9
17
18
10
E X 10⁻⁶
-2500
-2000
-1500
-1000
-500

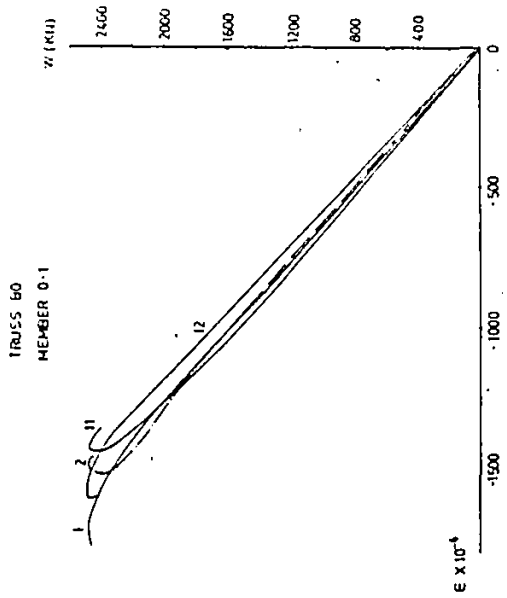
TRUSS 60
MEMBER 0-1
W (KN)
2400
2000
1600
1200
800
400
0
-500
-1000
-1500
ε X 10⁻⁶
1
2
11
12

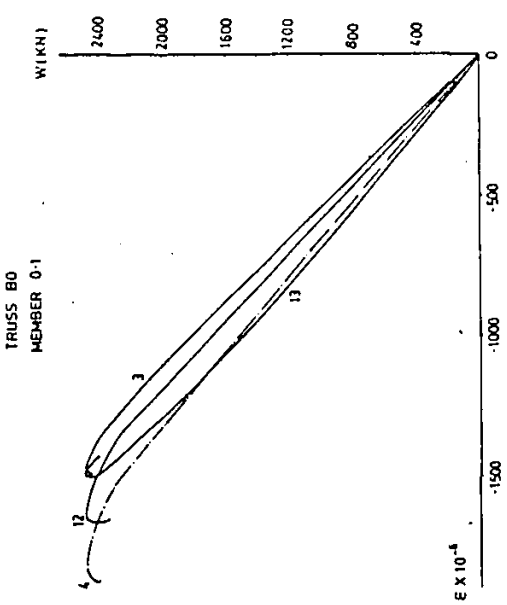
TRUSS 80
MEMBER 0-1
W(KN)
2400
2000
1600
1200
800
400
0
-500
-1000
-1500
ε X 10⁻⁶
3
4
12
13

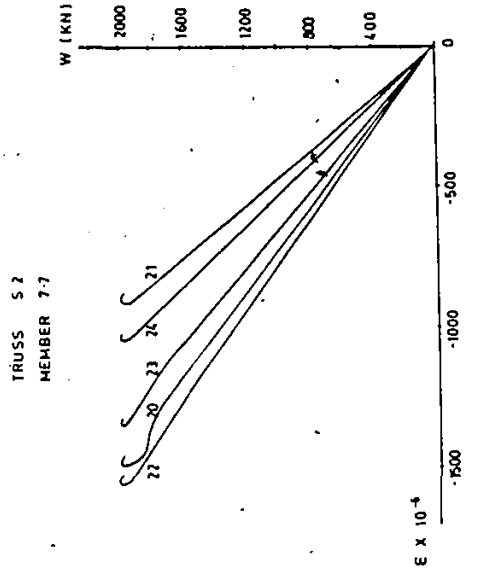
TRUSS S 2
MEMBER 7-7
W (KN)
2000
1600
1200
800
400
0
-500
-1000
-1500
ε X 10⁻⁶
21
24
23
20
22

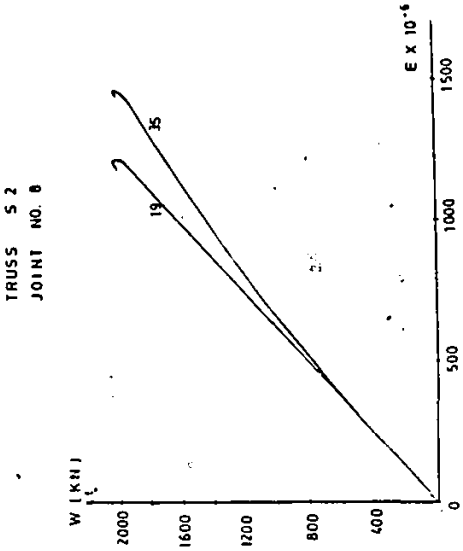
TRUSS S 2
JOINT NO. 8
W (KN)
2000
1600
1200
800
400
0
500
1000
1500
ε X 10⁻⁶
18
35

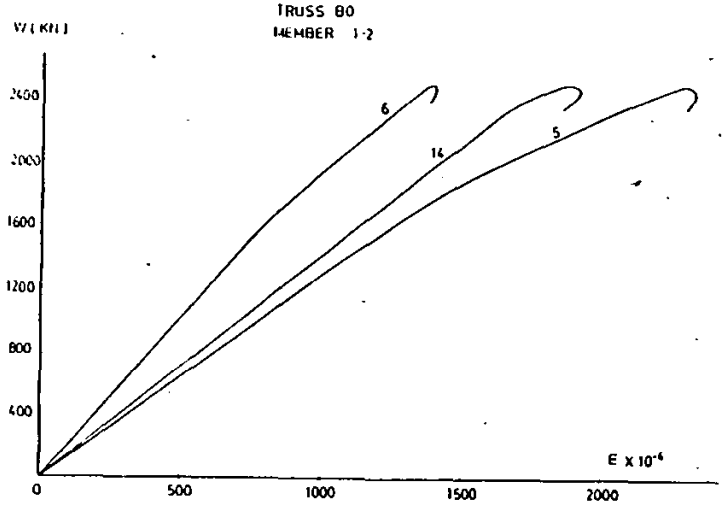
TRUSS 80
MEMBER 1-2
W(KN)
2400
2000
1600
1200
800
400
0
500
1000
1500
2000
E X 10⁻⁶
6
14
5

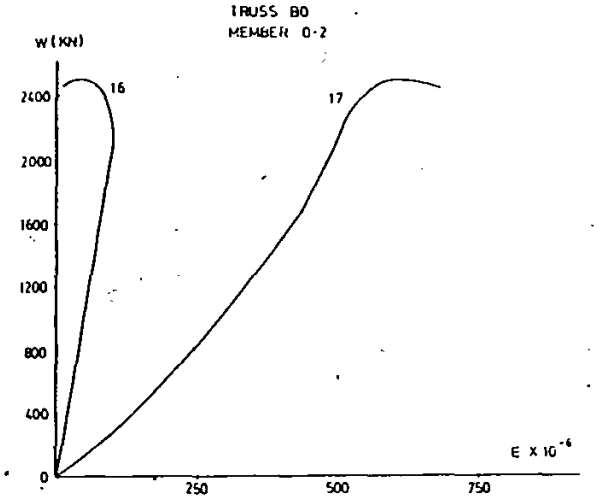
TRUSS 80
MEMBER 0-2
W(KN)
2400
2000
1600
1200
800
400
0
250
500
750
E X 10⁻⁶
16
17

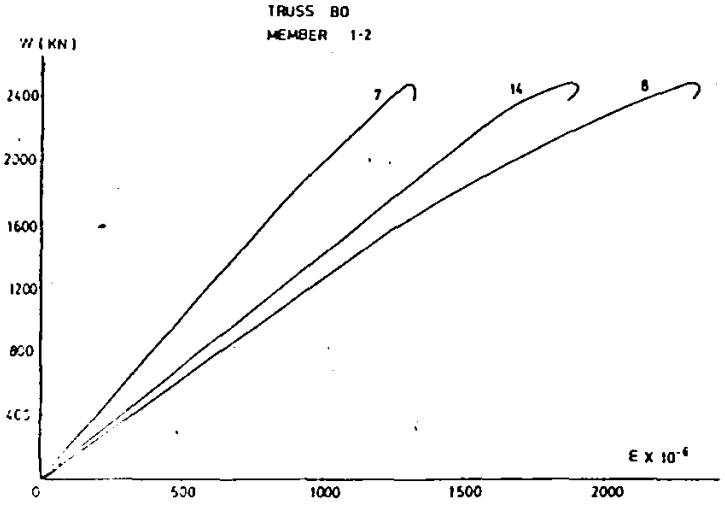
TRUSS 80
MEMBER 1-2
W(KN)
2400
2000
1600
1200
800
400
0
500
1000
1500
2000
E X 10⁻⁶
7
14
8

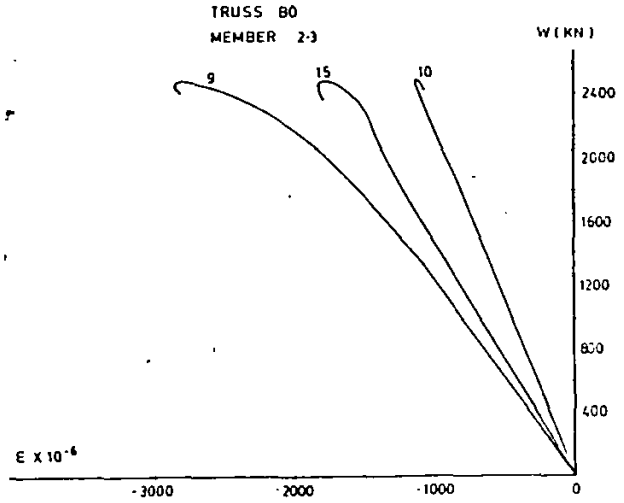
TRUSS 80
MEMBER 2-3
W(KN)
2400
2000
1600
1200
800
400
E X 10⁻⁶
-3000
-2000
-1000
0
9
15
10

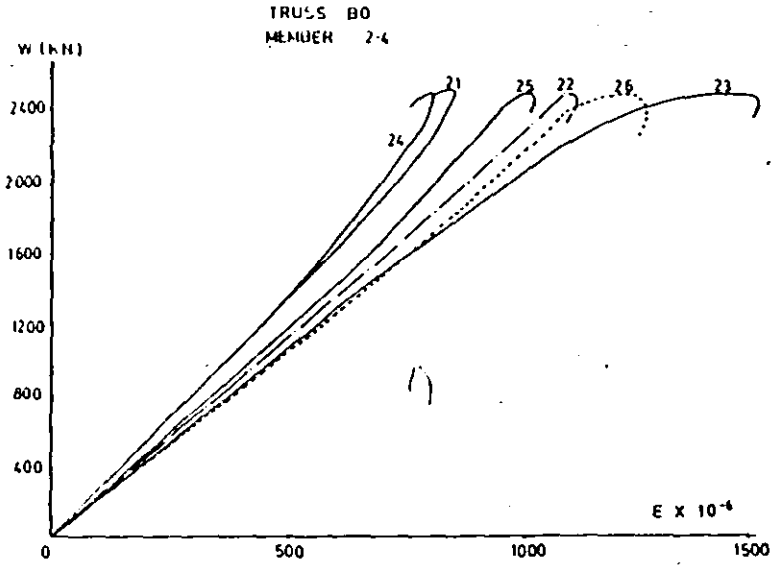
TRUSS BO
MEMBER 2-4
W (KN)
2400
2000
1600
1200
800
400
0
500
1000
1500
E X 10⁻⁶
21
25
22
26
23
24

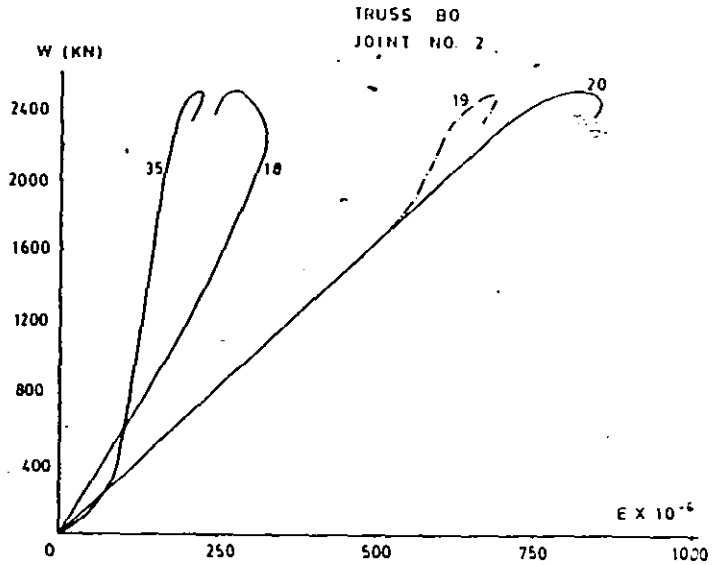
TRUSS BO
JOINT NO. 2
W (KN)
2400
2000
1600
1200
800
400
0
250
500
750
1000
E X 10⁻⁶
35
18
19
20

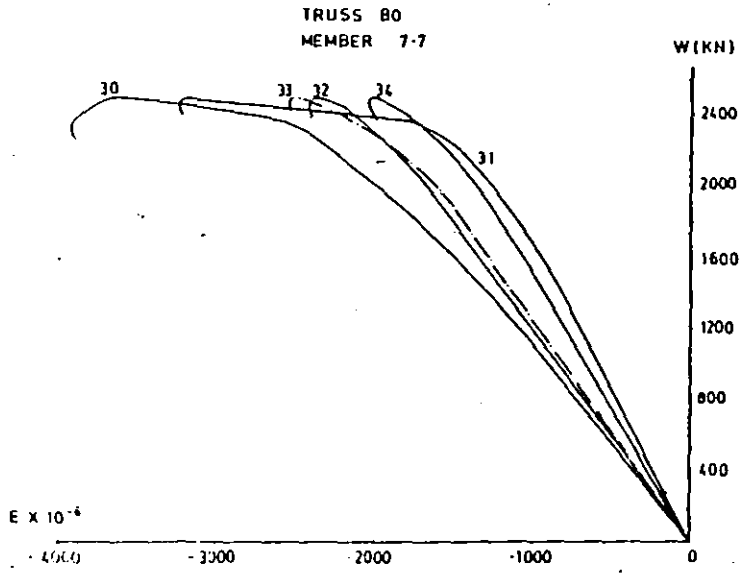
TRUSS BO
MEMBER 7-7
W(KN)
2400
2000
1600
1200
800
400
E X 10⁻⁶
-4000
-3000
-2000
-1000
0
30
33
32
34
31

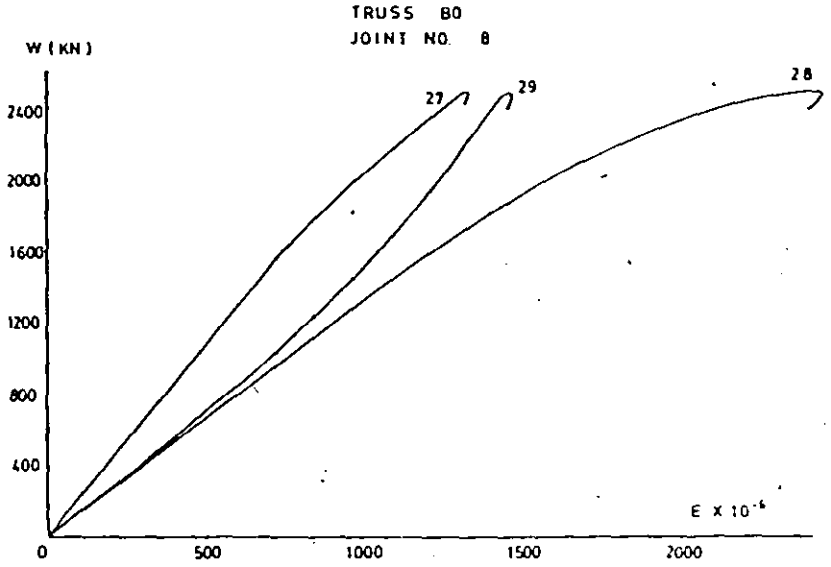
TRUSS BO
JOINT NO. 8
W (KN)
2400
2000
1600
1200
800
400
0
500
1000
1500
2000
E X 10⁻⁶
27
29
28

APPENDIX III

PARAMETER FUNCTIONS FOR m-ϕ-p INTERACTION DIAGRAMS

Chen and Atsuta [6] proposed a set of parametric functions such that the moment-curvature-thrust (m-ϕ-p) relationships for most hollow structural steel sections subjected to combined unaxial bending and compression can be closely approximated. The material is assumed to have an elastic-perfectly plastic stress-strain relationship.

Three domaines are defined as limiting elastic, primary elastic and fully plastic as shown in Fig. III.1. Non-dimensional initial yield moment, secondary yield moment and the ultimate flow moment are represented by the moment functions $\tilde{m}_1$, $\tilde{m}_2$ and $\tilde{m}_{pc}$, respectively as shown.

The following non-dimensional parameters are also defined for deriving the m-ϕ-p relationships.

$$\tilde{m} = \frac{M}{M_y} , \qquad \phi = \frac{\phi_c}{\phi_y} , \qquad p = \frac{P}{P_y}$$

For square hollow structural sections without residual stresses, the following parametric equations are all functions of thrust p, and are defined for its appropriate ranges.

$$\tilde{m}_1 = 1 - p$$

$$\phi_1 = 1 - p$$

For $0 < p < 0.467$

$$\tilde{m}_{pc} = 1.20 - 1.60p^2$$

$$\tilde{m}_2 = 1 + 0.9p - 3.25\ p^2$$

$$\phi_2 = \frac{1}{1 - 2.5p + 4.17p^2}$$

For $0.467 < p < 1$

$$\tilde{m}_{pc} = 1.51 - 1.31p - 0.2p^2$$

$$\tilde{m}_2 = 1.40\ (1 - p)$$

$$\phi_2 = 2.50\ (1 - p)$$

Using the equations above, the following constants are defined in order to determine moment-curvature relationships at various stages of loading.

$$a = \frac{\tilde{m}_1}{\phi}$$

$$b = \frac{\tilde{m}_2 - \tilde{m}_1 \sqrt{\phi_1/\phi_2}}{1 - \sqrt{\phi_1/\phi_2}}$$

$$g = \frac{\tilde{m}_2 - \tilde{m}_1}{1/\sqrt{\phi_1} - 1/\sqrt{\phi_2}}$$

$$d = S/Z$$

$$f = (\tilde{m}_{pc} - \tilde{m}_2)\phi_2^2$$

The moment-curvature-thrust relationships are then given by

$$\tilde{m} = \begin{cases} a\phi d & (\phi \leq \phi_1 : \text{Elastic}) \\ (b - g\sqrt{\phi})d & (\phi_1 < \phi \leq \phi_2 : \text{Primary plastic}) \\ (\tilde{m}_{pc} - f/\phi^2)d & (\phi_2 < \phi : \text{Fully plastic}) \end{cases}$$

After the thrust p has been determined from test results and/or numerical computations for a particular shape of cross section.

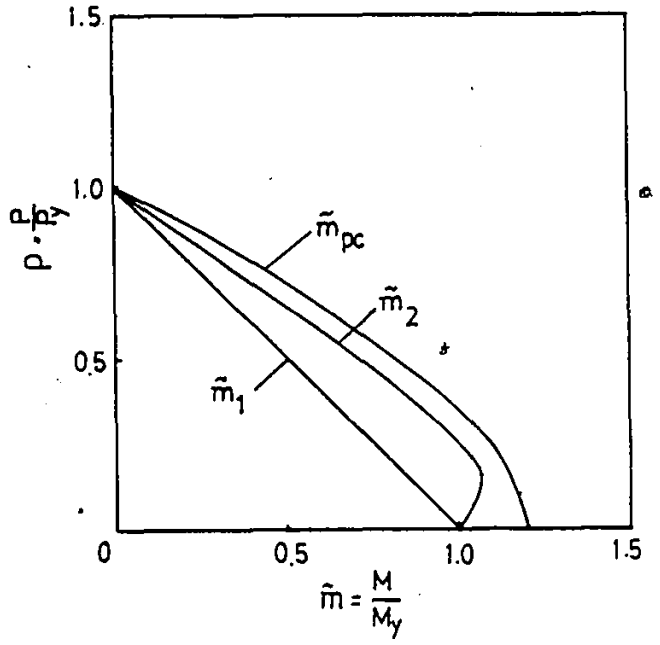

FIGURE III.1 m-p INTERACTION DIAGRAM FOR SHS

APPENDIX IV

m-ϕ-p INTERACTION DIAGRAMS FOR CRITICAL MEMBERS OF VARIOUS TRUSSES

Axial forces determined for the critical members, namely, member 0-1, 1-2, 2-3 and 7-7 during the various stages of loading of Trusses BBST, BBOV, S1, S2 and BO were substituted into the appropriate parametric equations in Appendix III to obtain the interaction diagrams in the following figures.

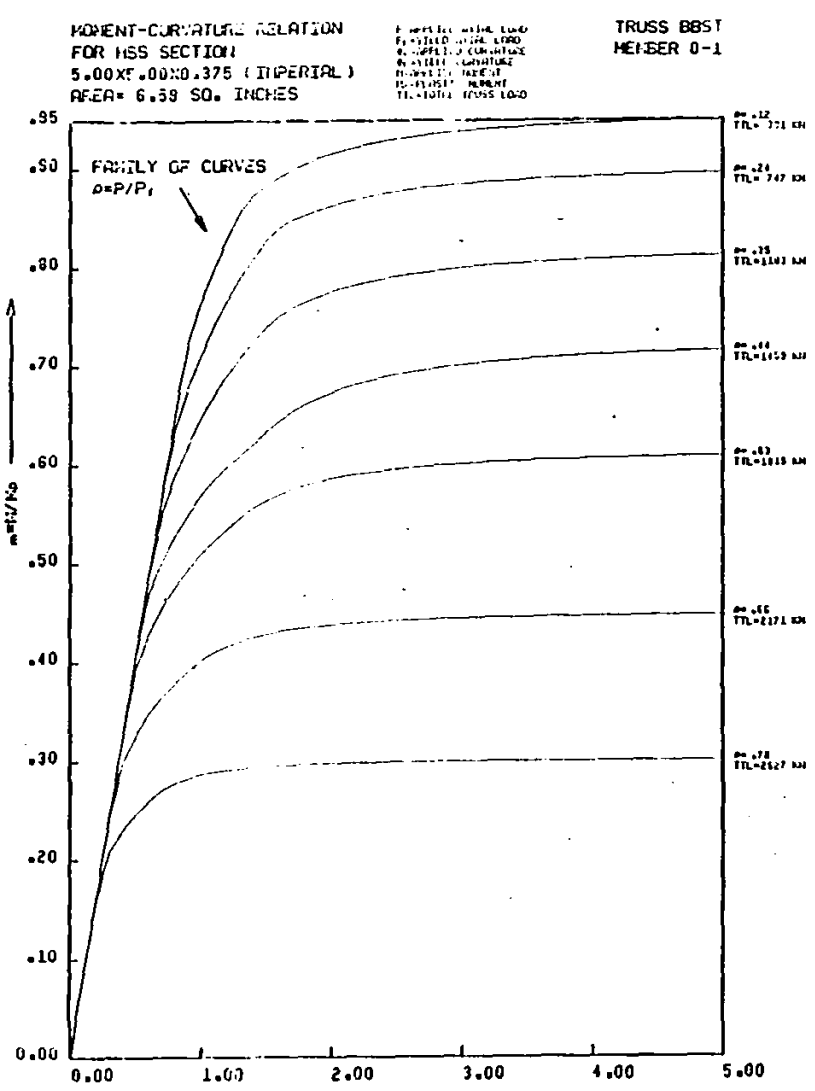
MOMENT-CURVATURE RELATION
FOR HSS SECTION
5.00X5.00X0.375 (IMPERIAL)
AREA= 6.59 SQ. INCHES
TRUSS BBST
MEMBER 0-1
FAMILY OF CURVES
ρ=P/P
.95
.90
.80
.70
.60
.50
.40
.30
.20
.10
0.00
0.00
1.00
2.00
3.00
4.00
5.00

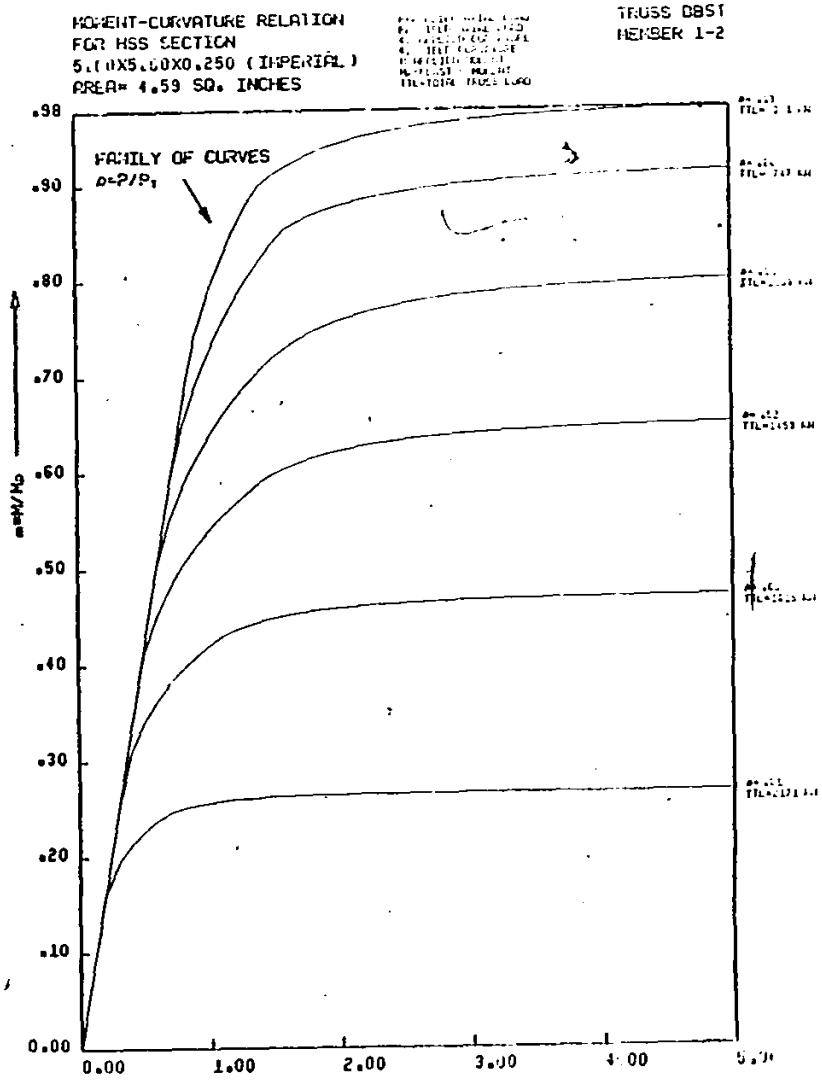
MOMENT-CURVATURE RELATION
FOR HSS SECTION
5.(0X5.00X0.250 (IMPERIAL)
AREA= 4.59 SQ. INCHES
TRUSS BBST
MEMBER 1-2
FAMILY OF CURVES
ρ=P/P
.98
.90
.80
.70
.60
.50
.40
.30
.20
.10
0.00
0.00
1.00
2.00
3.00

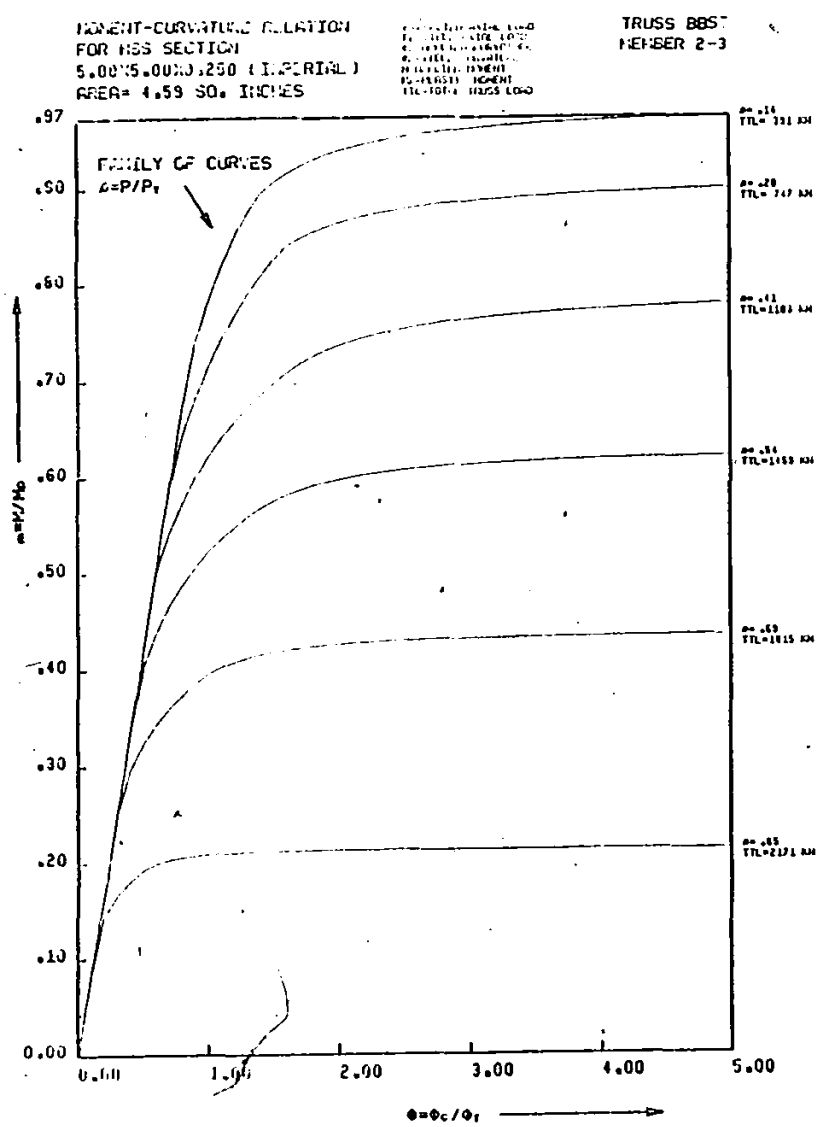
MOMENT-CURVATURE RELATION
FOR HSS SECTION
5.00X5.00X0.250 (IMPERIAL)
AREA= 4.59 SQ. INCHES
TRUSS BBST
MEMBER 2-3
FAMILY OF CURVES
α=P/Pr
m=M/Mp
ϕ=ϕc/ϕr
0.00
.10
.20
.30
.40
.50
.60
.70
.80
.90
.97
1.00
2.00
3.00
4.00
5.00

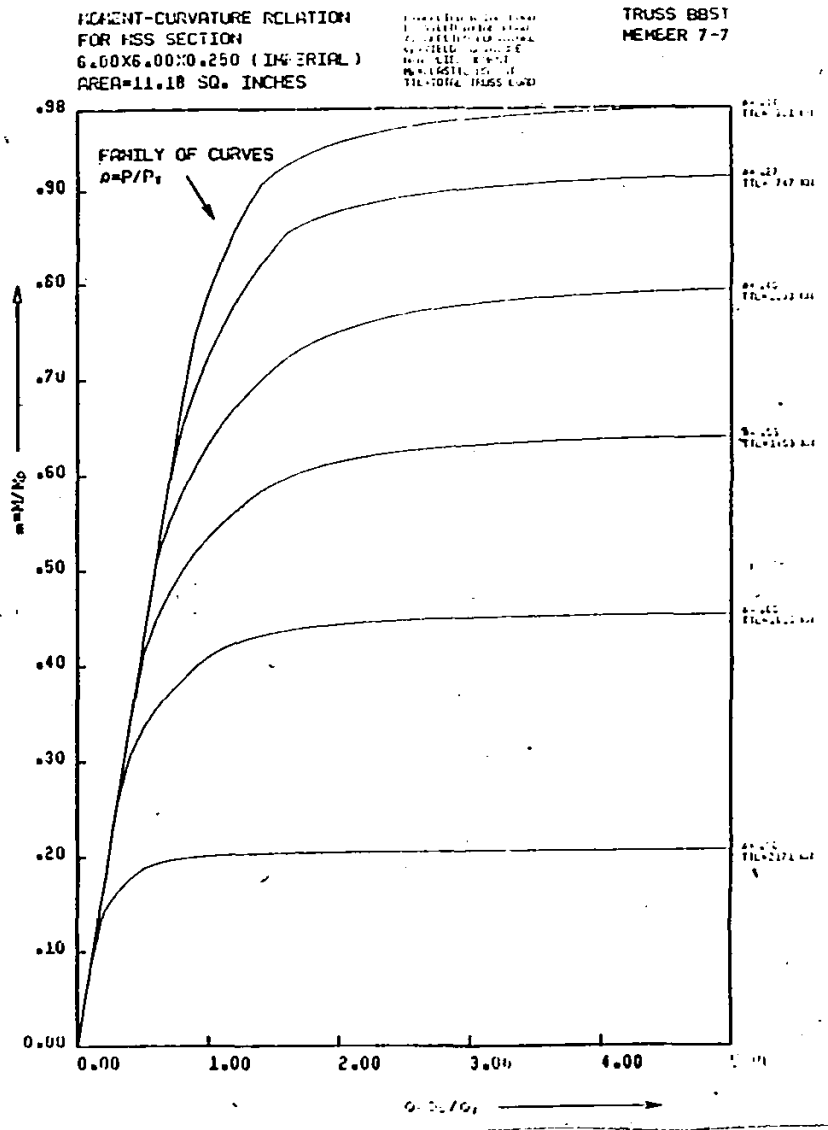
MOMENT-CURVATURE RELATION
FOR HSS SECTION
6.00X6.00X0.250 (IMPERIAL)
AREA=11.18 SQ. INCHES
TRUSS BBST
MEMBER 7-7
FAMILY OF CURVES
α=P/Pr
m=M/Mp
0.00
.10
.20
.30
.40
.50
.60
.70
.90
.98
1.00
2.00
3.00
4.00

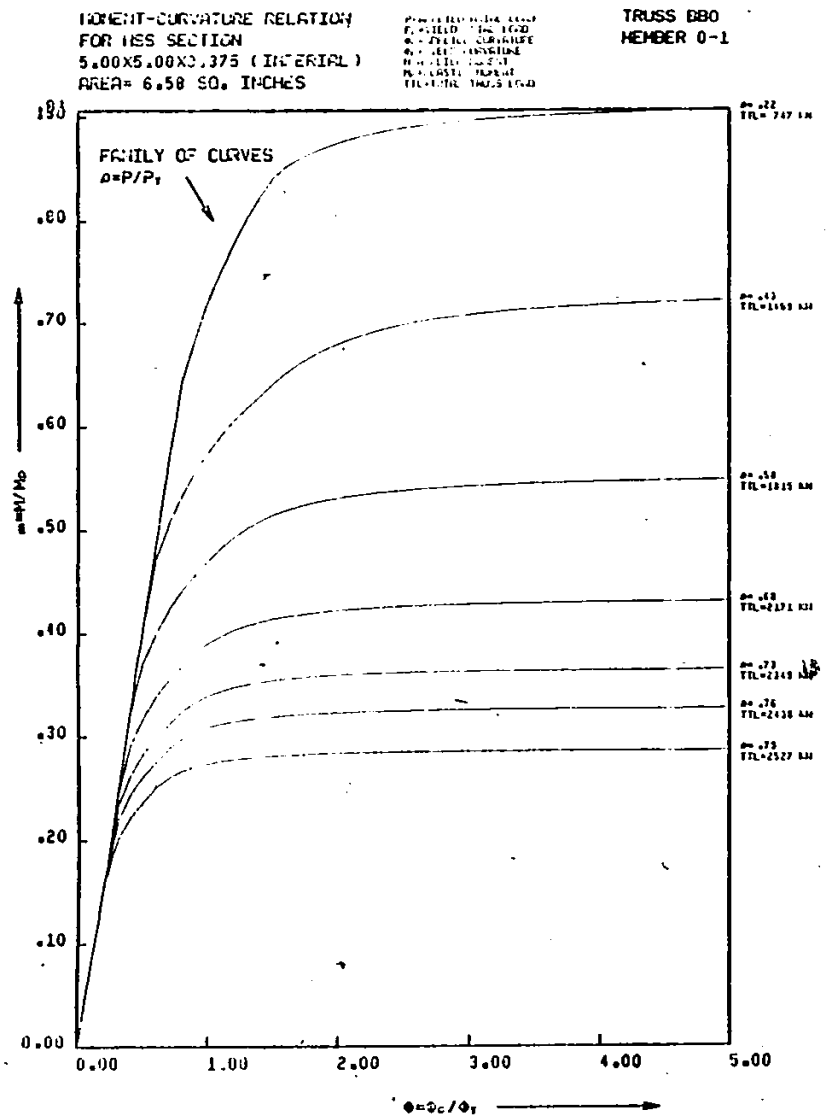
MOMENT-CURVATURE RELATION
FOR HSS SECTION
5.00X5.00X0.375 (IMPERIAL)
AREA= 6.58 SQ. INCHES
TRUSS BBO
MEMBER 0-1
FAMILY OF CURVES
ρ=P/Py
m=M/Mo
Φ=Φc/Φy
0.00
.10
.20
.30
.40
.50
.60
.70
.80
.90
1.00
2.00
3.00
4.00
5.00

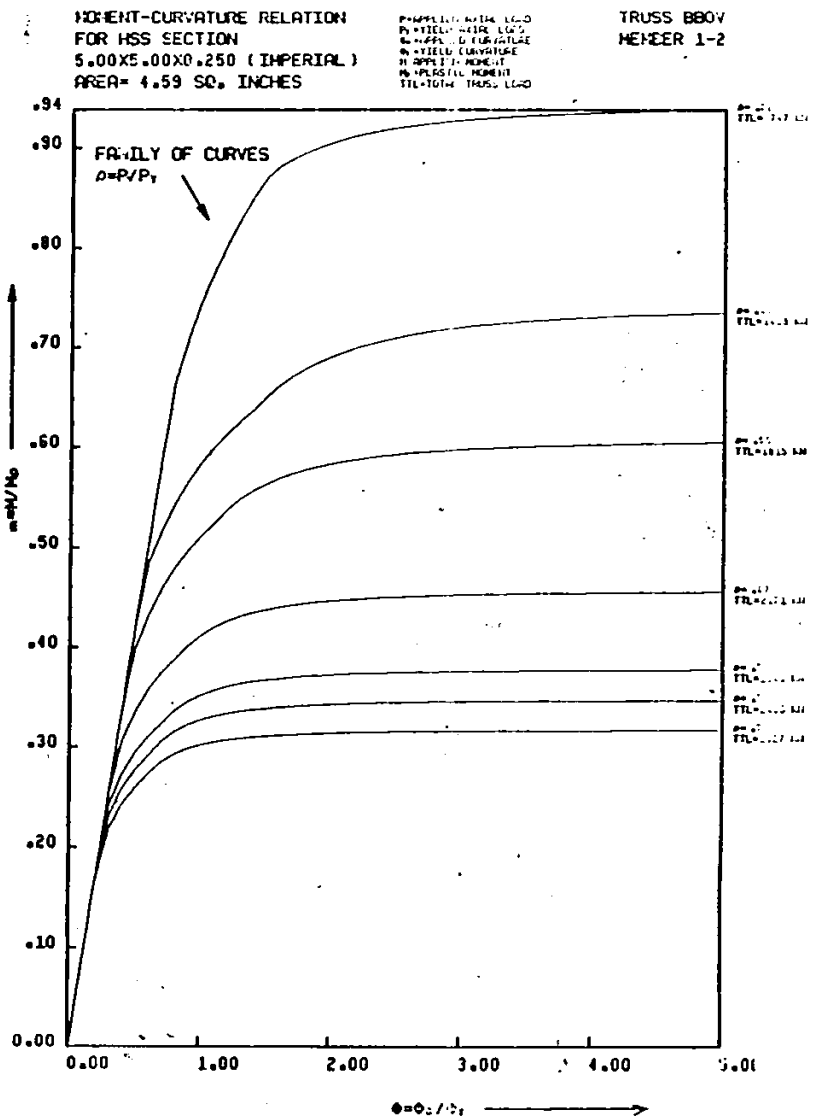
MOMENT-CURVATURE RELATION
FOR HSS SECTION
5.00X5.00X0.250 (IMPERIAL)
AREA= 4.59 SQ. INCHES
TRUSS BBOV
MEMBER 1-2
FAMILY OF CURVES
ρ=P/Py
m=M/Mo
Φ=Φc/Φy
0.00
.10
.20
.30
.40
.50
.60
.70
.80
.90
.94
1.00
2.00
3.00
4.00

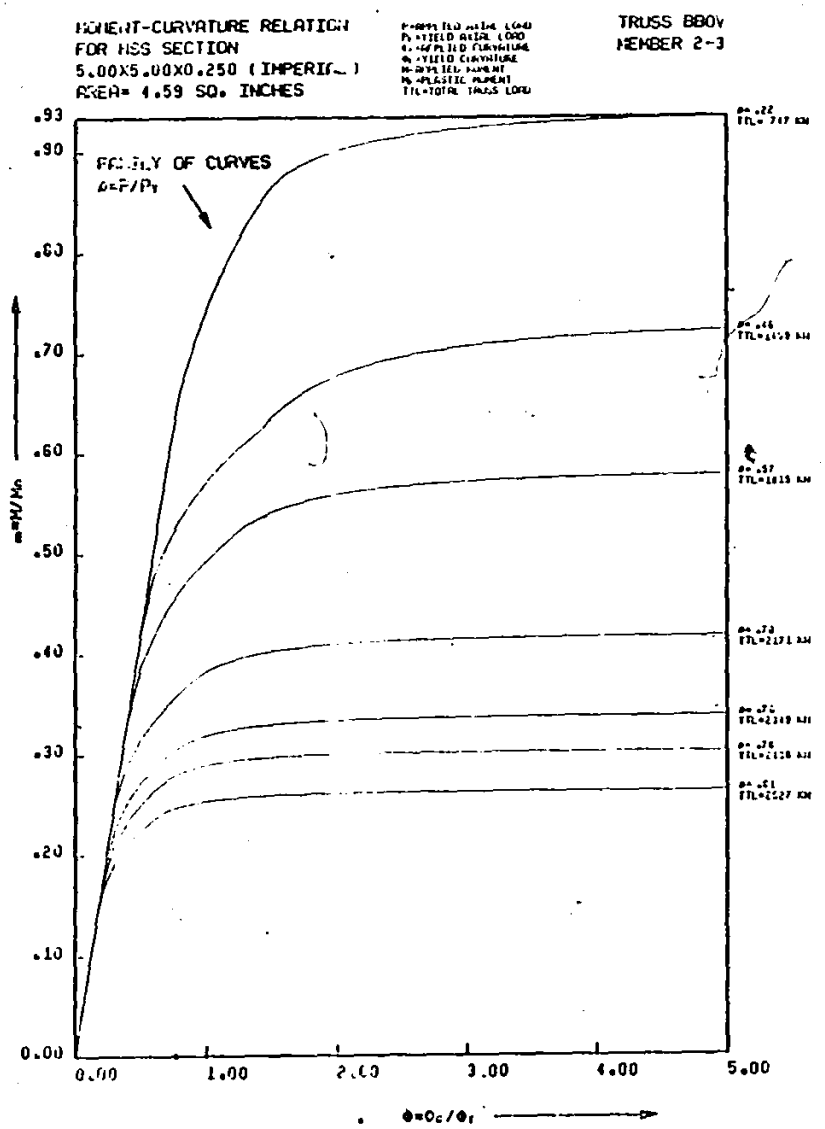
MOMENT-CURVATURE RELATION
FOR HSS SECTION
5.00X5.00X0.250 (IMPERIAL)
AREA= 4.59 SQ. INCHES
TRUSS BBOV
MEMBER 2-3
FAMILY OF CURVES
α=P/Py
m=M/Mo
φ=Oc/Oy
0.00
.10
.20
.30
.40
.50
.60
.70
.80
.90
.93
1.00
2.00
3.00
4.00
5.00

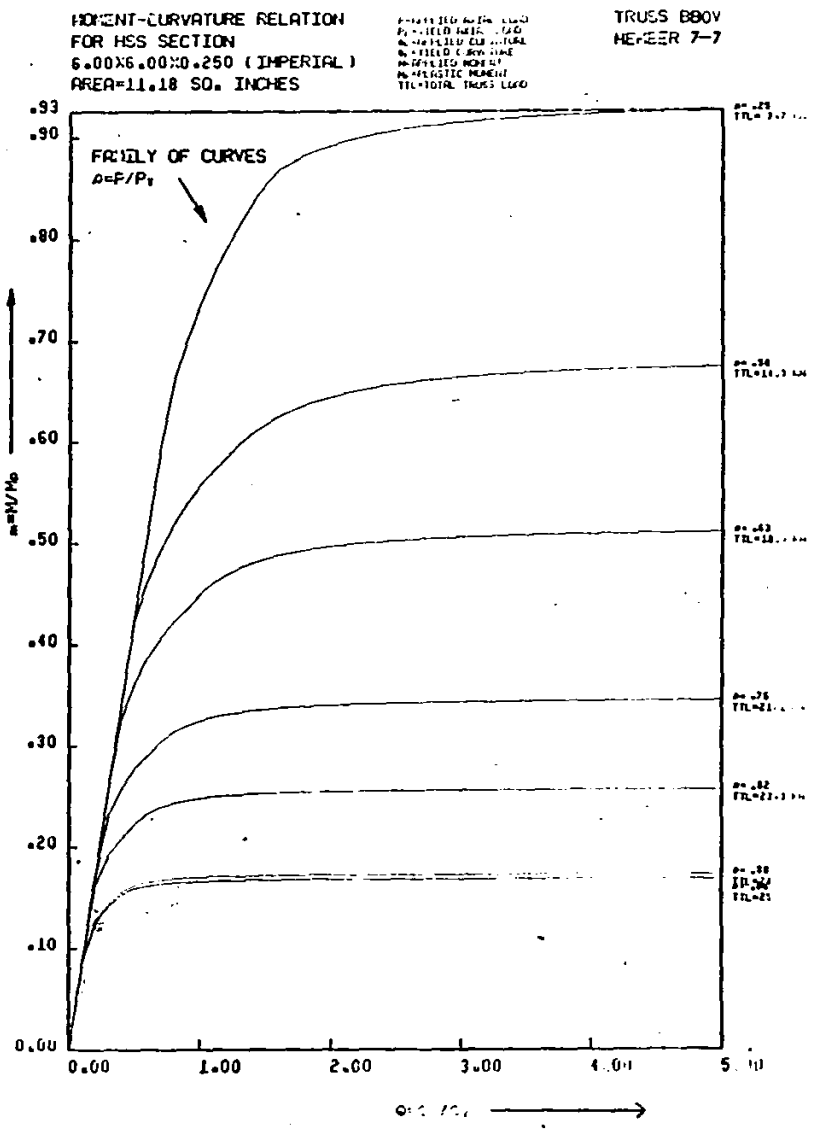
MOMENT-CURVATURE RELATION
FOR HSS SECTION
6.00X6.00X0.250 (IMPERIAL)
AREA=11.18 SQ. INCHES
TRUSS BBOV
MEMBER 7-7
FAMILY OF CURVES
α=P/Py
m=M/Mo
0.00
.10
.20
.30
.40
.50
.60
.70
.80
.90
.93
1.00
2.00
3.00
4.00
5.00

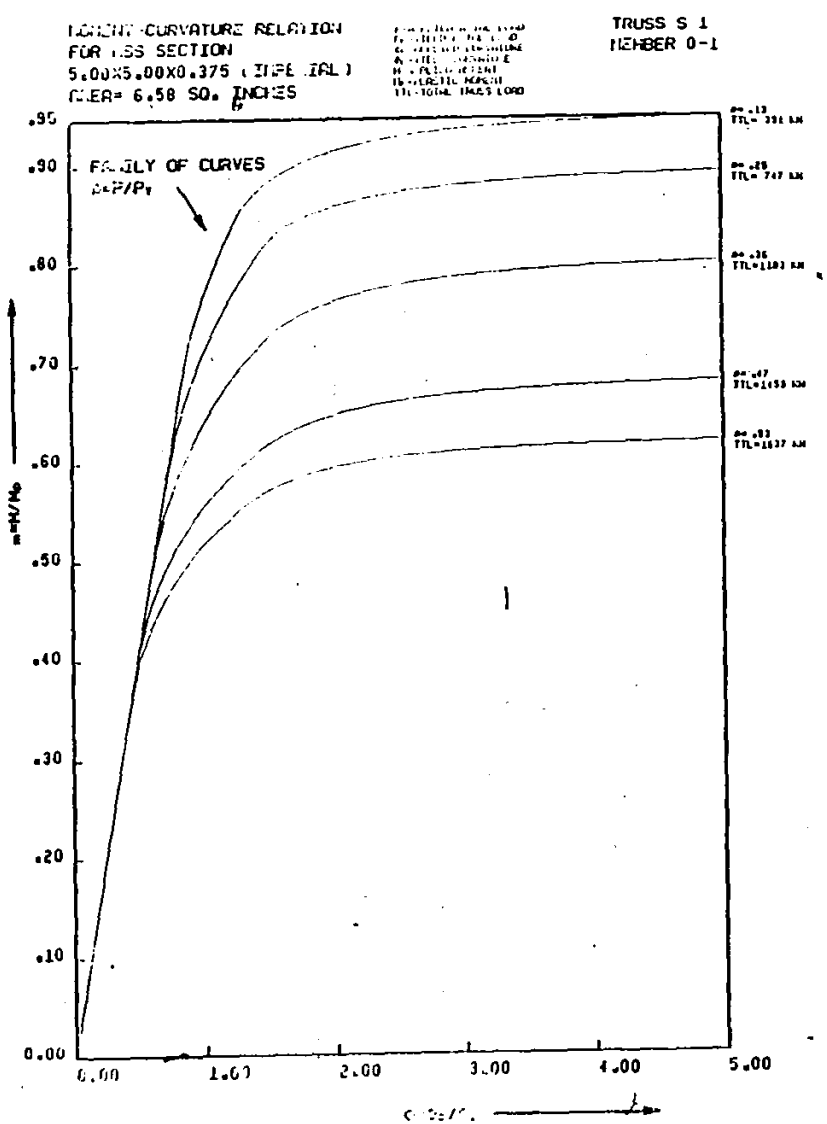
MOMENT-CURVATURE RELATION
FOR HSS SECTION
5.00X5.00X0.375 (IMPERIAL)
AREA= 6.58 SQ. INCHES
TRUSS S 1
MEMBER 0-1
FAMILY OF CURVES
Δ=P/Py
m=M/Mo
.00
.10
.20
.30
.40
.50
.60
.70
.80
.90
.95
0.00
1.00
2.00
3.00
4.00
5.00

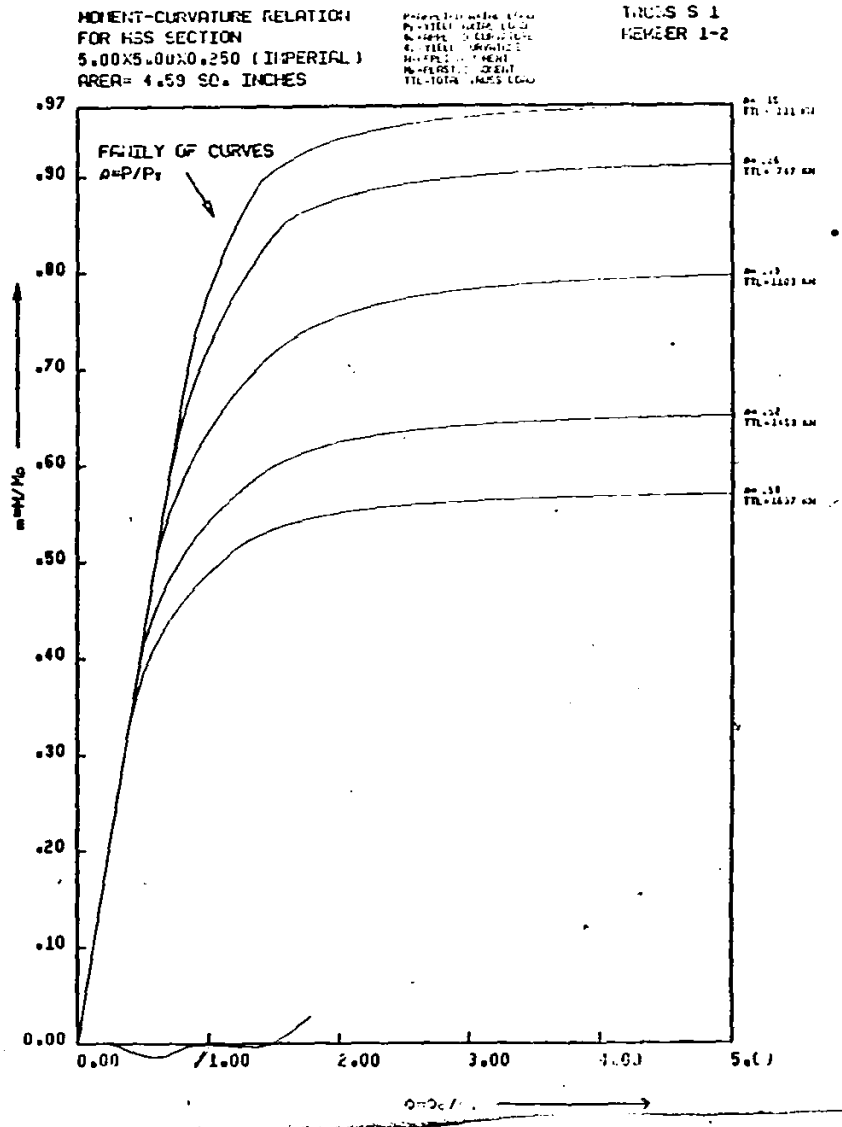
MOMENT-CURVATURE RELATION
FOR HSS SECTION
5.00X5.00X0.250 (IMPERIAL)
AREA= 4.59 SQ. INCHES
TRUSS S 1
MEMBER 1-2
FAMILY OF CURVES
Δ=P/Py
m=M/Mo
.00
.10
.20
.30
.40
.50
.60
.70
.80
.90
.97
0.00
1.00
2.00
3.00
5.00

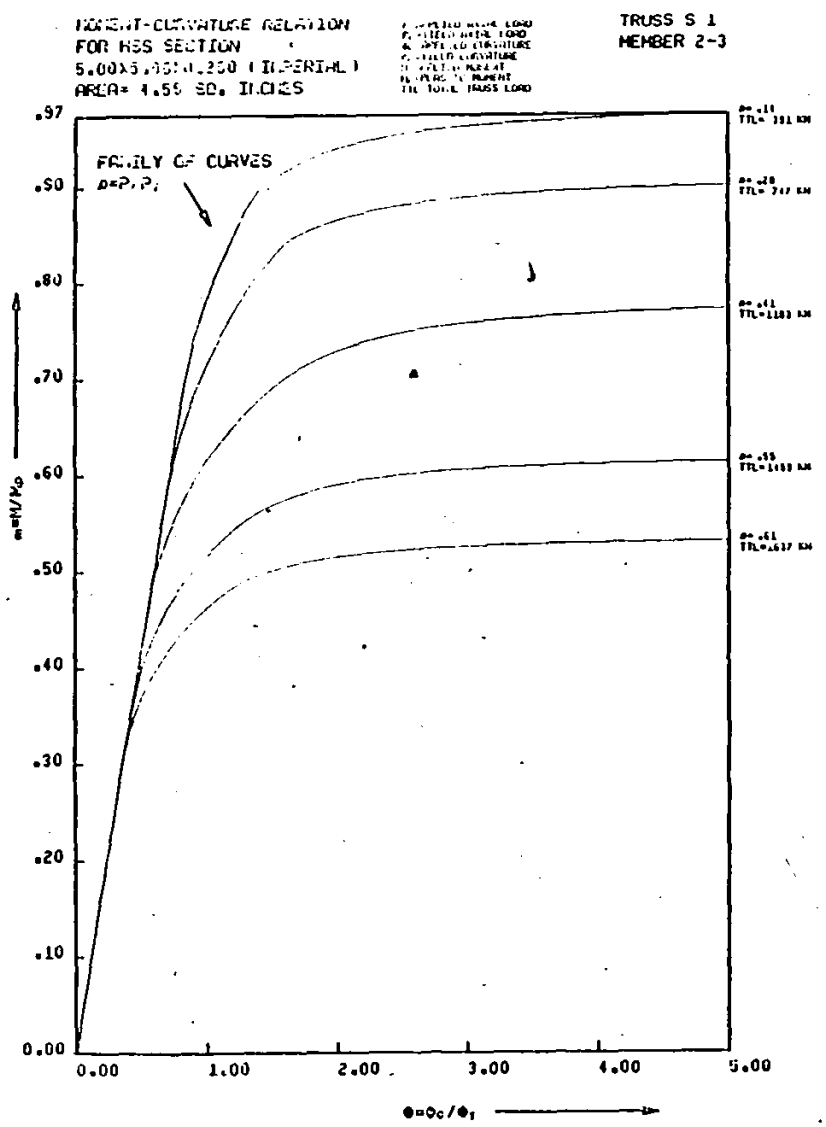
MOMENT-CURVATURE RELATION
FOR HSS SECTION
5.00X5.
AREA= 4.59 SQ. INCHES
TRUSS S 1
MEMBER 2-3
FAMILY OF CURVES
m=M/Mp
0.00
.10
.20
.30
.40
.50
.60
.70
.80
.90
.97
0.00
1.00
2.00
3.00
4.00
5.00

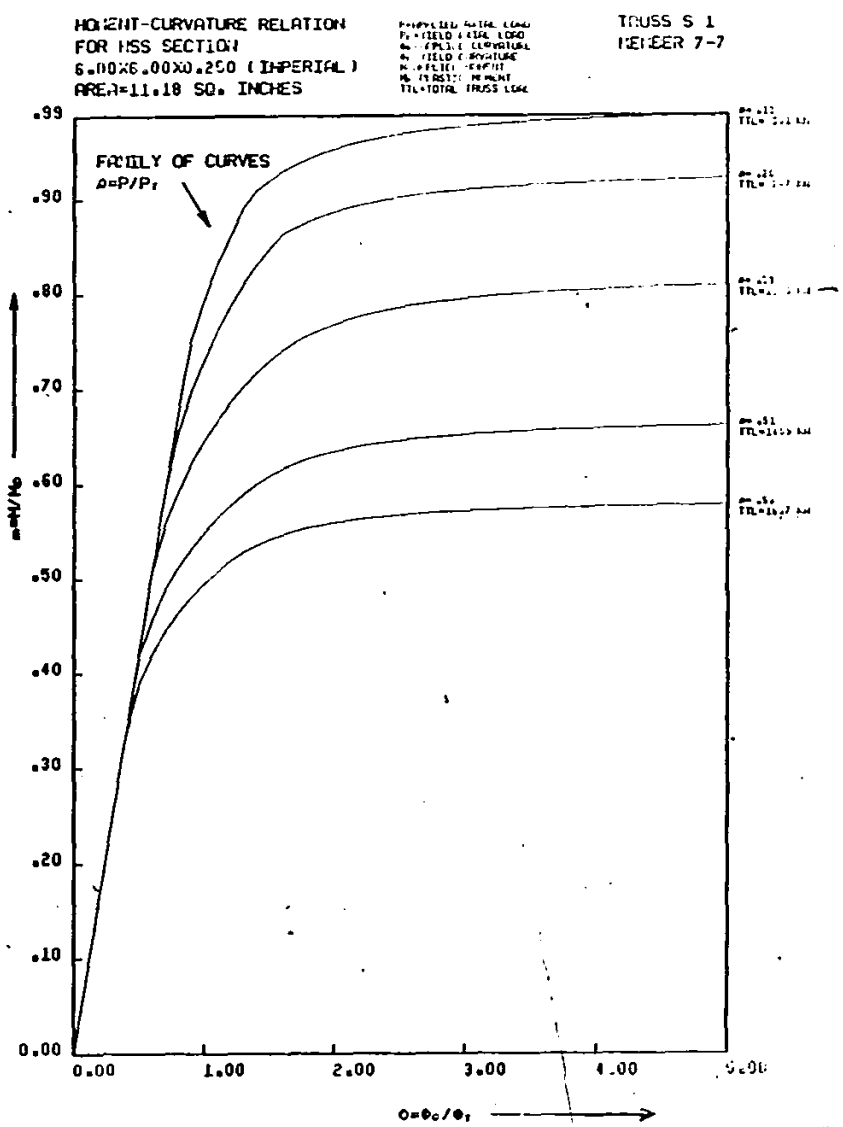
MOMENT-CURVATURE RELATION
FOR HSS SECTION
6.00X6.00X0.250 (IMPERIAL)
AREA=11.18 SQ. INCHES
TRUSS S 1
MEMBER 7-7
FAMILY OF CURVES
m=M/Mp
0.00
.10
.20
.30
.40
.50
.60
.70
.80
.90
.99
0.00
1.00
2.00
3.00
4.00

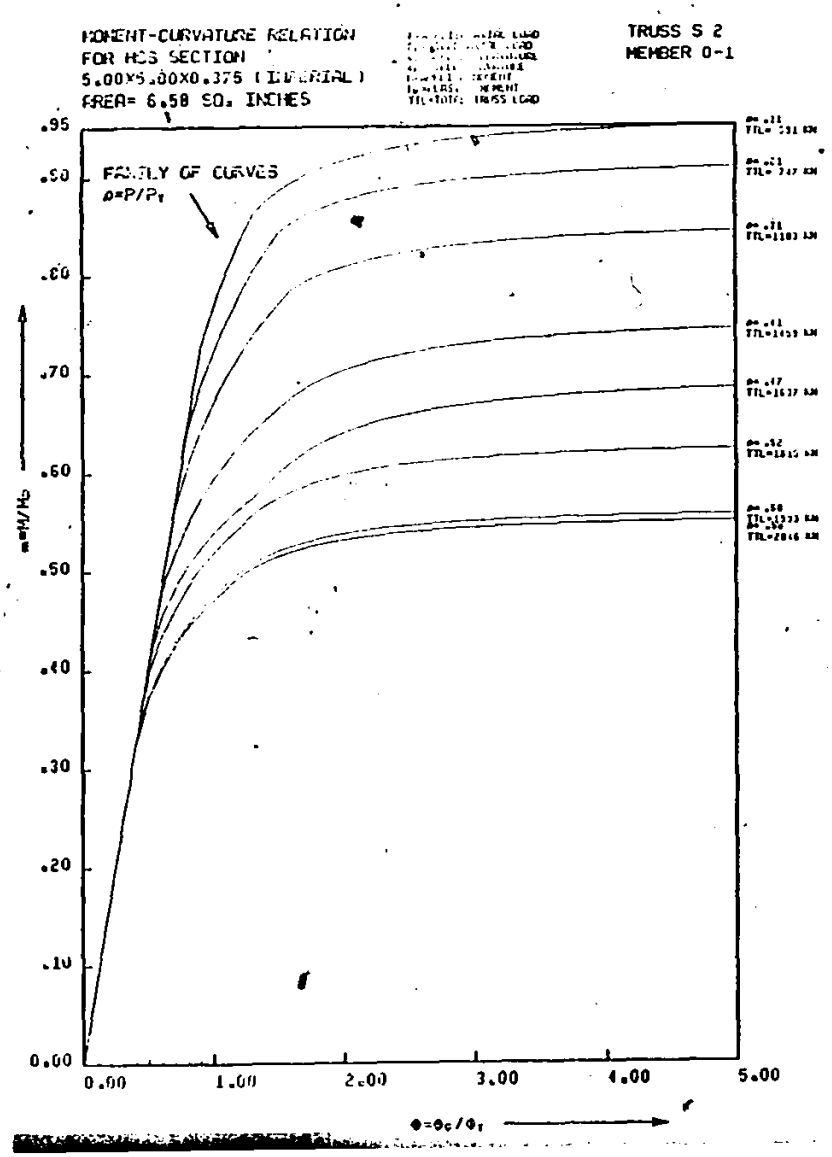
MOMENT-CURVATURE RELATION
FOR HSS SECTION
5.00X5.00X0.375 (IMPERIAL)
AREA= 6.58 SQ. INCHES
TRUSS S 2
MEMBER 0-1
FAMILY OF CURVES
β=P/Pf
m=M/Mb
.95
.90
.80
.70
.60
.50
.40
.30
.20
.10
0.00
0.00
1.00
2.00
3.00
4.00
5.00
φ=φc/φf

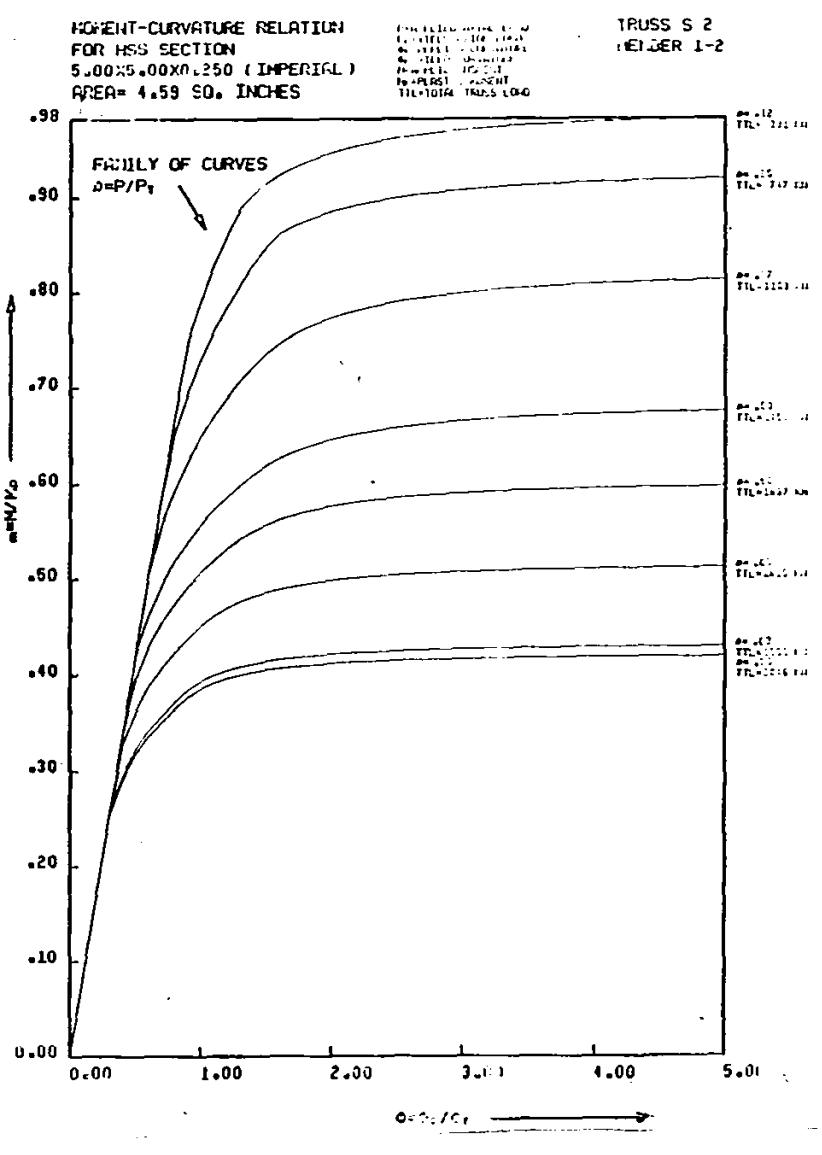
MOMENT-CURVATURE RELATION
FOR HSS SECTION
5.00X5.00X0.250 (IMPERIAL)
AREA= 4.59 SQ. INCHES
TRUSS S 2
MEMBER 1-2
FAMILY OF CURVES
β=P/Pf
m=M/Mb
.98
.90
.80
.70
.60
.50
.40
.30
.20
.10
0.00
0.00
1.00
2.00
4.00
5.00

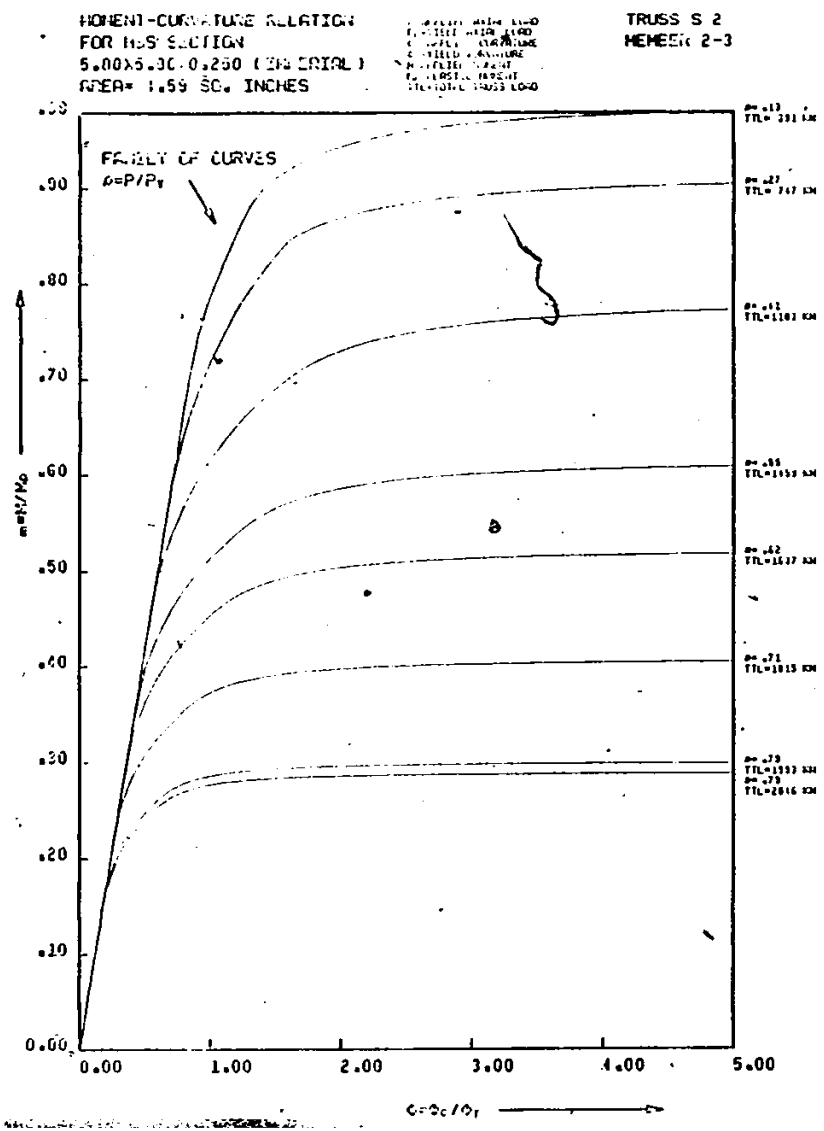
MOMENT-CURVATURE RELATION
FOR HSS SECTION
5.00X5.00X0.250 (IMPERIAL)
AREA= 4.59 SQ. INCHES
TRUSS S 2
MEMBER 2-3
FAMILY OF CURVES
ρ=P/Py
m=M/My
0.00
.10
.20
.30
.40
.50
.60
.70
.80
.90
.99
0.00
1.00
2.00
3.00
4.00
5.00
θ=θc/θy

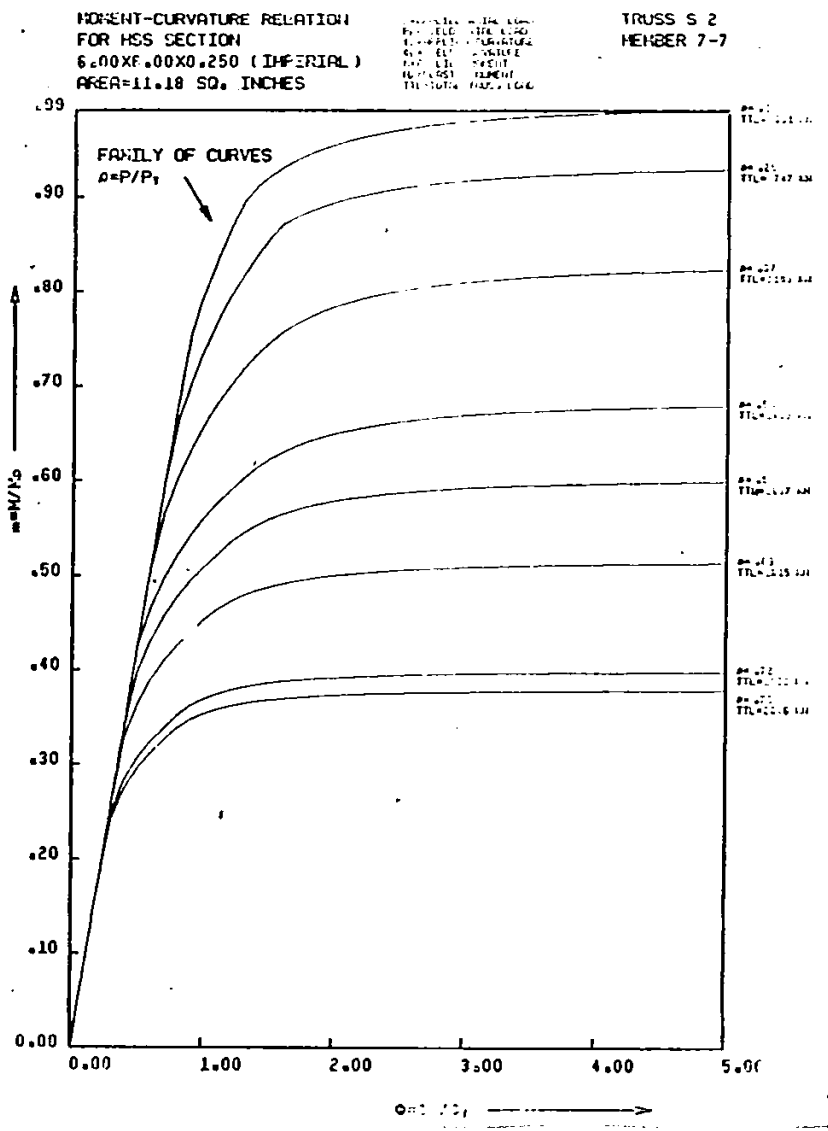
MOMENT-CURVATURE RELATION
FOR HSS SECTION
6.00X6.00X0.250 (IMPERIAL)
AREA=11.18 SQ. INCHES
TRUSS S 2
MEMBER 7-7
FAMILY OF CURVES
ρ=P/Py
m=M/My
0.00
.10
.20
.30
.40
.50
.60
.70
.80
.90
.99
0.00
1.00
2.00
3.00
4.00
5.00

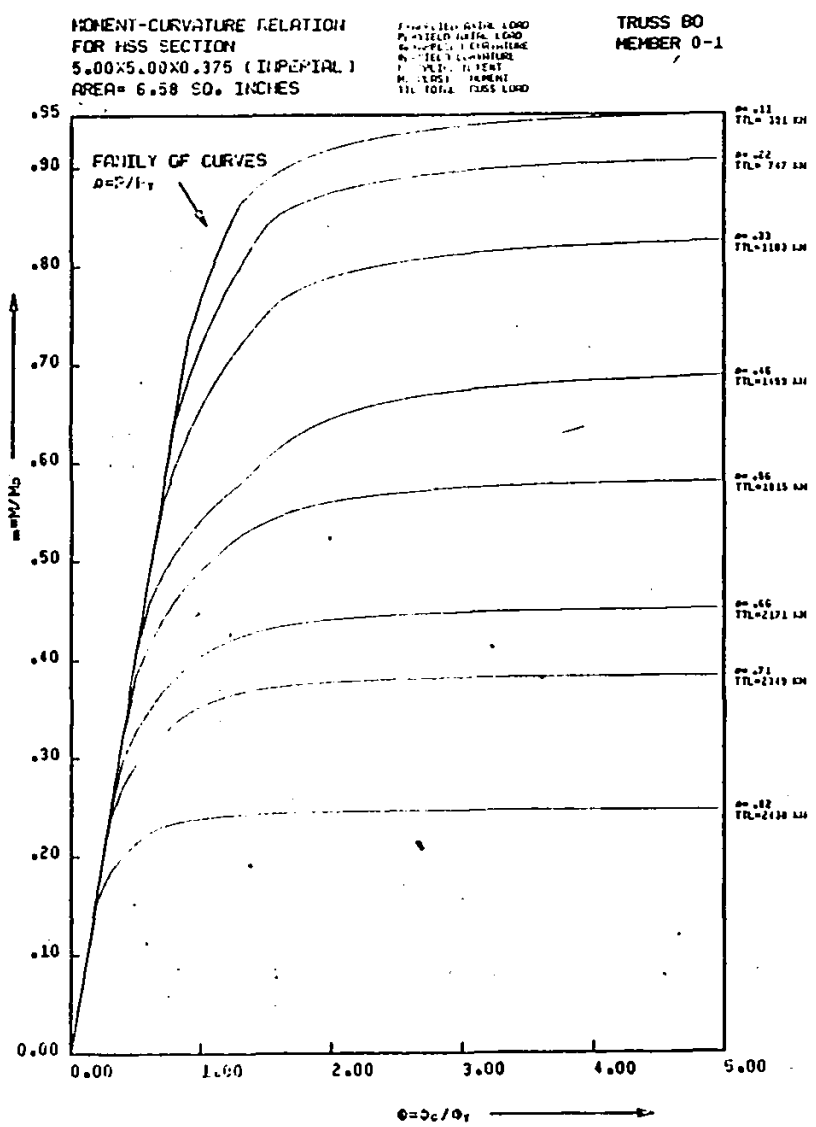
MOMENT-CURVATURE RELATION
FOR HSS SECTION
5.00X5.00X0.375 (IMPERIAL)
AREA= 6.58 SQ. INCHES
TRUSS B0
MEMBER 0-1
FAMILY OF CURVES
m=M/Mp
Φ=Φc/Φy
0.00
.10
.20
.30
.40
.50
.60
.70
.80
.90
.95
1.00
2.00
3.00
4.00
5.00

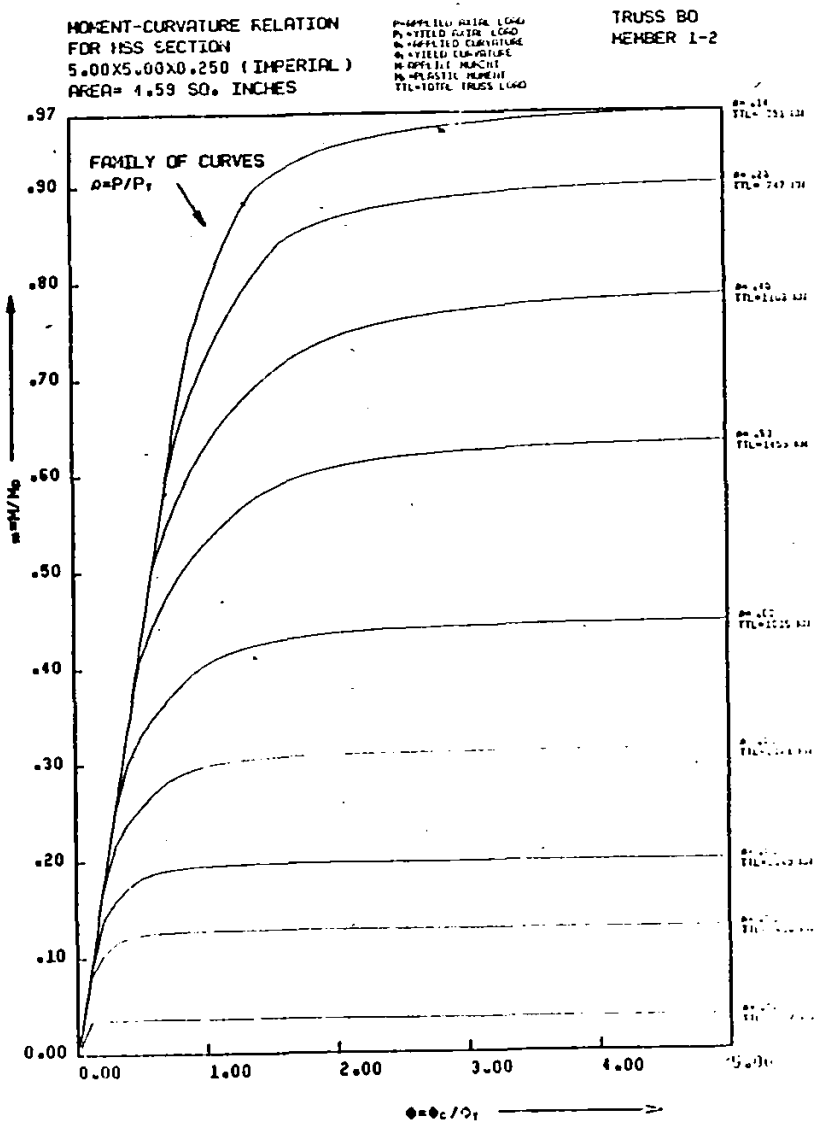
MOMENT-CURVATURE RELATION
FOR HSS SECTION
5.00X5.00X0.250 (IMPERIAL)
AREA= 4.59 SQ. INCHES
TRUSS B0
MEMBER 1-2
FAMILY OF CURVES
m=M/Mp
Φ=Φc/Φy
0.00
.10
.20
.30
.40
.50
.60
.70
.80
.90
.97
1.00
2.00
3.00
4.00

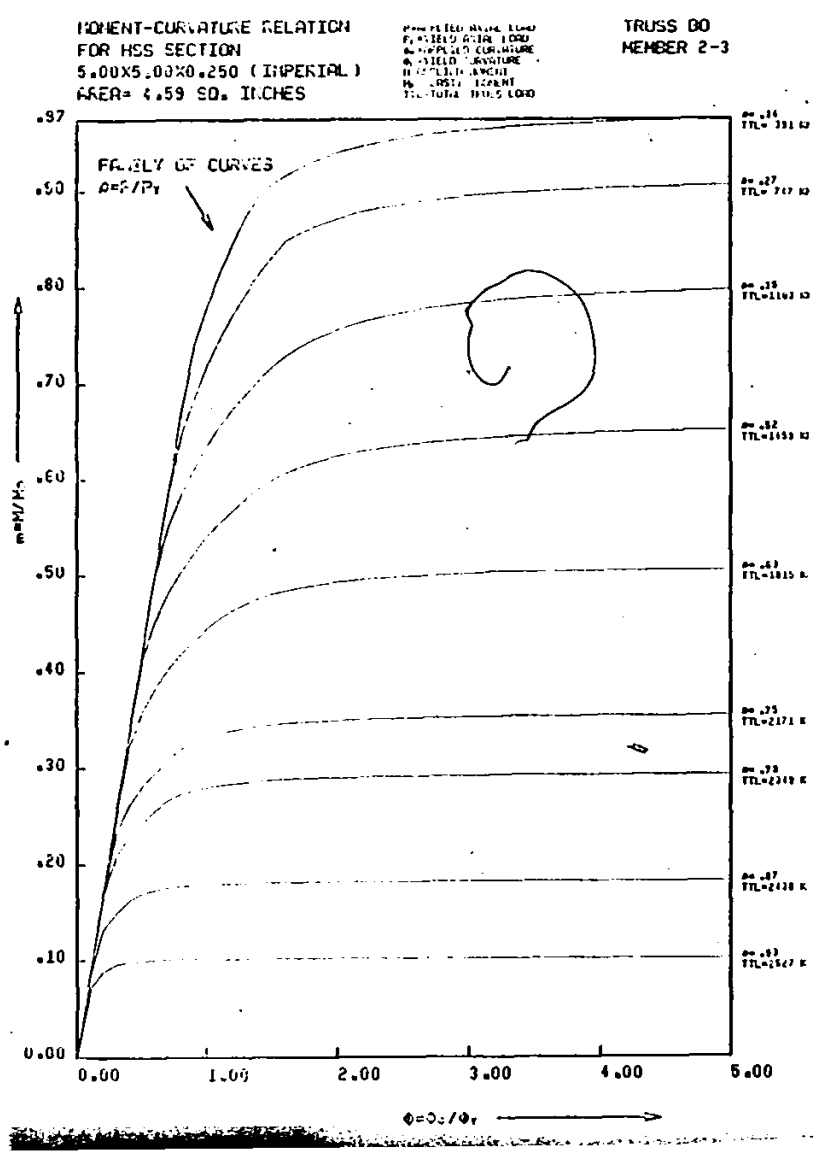
MOMENT-CURVATURE RELATION
FOR HSS SECTION
5.00X5.00X0.250 (IMPERIAL)
AREA= 4.59 SQ. INCHES
TRUSS BO
MEMBER 2-3
FAMILY OF CURVES
ρ=P/Py
m=M/My
.97
.90
.80
.70
.60
.50
.40
.30
.20
.10
0.00
0.00
1.00
2.00
3.00
4.00
5.00
Φ=Φx/Φy

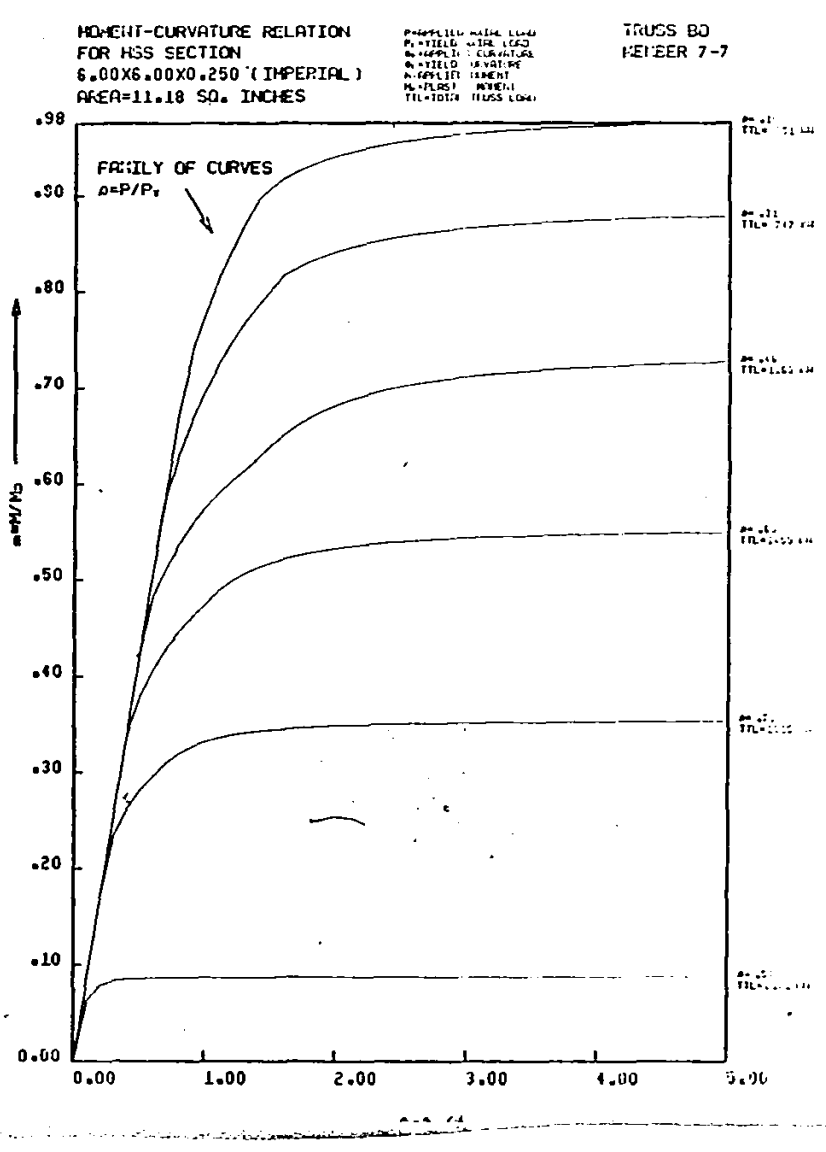
MOMENT-CURVATURE RELATION
FOR HSS SECTION
6.00X6.00X0.250 (IMPERIAL)
AREA=11.18 SQ. INCHES
TRUSS BO
MEMBER 7-7
FAMILY OF CURVES
ρ=P/Py
m=M/My
.98
.90
.80
.70
.60
.50
.40
.30
.20
.10
0.00
0.00
1.00
2.00
3.00
4.00
5.00

BIBLIOGRAPHY

[1] Korol, R.M. and Chidiac, M.A., "K-joints of double-chord square hollow sections", Canadian Journal of Civil Engineering, Vol. 7, No. 3, pp. 523-539, 1980.

[2] Chidiac, M.A., "K-joints of double chord square hollow sections", Ph.D. Thesis, McMaster University, Canada, 1979.

[3] British Steel Corporation Tubes Division. "Tests on complete girders". Draft Report CE 73/95, Corby, 1977.

[4] British Steel Corporation Tubes Division. "Tests on isolated joints". Report CE 73/96/D, Corby, August 1977.

[5] Haleem, A.S., "Some aspects on SHS welded joint behaviour", British Steel Corporation Tubes Division, Corby, January 1977.

[6] Dasgupta, A., "The behaviour of joints in tubular trusses", Ph.D. Thesis, University of Nottingham, England, November 1970.

[7] Chandrakeerthy, S., "Structural behaviour related to stress analysis of joints in cold-formed square hollow sections", Ph.D. Thesis, University of Sheffield, 1972.

[8] Walton, B.A., "Interaction of shear and tension in welded truss connection", Canadian Journal of Civil Engineering, Vol. 6, pp. 567-574, 1979.

[9] ASTM Annual Standards 1972, Part 31, Section E8 - "Standard Methods of Tensile Testing Metalic Materials".

[10] Hetenyi, M., "Handbook of experimental stress analysis", John Wiley and Sons, Inc., New York, 1957.

[11] Chen, W.F. and Atsuta, T., "Theory of Beam-Columns, Vol. 1", McGraw-Hill, New York, 1976.

[12] Neal, B.G., "The Plastic Methods of Structural Analysis", Chapman and Hall, 1977.

[13] Beedle, L.S., "Plastic Design of Steel Frames", John Wiley and Sons, New York, 1958.

[14] Yuru, J.A. and Lu, L.W., "Ultimate Load Tests on Braced Multi-storey Frames", Proc. of ASCE, Vol. 95, ST10, p. 2243, October 1969.

[15] Galumbos, T.V. and Lay, M.G., "Studies of the Ductility of Steel Members", Proc. of ASCE, Vol. 91, ST4, pp. 125-151, August 1965.

[16] Jennings, A. and Majid, K., "An elastic-plastic analysis by computer for framed structures loaded up to collapse", Structural Engineer, Vol. 43, No. 12, pp. 407-412, December 1965.

[17] Csagoly, P.F. and Bakht, B., "A computer program to determine the collapse load of steel trusses", Ministry of Transportation and Communications, Ontario, 1978.

[18] Gere, J.M. and Weaver, W., "Analysis of framed structures", D. Van Nostrand Company, New York, 1965.

[19] Wang, C.K., "Computer Methods in Advanced Structural Analysis", Intext Educational Publishers.

[20] ASCE - WRC Joint Committee, "Commentary on Plastic Design in Steel", ASCE Manual No. 41, 1981.

[21] Nadai, A., "Theory of flow and fractures of solids", McGraw-Hill, New York, 1950.

[22] Adams, P.F., Krentz, G.L. and Kulak, G.L., "Limit States Design in Structural Steel", CISC, July 1977.